

November 1992

**Water Quality Monitoring  
in Massachusetts  
and Cape Cod Bays:  
February-March 1992**

---

Massachusetts Water  
Resources Authority

Environmental Quality Department  
Technical Report No. 92-8





**WATER QUALITY MONITORING  
IN  
MASSACHUSETTS AND CAPE COD BAYS:  
FEBRUARY-MARCH 1992**

by  
**John R. Kelly  
Carl S. Albro  
John T. Hennessy  
Damian Shea**

prepared by:  
**Battelle Ocean Sciences  
397 Washington Street  
Duxbury, MA 12332  
(617) 934-0571**

prepared for:  
**Massachusetts Water Resource Authority  
Charlestown Navy Yard  
100 First Avenue  
Boston, MA, 02129  
(617) 242-6000**

**Environmental Quality Department Technical Report Series No. 92-8**

**November 1992**



## CONTENTS

<b>PREFACE</b> .....	<b>i</b>
<b>EXECUTIVE SUMMARY</b> .....	<b>ii</b>
<b>1.0 INTRODUCTION</b> .....	<b>1-1</b>
<b>1.1 Background</b> .....	<b>1-1</b>
<b>1.2 Survey Objectives</b> .....	<b>1-2</b>
<b>1.3 Survey Schedule for 1992 Baseline Water Quality   Monitoring Program</b> .....	<b>1-3</b>
<b>1.4 Summary of Accomplishments During February   and March 1992</b> .....	<b>1-3</b>
<b>2.0 METHODS</b> .....	<b>2-1</b>
<b>2.1 Field Procedures</b> .....	<b>2-1</b>
<b>2.1.1 Vertical Hydrographic Profiling</b> .....	<b>2-2</b>
<b>2.1.2 Tow-Yo Hydrographic Profiling</b> .....	<b>2-3</b>
<b>2.1.3 Sampling for Nutrients, Chlorophyll,     and Total Suspended Solids</b> .....	<b>2-3</b>
<b>2.1.4 Metabolism Measurements</b> .....	<b>2-4</b>
<b>2.1.5 Phytoplankton and Zooplankton Sampling</b> .....	<b>2-4</b>
<b>2.2 Laboratory Procedures</b> .....	<b>2-5</b>
<b>2.2.1 Nutrients and Carbon Analyses</b> .....	<b>2-5</b>
<b>2.2.2 Chlorophyll <i>a</i> and Phaeophytin</b> .....	<b>2-6</b>
<b>2.2.3 Total Suspended Solids</b> .....	<b>2-6</b>
<b>2.2.4 Dissolved Oxygen</b> .....	<b>2-6</b>
<b>2.2.5 Phytoplankton Taxonomy: Identification and Counts</b> .....	<b>2-6</b>
<b>2.2.6 Zooplankton Taxonomy: Identification and Counts</b> .....	<b>2-6</b>
<b>2.3 <i>In Situ</i> Instrument Comparison and Calibration Procedures</b> .....	<b>2-8</b>
<b>2.4 Data Management and Processing</b> .....	<b>2-9</b>
<b>2.5 Graphical Modeling and Statistical Analyses</b> .....	<b>2-9</b>
<b>3.0 FEBRUARY 1992 SURVEYS</b> .....	<b>3-1</b>
<b>3.1 Farfield Survey Results</b> .....	<b>3-1</b>
<b>3.1.1 Horizontal Distribution of Water Properties</b> .....	<b>3-1</b>
<b>3.1.2 Water Properties Along Selected Vertical Sections</b> .....	<b>3-3</b>
<b>3.1.3 Analysis of Water Types</b> .....	<b>3-3</b>
<b>3.1.4 Distribution of Chlorophyll and Phytoplankton</b> .....	<b>3-6</b>
<b>3.1.5 Distribution of Zooplankton</b> .....	<b>3-7</b>
<b>3.1.6 Whole-Water Metabolism Incubations</b> .....	<b>3-8</b>

## CONTENTS (Continued)

3.2	Nearfield Survey Results .....	3-9
3.2.1	Horizontal Distribution of Water Properties .....	3-9
3.2.2	Water Properties Along Vertical Transects .....	3-10
3.2.3	Comparison of Vertical and Towed Profiling .....	3-10
3.2.4	Analysis of Small-Scale Variability .....	3-11
3.2.5	Analysis of Water Types and Biological Properties .....	3-11
4.0	MARCH 1992 SURVEYS .....	4-1
4.1	Farfield Survey Results .....	4-1
4.1.1	Horizontal Distribution of Water Properties .....	4-1
4.1.2	Water Properties Along Selected Vertical Sections .....	4-2
4.1.3	Analysis of Water Types .....	4-3
4.1.4	Distribution of Chlorophyll and Phytoplankton .....	4-4
4.1.5	Distribution of Zooplankton .....	4-5
4.1.6	Whole-Water Metabolism Incubations .....	4-6
4.2	Nearfield Survey Results .....	4-7
4.2.1	Horizontal Distribution of Water Properties .....	4-7
4.2.2	Water Properties Along Vertical Transects and Analysis of Small-Scale Variability .....	4-7
5.0	DISCUSSION .....	5-1
5.1	Water Properties (Physical and Chemical) .....	5-1
5.1.1	Variability at the Regional Scale .....	5-1
5.1.2	Small-Scale Time and Space Variability in the Nearfield .....	5-1
5.1.3	Coherence of Nearfield and Farfield Station Properties .....	5-2
5.1.4	Comparison of Previous Studies .....	5-2
5.2	Water-Column/Nutrient Dynamics .....	5-2
5.2.1	Vertical Structure .....	5-2
5.2.2	Inshore - Offshore Gradients, Including Boston Harbor Mouth .....	5-3
5.2.3	Influence of Water from Northern Rivers/Special Features .....	5-3
5.2.4	Comparison to Previous Studies .....	5-3
5.3	Biology in Relation to Water Properties and Nutrient Dynamics .....	5-4
5.3.1	Phytoplankton - Zooplankton Relationships .....	5-4
5.3.2	Plankton Species and Water Properties .....	5-4
5.3.3	Chlorophyll Biomass and Nutrient Distribution .....	5-5
5.3.4	Metabolism and Environment .....	5-6

## CONTENTS (Continued)

5.3.5	Special Features/Anomalous Stations . . . . .	5-7
5.3.6	Comparison to Previous Studies . . . . .	5-7
5.4	Recommendations . . . . .	5-9
5.4.1	Station Locations . . . . .	5-9
5.4.2	Field and Laboratory Procedures . . . . .	5-10
6.0	<b>SUMMARY INTERPRETATION OF WINTER-SPRING SEASON DYNAMICS . . . . .</b>	<b>6-1</b>
6.1	Farfield Scale . . . . .	6-1
6.1.1	Water Properties in Space and Time . . . . .	6-1
6.1.2	Ecological Dynamics . . . . .	6-1
6.2	Nearfield Scale . . . . .	6-2
6.2.1	Water Properties in Space and Time . . . . .	6-2
6.2.2	Ecological Dynamics . . . . .	6-2
7.0	<b>REFERENCES . . . . .</b>	<b>7-1</b>
APPENDIX A.	February 1992 Station Data Tables	
APPENDIX B.	March 1992 Station Data Tables	
APPENDIX C.	February 1992 Cruises	
APPENDIX D.	Towing Profiles from February 1992 Nearfield Stations	
APPENDIX E.	March 1992 Cruises	
APPENDIX F.	Towing Profiles from March 1992 Nearfield Stations	
APPENDIX G.	Metabolism and Light Measurements from February 1992 Stations	
APPENDIX H.	Metabolism and Light Measurements from March 1992 Stations	
APPENDIX I.	Phytoplankton Species Data Tables for February 1992	
APPENDIX J.	Phytoplankton Species Data Tables for March 1992	
APPENDIX K.	Zooplankton Species Data Tables for February 1992	
APPENDIX L.	Zooplankton Species Data Tables for March 1992	

## **TABLES**

- Table 1-1**      **Summary of Samples Collected During Combined Nearfield-Farfield Survey, February 22-28, 1992**
- Table 1-2**      **Summary of Samples Collected During Combined Nearfield-Farfield Survey, March, 1992**
- Table 3-1**      **Analysis of Water Types**
- Table 3-2**      **Top 5 Dominant Phytoplankton Taxa, Excluding Microflagellates and Cryptomonads, in Near Surface Samples Collected in February, 1992**
- Table 4-1**      **Analysis of Water Types**
- Table 4-2**      **Top 5 Dominant Phytoplankton Taxa, Excluding Microflagellates and Cryptomonads, in Near Surface Samples Collected in March, 1992**



## FIGURES

- Figure 1-1 Massachusetts and Cape Cod Bays
- Figure 1-2 Planned Schedule of Water Quality Surveys for Calendar Year 1992. This report provides data from the combined Farfield-Nearfield (n1, n2) surveys in February and March.
- Figure 1-3 Water Quality Sampling Stations in Massachusetts and Cape Cod Bays. Station Codes — F: Farfield, N: Nearfield, P: Biology/Productivity
- Figure 3-1 Surface temperature ( $^{\circ}\text{C}$ ) in the region in February 1992.
- Figure 3-2 Surface salinity (PSU) in the region in February 1992.
- Figure 3-3 Surface  $\sigma_T$  in the region in February 1992.
- Figure 3-4 Surface beam attenuation ( $\text{m}^{-1}$ ) in the region in February 1992.
- Figure 3-5 Surface *in situ* fluorescence (as  $\mu\text{g Chl L}^{-1}$ ) in the region in February 1992.
- Figure 3-6 Surface dissolved inorganic nitrogen (DIN,  $\mu\text{M}$ ) in the region in February 1992.
- Figure 3-7 Surface ammonia ( $\mu\text{M}$ ) in the region in February 1992.
- Figure 3-8 Surface nitrate ( $\mu\text{M}$ ) in the region in February 1992.
- Figure 3-9 Surface phosphate ( $\mu\text{M}$ ) in the region in February 1992.
- Figure 3-10 Surface silicate ( $\mu\text{M}$ ) in the region in February 1992.
- Figure 3-11 Map showing position of four standard transects for which vertical contour plots were produced.
- Figure 3-12 Vertical section contours of  $\sigma_T$  in February for standard transects (see Figure 3-11).
- Figure 3-13 Vertical section contours of fluorescence (as  $\mu\text{g Chl L}^{-1}$ ) in February for standard transects (see Figure 3-11).
- Figure 3-14 Vertical section contours of dissolved inorganic nitrogen ( $\mu\text{M}$ ) in February for standard transects (see Figure 3-11).
- Figure 3-15 Scatter plots of data acquired by *in situ* sensor package during vertical casts at all farfield and nearfield stations occupied in February 1992.
- Figure 3-16 Map to show station groups designated in Figures 3-16 through 3-22.
- Figure 3-17 Scatter plots of nitrogen forms vs. phosphate during February 1992.

## FIGURES (Continued)

- Figure 3-18 Scatter plots of nitrogen vs. silicate during February 1992.
- Figure 3-19 Dissolved inorganic nitrogen vs. salinity and  $\sigma_T$  in February 1992.
- Figure 3-20 Ammonia vs. salinity and  $\sigma_T$  in February 1992.
- Figure 3-21 Phosphate vs. salinity and  $\sigma_T$  in February 1992.
- Figure 3-22 Silicate vs. salinity and  $\sigma_T$  in February 1992.
- Figure 3-23 The sum of dissolved inorganic nitrogen and particulate organic nitrogen vs. salinity and  $\sigma_T$  in February 1992.
- Figure 3-24 The sum of total dissolved nitrogen and particulate organic nitrogen (=total nitrogen) vs. salinity and  $\sigma_T$  in February 1992.
- Figure 3-25 Surface chlorophyll at BioProductivity stations and special station F25 in February 1992.
- Figure 3-26 Surface and deeper chlorophyll at BioProductivity stations and special station F25 in February 1992.
- Figure 3-27 Total phytoplankton abundance vs. extracted chlorophyll at BioProductivity stations in February 1992.
- Figure 3-28 Total phytoplankton abundance, by taxonomic groups, at BioProductivity stations in February 1992.
- Figure 3-29 Comparison of phytoplankton taxonomic composition of surface and deeper samples at station N4P in February 1992.
- Figure 3-30 Comparison of phytoplankton taxonomic composition of surface and deeper samples at station F2P in February 1992.
- Figure 3-31 Comparison of phytoplankton taxonomic composition of surface and deeper samples at station F23P in February 1992.
- Figure 3-32 Comparison of phytoplankton taxonomic composition of surface and deeper samples at station F13P in February 1992.
- Figure 3-33 Zooplankton abundance, by groups, at BioProductivity stations in February 1992.
- Figure 3-34 Net production (P) vs. irradiance (I) curves for station N4P in February 1992.
- Figure 3-35 Light extinction at a selection of stations in February 1992.

## FIGURES (Continued)

- Figure 3-36 Surface nutrient concentrations ( $\mu\text{M}$ ) during day 1 of nearfield sampling in February 1992.
- Figure 3-37 The salinity field in the nearfield viewed as horizontal slices at 2.5, 11, and 20 m water depths.
- Figure 3-38 Vertical section contours of  $\sigma_T$  generated from tow-yos (nearfield day 2) in February 1992.
- Figure 3-39 Vertical section contours of  $\sigma_T$  generated for tow-yos in February 1992.
- Figure 3-40 Vertical section contours of Fluorescence (as  $\mu\text{g Chl L}^{-1}$ ) generated for tow-yos in February 1992.
- Figure 3-41 Vertical section contours of Fluorescence (as  $\mu\text{g Chl L}^{-1}$ ) generated from tow-yos in February 1992.
- Figure 3-42 Comparison of contours of temperature generated from tow-yos sampling (top) vs. vertical casts at four stations along track, all nearfield day 2.
- Figure 3-43 Short-term variability at three corner stations of the nearfield grid in February 1992.
- Figure 3-44 Change in vertical profiles of parameters in 20 hours at station N1P.
- Figure 4-1 Surface temperature ( $^{\circ}\text{C}$ ) in the region in March 1992.
- Figure 4-2 Surface salinity (PSU) in the region in March 1992.
- Figure 4-3 Surface  $\sigma_T$  in the region in March 1992.
- Figure 4-4 Surface beam attenuation ( $\text{m}^{-1}$ ) in the region in March 1992.
- Figure 4-5 Surface *in situ* fluorescence (as  $\mu\text{g Chl L}^{-1}$ ) in the region in March 1992.
- Figure 4-6 Surface dissolved inorganic nitrogen (DIN  $\mu\text{M}$ ) in the region in March 1992.
- Figure 4-7 Surface ammonia ( $\mu\text{M}$ ) in the region in March 1992.
- Figure 4-8 Surface nitrate ( $\mu\text{M}$ ) in the region in March 1992.
- Figure 4-9 Surface phosphate ( $\mu\text{M}$ ) in the region in March 1992.
- Figure 4-10 Surface silicate ( $\mu\text{M}$ ) in the region in March 1992.
- Figure 4-11 Vertical section contours of  $\sigma_T$  in March for standard transects (see Figure 3-11).

## FIGURES (Continued)

- Figure 4-12 Vertical section contours of fluorescence (as  $\mu\text{g Chl L}^{-1}$ ) in March for standard transects.
- Figure 4-13 Vertical section contours of dissolved inorganic nitrogen in March for standard transects.
- Figure 4-14 Scatter plots of data acquired by *in situ* sensor package during vertical casts at all farfield and nearfield stations occupied in March 1992.
- Figure 4-15 Map to show station groups, the same as for February, designated in Figures 4-16 through 4-21.
- Figure 4-16 Scatter plots of nitrogen forms vs. phosphate during March 1992.
- Figure 4-17 Scatter plots of nitrogen vs. silicate during March 1992.
- Figure 4-18 Dissolved inorganic nitrogen vs. salinity and  $\sigma_T$  in March 1992.
- Figure 4-19 Ammonia vs. salinity and  $\sigma_T$  in March 1992.
- Figure 4-20 Phosphate vs. salinity and  $\sigma_T$  in March 1992.
- Figure 4-21 Silicate vs. salinity and  $\sigma_T$  in March 1992.
- Figure 4-22 The sum of dissolved inorganic nitrogen and particulate organic nitrogen vs salinity and  $\sigma_T$  in March 1992.
- Figure 4-23 The sum of total dissolved nitrogen and particulate organic nitrogen (=total nitrogen) vs. salinity and  $\sigma_T$  in March 1992.
- Figure 4-24 Surface chlorophyll at BioProductivity stations and special station F25 in March 1992.
- Figure 4-25 Surface and deeper chlorophyll at BioProductivity stations and special station F25 in March 1992.
- Figure 4-26 Total phytoplankton abundance vs. extracted chlorophyll at BioProductivity stations in March 1992.
- Figure 4-27 Total phytoplankton abundance in surface samples, by taxonomic groups, at BioProductivity stations in March 1992.
- Figure 4-28 Comparison of phytoplankton taxonomic composition of surface and deeper samples at station N4P in March 1992.
- Figure 4-29 Comparison of phytoplankton taxonomic composition of surface and deeper samples at station F2P in March 1992.

## FIGURES (Continued)

- Figure 4-30** Comparison of phytoplankton taxonomic composition of surface and deeper samples at station F23P in March 1992.
- Figure 4-31** Comparison of phytoplankton taxonomic composition of surface and deeper samples at station F13P in March 1992.
- Figure 4-32** Zooplankton abundance, by groups, at BioProductivity stations in March 1992.
- Figure 4-33** Net production (P) vs. irradiance (I) curves for station N4P in March 1992.
- Figure 4-34** Light extinction at a selection of stations in March 1992.
- Figure 4-35** Surface nutrient concentrations ( $\mu\text{M}$ ) during day 1 of nearfield sampling in March 1992.
- Figure 4-36** The salinity field in the nearfield viewed as horizontal slices at 2.5, 11, and 20 m water depths.
- Figure 4-37** Vertical section contours of salinity generated from tow-yos in March 1992.
- Figure 4-38** Vertical section contours of salinity generated from tow-yos in March 1992.
- Figure 5-1** Dissolved inorganic nitrogen vs. depth for all stations in February 1992.
- Figure 5-2** Dissolved inorganic nitrogen vs. depth for all stations in March 1992.
- Figure 5-3** Vertical section plots for silicate ( $\mu\text{M}$ ) across the Boston - Nearfield Transect 2 in February (top) and in March (bottom) 1992.
- Figure 5-4** Total dissolved nitrogen vs. depth from BioProductivity stations and special station F25 in February (top) and March (bottom) 1992.
- Figure 5-5** Silicate vs. depth for all stations in February (top) and March (bottom) 1992.
- Figure 5-6** Total dissolved nitrogen vs. dissolved inorganic nitrogen in February (top) and March (bottom) 1992.
- Figure 5-7** Zooplankton abundance vs. phytoplankton abundance (top) and chlorophyll (bottom) from all BioProductivity stations in February 1992.
- Figure 5-8** Zooplankton abundance vs. phytoplankton abundance (top) and chlorophyll (bottom) from all BioProductivity stations in March 1992.
- Figure 5-9** Chlorophyll vs dissolved inorganic nitrogen from all BioProductivity stations in February (top) and March (bottom) 1992 at two depths.

## FIGURES (Continued)

- Figure 5-10** Phytoplankton abundance vs dissolved inorganic nitrogen from all BioProductivity stations in February (top) and March (bottom) 1992 at two depths.
- Figure 5-11** Chlorophyll vs. phaeopigments from all BioProductivity stations in February (top) and March (bottom) at two depths.
- Figure 5-12** Estimated  $P_{max}$  from P-I curves vs. dissolved inorganic nitrogen in February (top) and March (bottom) 1992.
- Figure 6-1** Surface concentrations of total nitrogen ( $\Sigma$  TDN + PON,  $\mu$ M) at BioProductivity stations and special station F25 shown as relative height bars overlain upon horizontal contours of surface fluorescence (as  $\mu$ g Chl L<sup>-1</sup>) during February 1992.

## Preface

This report provides a description and summary of data collected for the Massachusetts Water Resources Authority Water Quality Monitoring during 1992. The authors played the primary role in report preparation including: data processing, interpretation, and presentation of survey objectives and findings. A larger group of individuals are gratefully acknowledged for tremendous efforts in the field, in the laboratory, in data analysis, and in report production. This group included:

Dr. Peter Doering, University of Rhode Island, who coordinated all aspects of the nutrient metabolism sampling and provided results of data analyses and modeling of metabolism. He was assisted by Laura Reed, Edwin Requintina, and Eric Kloss.

Dr. Jefferson Turner and David Borkman of the University of Massachusetts - Dartmouth, who performed phytoplankton and zooplankton sampling and analyses and provided interpretative assistance.

Chip Ryther, who coordinated the field efforts for Battelle Ocean Sciences, and who was assisted by Jack Bechtold, Tony Luksas, and Kevin King.

Ellie Baptiste, of Battelle Ocean Sciences, developed and managed the database and prepared many appendices for this report. Carole Peven and Lisa Ginsburg prepared many of the graphic results for the report.

Rosanna Buhl, of Battelle Ocean Sciences, who performed the Quality Assurance review of the data and the report. She was assisted by Suzanne Deveney.

The pool of Battelle Ocean Sciences staff who helped produce the report, including Karen Johnson, Diane Donovan, Heather Amoling, Barbara Greene, and Lynn Lariviere.

# WATER QUALITY MONITORING IN MASSACHUSETTS AND CAPE COD BAYS: FEBRUARY-MARCH 1992

## EXECUTIVE SUMMARY

The Massachusetts Water Resources Authority (MWRA) is implementing a long-term monitoring plan for the future MWRA effluent outfall that will be located in western Massachusetts Bay. The purpose of monitoring is to verify compliance with the discharge permit and to assess the potential environmental impact of effluent discharge into Massachusetts Bay. To help establish the present conditions as a baseline, Battelle will be conducting twenty-two water-quality surveys throughout Massachusetts Bay and Cape Cod Bay during 1992 for the MWRA. These water-quality surveys are to provide data on water properties, including nutrients and other parameters of importance relative to eutrophication.

This report encompasses the initial surveys for the year, covering those conducted in February and March. Included are results, from each month, of a "combined" survey. Each combined survey included stations located in the "nearfield," an approximately 100 km<sup>2</sup> region whose center is near the middle of the proposed outfall diffuser line, and the "farfield," defined as all other stations sampled in Massachusetts and Cape Cod Bays that fall outside the nearfield region. The report briefly provides background information on the water quality surveys and objectives and describes field, laboratory, and data analysis procedures. Results from the February and March surveys are presented and discussed in some detail. Survey activities and major results are summarized here.

### Overview of surveys

Measures of physical, chemical, and biological properties in Massachusetts Bay and Cape Cod Bay were made. Sampling was performed at predetermined stations, following the monitoring plan developed by the MWRA. Included were twenty-one nearfield stations in a regular grid around the proposed outfall location in Western Massachusetts Bay. Also included were twenty-five farfield stations; most of these were along transect lines set to provide description of water quality north, south, east, and west of the nearfield. Some stations were also established to characterize selected areas, such as along the axis of Stellwagen Basin, near Race Point off Provincetown at the tip of Cape Cod, and at two exit points from Boston Harbor.

There were two main types of stations: nutrient/hydrography stations and biology/productivity stations, both in the nearfield and the farfield. A variety of supplemental measurements were made at the latter type of station to provide intensive description of water quality.

There were two principal modes of sampling. Vertical profiles were made using sensors and bottles to sample throughout the water column at a station. In the nearfield, horizontal (tow-yo) towing also was conducted, in which instruments sampled the water column while oscillating from near surface to near bottom along prescribed transects.

The purpose of measurements was to determine *in situ* concentrations for most parameters and provide data on rates of several important processes. Sampling was performed using three general methods: (1) *in situ* sensors and electronic, or in one case (light) manual, data recording; (2) whole-



water samples retrieved from depth by closing bottles, or in some cases, by pumping; (3) towing of a net to obtain samples of zooplankton. From (2) and (3), laboratory analyses were performed to provide precise determinations of chemical or biological parameters and results were input to the MWRA monitoring database.

### **Overview of major results**

Both the February and March surveys were highly successful; results allowed useful and detailed characterization of physical, chemical, and biological properties in the nearfield and farfield regions. The major environmental features were similar in February and March and in general the conditions suggested that the Bays were relatively well-mixed physically. Nutrients were within the range previously measured in the Bays; even the highest measured concentrations did not indicate eutrophic conditions. The biological community was quite similar throughout the regions sampled and was best characterized as a pelagic community that was normal and expected for a shallow temperate coastal marine ecosystem.

It was revealing to examine results by contrasting variability of physical, chemical (nutrients), and biological parameters. The features of variability for each were as indicated by the following synopses.

***Physical variability.*** Conditions were well-mixed vertically. There were weak, but easily characterized, horizontal gradients from shore; thus water mass distinctions between shallow coastal and more offshore waters were possible. The shoreline had colder, slightly less saline, waters than offshore. At the regional scale, an inverse latitudinal temperature gradient was detected for mainstem Bay offshore waters. With respect to the nearfield, one can infer from the data that a surface water mass impinged on nearfield from the north during this season. Mixing of coastal water of obvious Boston Harbor origin with offshore water also was documented within the nearfield region. In the nearfield, where repeated sampling occurred on several days of a survey and where synoptic data were gathered during horizontal towing, results showed that short-term and small-scale time and space variability was high.

***Chemical (nutrients) variability.*** Following the physical regime, the Bays generally were vertically well-mixed with respect to most nutrients. Nutrients also followed physics with respect to offshore/inshore distinctions, and latitudinal patterns. Even given the weak horizontal physical gradients, it was possible to make a geochemical distinction between most coastal and offshore waters by virtue of either the quantity and quality of nutrients. In part, this was due to the large signal of nutrients from Boston Harbor, where nutrients were highly elevated in nitrogen, particularly so for ammonia-nitrogen, yet not so elevated in silicate. Spatial contours of the station data on nutrient concentrations suggested outflow from the Boston Harbor region, with mixing and advection occurring nearly conservatively to the nearfield (in February especially) and along the coast to the south. At the regional scale at the time of sampling, there were the north-south differences in dissolved inorganic nutrient concentration corresponding to physical latitudinal patterns, but amplified in part due to the Boston Harbor source towards the north and in part by high biological activity that removed nitrogen concentrations to near detection limits at Cape Cod Bay stations to the south.

***Biological variability.*** As with physics and nutrients, there were no strong vertical patterns in phytoplankton (chlorophyll) biomass or species compositions. There were some spatial and temporal variability in phytoplankton biomass, with high concentrations in Cape Cod Bay particularly in

February, but there were only minor differences in species composition throughout the Bays, either for phytoplankton or zooplankton. As for chlorophyll, there was spatial and temporal variation in net primary production.  $P_{max}$ , a measure of production potential under non-limiting surface light irradiance conditions, had about a four-fold variation across stations and depths. The variability of these rates, as well as variability in biomass and species abundances, was often as high between neighboring biology/productivity stations of the nearfield as between distant biology/productivity stations of the farfield. In spite of sharp differences in nutrient concentrations throughout the Bays, it appeared that light, rather than nutrients, was probably the most limiting factor, a phenomenon which is typical of coastal marine plankton communities during the winter-spring period at temperate latitudes. At the time of these surveys there was no strong linkage between the variations in dissolved inorganic nutrient concentrations and biological species distributions.

#### **Initial conclusions on monitoring design**

The station sampling design and sample analyses were very powerful in the sense of being able to distinguish with great confidence water masses having only very small differences in their parameter values. For the farfield in particular, physical *dynamics* could not be assessed fully because sampling did not include any measurements of water motion. The sampling for all measures in the nearfield was more powerful than for the farfield; in the nearfield the data indicated that there were short-term variations and an occasional small lens of water of Boston Harbor origin. Physical, chemical, and biological changes were noted within a tidal cycle, as well as over 2-3 days. In certain cases, the data allow one to suggest reasonably whether biological changes were due to advective processes (movement of water) rather than *in situ* processes within a confined mass of water.

## **1.0 INTRODUCTION**

This report is the first quarterly synthesis report for the water quality portion of the 1992 Massachusetts Water Resources Authority Outfall Monitoring Program. It includes physical, chemical, and biological data from the February and March combined nearfield-farfield surveys. The report structure is as follows.

1. Background information on the water quality surveys
2. Description of field, laboratory, and data analysis procedures
3. Results from the February 1992 surveys
4. Results from the March 1992 surveys
5. Discussion of the physical and chemical properties of the water, the water-column/nutrient dynamics, and the relationship between biological parameters and water properties/nutrient dynamics
6. Summary of the 1992 winter-spring season — water properties and ecological dynamics

Recognizing the need for dissemination of monitoring data and information, this report is intended to be a summary and preliminary synthesis of information resulting from the first two surveys in 1992. Survey plans were prepared for each survey to provide important operational details required to conduct each survey and summaries of each survey were given in survey reports that were submitted to MWRA about 4 weeks after completion of each survey (Ryther, 1992a and 1992b). Appendices of data from the February and March surveys, listed in the Table of Contents are attached as a separate volume of this report. Further interpretation of this information, and information gathered over the remainder of 1992, will be given in an annual report that will be prepared under a separate contract.

### **1.1 Background**

The Massachusetts Water Resources Authority (MWRA) is implementing a long-term monitoring plan (MWRA, 1991) for the future MWRA effluent outfall that will be located in Massachusetts Bay (see Figure 1-1). (Note that all tables and figures are at the end of each chapter). The purpose of the monitoring is to verify compliance with the discharge permit and to assess the potential environmental impact of effluent discharge into Massachusetts Bay. To help establish the present conditions with respect to water properties, nutrients, and other important parameters of eutrophication, Battelle will be conducting twenty-two water-quality surveys throughout Massachusetts Bay during 1992 for the MWRA.

A detailed description of the monitoring and its rationale are given in the Effluent Outfall Monitoring Plan (MWRA, 1991). The technical approach used to implement the water quality portion of this monitoring plan is presented in the Quality Assurance Project Plan (QAPjP), Shea *et al.* (1992). The QAPjP describes the technical activities performed at sea and in the laboratory, data quality requirements and assessments, project management, and a schedule of activities and deliverables.

## **1.2 Survey Objectives**

The objectives of the water quality surveys are discussed in detail in the MWRA Effluent Outfall Monitoring Plan (MWRA, 1991) and are summarized below.

### **Physical Oceanography**

- Obtain high-resolution measurements of water properties throughout Massachusetts Bay
- Use vertical-profile data on water properties at selected sites in Massachusetts and Cape Cod Bays for analysis of large-scale spatial (10s of km) and temporal (seasonal) variability in water properties and to provide supporting data to help interpret biological and chemical data
- Use high-resolution, near-synoptic, water-property measurements along transects within the nearfield area for analysis of smaller-scale spatial (km) and temporal (semi-monthly) variability in water properties, and develop a three-dimensional picture of water properties near the future outfall

### **Nutrients**

- Obtain nutrient measurements in water that is representative of Massachusetts and Cape Cod Bays
- Use vertical-profile data on nutrients at selected sites in Massachusetts and Cape Cod Bays for analysis of large-scale spatial (10s of km) and temporal (seasonal) variability in nutrient concentrations and to provide supporting data to help to interpret biological data
- Use vertical-profile data on nutrients along transects of closely-spaced stations within the nearfield area for analysis of smaller-scale spatial (km) and temporal (semi-monthly) variability in nutrient concentrations, and develop a three-dimensional picture of the nutrient field near the future outfall

### **Plankton**

- Obtain high-quality identification and enumeration of phytoplankton and zooplankton in water that is representative of Massachusetts and Cape Cod Bays
- Use vertical-profile data on plankton at selected sites in Massachusetts and Cape Cod Bays for analysis of large-scale spatial (10s of km) and temporal (seasonal) variability in plankton distribution

## **Water Column Respiration and Production**

- Using water that is representative of Massachusetts and Cape Cod Bays, obtain a reasonable estimate of the rates of water-column respiration and production as a function of irradiance.

## **General**

- Evaluate the utility of various measurements to detect change or to help to explain observed change
- Provide data to help to modify the monitoring program to allow a more efficient means of attaining monitoring objectives
- Use the data appropriately to describe the water-quality conditions (over space and time) in Massachusetts and Cape Cod Bays

### **1.3 Survey Schedule for 1992 Baseline Water Quality Monitoring Program**

The original survey schedule for the 1992 Baseline Water Quality Monitoring Program is shown in Figure 1-2. The February combined nearfield-farfield survey was completed ahead of schedule on 28 February 1992. Extremely bad weather (25-35-kn winds, 6-8-ft seas) delayed the start of the March combined nearfield-farfield survey until 14 March; the survey was completed 18 March. Because of this delay, the time window between the second and third combined nearfield-farfield surveys was reduced to just over two weeks. After consultation with the MWRA, it was decided to postpone the March nearfield survey, scheduled for March 24-25, until later in the year.

### **1.4 Summary of Accomplishments during February and March 1992**

To begin to meet the objectives listed above, Battelle conducted two farfield surveys in Massachusetts and Cape Cod Bays and two nearfield surveys in the vicinity of the future outfall during February and March 1992. *In situ* measurements were taken and samples were collected at the stations shown in Figure 1-3 for laboratory analyses to obtain the following types of data.

- Dissolved inorganic nutrients: nitrate, nitrite, ammonium, phosphate, and silicate
- Chlorophyll *a* and phaeopigments in extracts of filtered water
- *In situ* fluorometric measurements of chlorophyll, optical-beam transmittance (attenuation), light irradiance, salinity, temperature, and dissolved oxygen

- Total suspended solids and dissolved oxygen in discrete water samples
- Organic nutrients: dissolved carbon, nitrogen, and phosphorus; particulate carbon and nitrogen
- Phytoplankton and zooplankton identification and enumeration
- Rates of water-column respiration and production vs. irradiance from shipboard incubations.

The first two combined nearfield-farfield surveys were highly successful. Despite an intensive schedule for planning, preparing, and mobilizing the February survey and the bad weather encountered during the March survey, nearly all objectives were met. Details of the survey operations are provided in the survey reports (Ryther, 1992a and 1992b), which additionally provide the survey tracks for each cruise.

The EPA vessel, OSV *Peter W. Anderson*, served as an excellent platform for the February survey. The Battelle Ocean Sampling System (BOSS) and other equipment (rosette, navigation system, photosynthetron) were successfully installed onboard the *Anderson*; only minimal equipment downtime was experienced during the survey. Water sampling operations and onboard sample processing were very successful; 100% station coverage was achieved for the vertical hydrographic profiles and sample collections (see Table 1-1). The photosynthetron incubator, designed specifically for this program, worked very well. Oxygen titrations required nearly continuous (24-h) operation to provide incubator space, but the analyses were under control at all times. Oscillating (tow-yo) hydrographic profiles were successfully performed in the nearfield during the second day of the nearfield survey (Ryther, 1992a).

The March survey successfully utilized a new vessel, the R/V *Navaho*. The 53-ft vessel served as an excellent platform. Approximately 80% station coverage was achieved (40 out of 52 stations) for the vertical hydrographic profiling and sample collections (see Table 1-2); rough seas prevented full station coverage during this period. Sampling operations, onboard sample processing, and the use of all but one of the *in situ* sensors were very successful despite the rough seas and severe icing encountered on this survey. Tow-yo hydrographic profiling was completed along the outer nearfield box; towing was suspended several times due to rough seas (Ryther, 1992b).

All samples that were collected for analysis have been analyzed, and *in situ* sensor measurements have been calibrated and processed. The data have been subjected to an independent review for accuracy and technical reasonableness, synthesized and interpreted, and this information is discussed in this report.



Table 1-1 Summary of Samples Collected During Combined Nearfield-Farfield Survey, February 22-28, 1992

Station Numbers	Date	Time on Station	Latitude	Longitude	Bottom Depth (m)	Sample Method Rosette/ Pump	#depths Sampled	Hydro-graphic Profile	Irra-diance Profile	Phyto-plankton	Zoo-plankton	Dissolved Inorganic Nutrients	Biological/ Productivity Parameters
F4	2/23/92	0915	42°04.78'	70°16.88'	63.9	Rosette	5	X	-	-	-	X	-
F2P	2/23/92	1142	41°54.49'	70°13.70'	32.6	Rosette	5	X	X	X	X	X	X
F1P	2/23/92	1415	41°51.05'	70°27.20'	28.2	Rosette	5	X	X	X	X	X	X
F3	2/23/92	1609	41°57.00'	70°32.90'	18.1	Rosette	4	X	X	-	-	X	-
F5	2/23/92	1737	42°08.43'	70°38.96'	23.8	Rosette	5	X	-	-	-	X	-
F6	2/23/92	1841	42°10.24'	70°34.60'	35.5	Rosette	5	X	-	-	-	X	-
F7	2/23/92	1927	42°11.81'	70°30.95'	55.1	Rosette	5	X	-	-	-	X	-
F8	2/23/92	2017	42°16.68'	70°26.86'	83.4	Rosette	5	X	-	-	-	X	-
F12	2/23/92	2059	42°19.80'	70°25.40'	91.4	Rosette	5	X	-	-	-	X	-
F11	2/23/92	2200	42°15.90'	70°45.00'	54.1	Rosette	4	X	-	-	-	X	-
F10	2/23/92	2238	42°14.54'	70°38.24'	33.5	Rosette	4	X	-	-	-	X	-
F9	2/23/92	2311	42°12.70'	70°42.65'	20.5	Rosette	4	X	X	X	X	X	X
F13P	2/24/92	0800	42°16.04'	70°44.17'	26.2	Rosette	5	X	X	X	X	X	X
N7P	2/24/92	1120	42°21.38'	70°42.37'	48.4	Rosette	4	X	X	X	X	X	X
N10P	2/24/92	1310	42°19.89'	70°50.04'	23.8	Rosette	4	X	X	-	-	X	-
F14	2/24/92	1405	42°18.00'	70°48.50'	17.8	Rosette	4	X	X	-	-	X	-
F15	2/24/92	1450	42°18.93'	70°43.66'	39.8	Rosette	5	X	X	-	-	X	-
F16	2/24/92	1542	42°19.84'	70°38.97'	60.8	Rosette	5	X	X	-	-	X	-
F17	2/24/92	1630	42°20.75'	70°34.23'	75.4	Rosette	5	X	-	-	-	X	-
F19	2/24/92	1720	42°24.90'	70°38.20'	82	Rosette	5	X	-	-	-	X	-
F22	2/24/92	1804	42°28.79'	70°37.06'	80.7	Rosette	4	X	-	-	-	X	-
F21	2/24/92	1848	42°29.73'	70°42.56'	57.5	Rosette	5	X	-	-	-	X	-
F20	2/24/92	1934	42°29.63'	70°46.51'	35.4	Rosette	5	X	-	-	-	X	-
F18	2/24/92	2040	42°26.53'	70°53.30'	25	Rosette	4	X	-	-	-	X	-
F24	2/24/92	2126	42°22.50'	70°53.75'	20	Rosette	5	X	-	-	-	X	-
N16P	2/25/92	0800	42°23.64'	70°45.20'	43.5	Rosette	5	X	X	X	X	X	X
N20P	2/25/92	0900	42°22.90'	70°49.03'	32.1	Rosette	5	X	X	X	X	X	X
F25	2/25/92	1019	42°19.38'	70°52.48'	14.1	Rosette	4	X	X	X	X	X	X
F23P	2/25/92	1215	42°25.16'	70°51.87'	31	Rosette	5	X	X	X	X	X	X
N1P	2/25/92	1339	42°20.27'	70°56.61'	15.6	Rosette	4	X	X	X	X	X	X
N2	2/26/92	0712	42°25.16'	70°51.87'	30	Rosette	5	X	X	X	X	X	X
N3	2/26/92	0852	42°25.65'	70°49.31'	41	Rosette	5	X	-	-	-	X	-
N4P	2/26/92	0935	42°26.14'	70°46.75'	45	Rosette	5	X	-	-	-	X	-
N5	2/26/92	1005	42°26.63'	70°44.19'	50	Rosette	5	X	-	-	-	X	-
N6	2/26/92	1110	42°24.88'	70°43.58'	51	Rosette	5	X	-	-	-	X	-
N7P	2/26/92	1135	42°23.13'	70°42.97'	50	Rosette	5	X	-	-	-	X	-
N8	2/26/92	1252	42°21.38'	70°42.37'	51	Rosette	5	X	-	-	-	X	-
N9	2/26/92	1320	42°20.88'	70°44.93'	27	Rosette	5	X	-	-	-	X	-
N10P	2/26/92	1411	42°20.39'	70°47.48'	35	Rosette	5	X	-	-	-	X	-
N11	2/26/92	1428	42°19.89'	70°50.04'	23	Rosette	5	X	-	-	-	X	-
N12	2/26/92	1500	42°21.65'	70°50.65'	30	Rosette	5	X	-	-	-	X	-
N13	2/26/92	1526	42°23.40'	70°51.26'	25	Rosette	5	X	-	-	-	X	-
N14	2/26/92	1543	42°24.21'	70°49.49'	30	Rosette	5	X	-	-	-	X	-
N15	2/26/92	1605	42°24.58'	70°47.57'	33	Rosette	5	X	-	-	-	X	-
N16P	2/26/92	1626	42°24.95'	70°45.65'	45	Rosette	5	X	-	-	-	X	-
N21	2/26/92	1654	42°23.64'	70°45.20'	42	Rosette	5	X	-	-	-	X	-
N20P	2/26/92	1739	42°23.27'	70°47.12'	37	Rosette	5	X	-	-	-	X	-
N19	2/26/92	1814	42°22.90'	70°49.03'	33	Rosette	5	X	X	X	X	X	X
N18	2/26/92	1849	42°21.58'	70°48.58'	27	Rosette	5	X	X	X	X	X	X
N17	2/26/92	1905	42°21.95'	70°46.66'	25	Rosette	5	X	X	X	X	X	X
			42°22.32'	70°44.74'	40	Rosette	5	X	-	-	-	X	-

x: Samples collected or profiles performed.  
-: Samples not collected.



Table 1-2 Summary of Samples Collected During Combined Nearfield-Farfield Survey, March, 1992

Station Numbers	Date	Time on Station (EST)	Latitude (N)	Longitude (W)	Bottom Depth (m)	Sample Method Rosette/Pump	# Depths Sampled	Hydrographic Profile	Irradiance Profile	Phyto-plankton	Zoo-plankton	Nutrients/ Inorganic Nutrients	Biological/ Productivity Parameters
F3	3/14/92	0811	41°57.00'	70°32.90'	19	R	5	X	X	--	--	X	--
F1P	3/14/92	0940	41°51.05'	70°27.20'	26	R	5	X	X	X	X	X	X
F2P	3/14/92	1147	41°54.49'	70°13.70'	30	R	5	X	X	X	X	X	X
F5	3/14/92	1554	42°08.43'	70°38.96'	20	R	4	X	X	--	--	X	--
F6	3/14/92	1650	42°10.24'	70°34.60'	38	R	5	X	X	--	--	X	--
F7	3/14/92	1746	42°11.81'	70°30.95'	56	R	5	X	X	--	--	X	--
F13P	3/15/92	0839	42°16.04'	70°44.17'	29	R	5	X	X	X	X	X	X
F9	3/15/92	1013	42°12.70'	70°42.65'	22	R	4	X	X	--	--	X	--
F10	3/15/92	1044	42°14.54'	70°38.24'	34	R	5	X	X	--	--	X	--
N7P	3/15/92	1205	42°21.38'	70°42.37'	50	R	5	X	X	X	X	X	X
N16P	3/15/92	1355	42°23.64'	70°45.20'	40	R	5	X	X	X	X	X	X
N20P	3/15/92	1503	42°22.90'	70°49.03'	30	R	5	X	X	X	X	X	X
F14	3/15/92	1614	42°18.00'	70°48.50'	18	R	4	X	X	--	--	X	--
F15	3/15/92	1654	42°18.93'	70°43.66'	39	R	5	X	X	--	--	X	--
F16	3/15/92	1740	42°19.84'	70°38.97'	58	R	5	X	X	--	--	X	--
N10P	3/16/92	1020	42°19.89'	70°50.04'	25	R	5	X	X	X	X	X	X
F25*	3/16/92	1156	42°19.38'	70°52.48'	15	R	4	X	X	--	--	X	--
F23P	3/16/92	1239	42°20.27'	70°56.61'	25	R	4	X	X	X	X	X	X
F24	3/16/92	1356	42°22.50'	70°53.75'	20	R	4	X	X	--	--	X	--
N1P	3/16/92	1454	42°25.16'	70°51.87'	30	R	5	X	X	X	X	X	X
F18	3/16/92	1548	42°26.53'	70°53.30'	23	R	5	X	X	--	--	X	--
F20	3/16/92	1634	42°29.63'	70°46.51'	35	R	5	X	X	--	--	X	--
F21	3/16/92	1705	42°29.73'	70°42.56'	55	R	5	X	X	--	--	X	--
F22	3/16/92	1740	42°28.79'	70°37.06'	80	R	5	X	X	--	--	X	--
F19	3/16/92	1817	42°24.90'	70°38.20'	80	R	5	X	X	--	--	X	--
F11	3/16/92	1908	42°15.90'	70°45.00'	55	R	5	X	X	--	--	X	--
N1P	3/17/92	0830	42°25.16'	70°51.87'	33	R	5	X	X	X	X	X	X
N2	3/17/92	0909	42°25.65'	70°49.31'	42	R	5	X	X	--	--	X	--
N4P	3/17/92	1017	42°26.63'	70°44.19'	53	R	5	X	X	X	X	X	X
N10P	3/17/92	1230	42°19.89'	70°50.04'	25	R	5	X	X	X	X	X	X
N11	3/17/92	1316	42°21.65'	70°50.65'	30	R	5	X	X	--	--	X	--
N12	3/17/92	1355	42°23.40'	70°51.26'	27	R	5	X	X	--	--	X	--
N13	3/17/92	1436	42°24.21'	70°49.49'	30	R	5	X	X	--	--	X	--
N20P	3/17/92	1507	42°22.90'	70°49.03'	29	R	5	X	X	X	X	X	X
N21	3/17/92	1540	42°23.27'	70°47.12'	33	R	5	X	X	--	--	X	--
N18	3/17/92	1614	42°21.95'	70°46.66'	22	R	5	X	X	--	--	X	--
N8	3/17/92	1639	42°20.88'	70°44.93'	30	R	5	X	X	--	--	X	--
N7P	3/17/92	1704	42°21.38'	70°42.37'	50	R	5	X	X	X	X	X	X
N9	3/17/92	1735	42°20.39'	70°47.48'	33	R	5	X	X	--	--	X	--
N19	3/17/92	1759	42°21.58'	70°48.58'	25	R	5	X	X	X	X	X	X

x: Sample collected or profile performed.

--: Sample not collected.

Totals 40 13 15 10 40 10

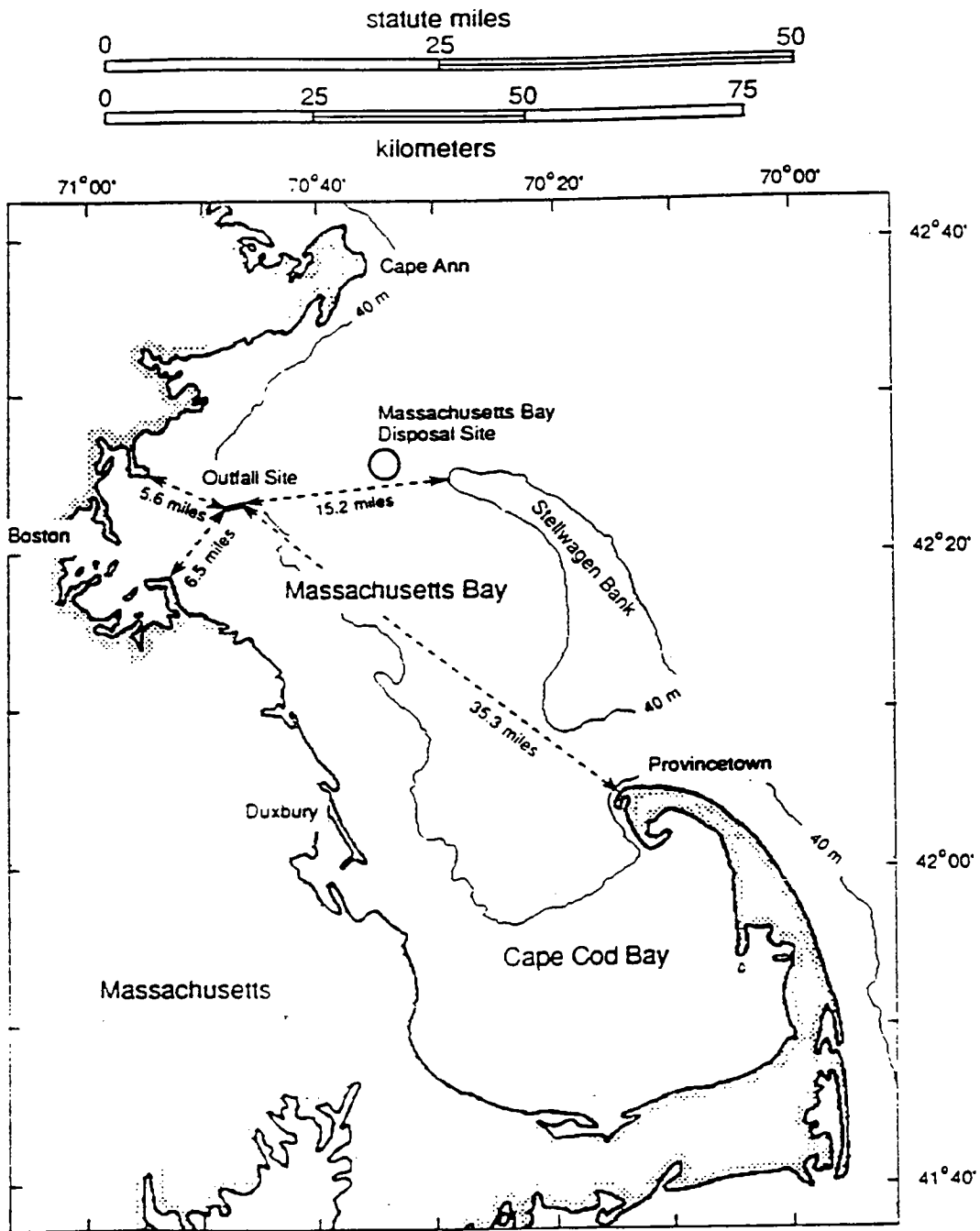


Figure 1-1. Massachusetts and Cape Cod Bays

	S	M	T	W	T	F	S		S	M	T	W	T	F	S	
				1	2	3	4					1	2	3	4	J
J	5	6	7	8	9	10	11		5	6	n1	n2	9	10	11	U
A	12	13	14	15	16	17	18		12	13	14	15	16	17	18	L
N	19	20	21	22	23	24	25		19	20	21	22	23	24	25	
	26	27	28	29	30	31	1		26	27	n1	n2	30	31	1	
F	2	3	4	5	6	7	8		2	3	4	5	6	7	8	A
E	9	10	11	12	13	14	15		9	10	n1	n2	13	14	15	U
B	16	17	18	19	20	21	22		16	17	18	19	20	21	22	G
	23	24	25	26	27	n1	n2		23	24	25	26	27	n1	n2	
M	1	2	3	4	5	6	7		30	31	1	2	3	4	5	S
A	8	9	10	11	12	n1	n2		6	7	8	n1	n2	11	12	E
R	15	16	17	18	19	20	21		13	14	15	16	17	18	19	P
	22	23	24	25	26	27	28		20	21	22	23	24	25	26	
	29	30	31	1	2	3	4		27	28	n1	n2	1	2	3	
A	5	6	7	8	9	n1	n2		4	5	6	7	8	9	10	O
P	12	13	14	15	16	17	18		11	12	13	14	15	16	n1	C
R	19	20	21	22	23	24	25		n2	19	20	21	22	23	24	T
	26	27	n1	n2	30	1	2		25	26	27	28	29	30	31	
M	3	4	5	6	7	8	9		1	2	n1	n2	5	6	7	N
A	10	11	12	13	14	15	16		8	9	10	11	12	13	14	O
Y	17	18	n1	n2	21	22	23		15	16	17	18	19	20	21	V
	24	25	26	27	28	29	30		22	23	24	25	26	27	28	
	31	1	2	3	4	5	6		29	30	n1	n2	3	4	5	D
J	7	8	9	10	11	12	13		6	7	8	9	10	11	12	E
U	14	15	16	17	18	19	20		13	14	15	16	17	18	19	C
N	21	22	23	24	25	n1	n2		20	21	22	23	24	25	26	
	28	29	30						27	28	29	30	31			

Legend: Nearfield nutrient/hydrography survey

Biology/productivity and farfield nutrient/hydrography survey

**Figure 1-2. Planned Schedule of Water Quality Surveys for Calendar Year 1992. This report provides data from the combined Farfield-Nearfield (n1, n2) surveys in February and March.**

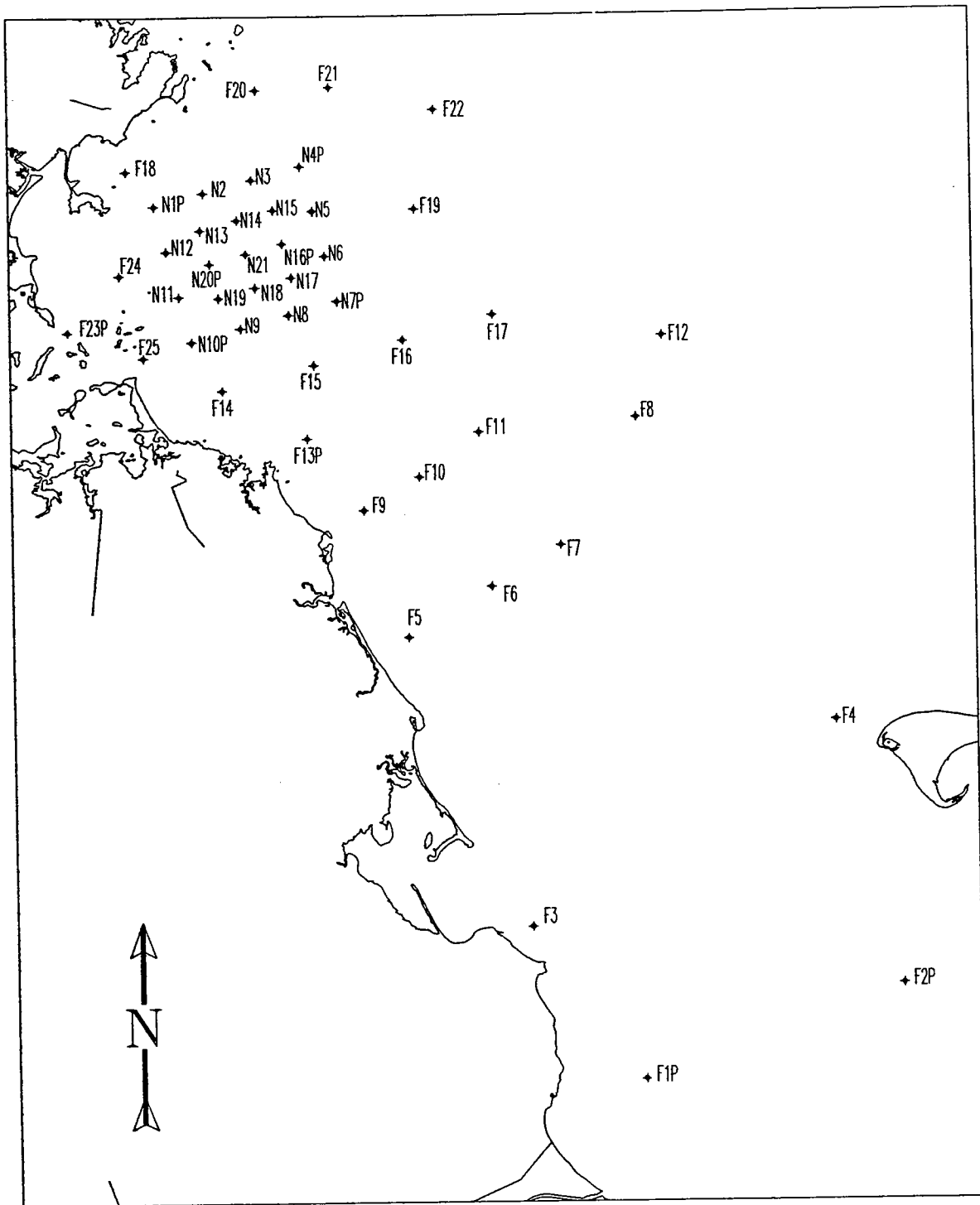


**Figure 1-3. Water Quality Sampling Stations in Massachusetts and Cape Cod Bays.**  
**Station Codes — F: Farfield, N: Nearfield, P: Biology/Productivity**

## 2.0 METHODS

Sampling equipment and procedures, sample handling and custody, sample processing and analysis, and instrument performance specifications and data quality objectives are discussed in detail in the Quality Assurance Project Plan (Shea *et al.*, 1992). A summary of this information is provided below, along with any significant modifications to the methods given in Shea *et al.* (1992). The methods used to process, manage, and analyze the data from the February and March surveys also are given in this section.

### 2.1 Field Procedures

The *OSV Anderson* and the *R/V Navaho* were used as platforms for the February and March surveys, respectively. Both surveys consisted of a farfield survey followed by a nearfield survey. During the farfield survey and the first day of the nearfield survey, continuous vertical hydrographic profiles of the water were performed and discrete water samples were collected at five depths. During the second day of the nearfield survey, continuous tow-yo hydrographic profiles were performed and discrete water samples were collected at some locations for instrument calibration and archival. Samples for water-column metabolism, and phytoplankton and zooplankton taxonomy were collected at the biology/productivity stations. Sample processing and analysis was performed both onboard the vessel and in laboratories on shore.

Positioning for both surveys was accomplished using a Northstar Model 800 Loran/GPS system with an absolute accuracy of 30-100 m. Depth measurements were collected with a JRC JFV-120 dual frequency color video echosounder. Transducers for this system were mounted on a swiveling boom assembly which was lowered into place upon arriving on station. The navigation system and depth sounder were interfaced to the BOSS navigation display and logging system. With this system, the Massachusetts Bay coastline, station locations, and the vessel track were all displayed on a color CRT. This system was also used to display and record bottom bathymetry and hydrographic data during profiling operations. Calibration checks of the Loran/GPS system were performed at dockside and at the B-buoy near the future outfall site.

During sampling operations, the BOSS computer displayed vessel position in relation to the target sampling location. When the vessel drifted more than 200-300 m off stations, the captain repositioned the ship. Hardcopies of the vessel position during sampling were printed after samples were collected.

### 2.1.1 Vertical Hydrographic Profiling

During each farfield survey and the first day of each nearfield survey, vertical hydrographic profiles were obtained using a SeaBird SBE-9 CTD and SeaBird SBE-13 dissolved oxygen sensor mounted in a General Oceanics Model 1015 rosette. The CTD system measures depth, temperature, conductivity, oxygen-sensor current, and oxygen-sensor temperature. Salinity, density, and dissolved oxygen concentrations were calculated from these measurements. The CTD system was interfaced to a SeaTech transmissometer (for beam attenuation) and Chelsea Instruments Aquatracka III fluorometer (for chlorophyll *a*). A submersible pump was also mounted on the SeaBird cage and water was pumped through a tube in the profiling cable to a Turner Model 10 fluorometer, providing a backup chlorophyll *a* measurement. At the completion of a cast, a color plot of the hydrographic profile data was produced and the profile data were recorded on computer hard disc. The data were backed up on floppy discs at regular intervals.

On the downcast, a hydrographic profile was obtained from near surface to within 5 m of the bottom for salinity, temperature, dissolved oxygen, beam transmittance, chlorophyll *a*, and depth. These data were graphically displayed in real time on the color CRT monitor and were used by the chief scientist to determine the depths for water sampling on the upcast.

Irradiance measurements were obtained with a Licor Spherical Quantum underwater irradiance sensor. The irradiance sensor was lowered by hand and values recorded from an analog deck box at 1-m intervals for the first 10 m and thereafter at 5-m intervals until the 1% light level was achieved. Variation in ambient light levels during profiling was measured simultaneously by a deck reference cell.

During the farfield survey and the first day of the nearfield survey, discrete water samples were collected with a General Oceanics Model 1015 rosette system equipped with 5- and 10-L GO-FLO (or Niskin) bottles. Samples for phytoplankton, dissolved inorganic nutrients, particulate and dissolved organic nutrients, chlorophyll, TSS, and DO were taken from these sample bottles. Bottles were lowered through the water column in an open position. On the upcast of a vertical profile, a bottle was electronically closed at each of five depths (bottom, intermediate bottom, mid-depth or chlorophyll maximum, intermediate surface, and surface) using the rosette deck unit. At stations where the bottom depth was about 20 m or less, only four depths were sampled. Discrete bottled-water sampling events were electronically flagged in the BOSS data file using an "event mark" so that the precise vessel position and the concurrent *in situ* water-column parameters (salinity, temperature, turbidity, dissolved oxygen, chlorophyll *a*, and depth) are linked with a particular bottle sample.

During the first day of each nearfield survey, water samples were collected for nutrients, phytoplankton, and calibration samples were also obtained at selected stations for chlorophyll *a*. Water samples for dissolved nutrients and chlorophyll *a* were filtered between sampling periods enroute to the next station.

Surface samples (~800-1000 mL) for phytoplankton taxonomy were also collected (using a bucket) at the biology/productivity stations.

### **2.1.2 Tow-Yo Hydrographic Profiling**

During the second day of the nearfield surveys, hydrographic data (depth, temperature, conductivity, oxygen, light transmission, and chlorophyll fluorescence) were obtained using the mini-BOSS equipped with an Ocean Sensors CTD, SeaTech transmissometer, Royce oxygen sensor, and water pumped on board through a Turner Model 10 fluorometer. The towfish was used to obtain continuous tow-yo profiles from near surface to about 5 m off bottom along the nearfield tracklines. Approximately six tow-yo profiles were performed between each nearfield station.

### **2.1.3 Sampling for Nutrients, Chlorophyll, and Total Suspended Solids**

Samples for dissolved nutrients, chlorophyll, and total suspended solids (TSS) were filtered onboard with a syringe-filter system. A sample of about 60 to 75 mL for dissolved inorganic nutrients was filtered through precombusted glass-fiber filters directly into 125-mL polyethylene bottles and preserved with chloroform. For dissolved organic carbon (DOC) about 60-75 mL of similarly filtered sample was placed directly into precleaned amber-glass bottles and then frozen. A 20-mL sample for dissolved organic nitrogen (DON) and dissolved organic phosphorus (DOP) analysis was filtered through the precombusted glass-fiber filter into a precleaned, capped test tube. The samples were fixed with buffered potassium persulfate solution and digested at 100°C in the field (Lambert and Oviatt, 1986).

Material retained on a precombusted glass-fiber filter from a 10-mL sample was used for chlorophyll *a* analysis. This small volume technique was developed by the Marine Ecosystems Research Laboratory and has been used in highly successful field and mesocosm studies for more than a decade. Filters were carefully folded, placed in aluminum foil, and frozen. Duplicate samples were taken and analyzed for chlorophyll at each sampling depth.

For combined particulate carbon and nitrogen analysis, about 50 mL of sample were passed through a precombusted glass-fiber filter; the filter was carefully folded and frozen. For TSS, about 100 mL of water was filtered through preweighed 0.4- $\mu$ m Nuclepore filters. The filters were placed in labeled petri dishes and frozen. All samples frozen on the ship remained frozen until analysis. All filtered sample volumes were recorded in a laboratory notebook.

#### 2.1.4 Metabolism Measurements

Metabolism was measured using the methods described in Lambert and Oviatt (1986). Phytoplankton production and respiration were measured by the light-dark bottle oxygen technique (Strickland and Parsons, 1972). Light and dark bottles were incubated in a photosynthetron using a modification of the methodology of Lewis and Smith (1983). Eighteen 300-mL biological oxygen demand (BOD) bottles were filled with water from a given depth (surface and mid-depth) at each of the biological/productivity stations. Up to 12 samples were incubated to simulate an irradiance gradient with light levels ranging from about 20 to 2000  $\mu\text{E}/\text{m}^2/\text{sec}$ . Light levels within the incubator were created by covering individual bottles with appropriate neutral density screening. For standardization, the light levels were fixed across stations and surveys. Three dark BOD bottles were placed in the photosynthetron to simulate zero irradiance. Three other BOD bottles were fixed (Lambert and Oviatt, 1986) immediately and represent both *in situ* DO concentrations, as well as initial values for the incubations. After about six hours (actual time was recorded), the remaining fifteen bottles from a given sampling location were fixed. The temperature of the photosynthetron was maintained at ambient surface water temperature by a flowing seawater system.

#### 2.1.5 Phytoplankton and Zooplankton Sampling

Seawater was collected in Niskin or Go-Flo bottles at five depths over the water column at each of the ten biological/productivity stations. An 800-mL subsample was collected from the Niskin bottle and was immediately preserved in 1% (final concentration) Utermohl's solution after Guillard (1973). Utermohl's solution is a mild iodine based preservative that does not destroy or greatly distort most delicate atecate dinoflagellates and microflagellates. Once collected and preserved, samples were labelled and stored in borosilicate glass jars. Two samples, one from the surface and one from the chlorophyll maximum, were analyzed for phytoplankton abundance and species composition at each biological/productivity station. The remaining samples, including those gathered from the surface during nearfield surveys, were archived at the University of Massachusetts-Dartmouth.

Net zooplankton were collected with a 0.5-m diameter 102- $\mu\text{m}$  mesh net equipped with a flowmeter. Vertical oblique tows were made at each of the ten biological/productivity stations. Tows were made over the depth of the whole water column at stations less than 50 m deep and over the upper 50 m at stations of greater than 50 m. Observation of the turning flowmeter at the end of each tow ensured that the net was not clogged during the tow. Aboard ship, samples were rinsed from the net into glass jars and immediately preserved in 5-10% formalin:seawater solution.



## 2.2 Laboratory Procedures

### 2.2.1 Nutrients and Carbon Analyses

Methods for nutrient analysis followed those described by Lambert and Oviatt (1986). Briefly, dissolved inorganic nutrient concentrations were determined on samples that had been passed through a 0.4- $\mu\text{m}$  Nuclepore membrane filter. The concentrations of ammonia, nitrate, nitrite, silicate, and phosphate were measured colorimetrically on a Technicon II Autoanalyzer. This instrument simply automates standard manual techniques for the analysis of nutrients. The analysis of ammonia is based on the technique of Solorzano (1969) in which absorbance of an indophenol blue complex is measured at 630 nm. Nitrite was measured by the method of Bendschneider and Robinson (1952). Nitrate and nitrite was measured by reducing all nitrate in the sample to nitrite and analyzing for nitrite as above. The concentration of nitrate was obtained by difference. The reduction of nitrate was accomplished with a cadmium column (Morris and Riley, 1963). The analysis of phosphate was based on the molybdate blue procedure of Murphy and Riley (1962). The colorimetric analysis of silicate was based on that of Brewer and Riley (1966).

Methods for particulate carbon and nitrogen followed those described by Lambert and Oviatt (1986). Particulate matter collected on a glass-fiber filter was ignited at high temperature (1050°C) in a Carlo Erba Model 1106 CHN elemental analyzer. The combustion releases total carbon and nitrogen in the sample in gaseous form. These products were quantified by the analyzer using a gas chromatography column and a thermal conductivity detector.

The concentrations of dissolved organic nitrogen were determined by the difference between total dissolved nitrogen and total dissolved inorganic nitrogen. Concentrations of dissolved organic phosphorus were determined in the same manner. The procedures by which the concentrations of dissolved inorganic nitrogen and phosphorus are obtained were described above. The concentrations of total dissolved nitrogen and phosphorus were determined using the method of Valderama (1981). This wet-chemistry technique utilizes persulphate to oxidize organic nitrogen and phosphorus to nitrate and phosphate. The concentrations of the latter were then determined colorimetrically on a Technicon Autoanalyzer, as described above.

Dissolved organic carbon was determined by persulphate digestion (Lambert and Oviatt, 1986) using an O.I. Model 700 TOC Analyzer. Some doubt concerning the accuracy of this method exists, and recent work suggests that the higher concentrations obtained by high temperature combustion more nearly reflect true levels of DOC in nature (Sugimura and Suzuki, 1988). The analysis used here has been intercalibrated with an Ionics high temperature combustion instrument; results for both fresh and salt

water agreed to within 6%. In addition a recent comparison of methods revealed no difference between concentrations obtained by wet oxidation with persulphate and high temperature combustion (J.I. Hedges, pers. comm.).

### **2.2.2 Chlorophyll *a* and Phaeophytin**

Methods were as described by Lambert and Oviatt (1986). The concentrations of chlorophyll *a* and phaeophytin was determined fluorometrically using a Turner fluorometer by the method of Yentsch and Menzel (1963) as modified by Lorenzen (1966).

### **2.2.3 Total Suspended Solids**

Methods were as described in Lambert and Oviatt (1986). Briefly, the weight of material suspended in seawater was determined by filtering an appropriate volume (up to 1 liter) through a pre-weighed 0.4- $\mu\text{m}$  Nuclepore membrane filter. The filter was rinsed with deionized water to remove salt, dried to constant weight at 60°C and reweighed. All weighings were performed on a Cahn electrobalance with removal of static charges on filters and sample prior to weighing.

### **2.2.4 Dissolved Oxygen**

Dissolved oxygen was measured in water samples using the method of Oudot *et al.* (1988) using the potentiometric endpoint. A Radiometer ABU91-21/TIM90-1 autotitrator was used with a Ag/AgCl combination electrode to perform all titrations. Titrations were performed within 24 h of sample collection. Titrations were done onboard the *Anderson* during the February survey and at URI during the March survey.

### **2.2.5 Phytoplankton Taxonomy: Identification and Counts**

At the laboratory, raw seawater samples were prepared for analysis by concentrating the sample via gravitational settling. Samples were placed in 40 cm tall glass settling chambers (graduated cylinders) that were scrubbed clean before each sample was processed. The initial volume of each sample was recorded to the nearest 0.5 mL and the sample was allowed to stand undisturbed in the covered settling chamber for a period of one week. After the one week settling period had passed, the settling chamber was uncovered and the upper 700-750 mL of seawater was siphoned out of the settling chamber with a

pipette attached to a 0.5 cm hose. Occasional examination of the supernatant fluid that had been siphoned off was done to ensure that no cells had inadvertently been removed from the settling chamber. The fluid remaining in the settling chamber (containing the settled out phytoplankton) was then gently mixed and transferred to a 250-mL jar. This concentrated (by a factor of approximately 10:1) plankton sample was the aliquot that was examined microscopically.

Enumeration of phytoplankton cells was done using a 1-mL subsample placed in a 1-mL Sedgwick-Rafter cell. Phytoplankton cells were observed, counted, and identified to lowest possible taxa at 200X magnification. However, 400X was used when needed to identify small cells or to discern important taxonomic features. A Whipple-grid disk placed in one ocular lens of the microscope allowed partitioning of the Sedgwick-Rafter chamber into areas of known volume (0.000195 mL per Whipple grid). A minimum of 200 cells and a maximum of 400 cells were counted for each sample. When 200 cells were counted in less than 200 Whipple grids, counting was continued until 200 Whipple grids were examined. Examining a relatively large subsample (200 Whipple grids) increases the probability of observing relatively rare cells, while counting between 200-400 cells per sample allows estimates of total phytoplankton abundance that have a precision of +/- 10% (for 400 cells counted) to +/- 20% (for 200 cells counted) of the mean (Anonymous, 1978).

Below is a sample calculation of determining total phytoplankton abundance using the above described method:

$$\frac{\# \text{ cells}}{\text{liter}} = \frac{\# \text{ cells counted}}{\# \text{ grids} * \text{ vol/grid}} * \frac{1000 \text{ mL}}{1 \text{ L}} * \frac{V_s}{V_o}$$

where:

$V_s$  = Volume of settled sample (typically 50-100 mL)

$V_o$  = Volume original sample minus volume of preservative (usually 800 mL)

Vol/grid = 0.000195 mL per Whipple grid (@200X)

Therefore, if 410 cells were counted in 200 Whipple grids (@ 200X) and the initial seawater sample was 800 mL settled to a volume of 80 mL, the density of phytoplankton in the water sample would be

$$\frac{\# \text{ cells}}{\text{liter}} = \frac{410 \text{ cells}}{200 \text{ grids} * 0.000195 \text{ mL/grid}} * \frac{1000 \text{ mL}}{1 \text{ L}} * \frac{80 \text{ mL}}{800 \text{ mL}}$$

$$\frac{\# \text{ cells}}{\text{liter}} = 1.051 * 10^6 \text{ cells per liter}$$

### 2.2.6 Zooplankton Taxonomy: Identification and Counts

Onshore, samples for zooplankton were transferred to 70% ethanol solutions to prevent inhalation of formalin fumes during counting. Samples were reduced to aliquots of at least 500 animals with a Folsom plankton splitter, and animals were counted under a dissecting microscope and identified to the lowest possible taxon. In most cases this was to species, and adult copepods were further characterized by sex. All copepodite stages of a given copepod genus were lumped, because copepod nauplii of small species cannot be reliably separated to genus under a dissecting microscope. Concentrations of total zooplankton and all identified taxa were calculated based on the number of animals counted, divided by the volume of water filtered by the net, multiplied by the aliquot concentration factor.

### 2.3 *In Situ* Instrument Comparison and Calibration Procedures

All *in situ* BOSS instruments were calibrated by the manufacturer prior to the February cruise. For chlorophyll and dissolved oxygen sensors, additional field calibration was performed by measuring these parameters in selected water samples using traditional laboratory methods (see above). For each cruise, discrete samples were collected in bottles from the biology/productivity stations (primarily) to provide a basis for post-calibrating the *in situ* sensors.

The average chlorophyll values that were measured from the discrete water samples were compared to the 20-s time-averaged *in situ* measurements that bracketed the opening and closing of the hydrocast bottle used to collect each sample. A regression of the paired values was made to provide a means of extrapolating sensor data throughout the survey. A functional regression method (Ricker, 1973) was used, and the data and statistics are provided in Appendices A and B.

During the second day of the February nearfield survey (towing operations), an in-line Turner fluorometer, with water pumped from the BOSS towfish, was used to measure *in situ* fluorescence, rather than the *in situ* Chelsea sensor. Both the Turner and Chelsea instruments ran simultaneously during the previous days of the survey; this entire electronically-stored database was used as a basis for regression and provided calibration of the Turner instrument (Appendix A). For March, the pump for the Turner was inoperable due to freezing conditions (see Ryther, 1992b) except for the towing (day 2) of the nearfield survey. Results for towing are presented as uncalibrated Turner readings (Appendix F).

A similar calibration method was used for dissolved oxygen, comparing the potentiometric endpoint titration values against the *in situ* sensor. This comparison was only satisfactory for the first cruise (Appendix A). The second survey was conducted under conditions where the instruments on the rosette

were icing-up on deck between casts. From examination of the data during post-cruise data processing, it became clear that the dissolved oxygen (DO) sensor was not operating properly. Probably, the severe weather conditions created an abnormal response time for the sensor; in any event, no extrapolations of sensor-collected data for the cruise were made as these data are unreliable. Approximately twenty potentiometric titrations were made on this survey; all of these data showed that conditions throughout the region were near saturation. It would be expected that the entire field would be fairly similar due to the fairly uniform and well-mixed physical, chemical, and biological conditions during this second survey.

## 2.4 Data Management and Processing

Samples were given unique sample/event identification numbers. These numbers were used to track data through the laboratories, to report the data and load it into the database developed specifically for the MWRA water quality monitoring program, and to link the laboratory data with the field data. All data from the *in situ* sensors and the BOSS navigation system were stored in electronic format. Sensor data associated with each bottle collection were extracted from the full time course of the electronic database, loaded into the MWRA database, and then used in data analysis, such as plots of nutrients vs. salinity. These "discrete bottle" data are provided in Appendices A and B. The full electronic database was used to provide high-resolution analyses, graphical display of vertical downcasts, and display of the oscillating towed data. These profile and time-series graphs are provided in the Appendices.

## 2.5 Graphical Modeling and Statistical Analyses

Both high-resolution *in situ* sensor data and data from measurements on discrete water samples were used for data analyses presented in this report. In general, the sources of the data are identified in figure legends and references are made to the appropriate Appendix.

Besides the statistical modeling done to calibrate instruments (see above), a model was used to fit data derived from metabolism incubations, as follows. From initial testing of P-I (Production-Irradiance) curves for several stations, a hyperbolic model was chosen as appropriate.

This model was

$$P_B = P_{\max} (1 - e^{-a}) - R_B,$$

where

$$a = \alpha I/P_{\max}.$$

$P_B$  = chlorophyll-normalized net production (units of  $\mu\text{g O}_2/\mu\text{g Chl/hr}$ ). For each Niskin/Go Flow sampling depth, this was calculated as the measured light bottle oxygen concentration minus the initial oxygen concentration (average of three replicates) divided by the chlorophyll concentration (average of two replicates) and the length of the incubation.

$P_{\max}$  = chlorophyll-normalized maximum production at light saturation (a model-derived value).

$\alpha$  = initial slope of the rise in net production with light increasing from zero irradiance [units of  $(\mu\text{g O}_2/\mu\text{g Chl/hr})/(\mu\text{E/m}^2/\text{sec})$ ], calculated from I (light irradiance level,  $\mu\text{E/m}^2/\text{sec}$ ) and  $P_{\max}$ .  $R_B$  = chlorophyll-normalized respiration (units of  $\mu\text{g O}_2/\mu\text{g Chl/hr}$ ), calculated from the model.

The three parameters,  $P_{\max}$ ,  $\alpha$ , and  $R_B$  were fit simultaneously, for each incubation series that measured paired  $P_B$  - I points, by least squares using the NLIN procedure in SAS (1985). Fitting was accomplished by the secant method where parameters were estimated if, within 50 iterations, the model converged on a suitable simultaneous fit (SAS, 1985). Note that bottle measurements of dark respiration were not used in this fitting procedure; rather,  $R_B$  was calculated from the P-I data. In general, however, it was clear that respiration was low and difficult to measure directly or to fit by the model (see Sections 3 and 4).

Tests of statistical significance of dark bottle oxygen concentrations ( $n = 3$ ) compared to initial concentrations ( $n = 3$ ) were conducted. These are presented along with model-fit parameters in the Appendices.

Finally, using light irradiance profiles with depth, the following standard model was assumed:

$$I_z = I_o e^{-Kz}$$

where

$I_o$  = incident irradiance, ( $\mu\text{E m}^{-2} \text{sec}^{-1}$ )

$I_z$  = irradiance at depth  $z(\text{m})$ , and

$K$  = the extinction coefficient in  $\text{m}^{-1}$ .

$I_o$  was measured by a deck cell and  $I_z$  with an *in situ* sensor. A correction factor for the immersion effect of the difference between air and water readings was applied. The quantity  $(I_z/I_o)$ , using paired underwater and deck cell readings (see Appendices G and H), was graphed against  $z$ , where the slope represented an estimate of  $K$ .

## 3.0 FEBRUARY 1992 SURVEYS

### 3.1 Farfield Survey Results

#### 3.1.1 Horizontal Distribution of Water Properties

In February 1992, nearshore surface waters were colder than offshore waters in Massachusetts Bay. Surface water temperatures in much of Cape Cod Bay were similar to the cold nearshore water along the coast of Massachusetts Bay, but the coldest water was found off Provincetown at the tip of Cape Cod. Other recent studies have also shown a cooler surface water mass off the tip of Cape Cod at this time of year (Geyer *et al.* 1992). The contoured pattern of surface temperature (Figure 3-1) shows the general cooling trend from  $>3^{\circ}\text{C}$  to  $<1.5^{\circ}\text{C}$ , progressing from the North to the South in the offshore waters, and with shallower coastal waters being mostly  $<2.6^{\circ}\text{C}$ .

Salinity in the surface waters showed a large-scale pattern with some similarities to temperature (Figure 3-2). Coastal nearshore waters in Massachusetts Bay, along with most of Cape Cod Bay, had salinities of about 32.1‰ or less. The freshest water was found coming from Boston Harbor. The bulk of offshore Massachusetts Bay water was from 32.0‰ to slightly over 32.3‰. Waters at both the northernmost edge of sampling (Station F22), and at Station F4 off Provincetown, were slightly fresher than their surrounding waters; these sentinel Bays-boundary stations suggested that water masses outside of the Bays may have been weak sources of fresher water at this time.

Seawater density, as reflected in surface  $\sigma_T$  values, varied over a very small range, but a regional pattern was evident nonetheless (Figure 3-3). There appeared to be sources of lighter water from Boston Harbor and from the North (perhaps the influence of rivers, including the Merrimack). A density gradient was most pronounced from Boston Harbor seaward, and also bent southward and stretched out from the coast along the South Shore. A small intrusion of slightly denser water directly from the North into the nearfield area was apparent. The main offshore axis of the Bay overlying Stellwagen Basin appeared as a body of denser water. The four Cape Cod stations had fairly similar density, in spite of the pronounced temperature variation at Provincetown, and thus that region appeared rather homogeneous.

Beam attenuation measurements in the surface waters showed the highest values (i.e., most turbid conditions) extending out from Boston Harbor (Figure 3-4). A general gradient from shore was apparent, with offshore waters being the clearest. Beam attenuation was elevated within Cape Cod Bay, corresponding to the phytoplankton bloom occurring there at this time (Figure 3-5). High

surface (1-3 m) fluorescence values ( $> 8 \mu\text{g/L}$  as chlorophyll) were seen at Station F4 off Provincetown and Station F3 off Plymouth. At Stations F1P and F2P the highest fluorescence readings were  $> 9 \mu\text{g/L}$  as chlorophyll, but were found just below the surface ( $\sim 5\text{-}7$  m). (See Appendix A.) The general regional trend was a latitudinal gradient of decreasing fluorescence from Cape Cod Bay to Massachusetts Bay, with slightly elevated fluorescence in the coastal water outside of Boston Harbor and another peak in fluorescence corresponding with the water mass edging into the northeast corner of the nearfield from the northern transect (Stations F20-F22).

High surface water concentrations of dissolved inorganic nitrogen (DIN) were seen at the two Boston Harbor exit points (Stations F23P and F25). A decreasing concentration gradient from those points seaward to the nearfield region was evident. The gradient also bent southward along the coastline until it reached values typical of the offshore body of Massachusetts Bay, and thus seemed to strongly follow temperature, salinity, and, especially,  $\sigma_T$  patterns (Figure 3-6). DIN concentrations were lowest in Cape Cod Bay, mirroring the higher phytoplankton biomass indicated by fluorescence. There did not appear to be elevated surface water nitrogen concentrations in waters that may have been intruding upon the nearfield region from the north/northeast. However, DIN concentrations in that corner of the Bay may have been drawn down by higher chlorophyll levels.

In general,  $\text{NH}_4$  contributed most strongly to DIN at nearshore stations, especially those around Boston Harbor. Offshore, nitrate represented nearly all of the DIN. Thus, the concentration contours in Figure 3-7 suggest that the Boston Harbor area acted as a strong source of  $\text{NH}_4$  into a low background of offshore water. The pattern in Figure 3-8 suggests that the Boston Harbor area also may have been acting as a weak source of nitrate. This could suggest some *in situ* nitrification of ammonia or a weak source of discharge  $\text{NO}_3$ . Note the lower  $\text{NO}_3$  values to the northeast and in Cape Cod Bay, where fluorescence was high. Note also for the middle of Massachusetts Bay, offshore from Scituate, there was high  $\text{NO}_3$  (and thus DIN) concentrations that corresponded to low chlorophyll fluorescence.

Phosphate ( $\text{PO}_4$ ) in surface water showed a geographic pattern that was similar to DIN (Figure 3-9). In contrast, surface waters had only slightly enriched  $\text{SiO}_4$  concentrations in the coastal area around Boston Harbor; some offshore stations with high salinity and high  $\sigma_T$  had the highest surface  $\text{SiO}_4$  concentrations (Figure 3-10). The regions of higher and lower silicate in the middle of Massachusetts Bay and Cape Cod Bays, respectively, roughly corresponded with the surface fluorescence patterns.



### 3.1.2 Water Properties Along Selected Vertical Stations

Section plots of T, S,  $\sigma_T$ , beam attenuation, *in situ* chlorophyll, and DIN were generated for four transects (Figure 3-11). All parameters are presented in Appendix C. Only  $\sigma_T$  chlorophyll and DIN are presented here. Transect 1, the Northern transect, displayed a surface cell of very slightly lighter (and fresher water) at Stations F21 and F22, which have water depths deeper than about 40m (Figure 3-12). Associated with this was a surface cell of high fluorescence (Figure 3-13), and slightly depleted DIN concentrations (Figure 3-14) relative to surrounding water. At the other three transects, there was very little vertical density gradient in waters deeper than about 30m. Transect 2, the Boston-Nearfield transect, showed the protrusion of lighter (cooler and fresher) coastal water into the center of nearfield (N20P and N16P), underlain with offshore water at depth. The outflow of DIN from Boston Harbor was evident in the striking similarity of  $\sigma_T$  and DIN contours, while fluorescence was relatively uniform across this gradient. It was of interest that fluorescence was highest at the surface of F19. Surface water had much higher temperature and lower salinity at this station and may have been influenced by water coming from the northern transect. However, this definitively was not coastal water, which could be seen mixing only out over the surface to about station N16P.

Transects 3 (Cohasset transect) and 4 (Marshfield transect) showed a nearshore cell of lighter water (Figure 3-12), probably a southward-flowing current, with offshore water not far from the coast. Fluorescence (Figure 3-13) showed a progressive increase along the length of this nearshore cell from stations F23P/F24 (Transect 2) to F14/15 (Transect 3) to F5/F6 (Transect 4). DIN, correspondingly, showed a progressive decrease until concentrations became similar to the offshore concentrations (Figure 3-14).

One other feature needs mentioning. The O<sub>2</sub> titrations at all Biology/Productivity (i.e., "BioProductivity") stations showed supersaturation at surface and deep stations. Vertical profiles from the *in situ* sensor, calibrated against these samples, showed little vertical structuring (Appendix C) and exhibited supersaturated values generally in the range of 11-13 mg O<sub>2</sub> L<sup>-1</sup>. Highest values, > 13 mg O<sub>2</sub> L<sup>-1</sup> were seen in Cape Cod Bay Stations F4, F2P, F1P, and F3, where there were high fluorescence levels and colder waters.

### 3.1.3 Analysis of Water Types

Though the range of most parameters was narrow throughout the breadth and the depth of the Bays, it was possible to distinguish waters with different physical and chemical characteristics. The high resolution hydrographic data, continuously recorded via the BOSS *in situ* sensors from all vertical profile stations (both farfield and nearfield), have been combined in scatter plots (Figure 3-15).

The composite temperature - salinity plot (T-S plot) reveals the main division of water masses was the distinction between shallow coastal stations and more offshore waters. With temperatures less than about 2.8°C, the string of coastal stations along the nearshore, from Boston Harbor southward, had substantially lower salinity (<32.2‰, extending horizontally to the left in the middle of the graph). Note: To examine individual stations in greater detail, see the individual station plots in Appendix C.

A string of points with increasing salinity and temperature, to the upper right of the graph, represent more offshore, deeper stations. The dense body of points centered around 3°C and slightly less than 32.3‰ are from the nearfield region. Thus, one can read this as suggesting that the nearfield at this time was a mixture of coastal and more offshore waters.

Two other distinctive water types can be seen in the T-S plot. In general, Cape Cod Bay stations were cooler and of intermediate salinity, but Station F4 stood out as very distinct from all others and to the lower right space of the T-S plot. This station may have represented, in part, the characteristics of the water mass outside Cape Cod Bay, since this station is the southern hydrodynamic link between the Bays and the open sea. On the other hand, it may represent mostly local cooling, since  $\sigma_T$  values were pretty similar to the entire Cape Cod Bay. The second minor grouping is the Northern transect (F20-F22), which was distinguished by surface waters that were relatively fresh for their temperature, as compared to other Massachusetts Bay offshore water (string stretching to left from the upper right collection of points). Data from this transect suggests a slightly different surface water mass existed at the northern point of the hydrodynamic link between the Bays and the open sea.

Using the high resolution data, there was a linear relation between beam attenuation and salinity (Figure 3-15), with station F4 abnormal and above the main body of points. Highest attenuation was seen in lower salinity coastal waters, with gradual decline towards higher salinity (clearer offshore waters). Cape Cod Bay Stations, as a group, had higher attenuation than others at similar intermediate salinity levels. This higher attenuation was clearly a function of higher plankton biomass levels; looking only at the Cape Cod Stations, a roughly linear relation was apparent for these two parameters. There was also, however, a general relation between fluorescence and salinity (Figure 3-15). Over the region as a whole, the relation between beam attenuation and fluorescence was complex because of absorbance due to plankton, inorganic suspended particles, and dissolved organic matter. These factors all complicate the attenuation-fluorescence relation at the coastal margin where water emerges from inshore harbors and estuaries. Stations around the mouth of Boston Harbor (F23P and F25, for example) had high beam attenuation for their fluorescence. The wet chemistry on discrete samples revealed that these stations had relatively low chlorophyll, but high total suspended solids, high dissolved organic carbon (DOC) and dissolved organic nitrogen (DON) concentrations.

To assess the geochemical variations among water types grouped by location and characterized by physical parameters (Table 3-1 and Figure 3-16), the monitoring program relies on discrete bottle sampling and the physical parameters associated with each bottle sample (full data, Appendix A). While not as rich in data points as Figure 3-15, dissolved inorganic nutrient data were still extensive. A standard geochemical convention is to examine nutrient concentrations relative to each other, as well as to examine chemical distributions as a function of salinity or water density. In this case, plots of concentration vs. salinity or density are not true mixing diagrams because there are more than two potential endmembers, or sources, being mixed at many stations. Nonetheless, very strong patterns emerged that revealed much about the water types in the Bays.

To begin, using data from all stations and depths (Appendix A) there was a strong relation between DIN and  $\text{PO}_4$  (Figure 3-17). With few exceptions, the data lay between isopleths that indicate N/P ratios of 8:1 to 16:1. Stations from around Boston Harbor (in the coastal group) were highest in both nutrients, but tended to be slightly more enriched in N than P, and thus closer to a 16:1 N/P ratio. Cape Cod Bay Stations were low in nutrients and tended to have N/P ratios closer to 8:1. Mostly intermediate in concentration and N/P ratio were samples from the nearfield group and offshore group. The Northern transect stations (F20-F22), were low to intermediate in these nutrients, the lower values being from the upper 20m of the water column (see Figure 3-14).

Using only  $\text{NO}_3$ , rather than DIN, a slightly different pattern is seen. Boston Harbor stations still had among the highest N concentrations, but a few fell more to the right because they had a high fraction of DIN as  $\text{NH}_4$ . Except for this difference, and the fact that the  $\text{NO}_3/\text{PO}_4$  ratio was slightly less than the DIN/ $\text{PO}_4$  ratio, the trend among groups was about the same.

The absolute values of nitrogen and phosphate, as well as subtle shifts in their relative concentrations thus provide an additional biogeochemical descriptor of water types in different geographic regions. Examination of nitrogen forms relative to silicate ( $\text{SiO}_4$ ), however, provided a more striking biogeochemical distinction between inshore and offshore waters (Figure 3-18). Considering either DIN or  $\text{NO}_3$ , it was apparent that offshore stations as well as those of Northern transect had more silicate per atom of nitrogen. The ratio of N/Si was on the order of 1:1 for these offshore waters throughout the water column, somewhat less in surface waters. In contrast, Boston Harbor area stations were relatively enriched with nitrogen and had an N/Si ratio on the order of 2:1. The nearfield appeared intermediate again, and Cape Cod Bay was low in both N and Si, due to high diatom levels there.

Examination of nutrients relative to salinity or  $\sigma_T$  (Figures 3-19 to 3-24) revealed a picture of mixing from the Boston Harbor area to the nearfield, where mixing with surface offshore waters was also apparent. Cape Cod Bay appeared low in nutrients (relative to similar salinity observed at stations in

the nearfield). The Northern transect appeared similar to offshore water, and both had some similarity to the nearfield. For DIN and PO<sub>4</sub>, the plots show a descending arm of concentration with increasing salinity to the approximately 32.2‰ characteristic of the Nearfield. Concurrently, there was an ascending arm of nutrient concentration with higher salinity (offshore waters) above the 32.2‰ level. For these offshore waters, there was a pattern of increasing concentration and salinity with depth. The deep-water intrusion of nutrients to the nearfield is considered below.

For NH<sub>4</sub> (Figure 3-20), with the strong Harbor signal, there was a sharp descending arm from the left (lower salinity). However, with the low offshore deep source, there was no real ascending arm of higher NH<sub>4</sub> with higher salinity. Silicate (Figure 3-22) showed the opposite trend of NH<sub>4</sub>. There was a strong *deep* offshore source of higher SiO<sub>4</sub>/higher salinity leading towards the nearfield, with very slight enrichment from the Harbor as shown by the small difference in SiO<sub>4</sub> within the range 31-32‰. *Surface* waters of the offshore (e.g., Figure 3-10) were similar to the nearshore.

Examining combined nitrogen fractions (Figures 3-23 and 3-24) from station data, showed a sharp gradient of mixing that corresponds with salinity changes from the Harbor to the nearfield. Again, Cape Cod Bay had the lowest concentrations. DIN+PON has been a useful measure in assessing the gradient of nitrogen from Boston Harbor (Kelly, 1991), but the data in this report also allow examination of all dissolved and particulate forms of N ("Total N") (Figure 3-24). Total N exhibited a most striking linear relation with salinity, implying almost conservative mixing out to the nearfield as well as along the coast to station F13P. Since total nitrogen encompasses the nitrogen incorporated into the tissue plankton, it is not responsive to uptake or conversion between nitrogen forms and species. The linear relation in Figure 3-24 therefore suggests little sinking loss as the Harbor water advects and mixes into the Bay.

In summary, a rough classification of the heterogeneities in waters of the Massachusetts and Cape Cod Bays is provided in Table 3-1, based on observations from this first survey. It was interesting that nutrients and fluorescence showed a greater absolute dynamic range, but physical characteristics were nevertheless also very powerful at identifying and classifying large-scale and fine-scale features.

#### 3.1.4 Distribution of Chlorophyll and Phytoplankton

*In situ* fluorescence measurements indicated that the highest chlorophyll levels were in Cape Cod Bay and also extended from the northeast corner of the nearfield to the North. Correspondingly, the chlorophyll in these same regions had the highest concentrations (measured by standard filter-extraction) of all the BioProductivity stations that were sampled. These stations included F1P (> 8 µg

L<sup>-1</sup>) and F2P (>4.5 µg L<sup>-1</sup>) in Cape Cod Bay, and N4P (>6 µg L<sup>-1</sup>) in Massachusetts Bay (Figure 3-25).

Other stations had chlorophyll values in the range of 1.0 µg L<sup>-1</sup> (N1P surface) to about 3.5 µg L<sup>-1</sup> (F13P surface), most being about 2-2.5 µg L<sup>-1</sup>. There was only minor variation between surface and deeper (~9-15m) chlorophyll concentrations (Figure 3-26) at the stations measured.

Total phytoplankton abundances were distributed roughly the same as chlorophyll (Figure 3-27). Stations F1P, F2P and N4P had high surface counts, above 10<sup>6</sup> cells L<sup>-1</sup> (Figure 3-28). One other station (N20P) exceeded 10<sup>6</sup> cells L<sup>-1</sup>, the rest were in a small range of about 0.5 to 0.9 × 10<sup>5</sup> cells L<sup>-1</sup>. Surface and deeper samples at each station were similar in total abundance (see Appendix I), as well as numbers of dominant species (Figures 3-29, 3-30, 3-31, and 3-32), reflecting the generally well-mixed nature of the water column at all stations.

With respect to the composition of the phytoplankton community, the stations were remarkably similar. Where higher chlorophyll was observed, diatoms were greater than 75% of the cells, but diatoms were always the major component (Figure 3-28). Microflagellates numerically were the second most important component. Dinoflagellates were rare.

The expected diatom species typical of northeastern coastal waters in winter-spring were present. There were few, if any, regional distinctions in species composition (Table 3-2). *Thalassiosira nordenskioldii* was among the dominants at all ten BioProductivity stations and was the top species at both F1P (Cape Cod Bay) and F23P (Boston Harbor mouth) as well as N4P (Massachusetts Bay). A relatively small number of species constituted the list of dominants at all stations. There were appearances of minor species at some stations that may relate to observed physical-chemical differences and water types, and these may be examined further as indicator species. However, overall the biology of the whole field did not appear very sensitive, in an ecologically significant fashion, to these relatively subtle features.

### 3.1.5 Distribution of Zooplankton

Total abundance of zooplankton measured at the ten BioProductivity stations varied only by a factor of about two and variations did not reflect the highs and lows of chlorophyll/phytoplankton abundance. In general, copepod adults and copepodites were a major fraction of the community (Figure 3-33). The only regional distinction of note was the finding of high barnacle nauplii at shallower nearshore stations in Massachusetts Bay outside of Boston Harbor (F23P, F13P, N10P, N1P).

Two smaller (<1mm in length) copepod species dominated the whole region, *Oithona similis* and *Paracalanus parvus*. In general, the minor cast of copepod species (~4 to 8 taxa) showed no distinct regional distribution. Perhaps the only subtle distinction related to water type was the presence of relatively high *Oikopleura*, possibly a more "oceanic" indicator species, at the eastern edge of the nearfield. In general, the composition everywhere suggests the typical assemblage of shelf species/taxa expected at this time of year.

### 3.1.6 Whole-Water Metabolism Incubations

The data generated from 6-hr light bottle incubations consistently showed that net production rates rose very sharply as a function of increasing irradiance, then reached a plateau. In some cases, net production may have decreased slightly at the highest irradiance levels used (> 1500  $\mu\text{E m}^{-2} \text{sec}^{-1}$ ). Nearly all cases suggested the approximate plateau, or light-saturation level where maximum net production rates ( $P_{\text{max}}$ ) were reached, occurred at an irradiance level below 250  $\mu\text{E m}^{-2} \text{sec}^{-1}$ ; many were in the range of 100-250  $\mu\text{E m}^{-2} \text{sec}^{-1}$ .  $P_{\text{max}}$ , as estimated directly from the plots at most stations, was in the range of about 10-40  $\mu\text{g O}_2 (\mu\text{g Chlorophyll})^{-1} \text{hr}^{-1}$ . Expressed as a whole-water rate, rather than  $P_{\text{max}}$  normalized to chlorophyll, the graphical estimate of  $P_{\text{max}}$  was roughly in the range of 20-140  $\mu\text{g O}_2 \text{L}^{-1} \text{hr}^{-1}$  (see Appendix G). Not surprisingly, the maximum light-saturated net production rates on a per volume basis were highest at stations F1P and N4P, where both chlorophyll levels and phytoplankton cell counts were very high. Variability is discussed further in Section 5.3.4.

An example plot for Station N4P (Figure 3-34) shows a case where the data were reasonably well described by a rectilinear hyperbola, the model chosen (see Section 2). In this case, the surface and deeper chlorophyll maximum water samples had highly similar P-I curves. With some variance, most stations had fairly similar results for surface and deep samples, and certainly no strong depth-related pattern was evident. Data from some stations could not all be fit with the model (see Appendix G). Other stations gave reasonable statistical fits, but provided parameters that were not sensible and did not adequately model the data. While in general  $P_{\text{max}}$  could be reasonably estimated by eye from the graphs, the initial slope ( $\alpha$ ) was too sharp to be estimated with confidence (see, however, the model fits in Appendix G).

Measured light readings showed that attenuation of Photosynthetically Active Radiation (PAR) varied somewhat across stations, and the approximate level of 1% (of surface incident) light ranged from about 10 m to >25 m (see Appendix G for all station data). Figure 3-35 shows examples of light attenuation for three stations. The slopes of the lines in Figure 3-35 offer a valid comparison between stations. The slope is the estimate of the extinction coefficient, K, from  $I_z = I_0 e^{-Kz}$  where the subscript z denotes the *in situ* reading at depth z and the subscript o denotes incident irradiance. During the

survey, the sky was mostly cloudy. Actual *in situ* readings of irradiance at 1 m were less than  $500 \mu\text{E m}^{-2} \text{sec}^{-1}$  and more usually in the range of about  $40\text{-}200 \mu\text{E m}^{-2} \text{sec}^{-1}$ . Using even the highest (clearest sky) incident irradiance observed one day near noon ( $\sim 1125 \mu\text{E m}^{-2} \text{sec}^{-1}$ ), irradiance within the first few ( $\sim 3\text{-}5$ ) meters of the surface would have decreased to a level marginal for maintaining  $P_{\text{max}}$  (i.e.,  $\leq 200 \mu\text{E m}^{-2} \text{sec}^{-1}$ ) using the P-I curves generated (e.g. Figure 3-34).

Thus, the P-I and *in situ* light field data seem to suggest that at this time of year, several clear sunny days in a row may initiate a phytoplankton growth, but on a cloudy day the entire water column may be strongly limited by light, rather than nutrients. In later discussion (Section 5), we will provide a rough calculation of daytime net production using February data.

In addition to light bottles, dark incubations were performed in an effort to measure dark respiration. In general, the rates were too low to be of statistical significance (Appendix G), and respiration could not be estimated with a 6-hr incubation.

## 3.2 Nearfield Surveys Results

### 3.2.1 Horizontal Distribution of Water Properties

The spatial distribution of nutrients at the surface of the 21 stations sampled on the first day of the nearfield cruise is shown in Figure 3-36. The patterns differ from the images generated on the basis of the preceding farfield sampling, which included only 6 BioProductivity stations (see Figures 3-6 through 3-10).

Due to the higher density of samples, the resolution is greater, the variability is also higher and some differences relative to the farfield cruise sampling were implied. Some differences were not simply a function of the change in scale of resolution, discussed below; rather they appeared to be real due to physical dynamics that caused temporal change within the nearfield in a matter of a day or less. Nevertheless, many gross features were the same, including higher values of DIN and  $\text{PO}_4$  at the northwest, southwest, and southeast corners of the grid and the lowest concentration of all nutrients were seen in the northeast corner.

A summary three-dimensional perspective is provided, using salinity data collected at the same time as the nutrient data, in Figure 3-37. This plot suggests impingement of fresher water from a coastal water mass spreading from mid depth to the surface in the southeast corner—the edge of an otherwise

fairly homogeneous, saline cube. This perspective can be contrasted with that provided in the next section, for which sampling occurred the following day.

### 3.2.2 Water Properties Along Vertical Transects

Towing was conducted along the outer track of the nearfield grid, with approximately 6-8 tow-yo oscillations between each nearfield station. The section profiles produced from towing are given in Appendix D. Examples of  $\sigma_T$  and fluorescence are given in Figures 3-38, 3-39, 3-40, and 3-41, respectively. North-south and east-west tracks are paired to give two views of the field. Many features are evident in these graphics, such as: (1) the density contours similar to those evident from the day before (Figure 3-37) that again emerge at the surface between N10 and N9 (South Track), (2) the lighter water, probably from the northern source, just impinging on the northeast edge of the nearfield at N4 (East and North Tracks), and (3) a surface lens of lighter water, likely from Boston Harbor, resting between N11 and N12 (West Track). With respect to chlorophyll, the towing captured a high chlorophyll feature that apparently had progressed from the North/Northeast along the North Track since the course of farfield/nearfield sampling (compare Figure 3-40 and 3-41 to surface contours in Figure 3-5). Chlorophyll was still high at N4P, as it had been several days before, and the surface wave of chlorophyll following the density contours along the East Track is striking. The northwest corner of the field (North and West Tracks) with high  $\sigma_T$ , had high chlorophyll also, whereas the two intrusions of lighter coastal waters on the West Track had lower chlorophyll. Thus, the striking feature is the development of a chlorophyll bloom from the offshore in, which confirms the gross pattern and portrays the short-term dynamics implied from the farfield cruise results.

### 3.2.3 Comparison of Vertical and Towed Profiling

Figure 3-42 provides an example of high-resolution data from the tow-yo profiling as the ship was underway along the outer east track of the nearfield from Station N4P to Station N7P. The track of the towfish can be seen dropping nearly vertically to depth, then rising to the surface; each drop forms a V-pattern. Compared to this, is the image one would obtain having used only the vertical downcast portion at each of the four designated nearfield stations. The difference was that subtle gradient features were lost, in this case being primarily the gradual sloping of temperature isopleths towards the surface at N7P, but also some contours appeared horizontal (e.g., midwater of N6) when the more accurate depiction was a wedge shape. Contouring can be done following different algorithms, some which may be less sensitive to the feature seen here. Clearly, the tows, because they provide ~5 times the resolution of the casts, provide a more realistic image of existing conditions along a section and have less tendency to exaggerate or miss small-scale flatness. At issue



is the difficulty of contouring when the distance between points in the x- and y- directions is disproportionate. Nonetheless, the confidence one has in defining smaller-scale features is vastly improved by having the higher-resolution towing data.

#### **3.2.4 Analysis of Small-Scale Variability**

Three corner stations of the nearfield were visited three times during the course of the February cruise. These visits provided data to examine short-term variability at fixed points. Displayed as  $\sigma_T$  changes as a function of time, it is illustrated that points within the region can indeed be dynamic (Figure 3-43). Station N10P was least variable at the surface but had some incursion of higher density water near bottom on the second sampling day (26 Feb 92). This could be a bottom water tidal oscillation, but we have not examined differences in the stage of tide to assess this. In contrast, Stations N1P and N7P both experienced passage of lighter surface water. N1P had a progressive decreasing density top-to-bottom. These density changes are very small, but indicate some of the dynamic motion in the nearfield area. N7P had a lighter surface water layer ( $\sim 0$  to 20 m) recorded on the second sampling day (26 Feb 92), coupled with slightly higher salinity bottom water. By the third sampling (27 Feb 92), the profile was almost uniform with  $\sigma_T \geq 25.7$ , suggesting offshore water was now at this station.

#### **3.2.5 Analysis of Water Types and Biological Properties**

The dynamic shown for Station N1P in Figure 3-44 may suggest the passage of a front. As the density progression occurred, the chlorophyll went from near zero to almost  $6 \mu\text{g L}^{-1}$ , as estimated by the fluorometer, from about noon on 25 February to 0820 on 26 February. On the 26th, the chlorophyll profile had a mid-depth maximum near the weak pycnocline evident in Figure 3-43, and decreased sharply below about 10 m to less than  $3 \mu\text{g L}^{-1}$ . The chlorophyll persisted on the 27th (the tow-yo day) when this corner of the nearfield had chlorophyll  $>4 \mu\text{g L}^{-1}$  to a depth of 25 m (see Section 3.2.2).

The sampling strategy of repeated visits to the corner stations of the nearfield provide an ability to describe some dynamic features of ecological interest to the monitoring program, and that were, in this case, detected when changes in physical characteristics occurred over a very small range (i.e., such as  $\sigma_T$  going from 25.69 to 25.57).

**TABLE 3-1. ANALYSIS OF WATER TYPES**

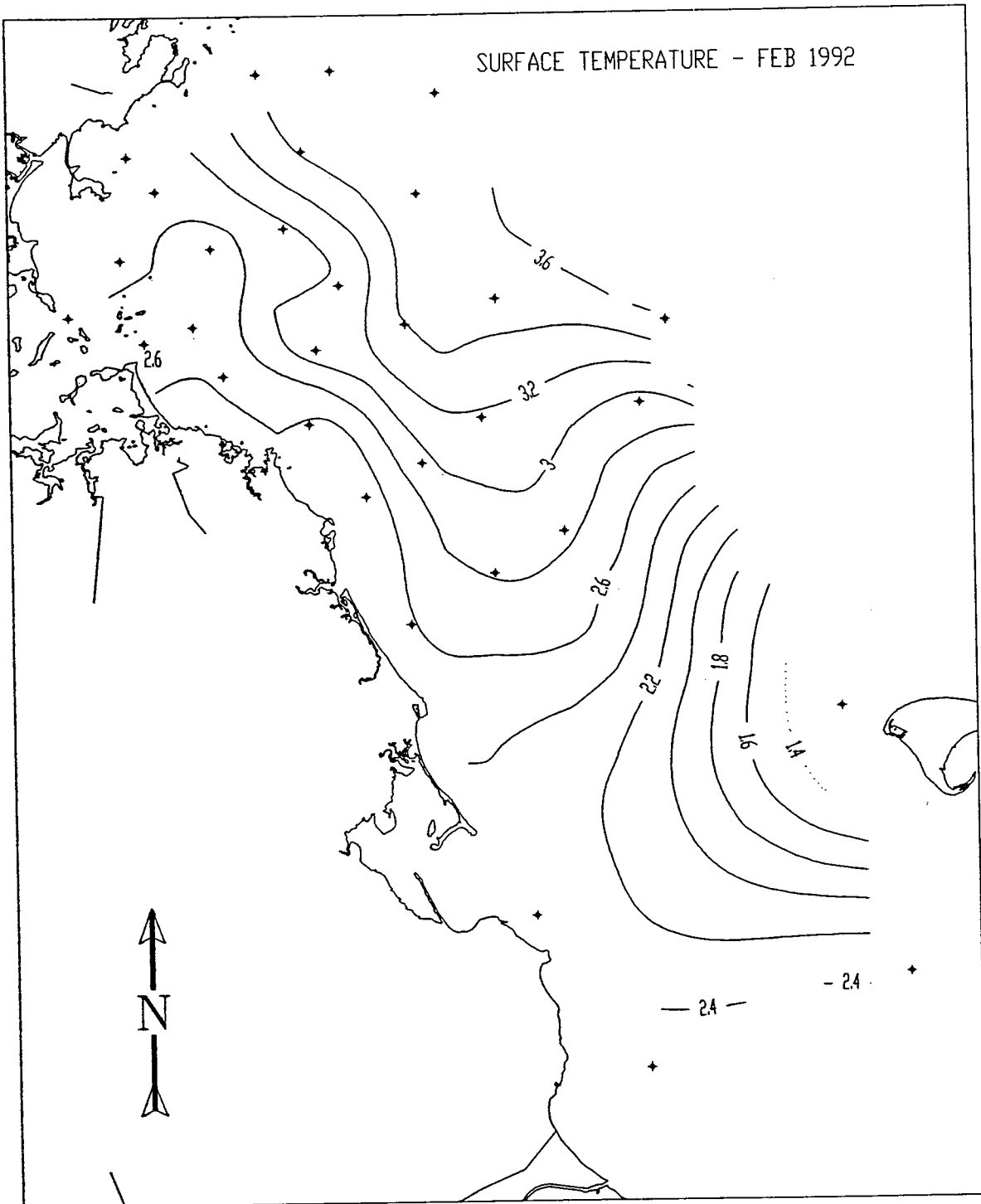
Water Type		Characteristics by Parameter					
		Geographic Descriptor	T	S	Beam Attenuation	Chlorophyll Fluorescence	Nutrients
Coastal	Most of Nearshore Mass. Bay (~ less than 30m)	Cold	Freshest	High	Mixed, Intermediate	All High	
Northern Transect	Transect along Northern entrance to Mass. Bay (F20-F22)	Warm	Intermediate saline to intermediate fresh	Low	High	Intermediate	
Nearfield	Within Nearfield Sampling Grid	Inter-mediate	Intermediate	Intermediate	Mixed	Mixed	
Offshore	Mainstem Mass. Bay (~ greater than 40m)	Warm	Most saline	Low	Low	Intermediate, but high SiO <sub>4</sub> deep	
Cape Cod A	Body of Cape Cod Bay	Colder	Intermediate fresh	High	High	Low	
Cape Cod B	Tip of Cape Cod, Station F04	Very cold	Intermediate	Very High	Very High	Low	

TABLE 3-2. TOP 5 DOMINANT PHYTOPLANKTON TAXA, EXCLUDING MICROFLAGELLATES AND CRYPTOMONADS, IN NEAR SURFACE SAMPLES COLLECTED IN FEBRUARY, 1992

Species	Station												
	F1P	F2P	F13P	F23P	N1P	N10P	N20P	N16P	N7P	N4P			
<i>Skeletonema costatum</i>	(3) 0.194	(1) 0.318	(4) 0.046		(2) 0.062								
<i>Leptocylindricus minimus</i>		(1) 0.318											
<i>Chaetoceros debilis</i>	(2) 0.267	(3) 0.256				(2) 0.060	(3) 0.109	(5) 0.031	(4) 0.039		(4) 0.087		
<i>Thalassiosira nordenskioldii</i>	(1) 0.289	(4) 0.226	(2) 0.063	(1) 0.105	(3) 0.053	(3) 0.051	(5) 0.060	(5) 0.031	(3) 0.053		(1) 0.235		
<i>Thalassionema nitzschoides</i>		(5) 0.154	(3) 0.051		(1) 0.075	(1) 0.090		(1) 0.155	(2) 0.077		(5) 0.059		
<i>Detonula confervacea</i>	(4) 0.163						(2) 0.143						
<i>Chaetoceros</i> spp.	(5) 0.118			(4) 0.029		(3) 0.051		(3) 0.040					
<i>Thalassiosira gravida</i>			(4) 0.046	(3) 0.038					(5) 0.030		(3) 0.090		
<i>Chaetoceros socialis</i>			(1) 0.094	(1) 0.105	(5) 0.025	(5) 0.047	(1) 0.188	(2) 0.043	(1) 0.083		(2) 0.138		
<i>Chaetoceros compressus</i>									(5) 0.030				
<i>Rhizosolenia delicatula</i>								(4) 0.034					
<i>Thalassiosira</i> spp.							(4) 0.071						
<i>Nitzschia closterium</i>					(4) 0.028								
<i>Coscinodiscus excentricus</i>				(5) 0.023									

( ) = rank

Number = millions of cells L<sup>-1</sup>



**Figure 3-1** Surface temperature ( $^{\circ}\text{C}$ ) in the region in February 1992. Data are from Appendix A, the surfacemost sample at all farfield survey stations, including the BioProductivity stations within the nearfield grid. The contour interval is  $0.2^{\circ}\text{C}$ . The dotted contour line (F4, Cape Cod) indicates the value was different and contours should be regarded with caution (see text).

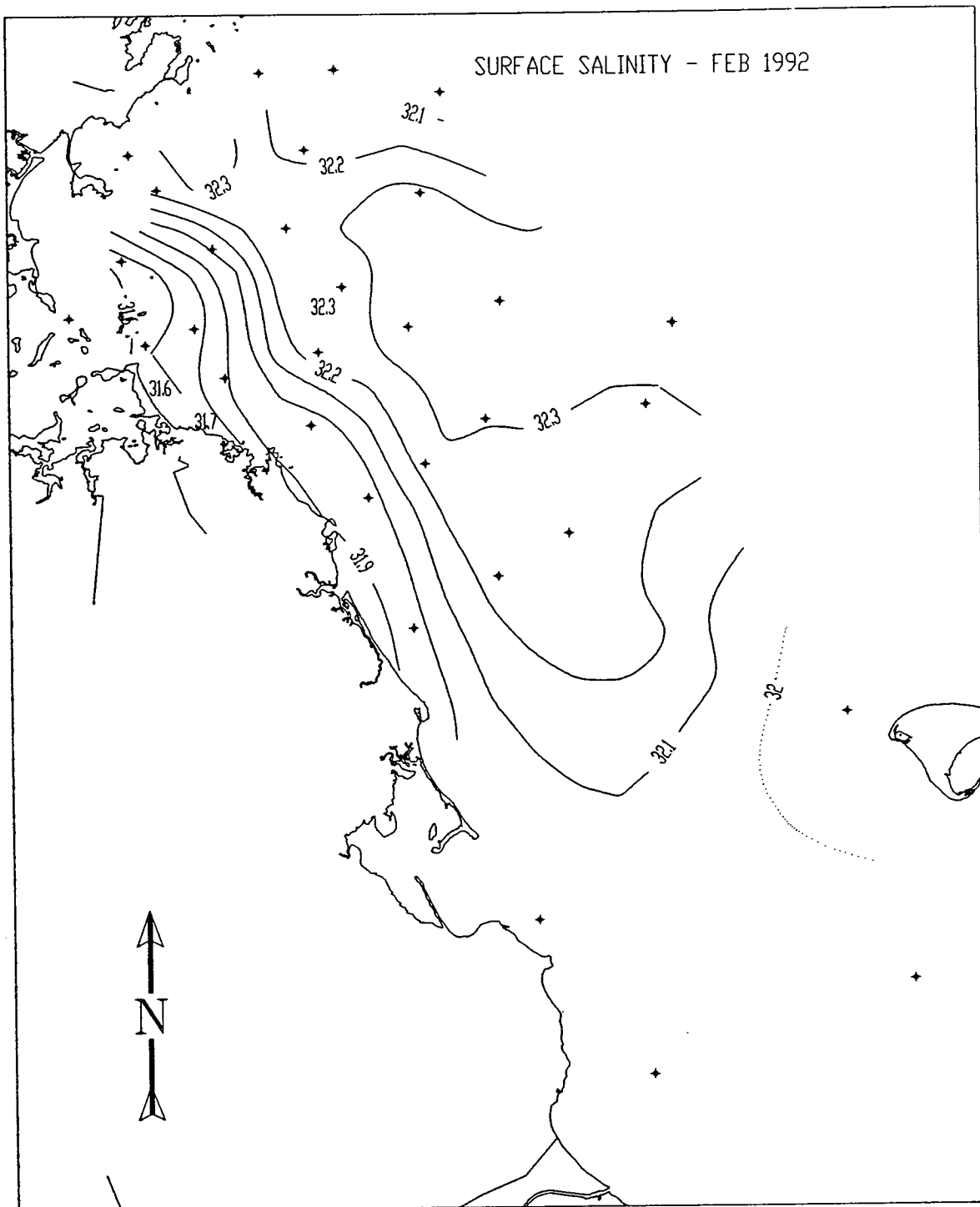


**Figure 3.2** Surface salinity (PSU) in the region in February 1992. Data are from Appendix A, the surfacemost sample at all farfield survey stations, including the BioProductivity stations within the nearfield grid. The contour interval is 0.1 PSU. The dotted contour line (F4, Cape Cod) indicates the value was different and contours should be regarded with caution (see text).

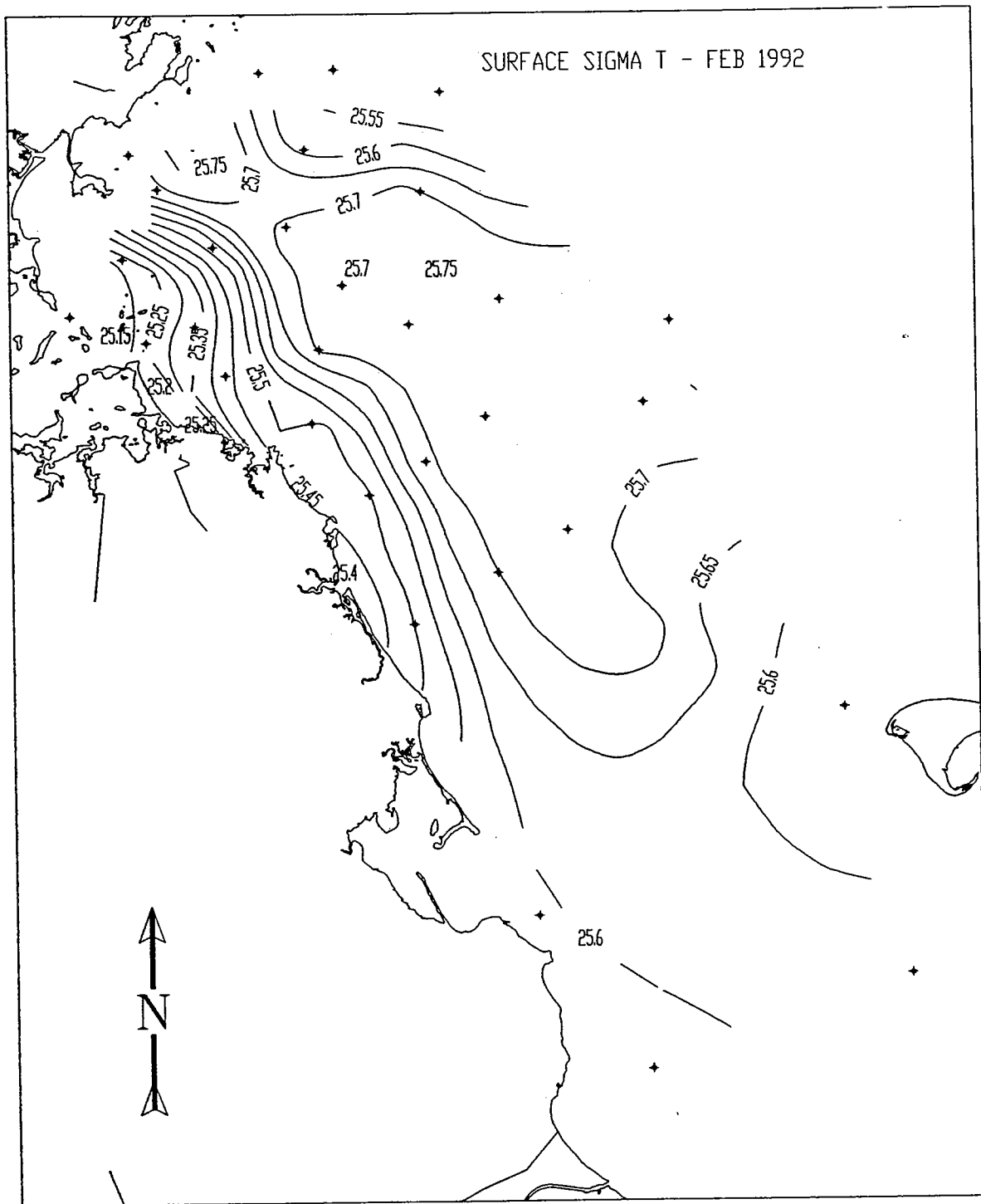


**Figure 3-3** Surface  $\sigma_T$  in the region in February 1992. Data are from Appendix A, the surfacemost sample at all Farfield survey stations, including the BioProductivity stations within the nearfield grid. The contour interval is 0.05 units.

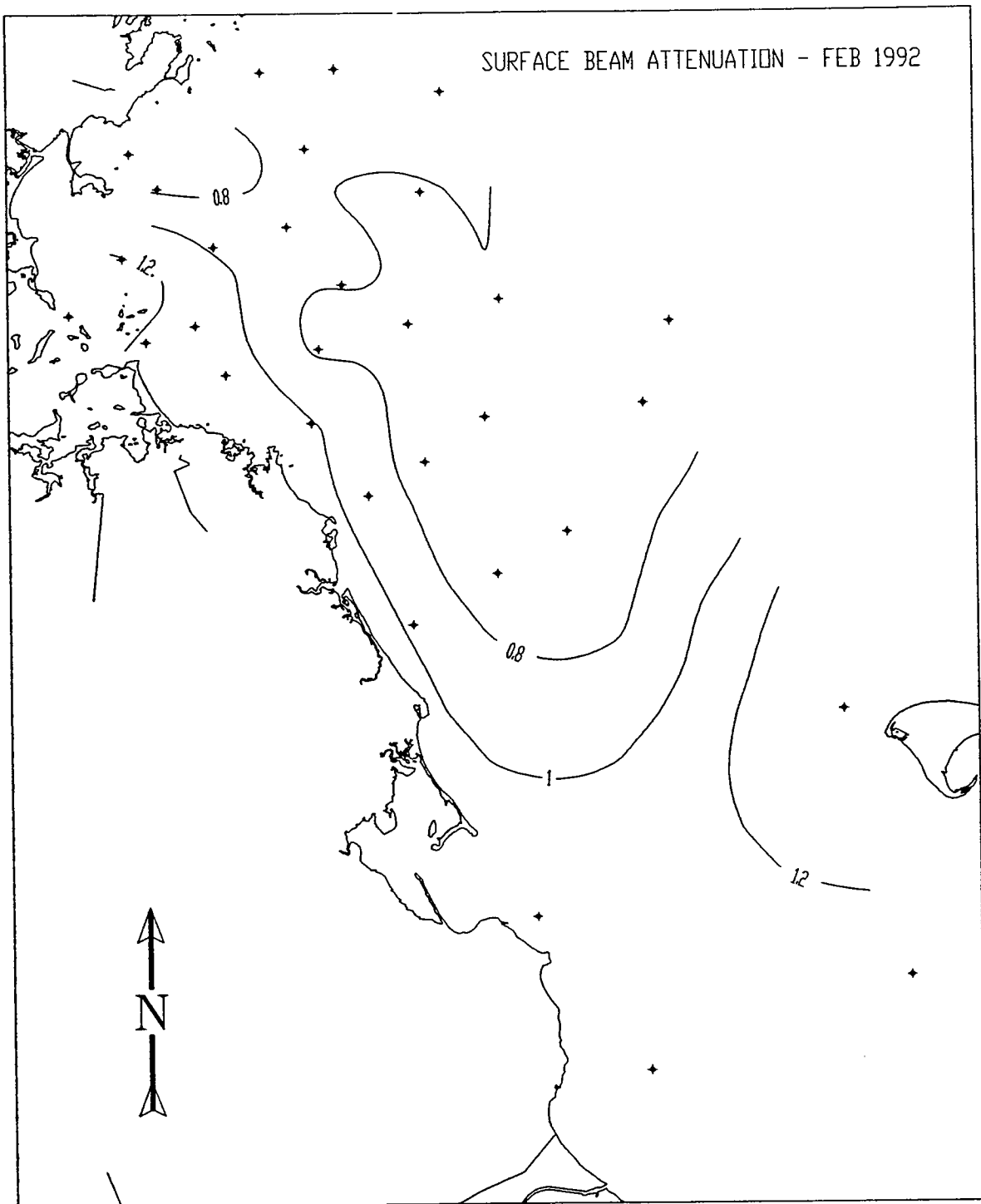


**Figure 3-4** Surface beam attenuation ( $m^{-1}$ ) in the region in February 1992. Data are from Appendix A, the surfacemost sample at all farfield survey stations, including the BioProductivity stations within the nearfield grid. The contour interval is  $0.2 m^{-1}$ .

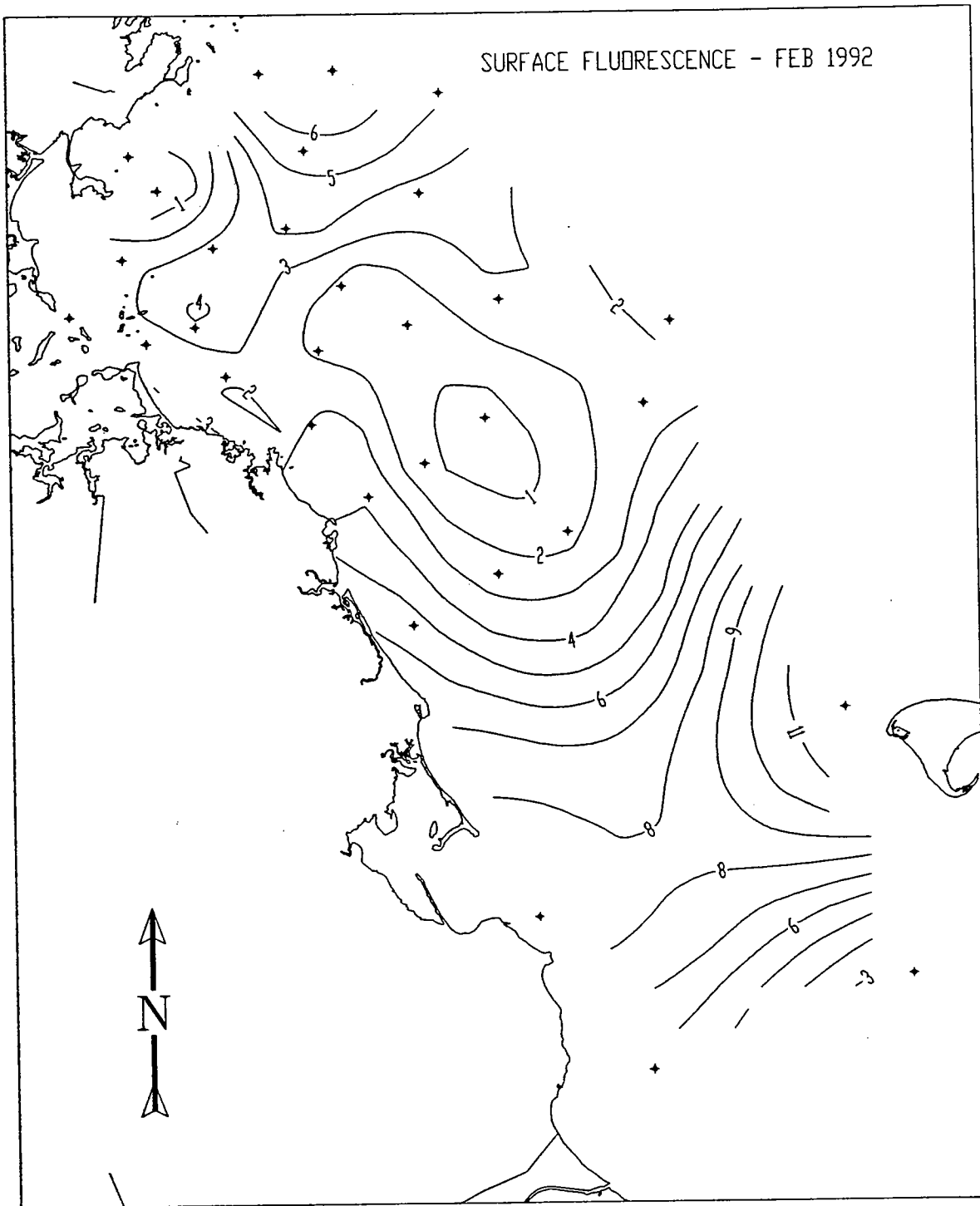


**Figure 3-5** Surface *in situ* fluorescence (as  $\mu\text{g Chl L}^{-1}$ ) in the region in February 1992. Data are from Appendix A, the surfacemost sample at all farfield stations, including the BioProductivity stations within the nearfield grid. The contour interval is  $1.0 \mu\text{g L}^{-1}$ .



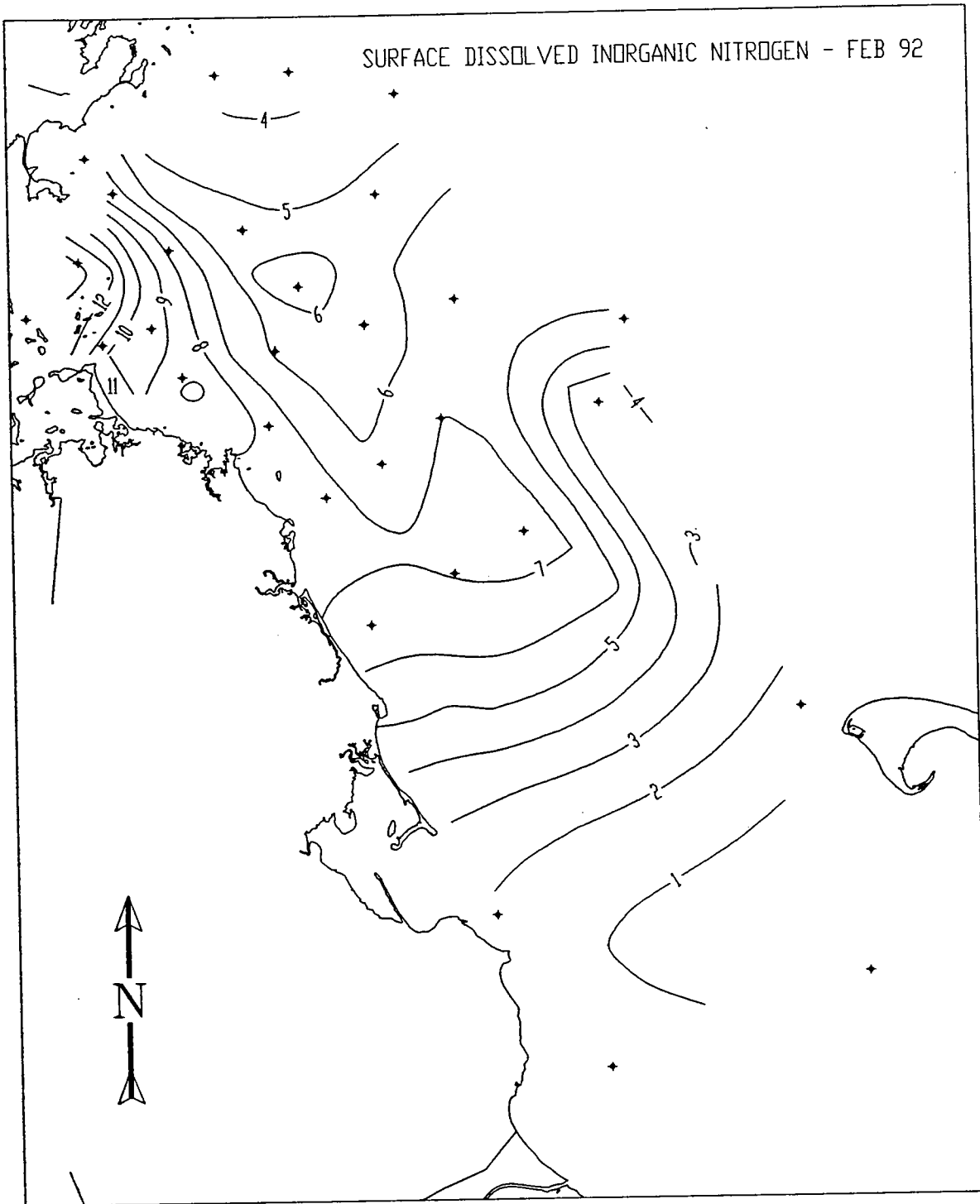


**Figure 3-6** Surface dissolved inorganic nitrogen (DIN,  $\mu\text{M}$ ) in the region in February 1992. Data are from Appendix A, the surfacemost sample at all farfield survey stations, including the BioProductivity stations within the nearfield grid. The contour interval is 1.0  $\mu\text{M}$ .

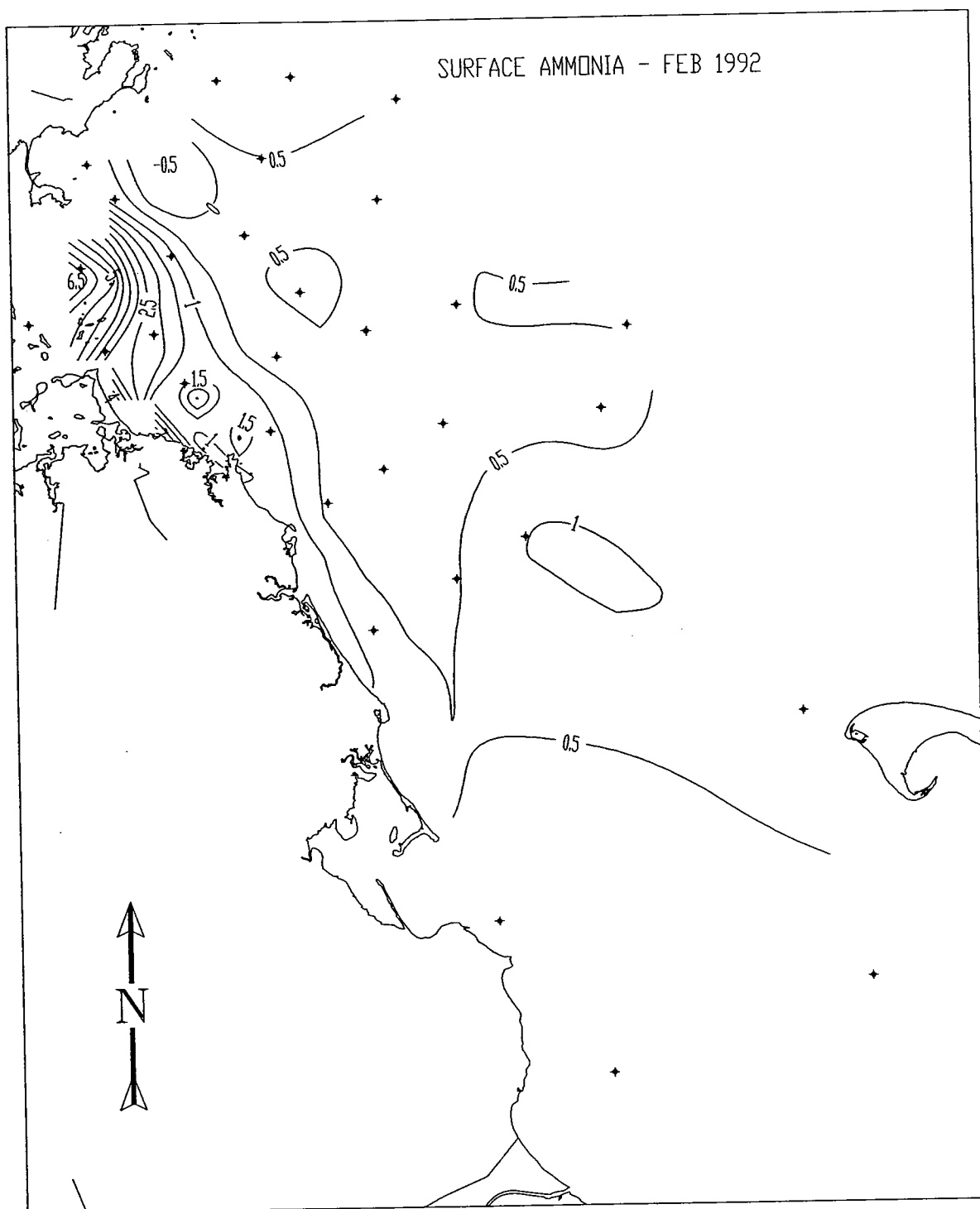


**Figure 3-7** Surface ammonia ( $\mu\text{M}$ ) in the region in February 1992. Data are from Appendix A, the surfacemost sample at all farfield survey stations, including the BioProductivity stations within the nearfield grid. The contour interval is 0.5  $\mu\text{M}$ .

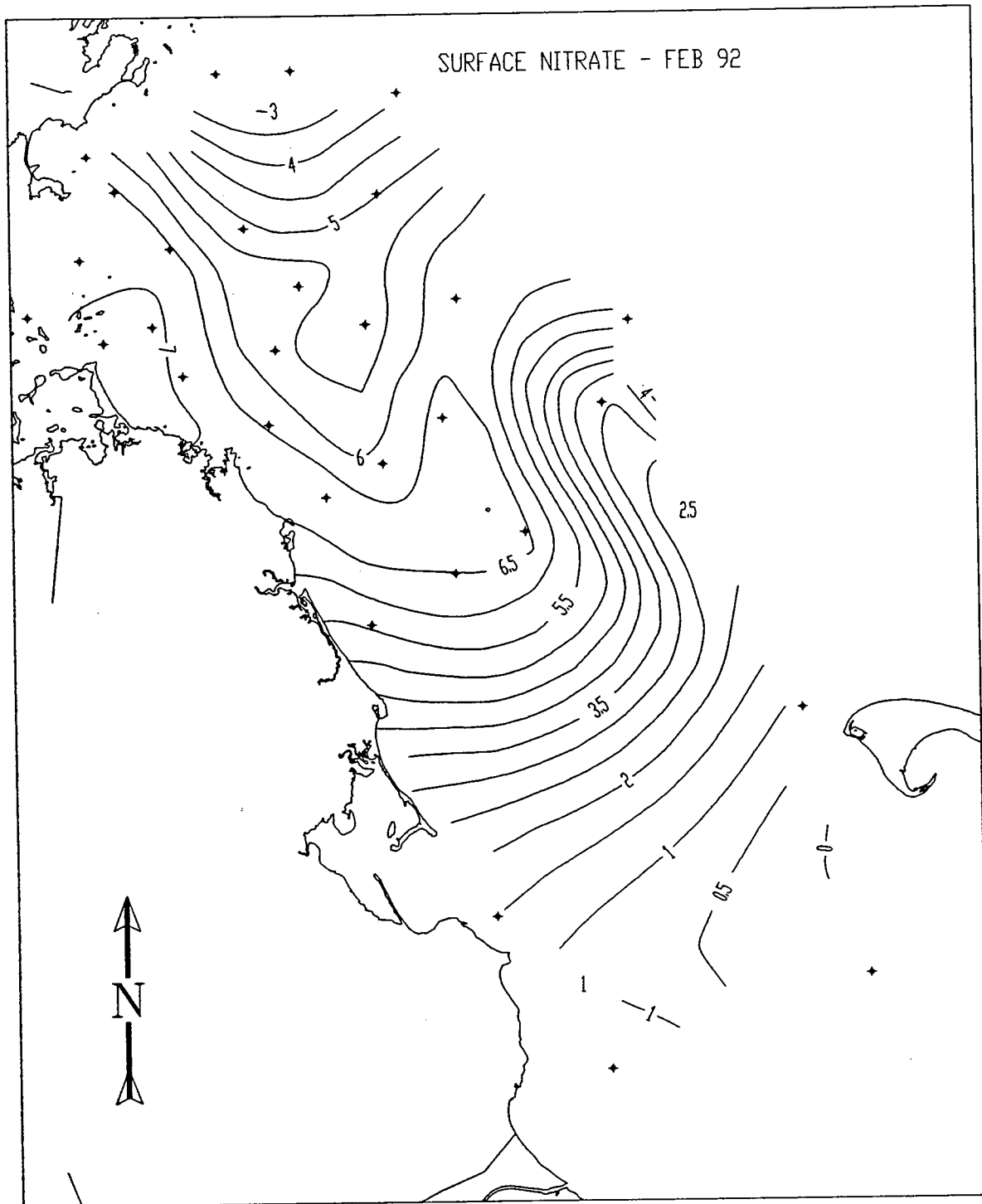


**Figure 3-8** Surface nitrate ( $\mu\text{M}$ ) in the region in February 1992. Data are from Appendix A, the surfacemost sample at all farfield survey stations, including the BioProductivity stations within the nearfield grid. The contour interval is 0.5  $\mu\text{M}$ .

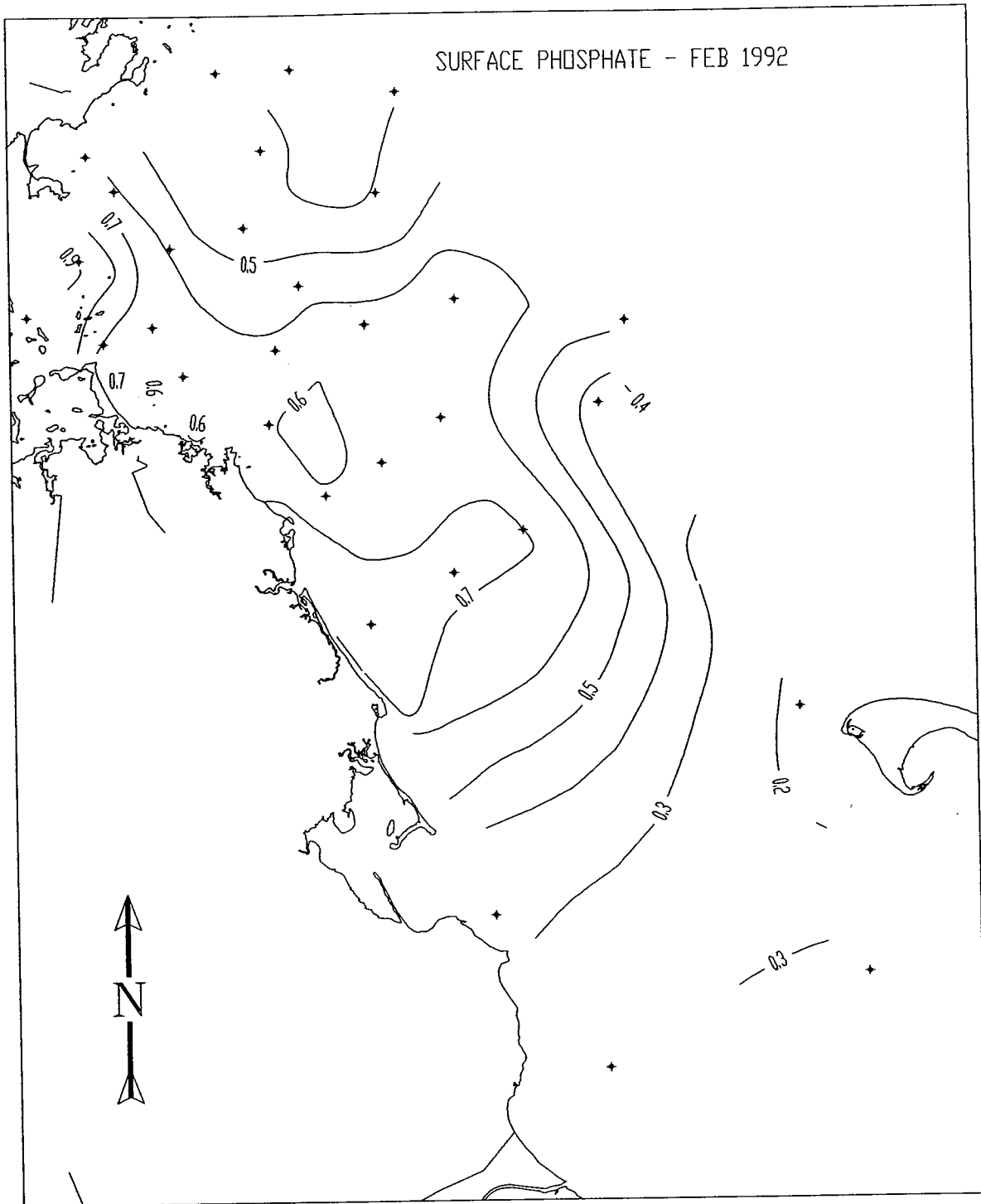


**Figure 3-9** Surface phosphate ( $\mu\text{M}$ ) in the region in February 1992. Data are from Appendix A, the surfacemost sample at all farfield stations, including the BioProductivity stations within the nearfield grid. The contour interval is 0.1  $\mu\text{M}$ .

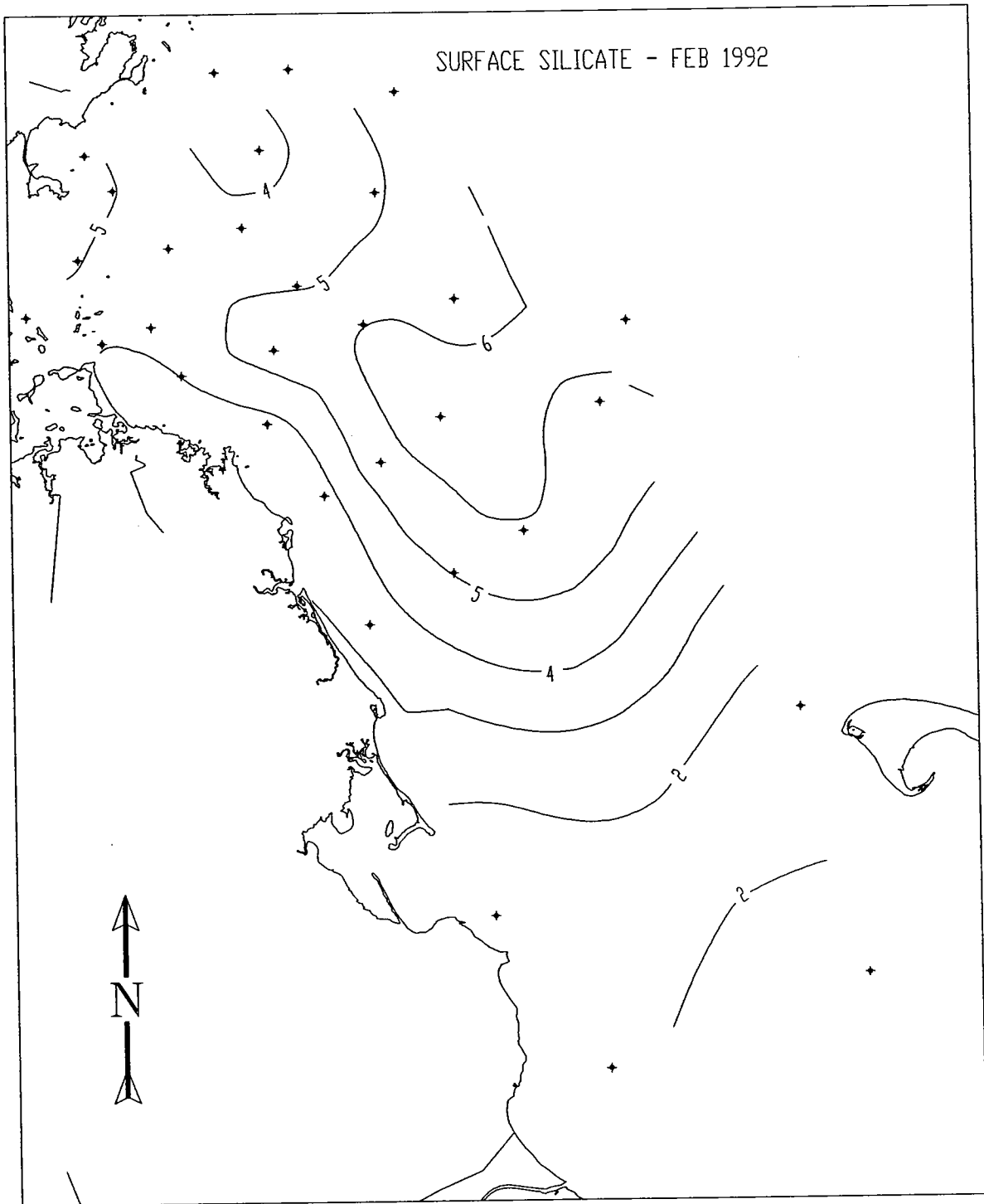


**Figure 3-10** Surface silicate ( $\mu\text{M}$ ) in the region in February 1992. Data are from Appendix A, the surfacemost sample at all farfield stations, including the BioProductivity stations within the nearfield grid. The contour interval is 1.0  $\mu\text{M}$ .

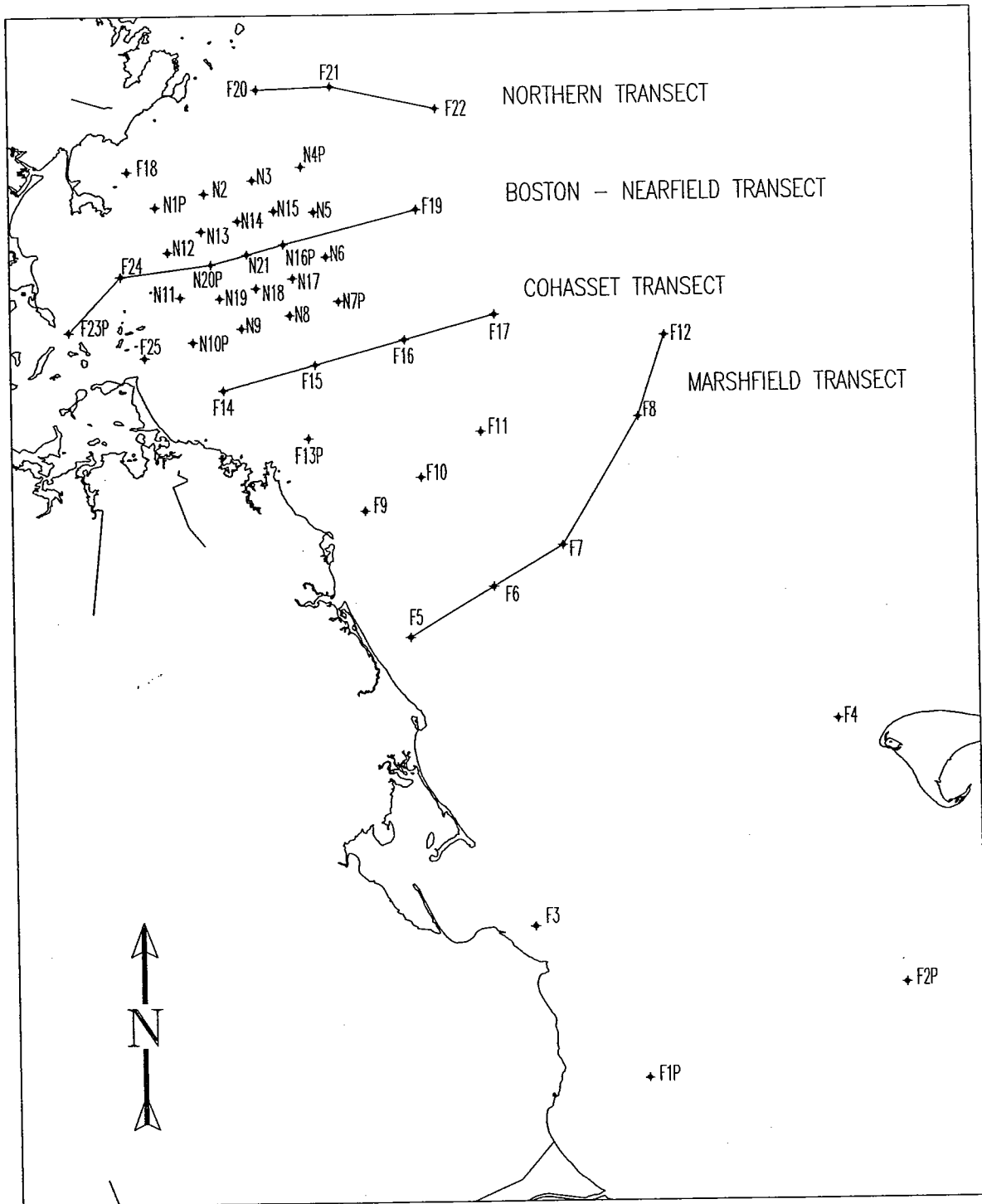


**Figure 3-11** Map showing position of four standard transects for which vertical contour plots were produced. The Northern Transect = Transect 1, Boston-Nearfield = Transect 2, Cohasset = Transect 3, and Marshfield = Transect 4 in Figures 3-12 to 3-14.

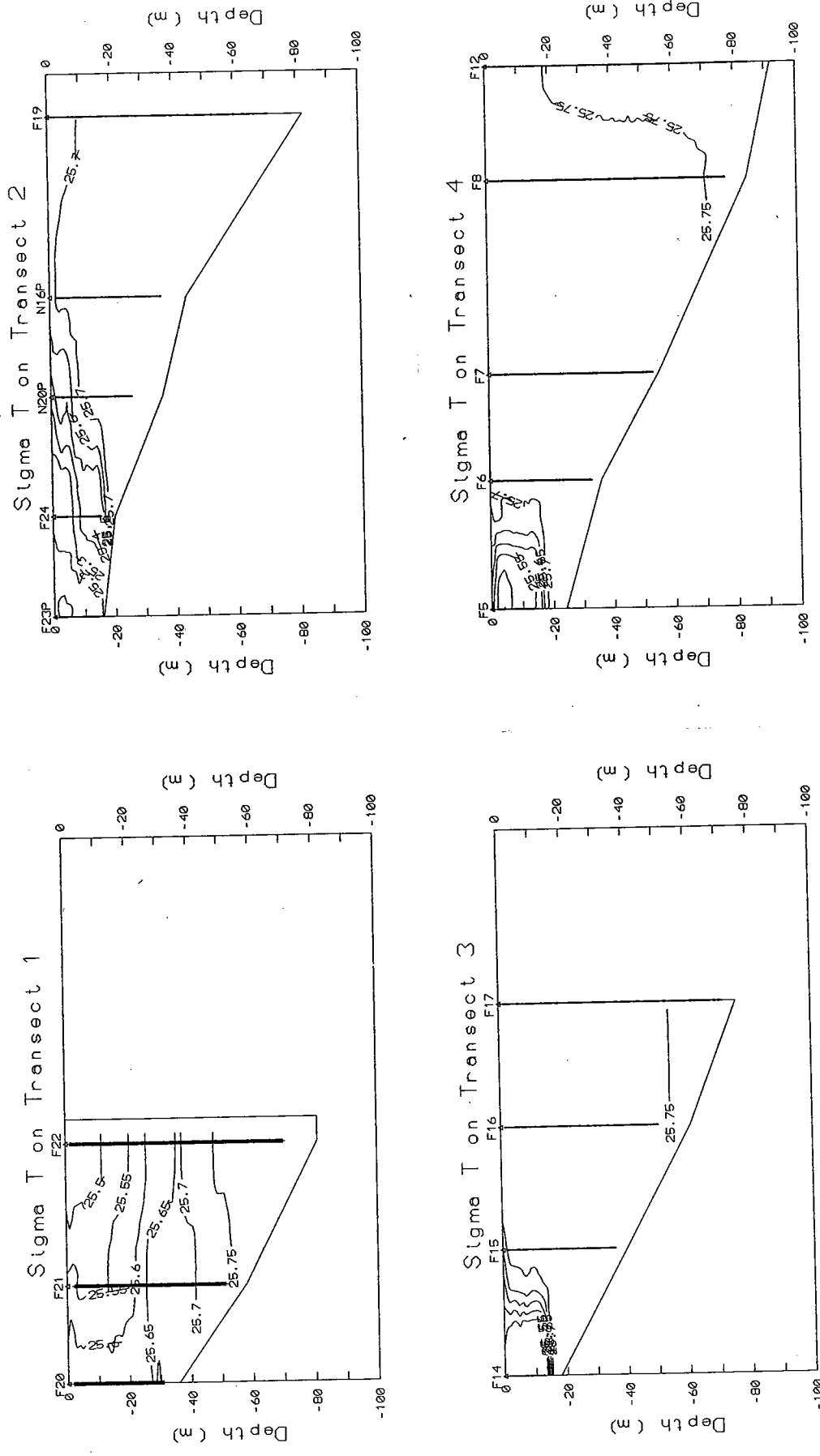


**Figure 3-12** Vertical section contours of  $\sigma_T$  in February for standard transects (see Figure 3-11). The data used to produce contours are from high-resolution continuous vertical profiles taken from the downcast at each station. The contour interval is 0.05 or 0.1 units.

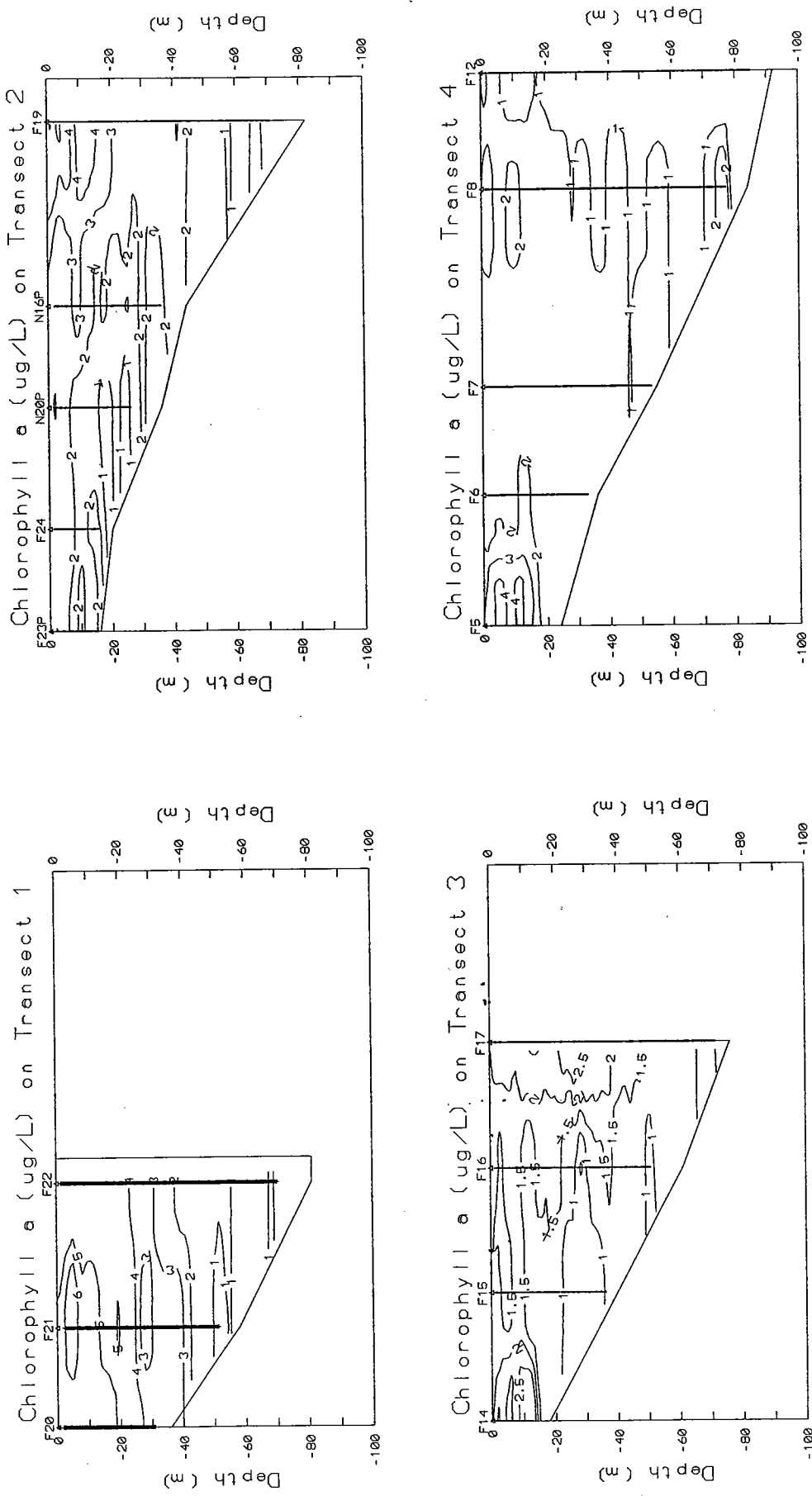


**Figure 3-13** Vertical section contours of fluorescence (as  $\mu\text{g Chl L}^{-1}$ ) in February for standard transects (see Figure 3-11). The data used to produce contours are from high-resolution continuous vertical profiles taken from the downcast at each station. The contour interval is 0.5 or 1.0  $\mu\text{g L}^{-1}$ .



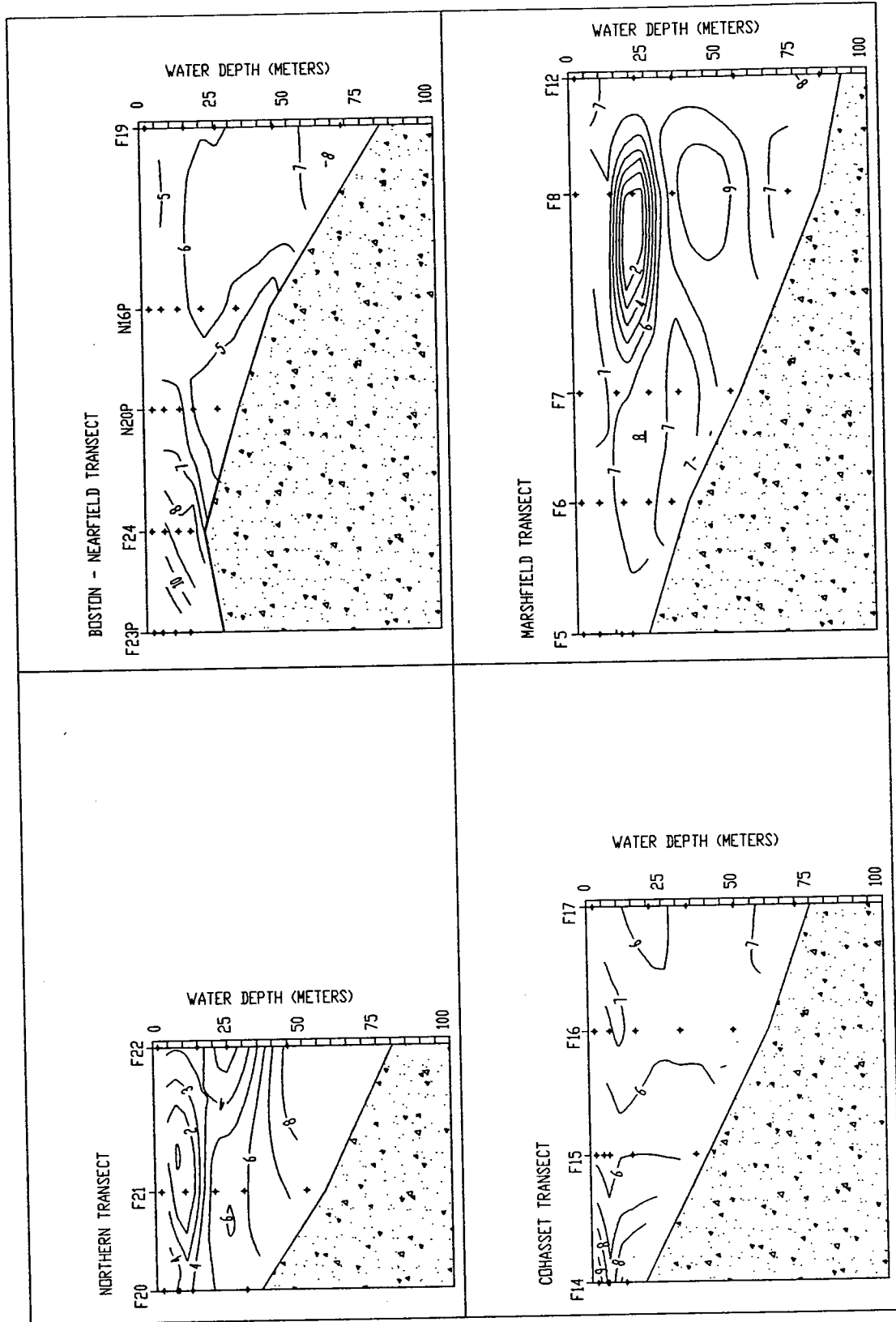
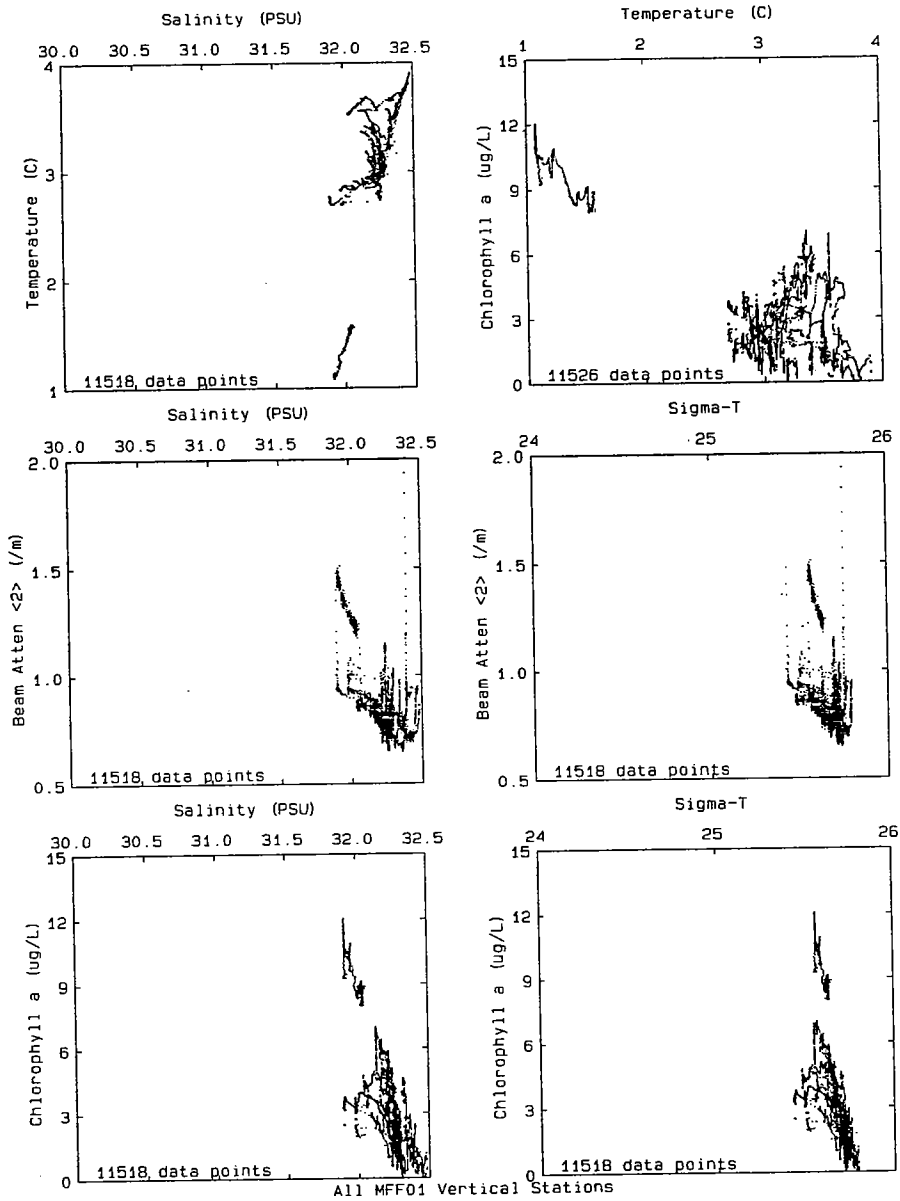
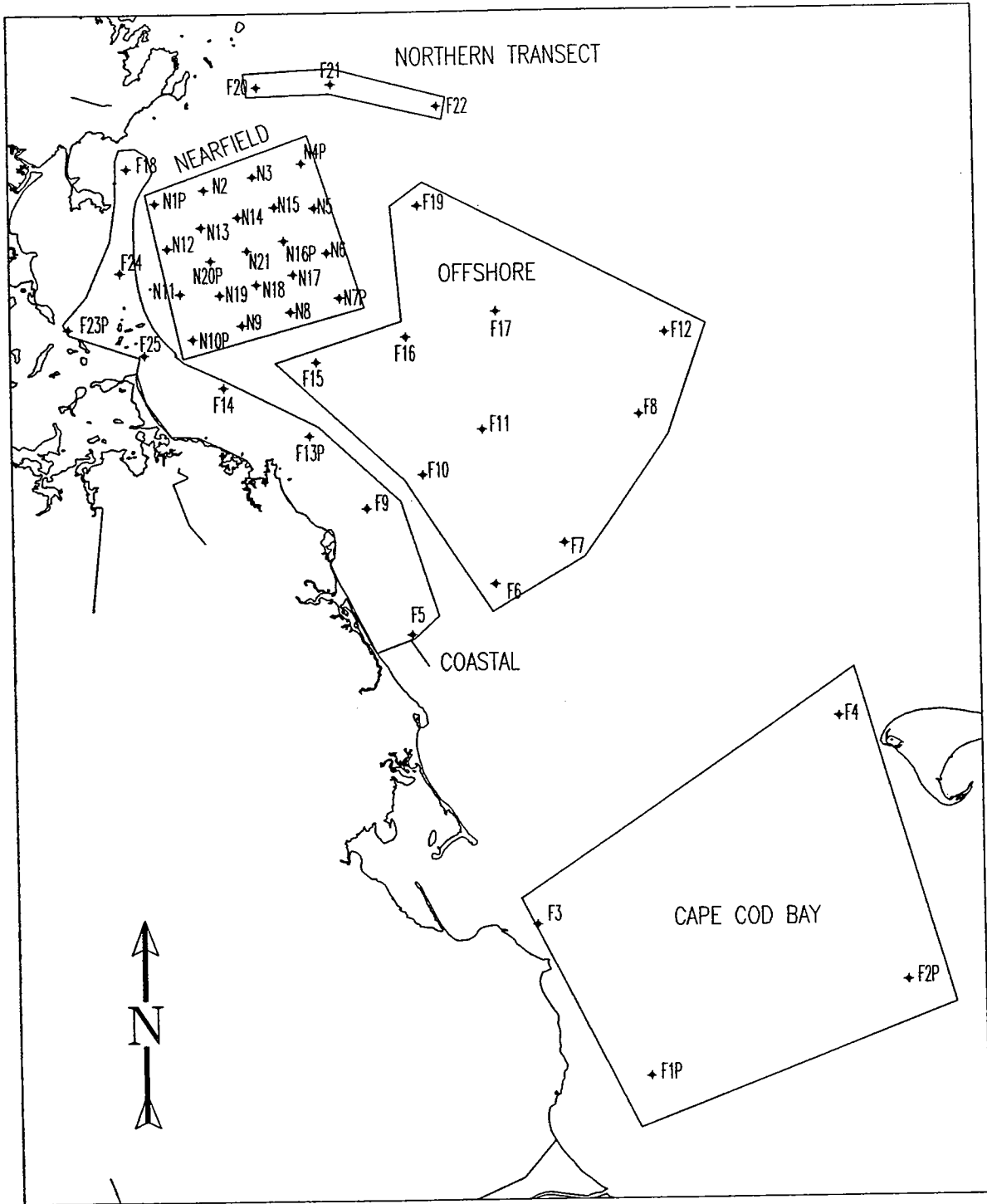


Figure 3-14 Vertical section contours of dissolved inorganic nitrogen ( $\mu\text{M}$ ) in February for standard transects (see Figure 3-11). The data used to produce contours are from discrete bottle samples as given in Appendix A. The contour interval is 1  $\mu\text{M}$ .



**Figure 3-15** Scatter plots of data acquired by *in situ* sensor package during vertical casts at all farfield and nearfield stations occupied in February 1992. Individual station casts plots that were used to produce this composite are in Appendix C.



**Figure 3-16** Map to show station groups designated in Figures 3-16 through 3-22. Massachusetts Bay was separated into 4 groups based on water depth and geographic position.

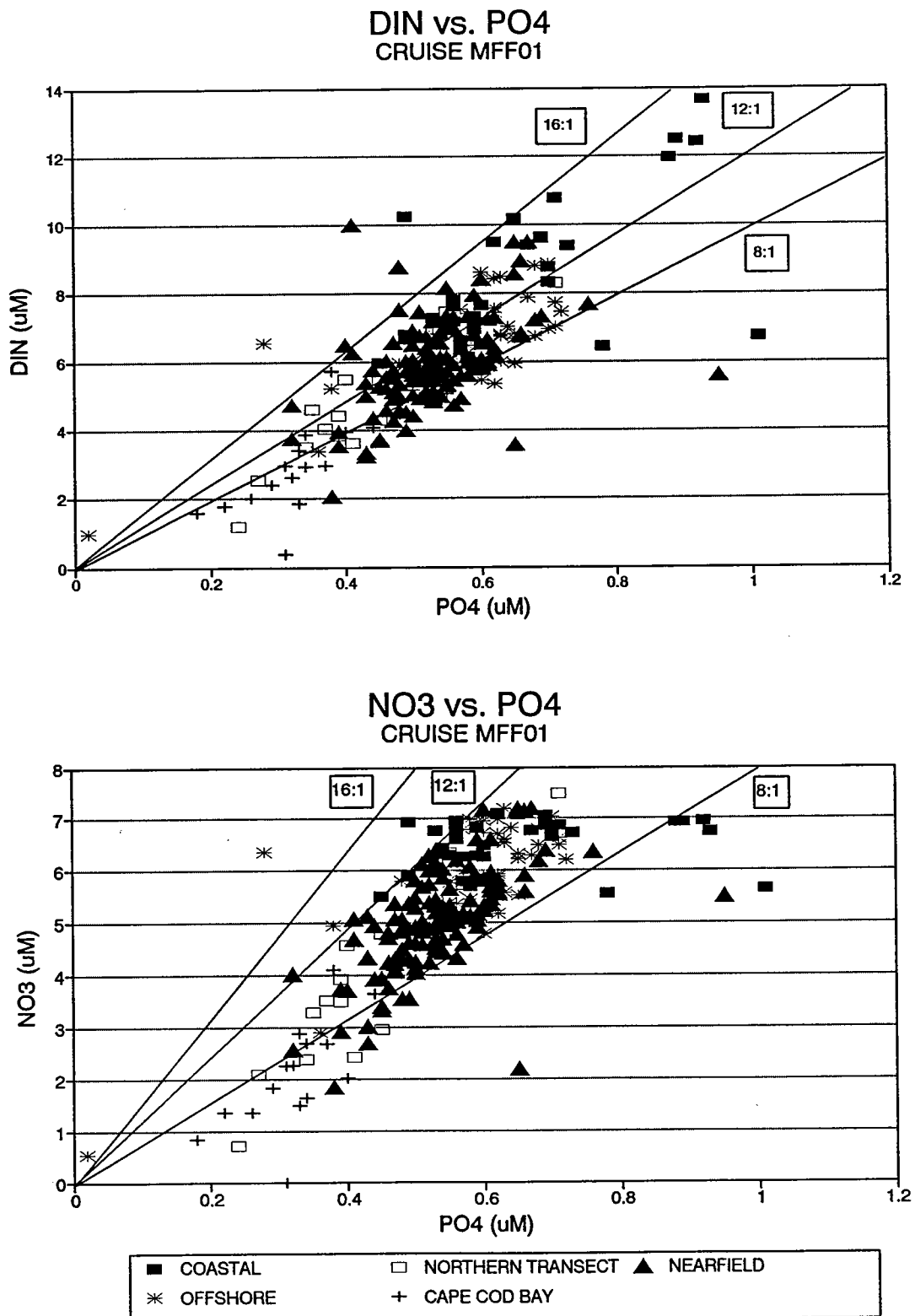


**Figure 3-17** Scatter plots of nitrogen forms vs. phosphate during February 1992. All stations and depths are included, and data are given in Appendix A. Lines show constant proportions of nitrogen relative to phosphorous across a range of N:P ratios.

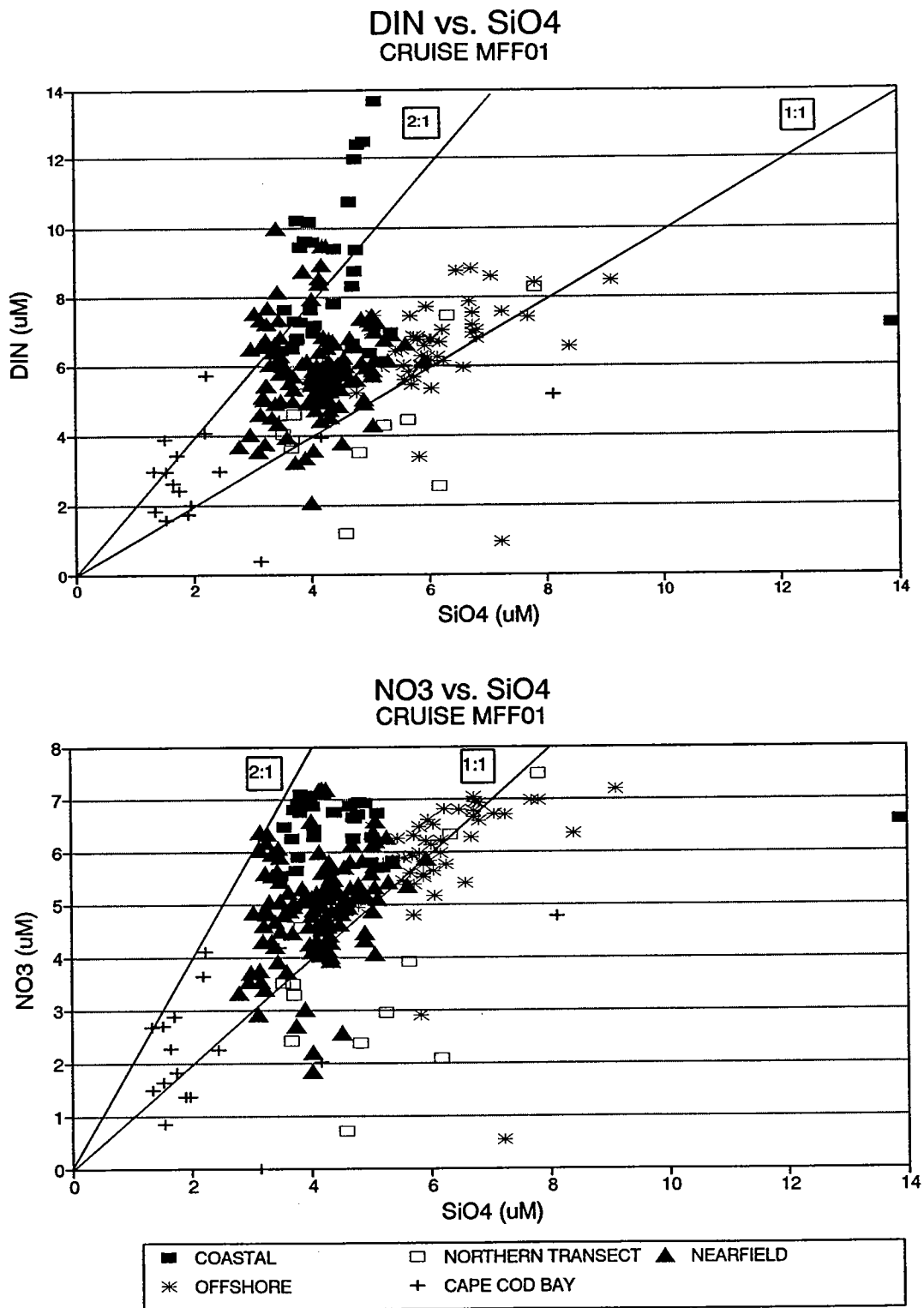


**Figure 3-18** Scatter plots of nitrogen vs. silicate during February 1992. All stations and depths are included, and data are given in Appendix A. Lines show constant proportions of nitrogen relative to silicate across a range of N:Si ratios.

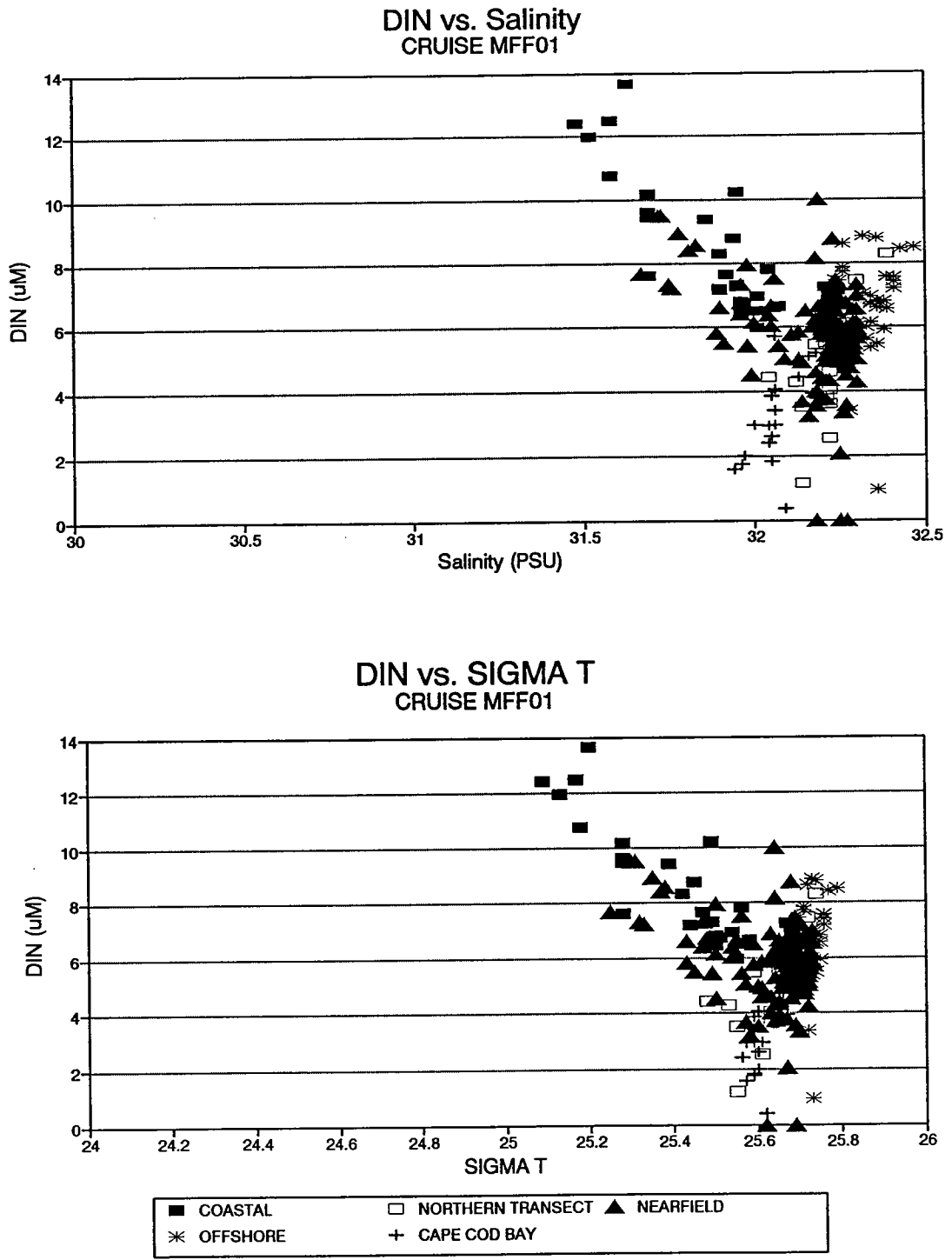


**Figure 3-19** Dissolved inorganic nitrogen vs. salinity and  $\sigma_T$  in February 1992. All stations and depths are included, and data are given in Appendix A.

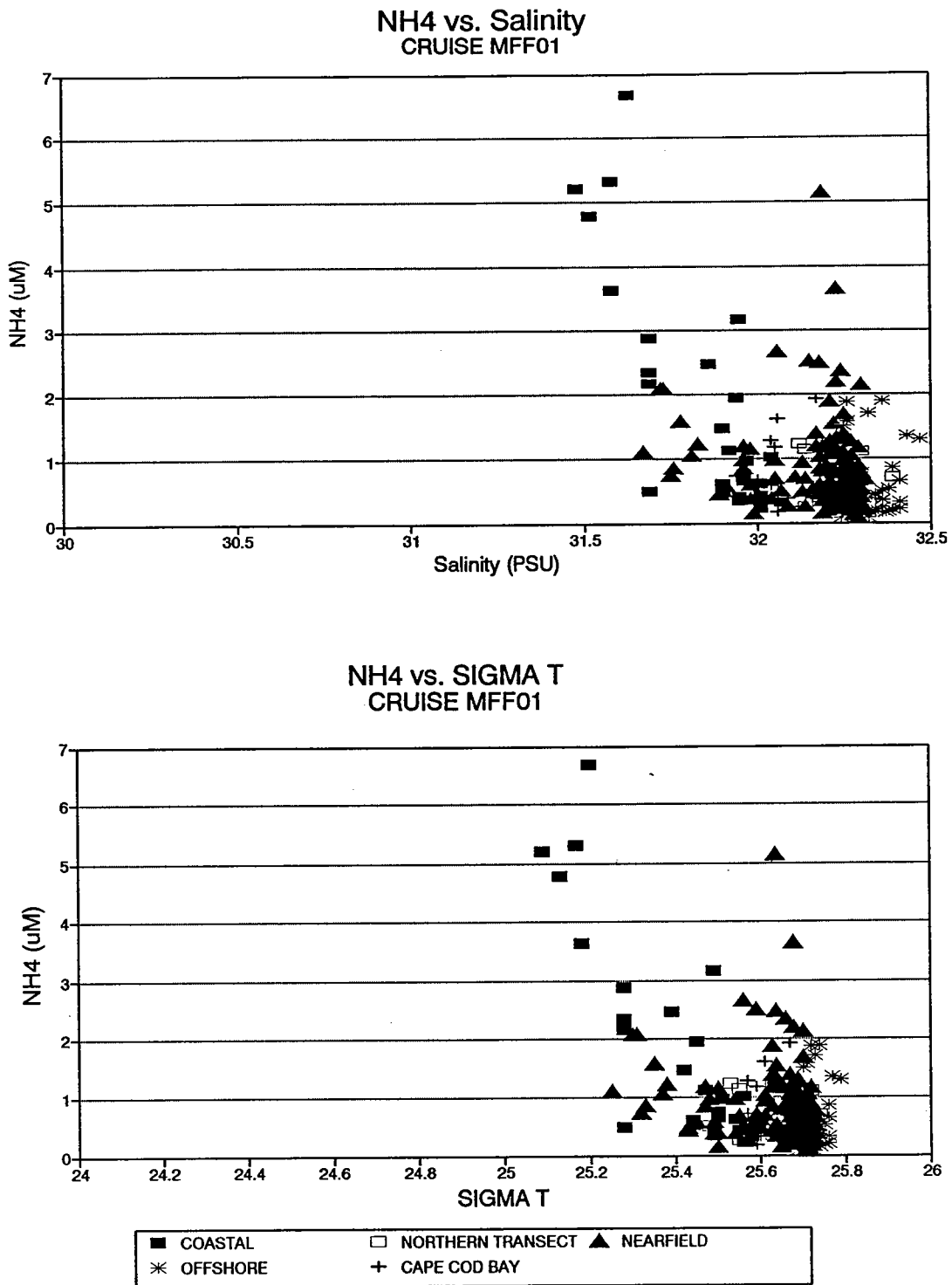
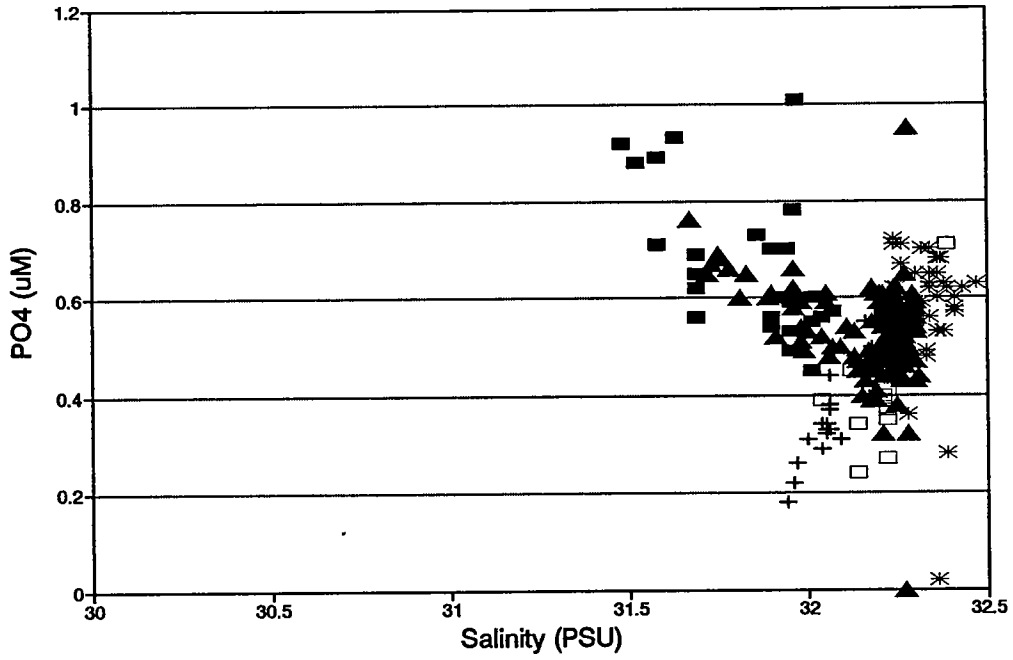


**Figure 3-20** Ammonia vs. salinity and  $\sigma_T$  in February 1992. All stations and depths are included, and data are given in Appendix A.

PO4 vs. Salinity  
CRUISE MFF01



PO4 vs. SIGMA T  
CRUISE MFF01

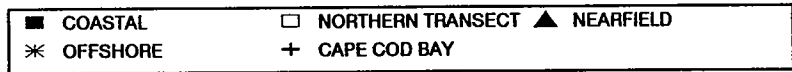
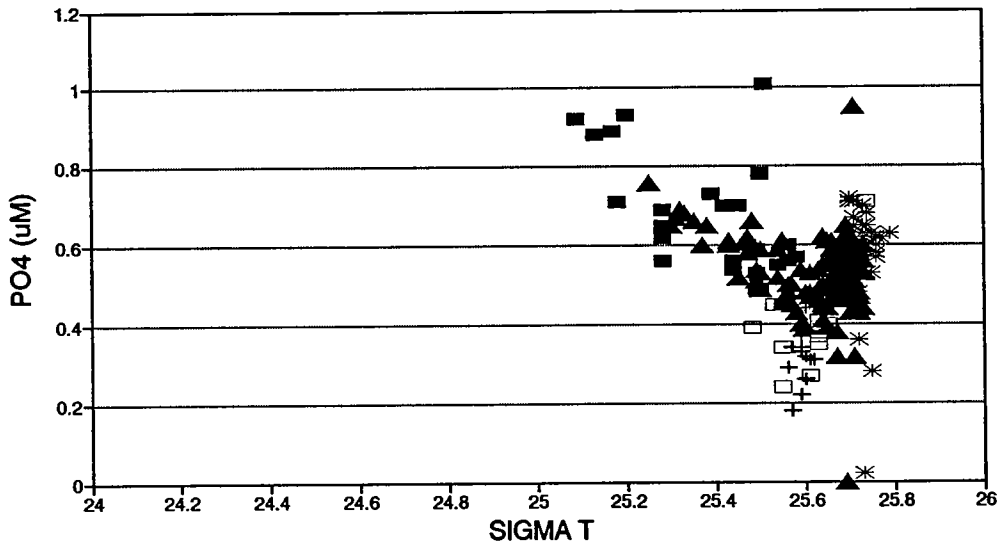
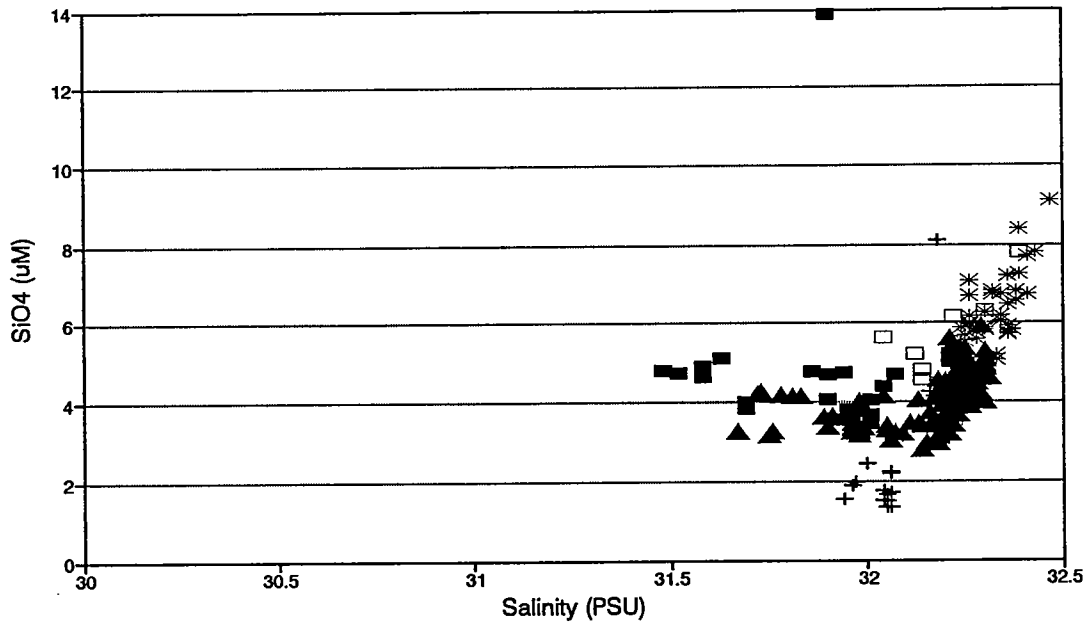


Figure 3-21 Phosphate vs. salinity and  $\sigma_T$  in February 1992. All stations and depths are included, and data are given in Appendix A.



SiO<sub>4</sub> vs. Salinity  
CRUISE MFF01



SiO<sub>4</sub> vs. SIGMA T  
CRUISE MFF01

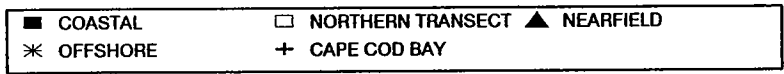
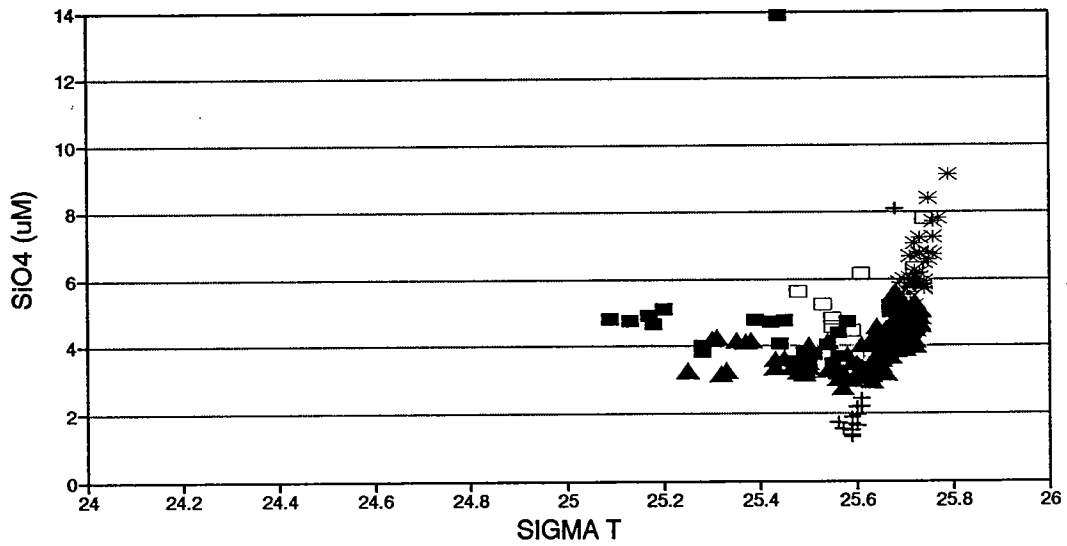
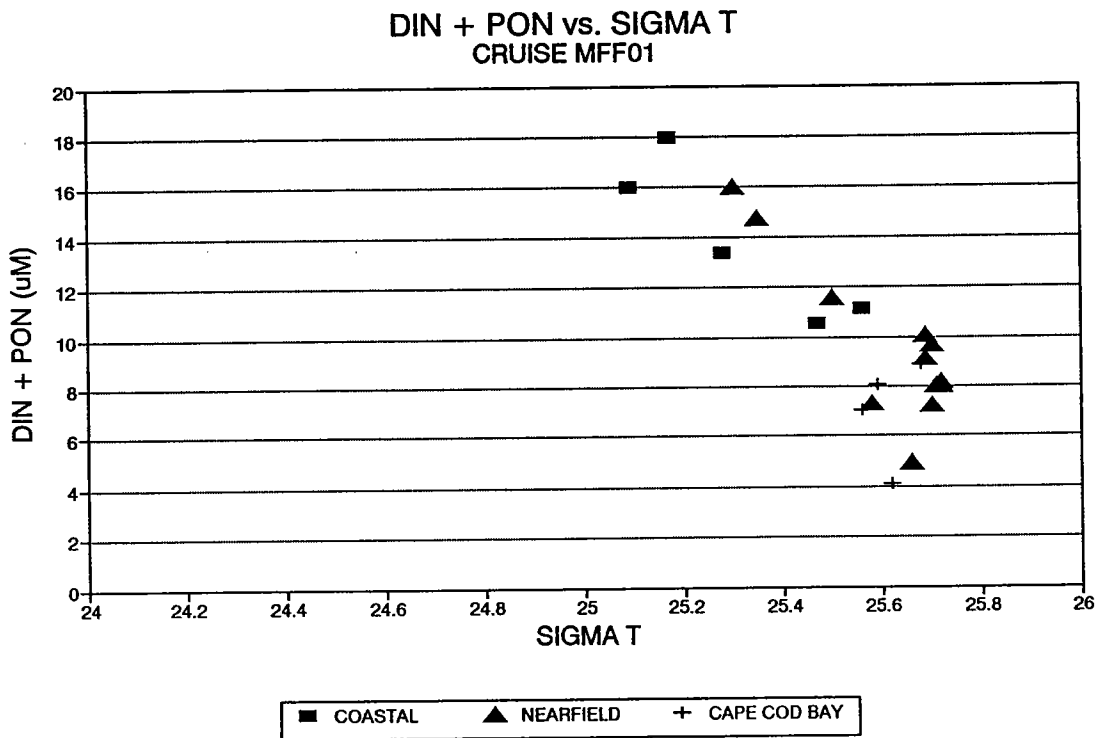
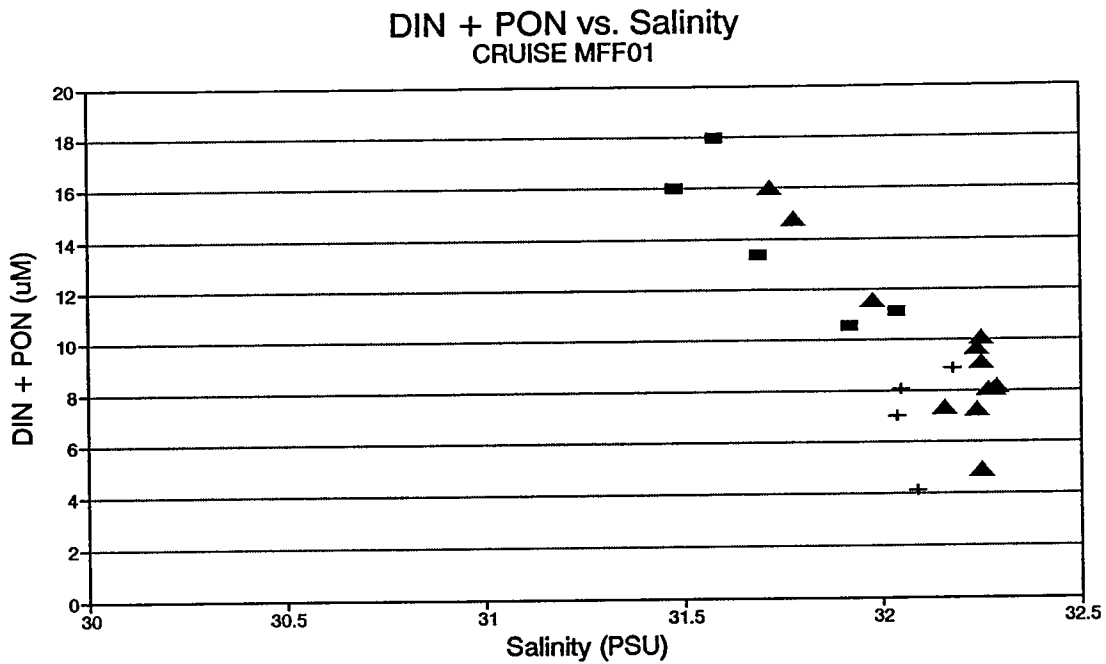
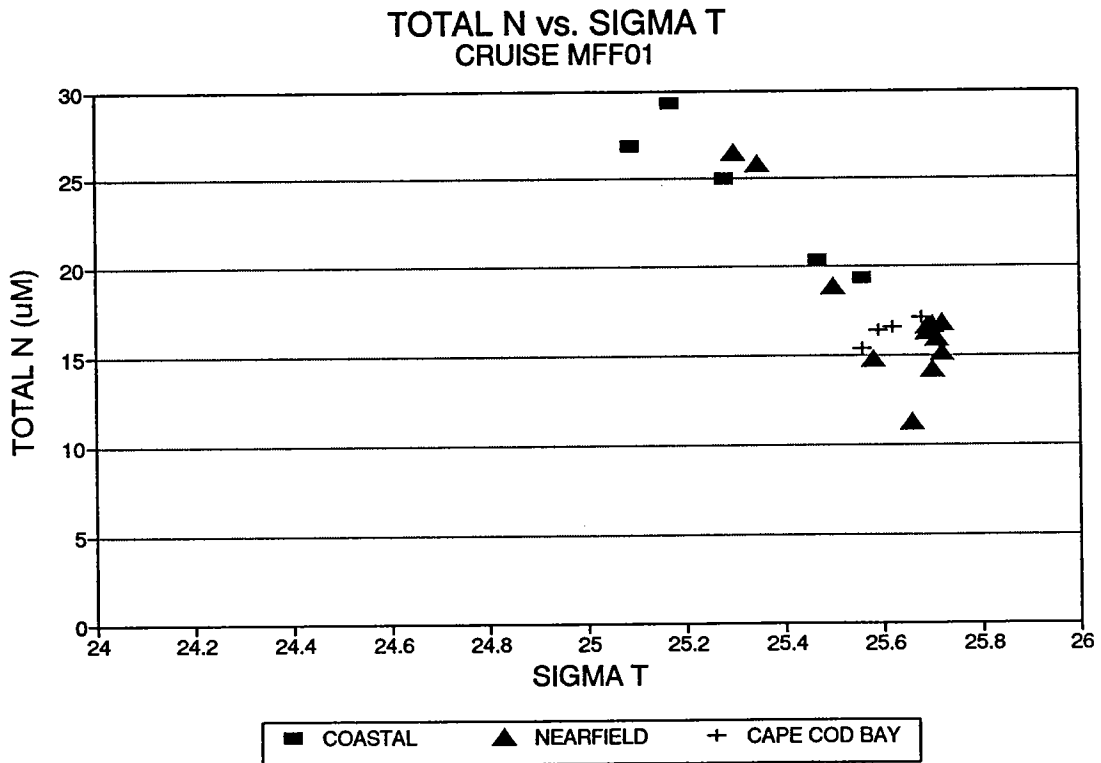
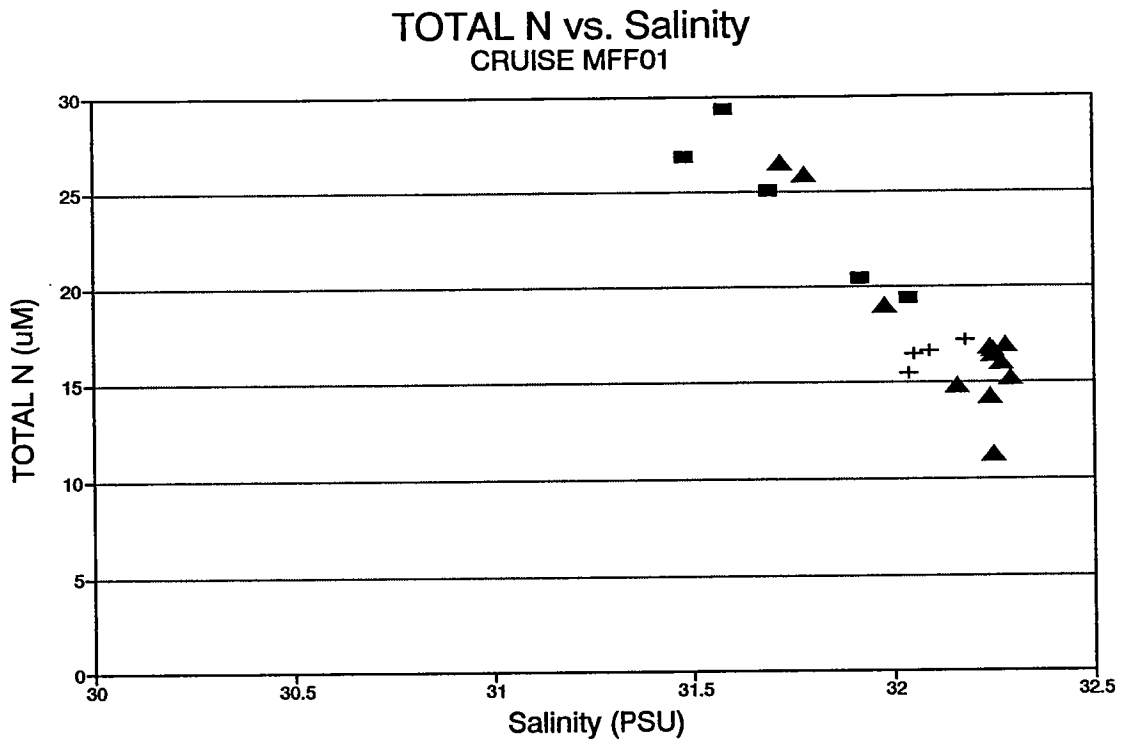


Figure 3-22 Silicate vs. salinity and  $\sigma_T$  in February 1992. All stations and depths are included, and data are given in Appendix A.



**Figure 3-23** The sum of dissolved inorganic nitrogen and particulate organic nitrogen vs. salinity and  $\sigma_T$  in February 1992. Data are from BioProductivity stations and special station F25 and are given in Appendix A. The station groups are coded as given in Figure 3-16; there are no BioProductivity stations in the Offshore or Northern Transect groups.



**Figure 3-24** The sum of total dissolved nitrogen and particulate organic nitrogen (=total nitrogen) vs. salinity and  $\sigma_T$  in February 1992. Data are from BioProductivity stations and special station F25 and are given in Appendix A. Groups are the same Figure 3-16.

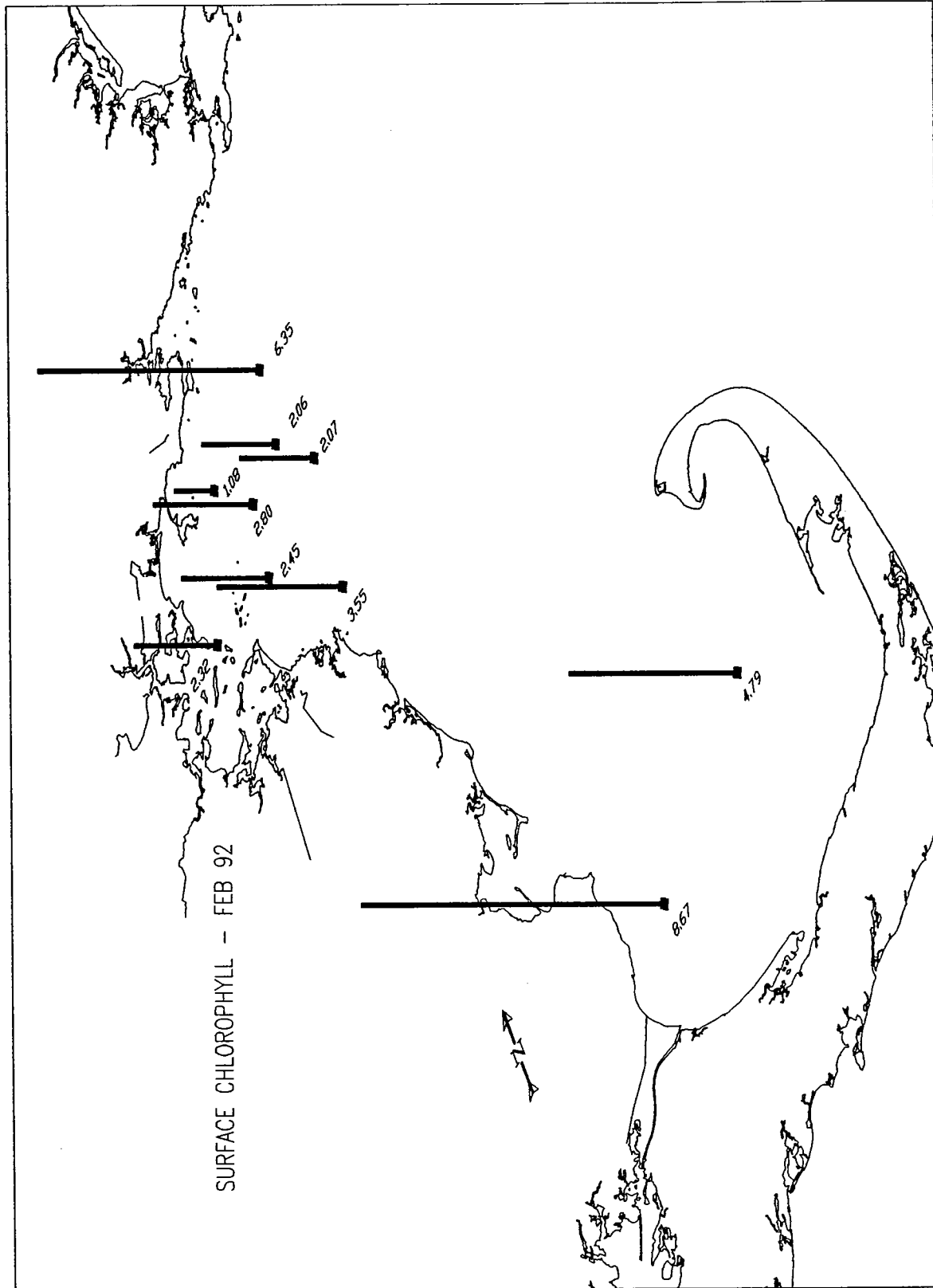
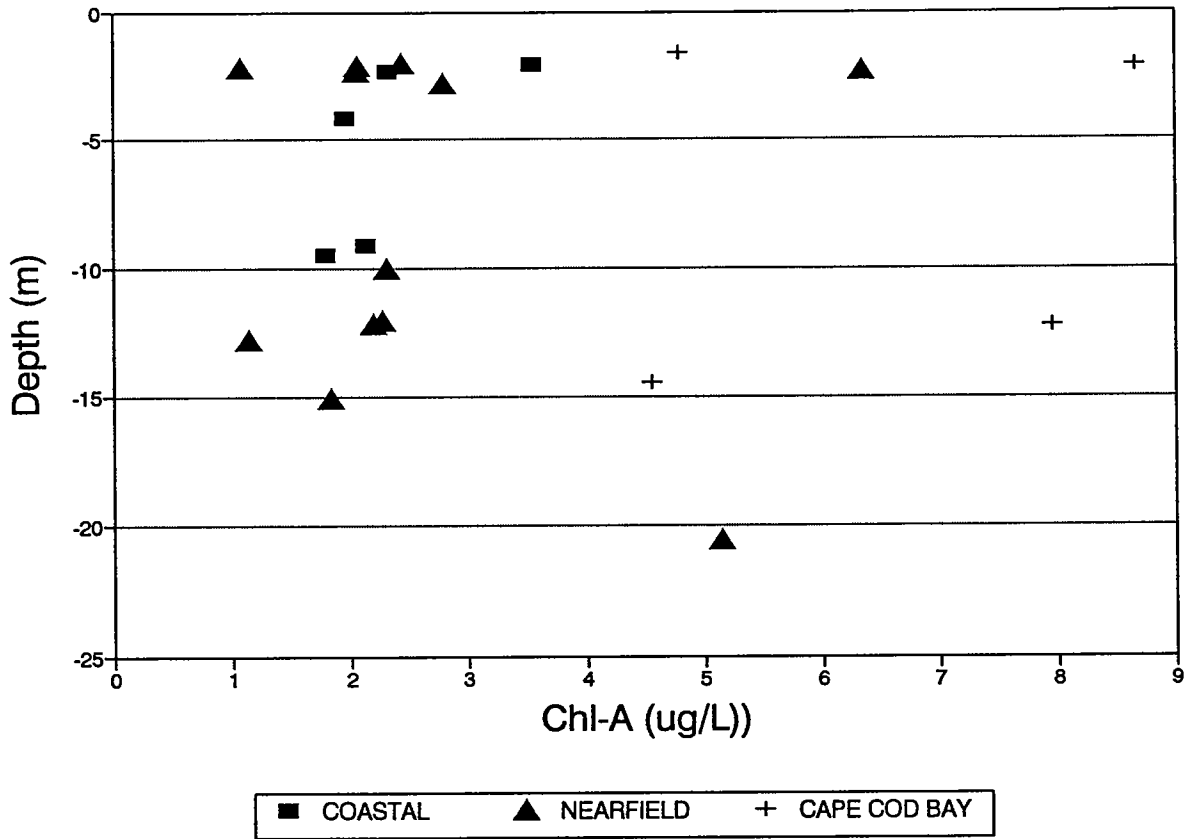
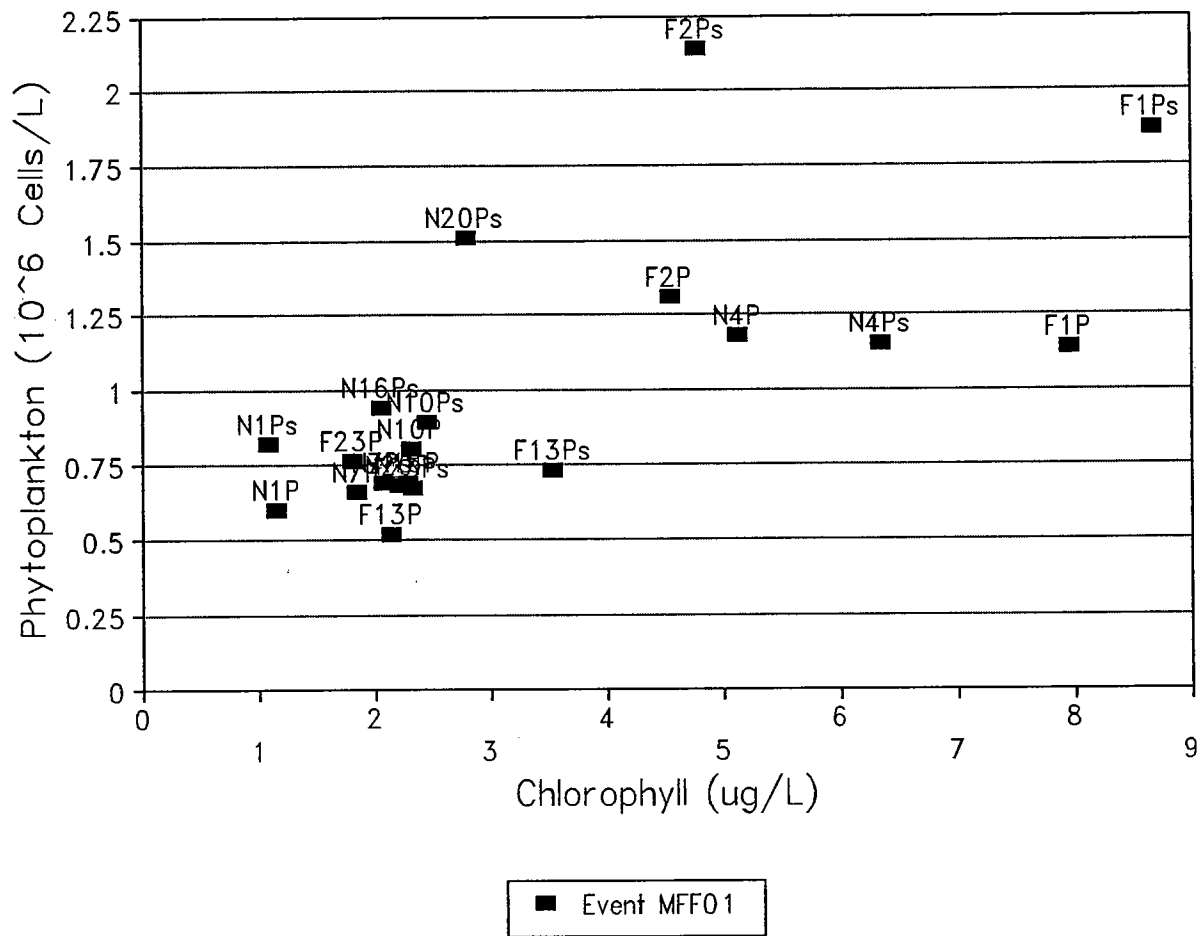


Figure 3-25 Surface chlorophyll at BioProductivity stations and special station F25 in February 1992. Data are the average of duplicate determinations by standard chlorophyll extraction (Appendix A.)

# CHL-A vs. DEPTH CRUISE MFF01



**Figure 3-26** Surface and deeper chlorophyll at BioProductivity stations and special station F25 in February 1992. Data are the average of duplicate determinations by standard chlorophyll extraction (Appendix A.) Groups are the same as Figure 3-16.



**Figure 3-27** Total phytoplankton abundance vs. extracted chlorophyll at BioProductivity stations in February 1992. Data are given in Appendices A and I.

# Phytoplankton - Feb 92

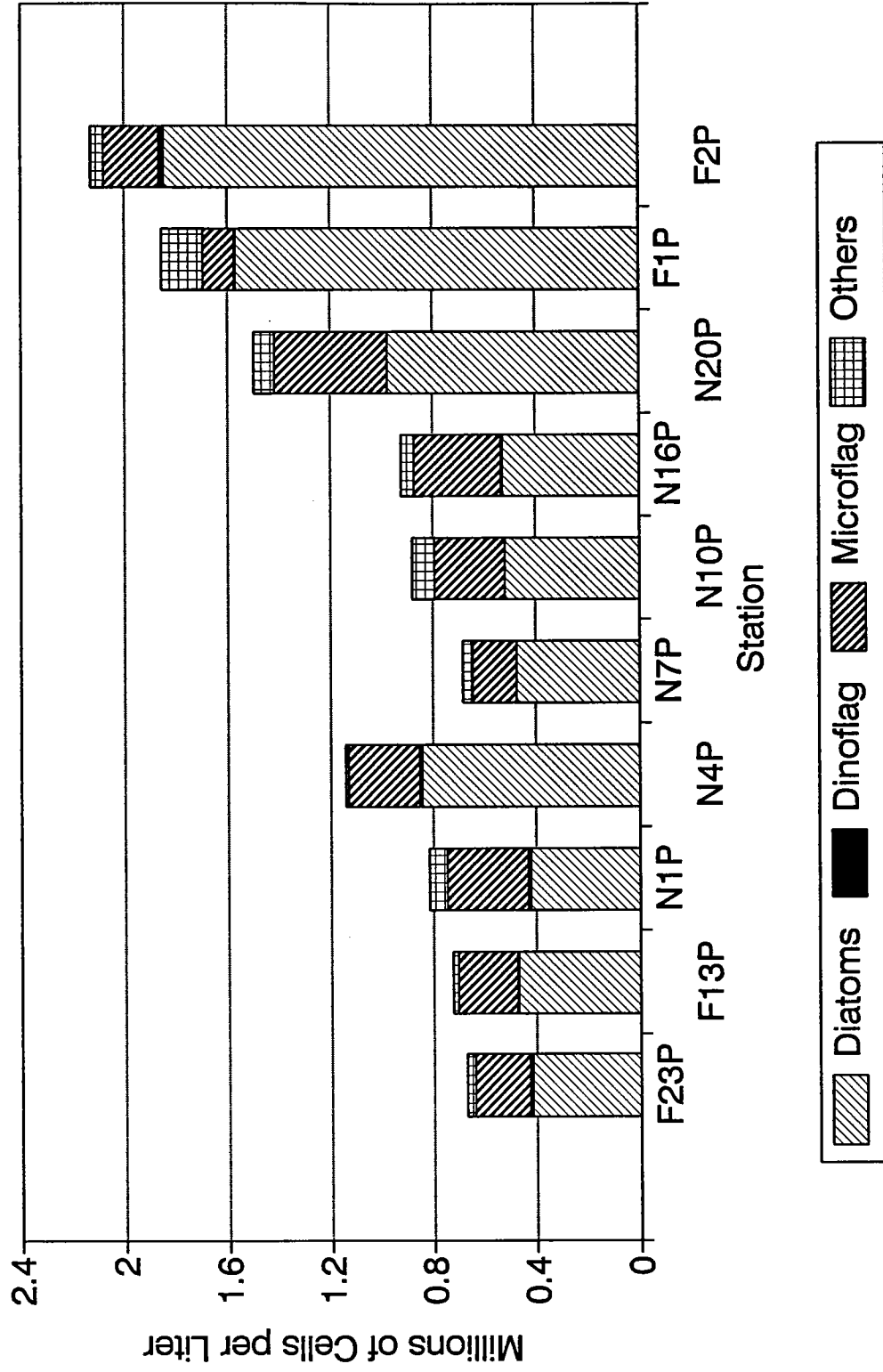
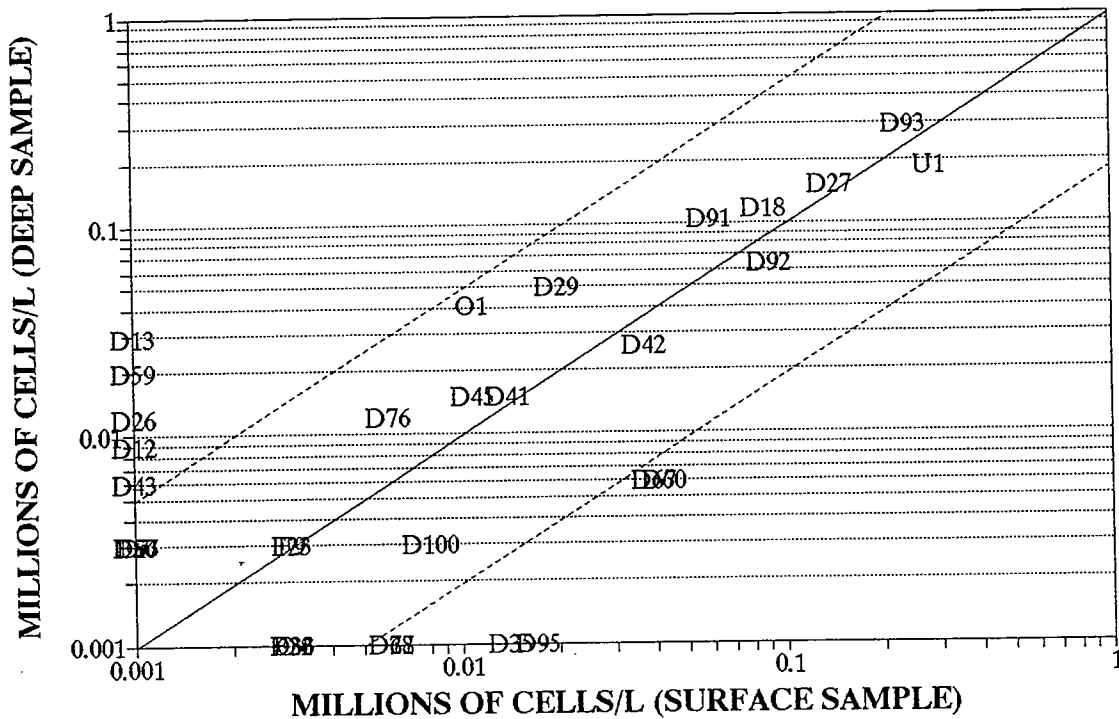


Figure 3-28 Total phytoplankton abundance, by taxonomic groups, at BioProductivity stations in February 1992. Data are given in Appendix I.

## PHYTOPLANKTON SPECIES ABUNDANCE STATION N4P - CRUISE MFF01



**Figure 3-29** Comparison of phytoplankton taxonomic composition of surface and deeper samples at station N4P in February 1992. Full species codes are given in Appendix I, but the alphabetical prefix indicates the following: D= diatom, F= dinoflagellate, U= microflagellates, O= other. Solid line shows 1:1 relationship, dotted lines show 1:5 and 5:1 isopleths.



## PHYTOPLANKTON SPECIES ABUNDANCE STATION F2P - CRUISE MFF01

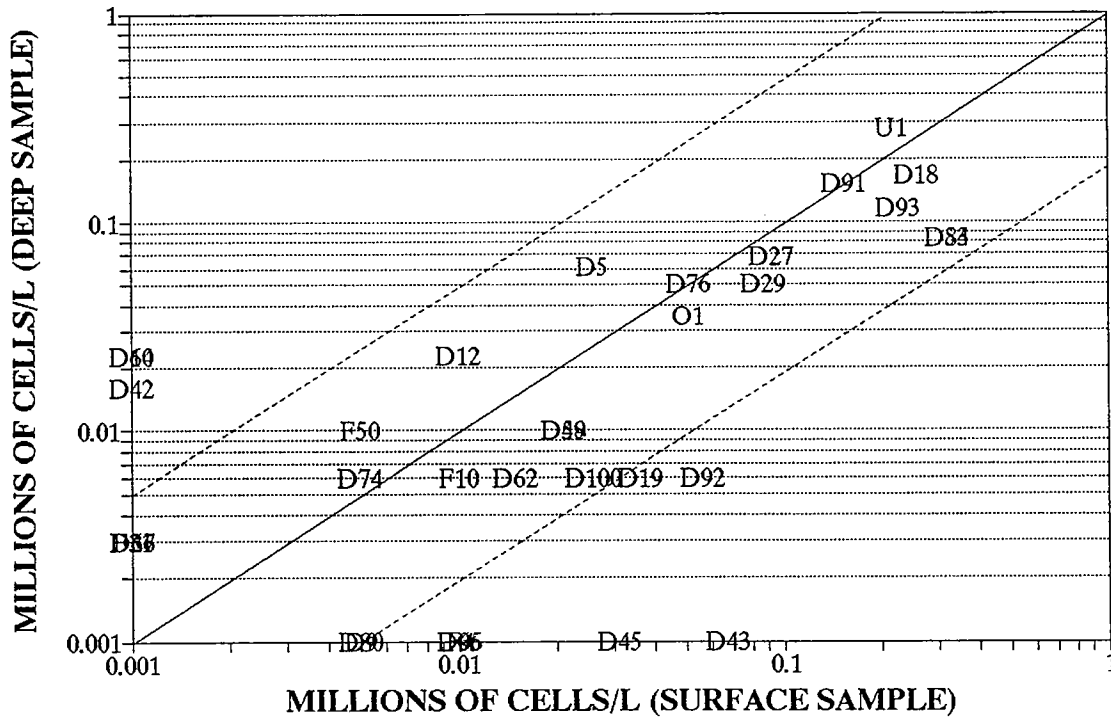
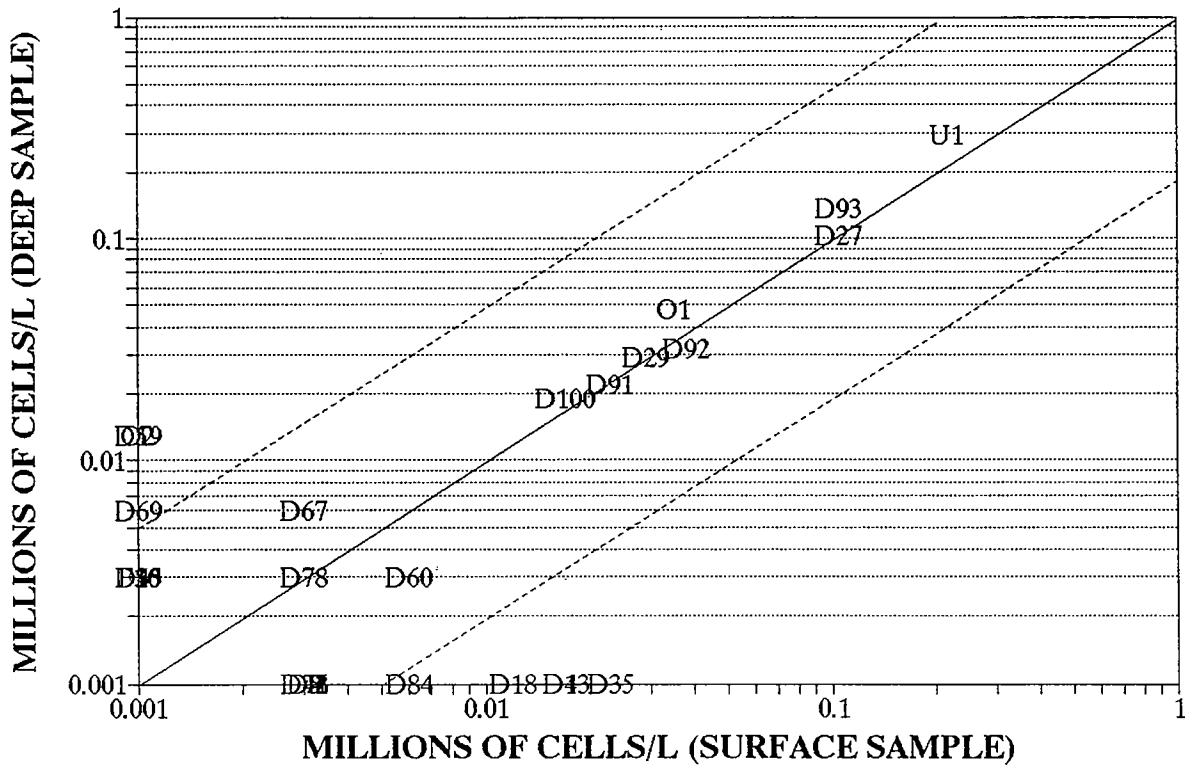


Figure 3-30 Comparison of phytoplankton taxonomic composition of surface and deeper samples at station F2P in February 1992. Species codes are given in Appendix I.

## PHYTOPLANKTON SPECIES ABUNDANCE STATION F23P - CRUISE MFF01



**Figure 3-31** Comparison of phytoplankton taxonomic composition of surface and deeper samples at station F23P in February 1992. Species codes are given in Appendix I.

## PHYTOPLANKTON SPECIES ABUNDANCE STATION F13P - CRUISE MFF01

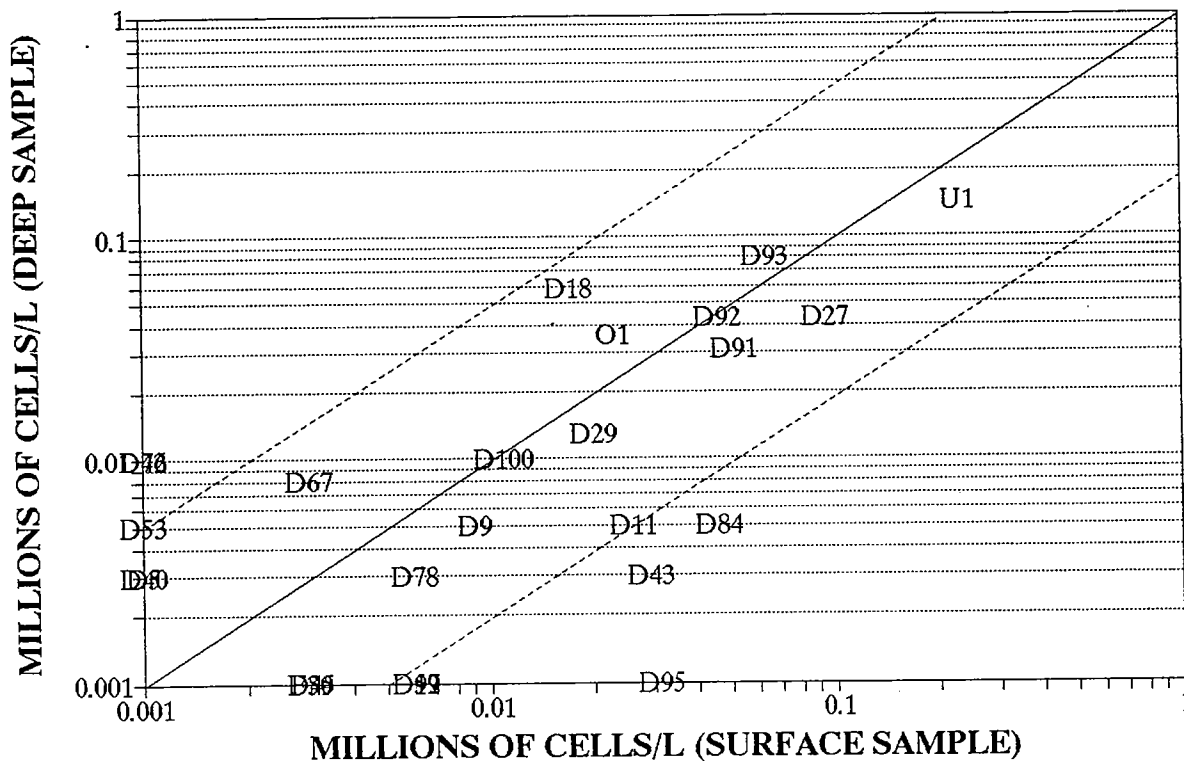


**Figure 3-32** Comparison of phytoplankton taxonomic composition of surface and deeper samples at station F13P in February 1992. Species codes are given in Appendix I.

# Zooplankton - Feb 92

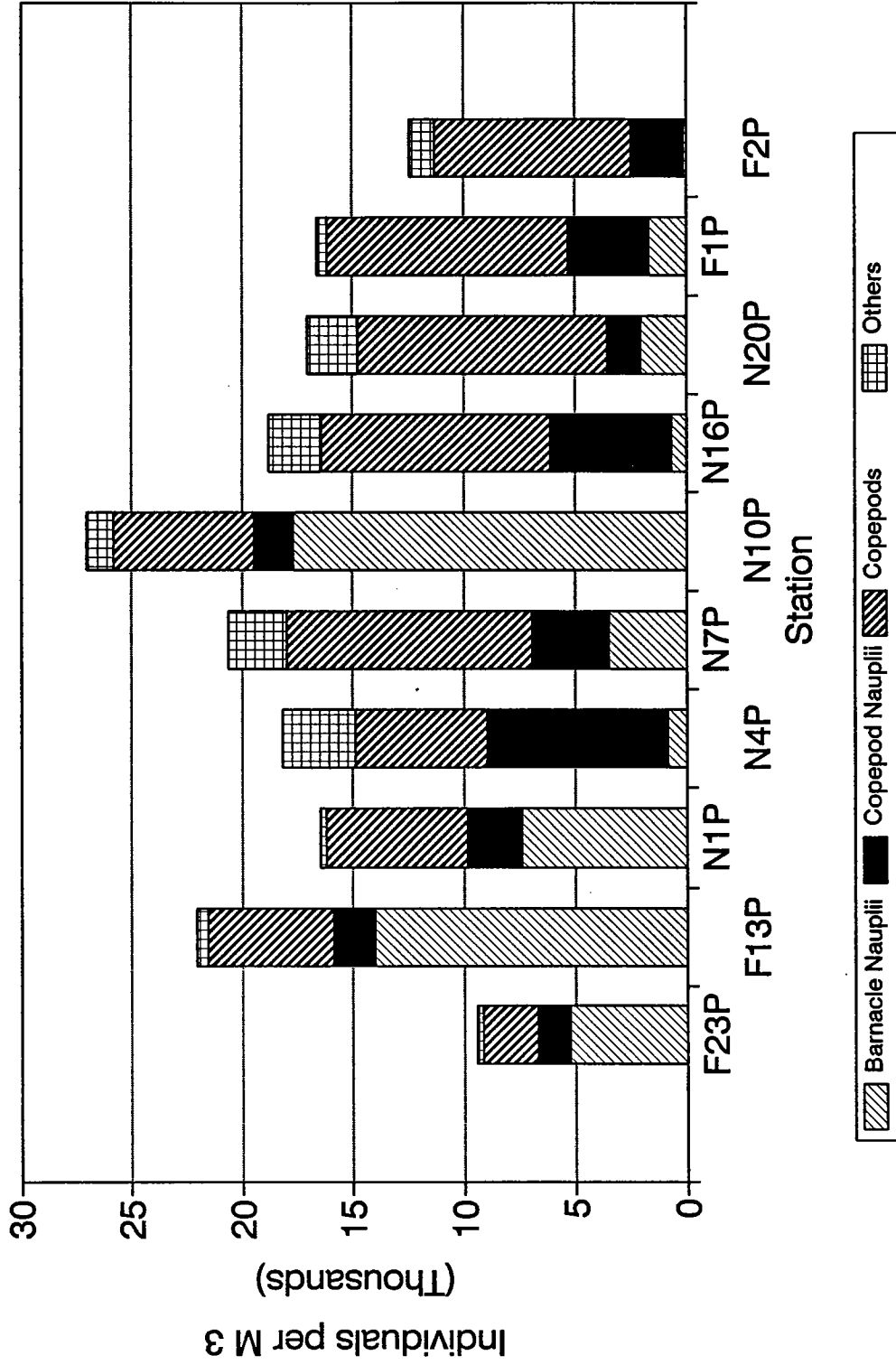


Figure 3-33 Zooplankton abundance, by groups, at BioProductivity stations in February 1992. Data are given in Appendix K.

# STATION N4P CRUISE 1

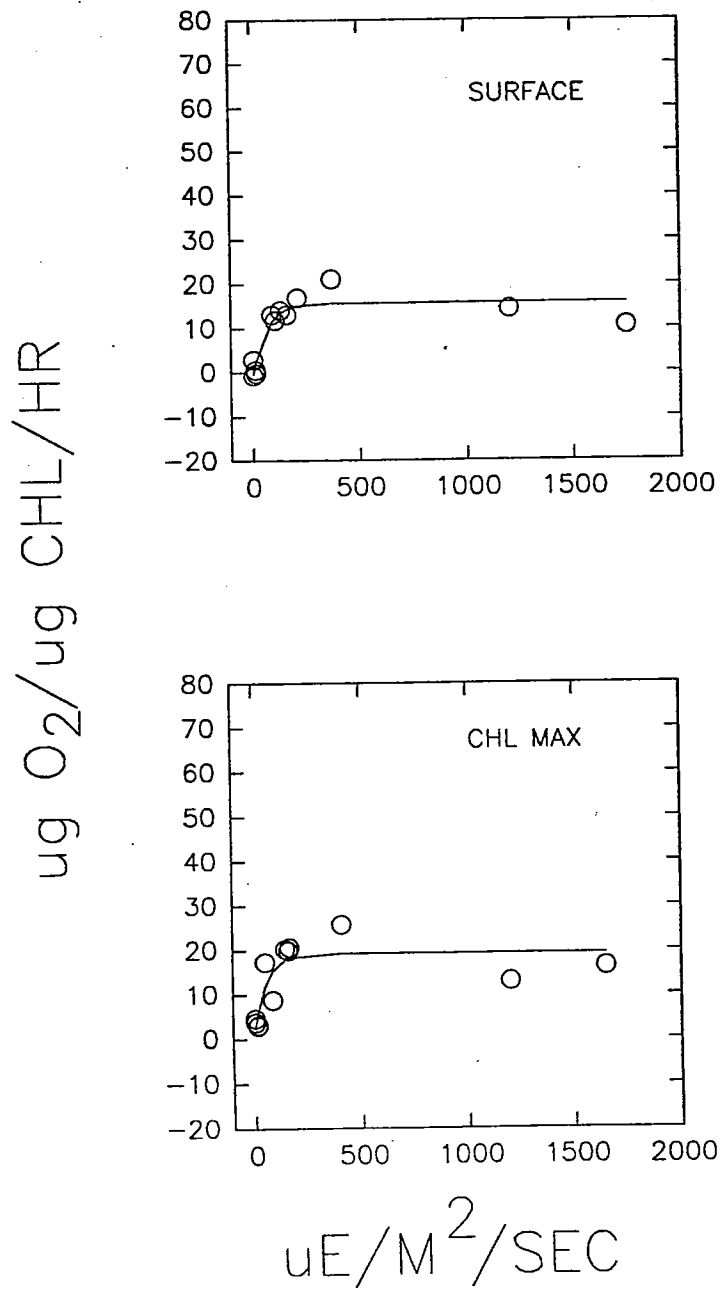


Figure 3-34 Net Production (P) vs. Irradiance (I) curves for station N4P in February 1992. Data are chlorophyll-normalized rates see Appendix G.

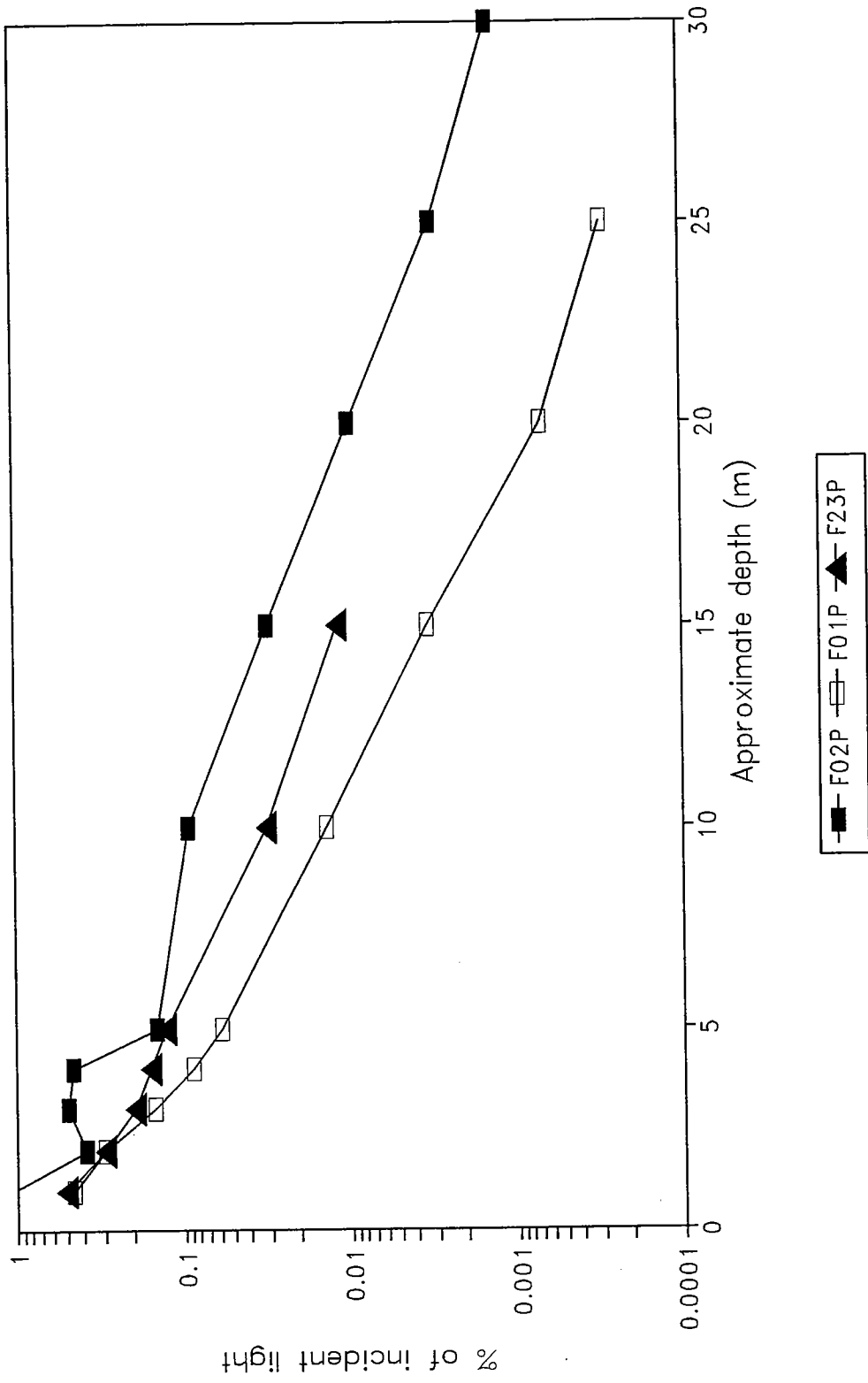
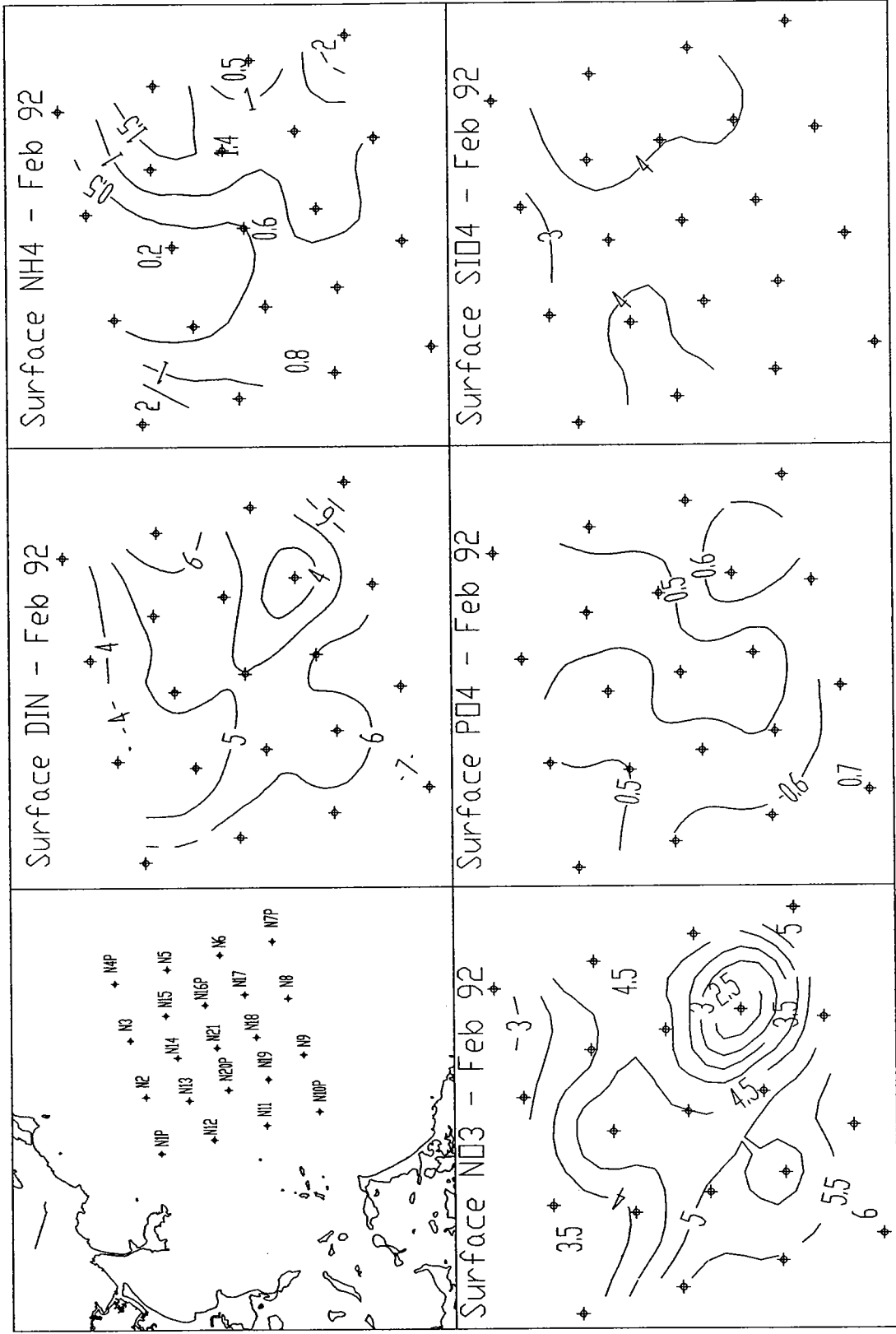
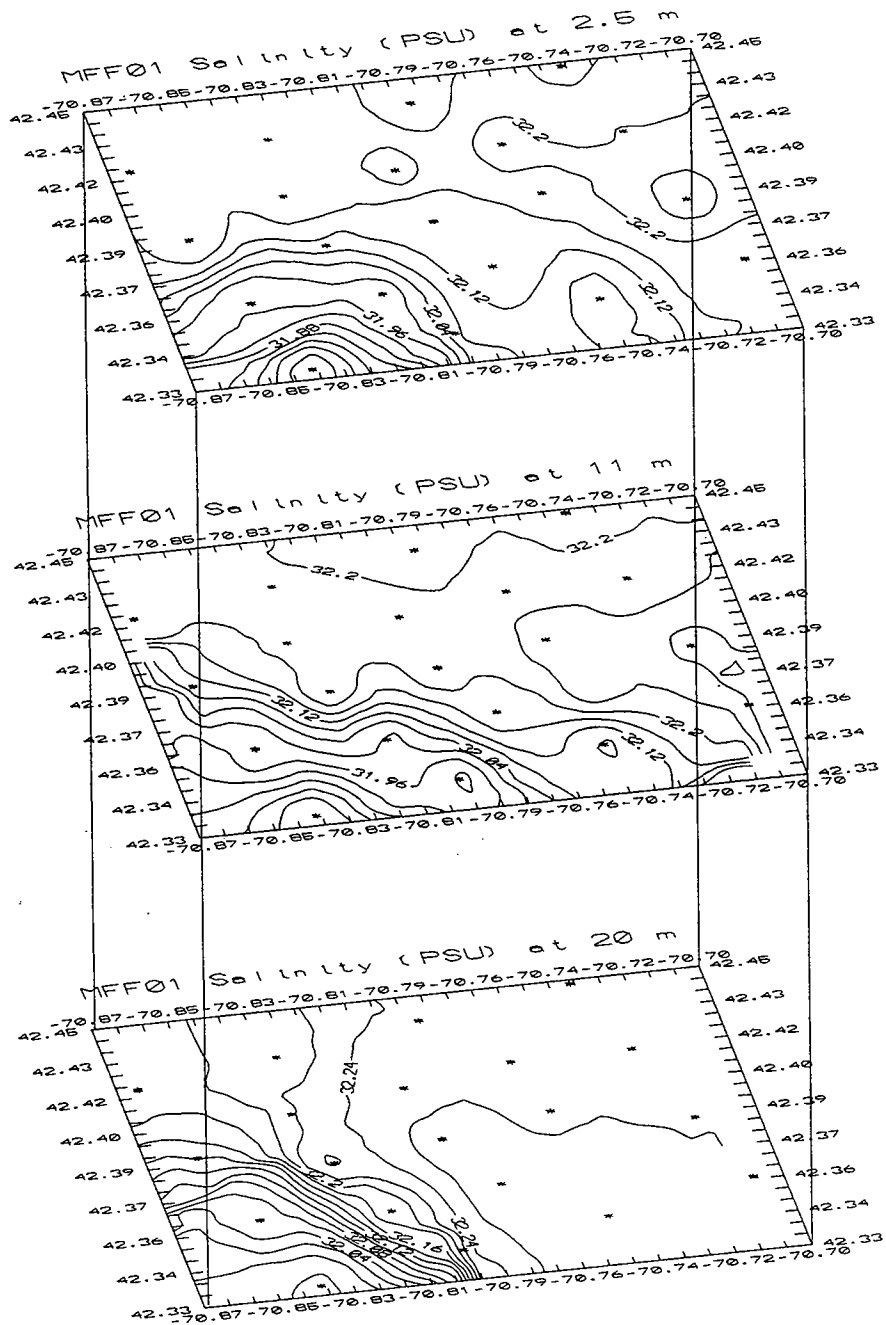


Figure 3-35. Light extinction at a selection of stations in February 1992. Data are given in Appendix G.



**Figure 3-36** Surface nutrient concentrations ( $\mu\text{M}$ ) during day 1 of nearfield sampling in February 1992. Data are given in Appendix A. Contour intervals are  $1 \mu\text{M}$  for  $\text{DIN}$  and  $\text{SiO}_4$ ,  $0.5 \mu\text{M}$  for  $\text{NH}_4$  and  $\text{NO}_3$ , and  $0.1 \mu\text{M}$  for  $\text{PO}_4$ .



**Figure 3-37** The salinity field in the nearfield viewed as horizontal slices at 2.5, 11, and 20 m water depths. The water depth along the western edge (left) is as shallow as 25 m whereas, the water depth on the eastern edge (right) is on the order 45-50 m. Data are from vertical casts on nearfield day 1 at stations whose positions are indicated. The contour interval is 0.02 PSU.



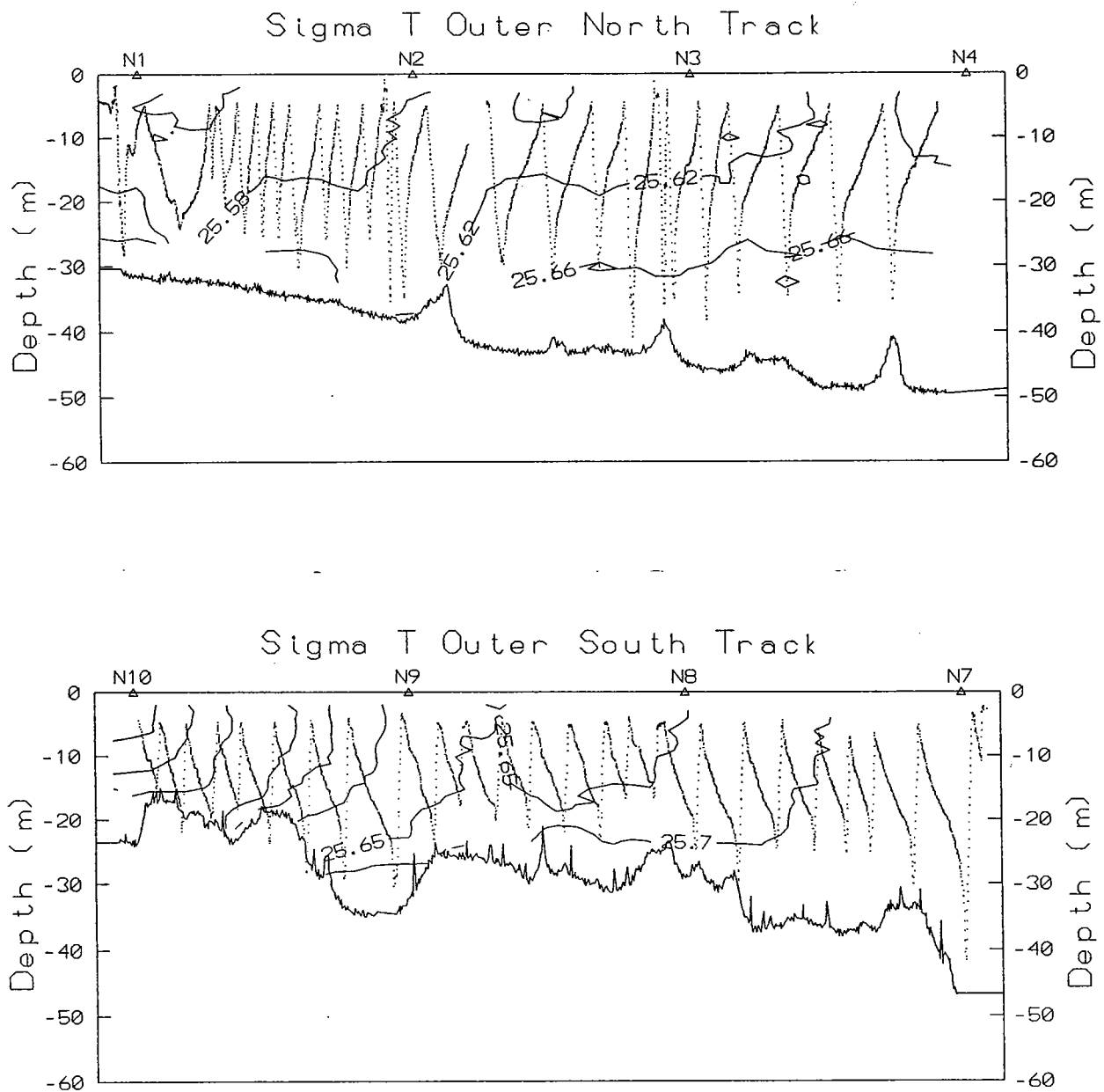


**Figure 3-38** Vertical section contours of  $\sigma_T$  generated from tow-yos (nearfield day 2) in February 1992. The view is towards the North, with a corner of the Nearfield grid at either end of a track. Bottom bathymetry is shown, with increasing water depth to the offshore (right). The V-pattern shows the position of the towfish along the track, where data were collected as the basis for the contouring.

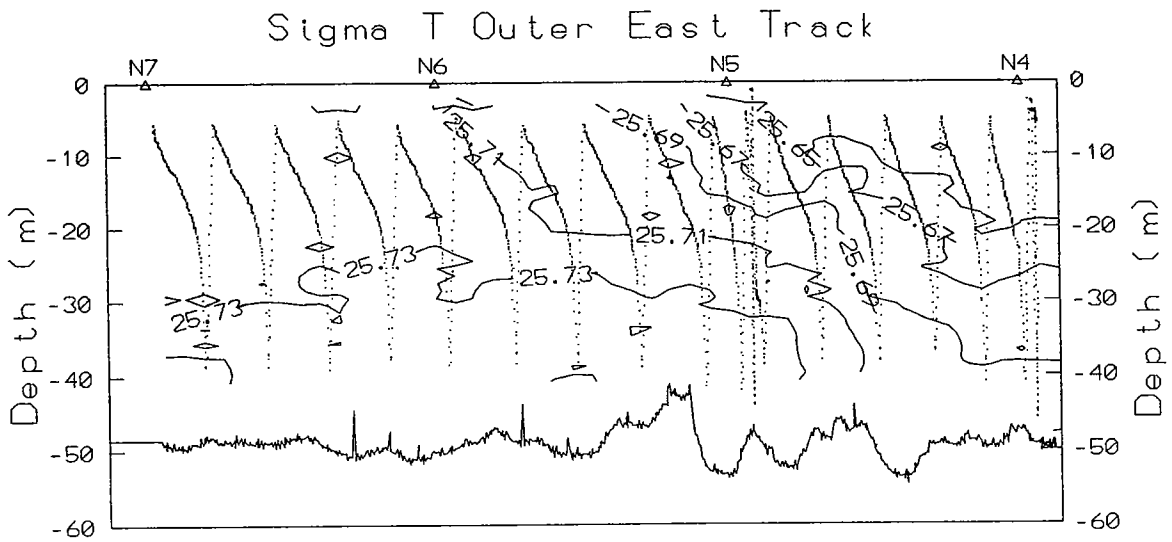
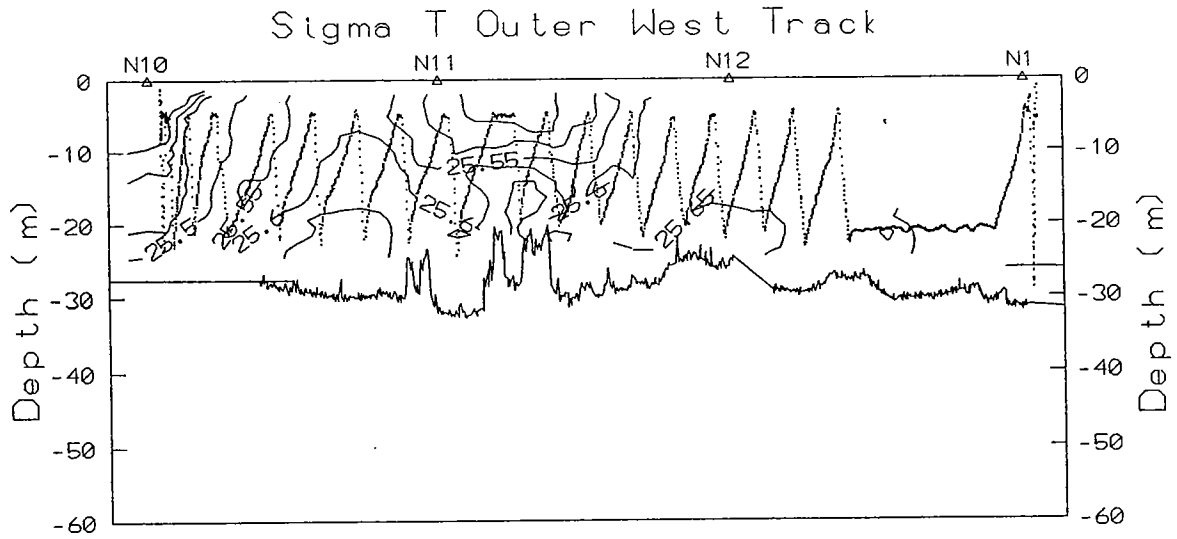


**Figure 3-39** Vertical section contours of  $\sigma_T$  generated for tow-yos in February 1992. The view is towards Boston Harbor.

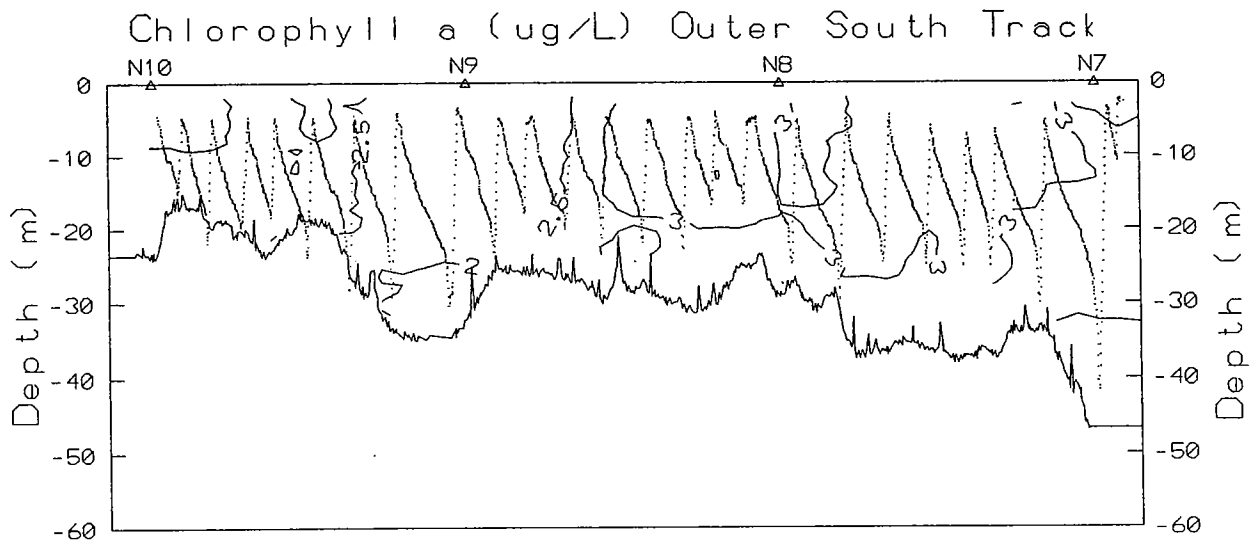
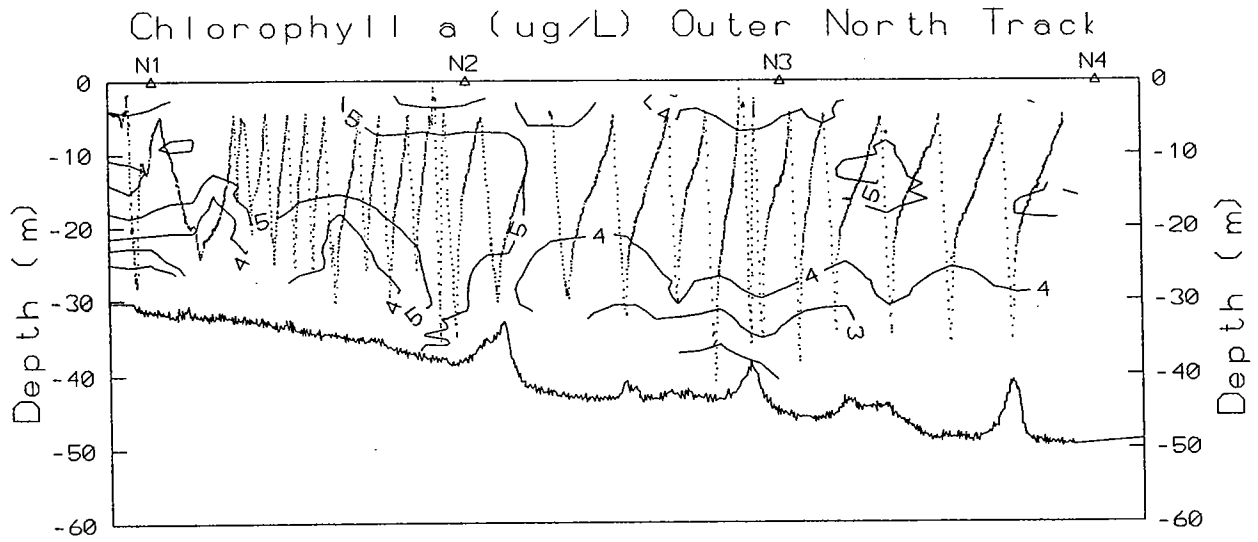


**Figure 3-40** Vertical section contours of fluorescence (as  $\mu\text{g Chl L}^{-1}$ ) generated for tow-yos in February 1992. The view is towards the North.

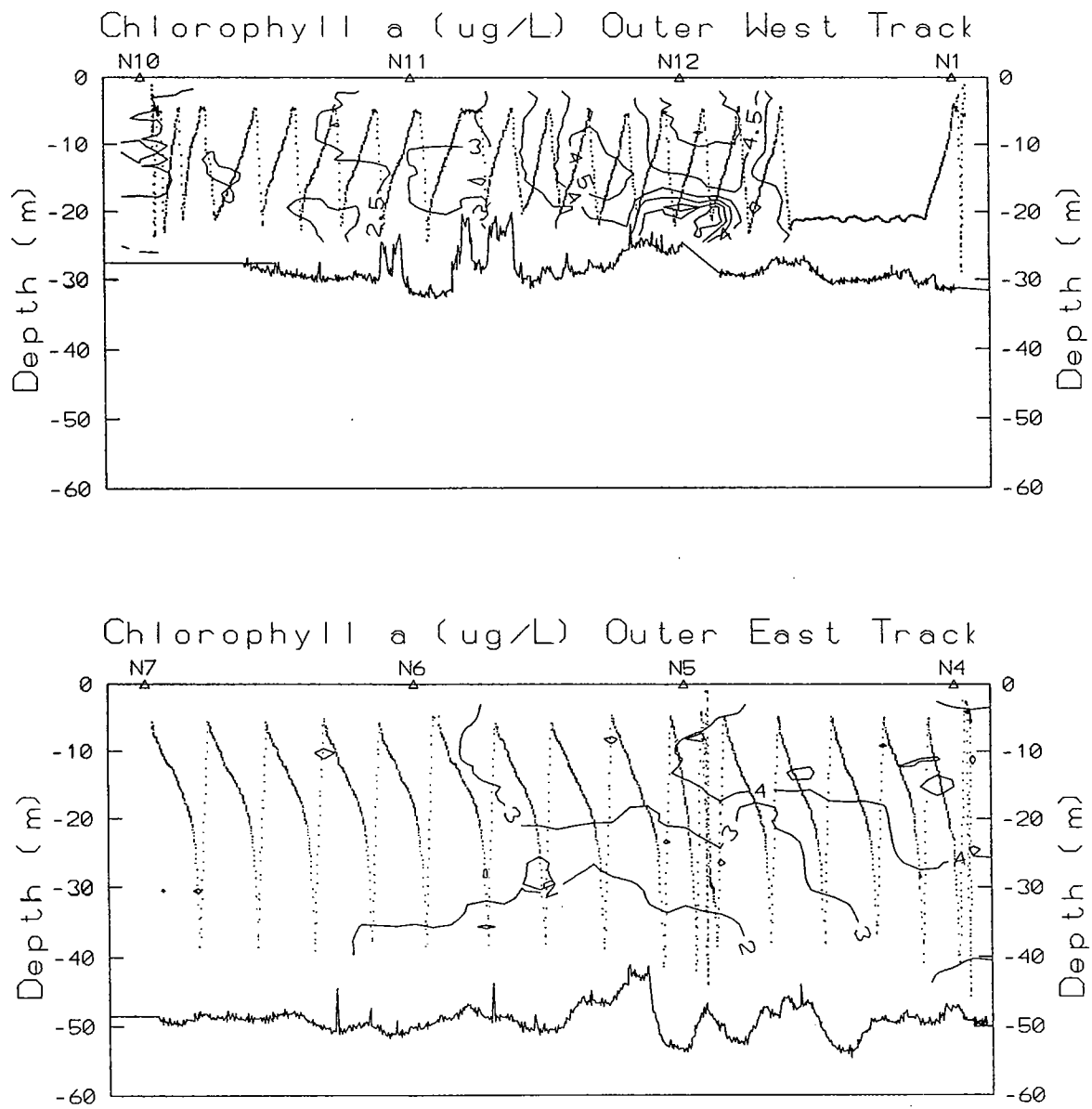


**Figure 3-41** Vertical section contours of fluorescence (as  $\mu\text{g Chl L}^{-1}$ ) generated from tow-yos in February 1992. The view is towards the Boston Harbor.

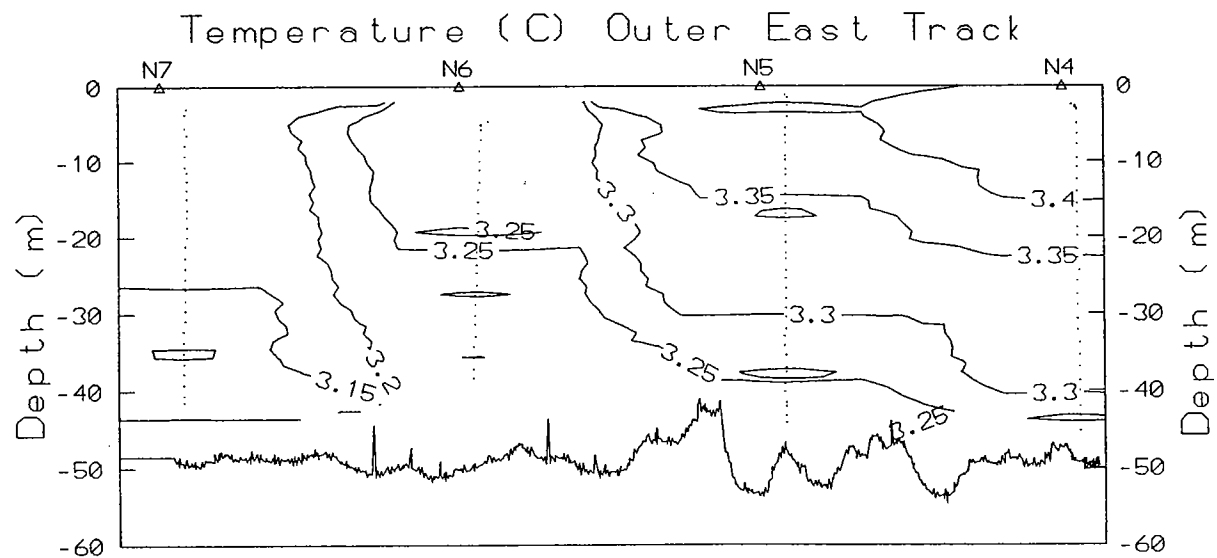
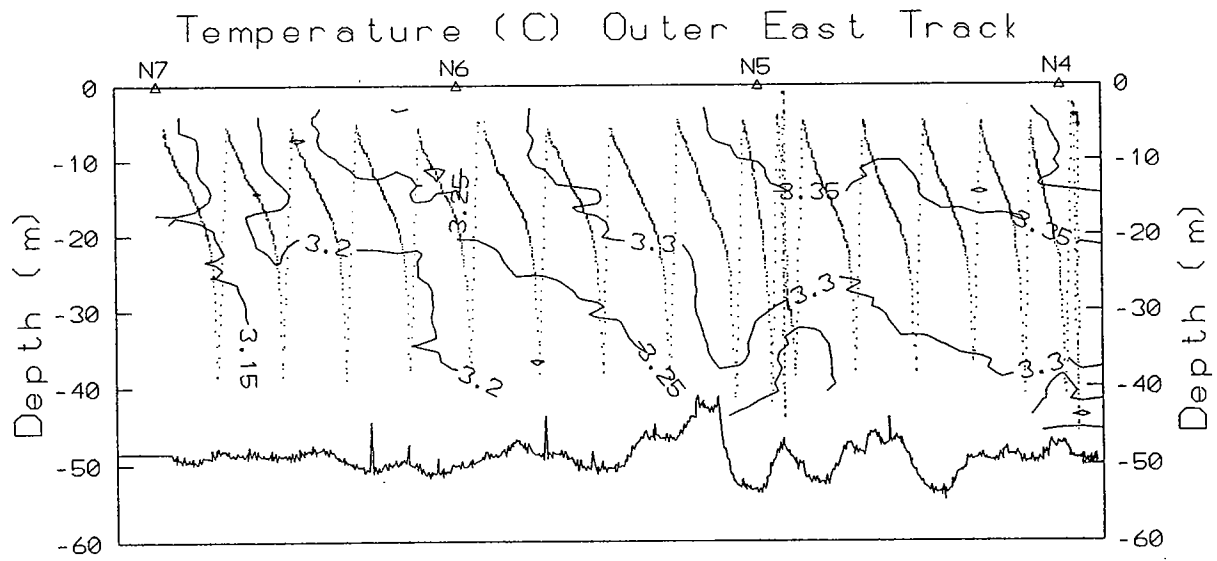


**Figure 3-42 Comparison of contours of temperature generated from tow-yos sampling (top) vs. vertical casts at four stations along track, all nearfield day 2.**

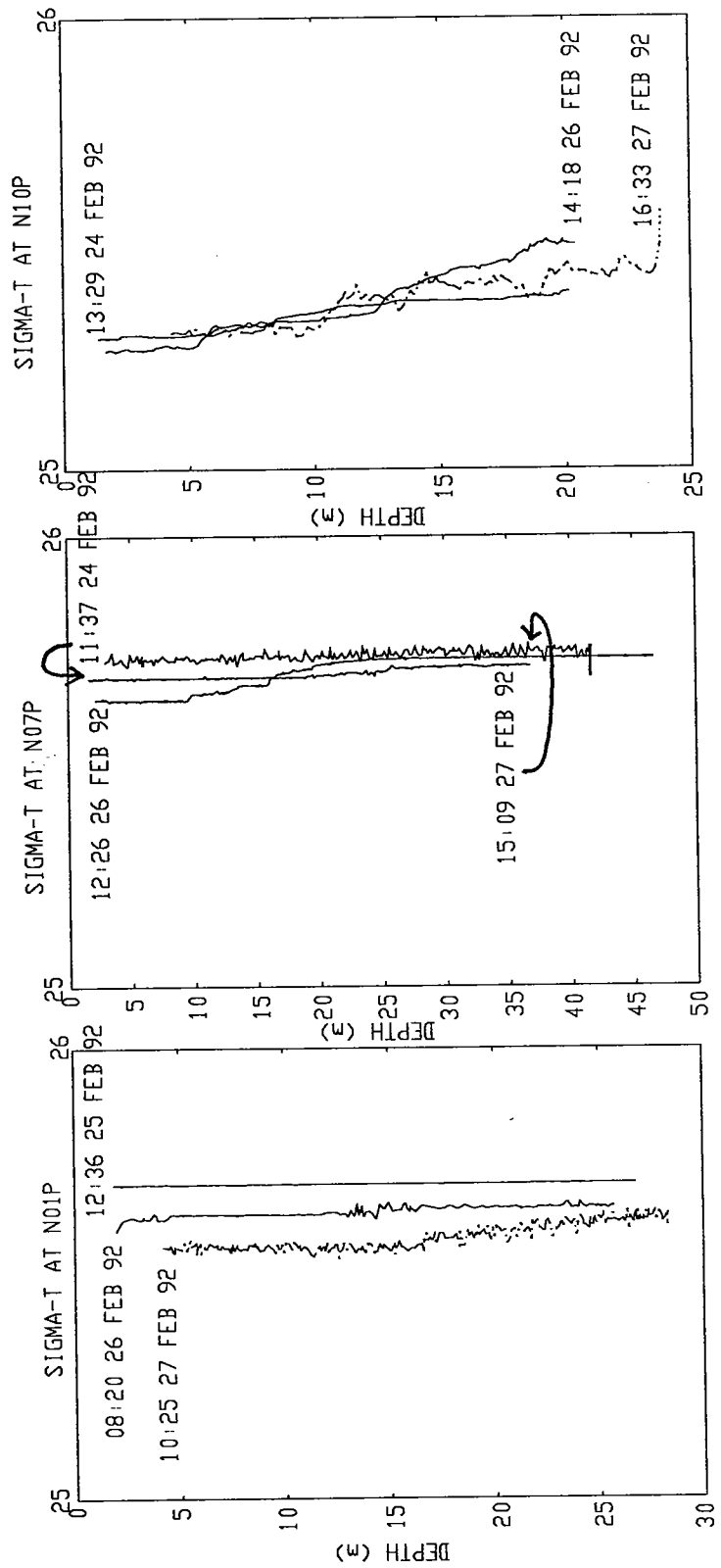


**Figure 3-43** Short-term variability at three corner stations of the nearfield grid in February 1992. Data on  $\sigma_T$  from three vertical casts are shown.

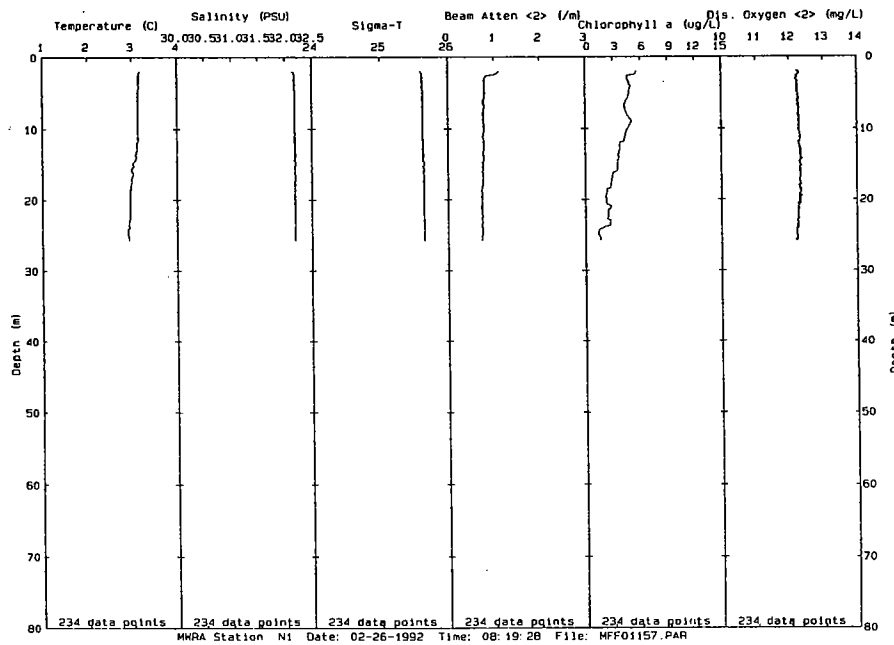
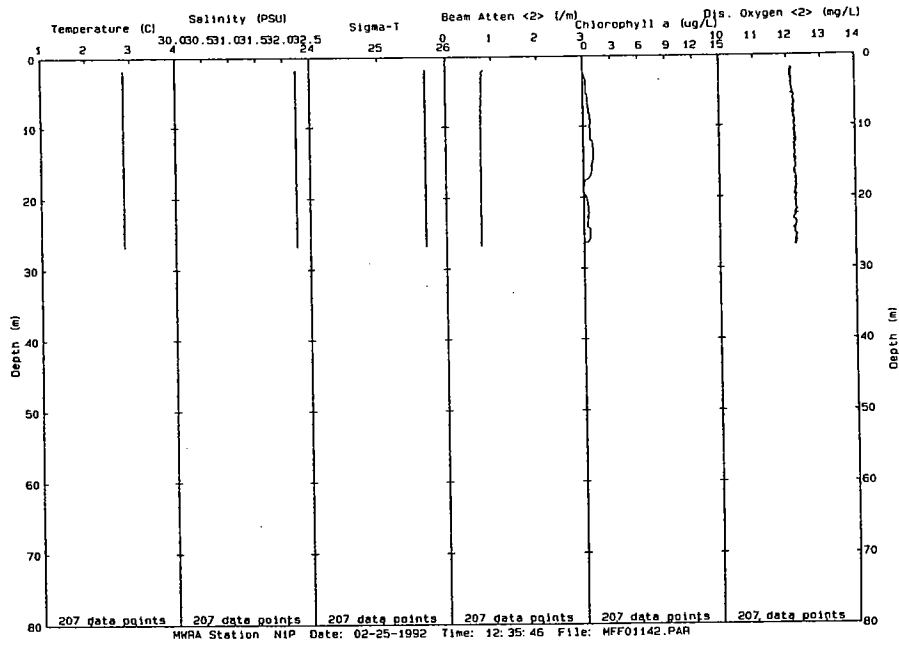


**Figure 3-44** Change in vertical profiles of parameters in 20 hours at station N1P. Data are those used to generate top plot for  $\sigma_T$  in Figure 3-43; note large difference in chlorophyll with very small change in other parameters.





## 4.0 MARCH 1992 SURVEYS

### 4.1 Farfield Survey Results

#### 4.1.1 Horizontal Distribution of Water Properties

During the March survey, temperature contours from Nahant to about Marshfield roughly paralleled the coast, with colder water hugging the shore (Figure 4-1). Contours south of Marshfield bent outward, making Cape Cod Bay look like a large, fairly homogeneous cell of cold surface water. Thus, similar to February, the general regional gradient of temperature was a decrease north-to-south down the mainstem of Massachusetts/Cape Cod Bays. Coldest temperatures, however, were around the mouth of Boston Harbor. There was also a mild intrusion of warmer surface water from offshore through the southeast corner of the nearfield region, along with a corresponding extrusion of cooler water ( $3^{\circ}\text{C}$  isopleth) in the middle of the nearfield grid.

This temperature variability was more pronounced than that shown by the associated salinity distribution in this region (Figure 4-2). Most of Massachusetts Bay that is deeper than about 30-40 m had a surface salinity greater than  $32.2^{\circ}/_{\text{oo}}$ . Fresher water from the Boston Harbor area ( $<31^{\circ}/_{\text{oo}}$ ) and paralleling the coast ( $31\text{-}32^{\circ}/_{\text{oo}}$ ) was evident. All four Cape Cod Stations had similar surface salinities, between 32 and  $32.2^{\circ}/_{\text{oo}}$ .

The surface water density pattern shown by  $\sigma_{\text{T}}$  had a sharp shore-to-sea gradient from Boston Harbor out to the nearfield region (Figure 4-3), with the gradient weakening as one progressed south along the South Shore. Other than a minor anomaly in the nearfield, the gradient was rather smooth and there was little variation throughout most of Massachusetts and Cape Cod Bays.

The pattern for beam transmittance showed local highs in attenuation along the Boston Harbor mouth, but also just off the southeast corner of the nearfield and at Station F2P in Cape Cod (Figure 4-4). The latter two areas corresponded with higher fluorescence readings (Figure 4-5). Slightly higher fluorescence was also apparent outside the mouth of South Boston Harbor extending to Cohasset. Extracted chlorophyll samples showed that nearshore Boston Harbor Stations (F23P, F25, and F13P) had high values that may have been underestimated by *in situ* fluorescence (discussed further below).

As in February, the latitudinal pattern in DIN showed the general north-to-south decrease (Figure 4-6). Coastal waters in the Boston Harbor area were higher in DIN than the nearfield, but the northeast corner of the nearfield also had relatively high DIN. Enrichment of ammonia from Boston Harbor was apparent,

though less pronounced than in February (due to higher chlorophyll, see below), and ammonia was high out of Plymouth-Duxbury Bay (Station F3) as well as at the Northern transect area (Figure 4-7).

The nitrate ( $\text{NO}_3$ ) pattern for surface waters was complex; there was some general latitudinal decrease from north to south (Figure 4-8). There was also a general gradient of decreased  $\text{NO}_3$  from offshore to nearshore; but the area exceptions to this trend included Boston Harbor and outside of Plymouth (Station F3). The enrichment of  $\text{NO}_3$  at the mouth of Boston Harbor appeared less strong than it had during February.

Other than one anomalous (and suspicious) high value which biased the contours in the middle of the nearfield region,  $\text{PO}_4$  again strongly followed DIN throughout the Bays (Figure 4-9). Silicate more strongly mimicked  $\text{NO}_3$ , with offshore having highest concentrations of the surface waters in the region (Figure 4-10).

#### 4.1.2 Water Properties Along Selected Vertical Sections

The same four transects (1=Northern transect, 2=Boston-Nearfield transect, 3=Cohasset transect, and 4=Marshfield transect) from shore that were examined in February were reexamined for the March cruise (Figures 4-11, 4-12, 4-13; other plots are given in Appendix E).

Conditions during this cruise were very cold and seas were rough, and apparently had caused some offshore cooling and continued vertical mixing. There was a shoreline coastal cell of colder, fresher, less dense water at each transect, but this was only pronounced at transects 2 and 3. Offshore waters, identified by a  $\sigma_T$  of 25.7 were closer to shore in most cases compared to February. For example, the physical-chemical gradient from Boston Harbor was only evident to the western third of the nearfield. Even so, a DIN gradient from the Harbor outward to the nearfield was seen (Figure 4-13). Most of the nearfield along the Boston-Nearfield transect appeared uniform in surface DIN concentration, with higher values both inshore and offshore. There appeared to be a fluorescence maximum close to the Harbor, but the surface of the mid-nearfield was remarkably uniform (Figure 4-12). The strong coastal cell that had been observed in February to radiate outward may have been compressed towards shore. In any event, the observed pattern was a fairly uniform distribution for most parameters across transects and few striking vertical or latitudinal features.

### 4.1.3 Analysis of Water Types

High-resolution *in situ* hydrographic data showed that there was again a low temperature, lower salinity coastal water type in the region. Surface salinity at the mouth of Boston Harbor was lower than in February. Figure 4-14 shows the composite data that suggest that the physical distinction between coastal and offshore water was very sharply defined and that there were at this time few distinct features at the northern transect, or at any Cape Cod Bay stations such as had been seen in February (Table 3-1).

High beam attenuation was associated with stations around Boston Harbor. Therefore, a strong relation of beam attenuation with salinity and  $\sigma_T$  was apparent across the region (Figure 4-14). Fluorescence varied over a small range, some of the highest points were just outside of the Harbor, but otherwise there was no striking coastal/offshore distinction. Excepting stations that were not visited, we used the same geographic groupings as we had in February to compare different areas (Figure 4-15).

Nutrient analyses (Figure 4-15 through Figure 4-17) showed, in comparison to February, many lower N/P ratios, with wider variance in the nearfield. Again, relatively higher  $\text{SiO}_4$  was detected in offshore and Northern transect waters, and lower concentrations of silicate and nitrate were found outside the Boston Harbor area. The generally larger scatter in the nutrient vs. nutrient plots is probably a result of the considerable mixing of waters that had occurred, but also a result of the phytoplankton in the northern region depleting the dissolved nutrients more actively. Therefore, some of the previous water type distinctions based on dissolved inorganic nutrients were less strong at this time.

The two end members of water, characterized by salinity or  $\sigma_T$ , and which seemed to meet in the nearfield — the offshore and coastal waters — had for the most part similar ranges of DIN, ammonia, and phosphate (Figures 4-18 through 4-20).

Silicate concentrations for near-coastal Harbor waters remained strongly different from those in more offshore waters (Figure 4-21); this again was due primarily to  $\text{SiO}_4$  concentrations in deeper water, rather than surface water. Mixing of offshore and inshore waters could produce many combinations of nutrient ratios and concentrations at a selected salinity or  $\sigma_T$ . Thus, the scatter observed in plots versus salinity may be partly due to this mixing.

In spite of preserved mixing and observed scatter, total nitrogen remained relatively high outside Boston Harbor, as did DIN + PON (Figures 4-22, 4-23). Again, these variables (as opposed to dissolved forms alone) reflect in part incorporation of DIN into plankton and thus tend to be a more conservative tracer. Even so, these variables would be non-conservative with sedimentation losses. The temporal changes around Boston Harbor could indicate some sinking, for the slopes of total N and DIN + PON relative to salinity changed from February to March. N4P stood out as somewhat high; it is curious that this

occurred with a blue-green (Cyanophyceae) bloom (see below) and thus it is tempting to speculate that N-fixation was active in this population, creating higher N concentrations than expected for a given salinity level by drawing N<sub>2</sub> from the atmosphere into the seawater nutrient cycle. Note, however, the same parameters for most other BioProductivity stations did not change markedly during this period.

In summary, the types of water found in the Massachusetts and Cape Cod Bays region changed considerably over the month of March (compare Table 4-1 and Table 3-1).

#### 4.1.4 Distribution of Chlorophyll and Phytoplankton

In March, chlorophyll concentrations measured in discrete samples at BioProductivity stations were highest ( $> 3 \mu\text{g L}^{-1}$ ) at the mouth of Boston Harbor (F25, F23P) and at the eastern side of Cape Cod Bay (F2P) (Figure 4-24). Next highest was off Cohasset (F13P), where surface values were  $\sim 2.3 \mu\text{g L}^{-1}$ . The high values outside Boston Harbor were not evident in the fluorescence data (Figure 4-5). In calibrating the fluorometer, it was clear that the chlorophyll measurements at these stations were above the main regression line (Appendix B). The high beam attenuation at this location may have caused an interference with the fluorescence measurements.

The lowest chlorophyll values were at Station N1P ( $< 1 \mu\text{g L}^{-1}$ ). Otherwise, concentrations were in the range of  $1\text{-}2 \mu\text{g L}^{-1}$  and little spatial pattern was evident (Figure 4-24).

In general, the chlorophyll levels between surface and deeper ( $\sim 10\text{-}23$  m) samples were not different, reflecting well-mixed conditions (Figure 4-25). Once again there was similarity in total cell counts, between surface and deeper water, as well as similar species composition.

Total phytoplankton abundance was high at stations where chlorophyll was also high (Figure 4-26). Station F2P levels exceeded  $10^6$  cells L<sup>-1</sup> and Station F23P levels approached  $10^6$  cells L<sup>-1</sup>. Most other stations were in the range of  $\sim 0.5$  to  $0.7 \times 10^6$  cells L<sup>-1</sup>. However, cell counts were also high ( $> 10^6$  cells L<sup>-1</sup>) at Station N4P, where chlorophyll was only intermediate ( $\sim 2 \mu\text{g L}^{-1}$ ). Curiously, this station was dominated by a blue-green (Cyanophyceae); perhaps it's amount of chlorophyll per cell was less than for the diatoms that were dominant at other stations (Figure 4-27).

Figures 4-28 through 4-31 show examples of the compositional similarity between surface and deeper samples. Only minor, rare species deviated strongly from a 1:1 relationship, with the exception of the blue-green at N4P (code "O2", Figure 4-28), which were much more abundant at the surface. With respect to total N or DIN + PON at this station and the possibility of N-fixation (Figures 4-22, 4-23), it was interesting to note that higher concentrations were at the surface, but not at depth.

Further inspection of Figures 4-28 to 4-31 shows that many of the same diatom species are dominant at the different stations and that microflagellates (code "U1") as a group were usually nearly as numerous as the most dominant diatoms.

With respect to species composition, as in February, a small group of diatom species could be found among the dominants at virtually all stations (Table 4-2). Microflagellates made up < 10% to about 39% of the total numbers, with lower percentages seen at higher chlorophyll concentrations and at both Cape Cod stations. The diatoms *Chaetoceros debilis* and (< 10 mm) *Chaetoceros* spp. were virtually ubiquitous. In general, a normal progression of diatom species succession from February appeared to be taking place.

The only distinctive features were the high relative numbers of the diatom *Leptocylindricus minimus* at both Cape Cod stations and the prevalence of blue-greens at N4P, as noted. Overall, the entire field, again in spite of detectable, but subtle, differences in water characteristics, was rather homogeneous in terms of dominant phytoplankton taxa and the overall community mix.

#### 4.1.5 Distribution of Zooplankton

During March, highest total numbers of zooplankton were observed at Station N4P, where high concentrations of blue-green (Cyanophyceae) were observed. Cape Cod Bay had slightly higher total numbers than the rest of the Massachusetts Bay Stations (Figure 4-32). In general, the abundance varied by a factor less than three across all the Stations ( $\sim 9$  to  $25 \times 10^3 \text{ M}^{-3}$ , a range about the same as the previous month — see Appendices K and L). Barnacle nauplii were again a strong component at F13P off Cohasset, but otherwise their numbers were diminished from February at nearshore Boston Harbor Stations. Copepod nauplii were a substantial contribution to total numbers, being over 40% of the total in Cape Cod Bay and usually roughly  $\frac{1}{3}$  of the total elsewhere. Roughly another  $\frac{1}{3}$  of the total was copepods, with barnacle nauplii and "other" taxa contributing the remainder.

Among the "other" category were *Oikopleura*, the appendicularian again present at N4P, as well as pteropods. These were both a pronounced feature of the zooplankton community at N4P, along with *Metridia lucens*, a copepod more typical of "oceanic" waters. *Metridia* was not observed at any other stations.

Pteropods were also a dominant taxa at N7P, the southeast corner of the Nearfield. In general, the same compliment of expected, typical "shelf" copepod species were present as had been in February. *Oithona similis* and *Paracalanus parvus* were once again ubiquitous as the two most dominant taxa at every

station except N4P and N7P, where *Oithona similis* ranked first, and pteropods ranked second numerically.

#### 4.1.6 Whole-Water Metabolism Incubations

Results of metabolism incubations for the cruise, by and large, were similar to February. Once again Station N4P is used as the example of a case where the hyperbolic model could be fit to describe the P-I curve fairly well (Figure 4-33). The majority, but not all stations, were about as well fit as this case. The data for most stations and depths showed the expected light saturation and, for these,  $P_{\max}$  could be estimated from graphs (Appendix H).

Graphically estimated,  $P_{\max}$  ranged from about 10-40  $\mu\text{g O}_2$  ( $\mu\text{g chlorophyll}$ )<sup>-1</sup> hr<sup>-1</sup>, or about the same as February. Whole-water rates for  $P_{\max}$ , not normalized for chlorophyll, ranged from about 18-90  $\mu\text{g O}_2 \text{ L}^{-1} \text{ hr}^{-1}$ , and were highest as F23P, which had the highest measured chlorophyll.

With minor exception, (e.g., N16P at the chlorophyll maximum; see Appendix H), curves showed saturation by about 250  $\mu\text{E m}^{-2} \text{ sec}^{-1}$  or less. As in February, the initial rise was sharp, but it was difficult to discriminate differences for  $\alpha$  among samples due to the steepness and the variability among points at very low light levels.

The same stations from which light extinction was described for February are shown for March in Figure 4-34. The slope appeared sharpest through the whole water column at F23P at the mouth of Boston Harbor; this was expected since beam attenuation there was very high. This station contrasted, for example, with clearer waters in Cape Cod Bay (F1P and F2P), graphically below the surface few meters. The 1% light level for this selection of stations ranged from about 12-22 m.

For many stations measured at midday between about 1000 and 1500h, the top two meters had *in situ* light levels near or above 200  $\mu\text{E m}^{-2} \text{ hr}^{-1}$ . Thus, the threshold for allowing maximum productivity was approached for the very surface waters (~ 1 to 5 m) during midday at many stations during this cruise. Below the surface, the *in situ* rates, in theory, would have been light limited and followed the initial rise portion of the P-I curve.

Dark respiration, with station temperatures similar to or colder than February, was not measurable at any station (Appendix H).

station except N4P and N7P, where *Oithona similis* ranked first, and pteropods ranked second numerically.

#### 4.1.6 Whole-Water Metabolism Incubations

Results of metabolism incubations for the cruise, by and large, were similar to February. Once again Station N4P is used as the example of a case where the hyperbolic model could be fit to describe the P-I curve fairly well (Figure 4-33). The majority, but not all stations, were about as well fit as this case. The data for most stations and depths showed the expected light saturation and, for these,  $P_{\max}$  could be estimated from graphs (Appendix H).

Graphically estimated,  $P_{\max}$  ranged from about 10-40  $\mu\text{g O}_2$  ( $\mu\text{g chlorophyll}$ )<sup>-1</sup> hr<sup>-1</sup>, or about the same as February. Whole-water rates for  $P_{\max}$ , not normalized for chlorophyll, ranged from about 18-90  $\mu\text{g O}_2 \text{ L}^{-1} \text{ hr}^{-1}$ , and were highest as F23P, which had the highest measured chlorophyll.

With minor exception, (e.g., N16P at the chlorophyll maximum; see Appendix H), curves showed saturation by about 250  $\mu\text{E m}^{-2} \text{ sec}^{-1}$  or less. As in February, the initial rise was sharp, but it was difficult to discriminate differences for  $\alpha$  among samples due to the steepness and the variability among points at very low light levels.

The same stations from which light extinction was described for February are shown for March in Figure 4-34. The slope appeared sharpest through the whole water column at F23P at the mouth of Boston Harbor; this was expected since beam attenuation there was very high. This station contrasted, for example, with clearer waters in Cape Cod Bay (F1P and F2P), graphically below the surface few meters. The 1% light level for this selection of stations ranged from about 10 - 20m.

For many stations measured at midday between about 1000 and 1500h, the top two meters had *in situ* light levels near or above 200  $\mu\text{E m}^{-2} \text{ hr}^{-1}$ . Thus, the threshold for allowing maximum productivity was approached for the very surface waters (~ 1 to 2 m) during midday at many stations during this cruise. Below the surface, the *in situ* rates, in theory, would have been light limited and followed the initial rise portion of the P-I curve.

Dark respiration, with station temperatures similar to or colder than February, was not measurable at any station (Appendix H).

## **4.2 Nearfield Survey Results**

### **4.2.1 Horizontal Distribution of Water Properties**

The high resolution sampling for nutrients in the nearfield (Figure 4-35) demonstrated significant variation from the broad-scale farfield plots (Figure 4-6 through 4-10). However, an intrusion of nutrients (especially  $\text{NH}_4$ ,  $\text{PO}_4$  and  $\text{SiO}_4$ ) into the nearfield at the surface of the southwest corner was suggested. It is suspected that, as for February, rather than a difference in scales of resolution, the main difference between this day and the preceding farfield data was due to dynamic processes.

The associated salinity field on the day nutrients were measured (Figure 4-36) indeed showed that a tongue of less saline water, pronounced more at the surface, was at the corner of the nearfield. This finding confirmed that higher nutrient values were associated with fresher water.

### **4.2.2 Water Properties Along Vertical Transects and Analysis of Small-Scale Variability**

Figures 4-37 and 4-38 show the salinity field measured in the nearfield during towing of the outer box, an activity conducted the day after that represented in Figure 4-36. The towing started in the morning between stations N10 and N11, proceeded on the Outer West Track, around the box, and returned to N10 in the evening along the Outer South Track. During this time, the vertically well-mixed and early saline water near N10 in the morning had changed by the evening to be similar to the salinity tongue surfacing at this corner from the coastal direction the previous day. Such temporal comparisons give strong evidence for diurnal and, probably tidal, dynamics in the nearfield and illustrate the high physical variability that seems to occur in this region.



**TABLE 4-1. ANALYSIS OF WATER TYPES**

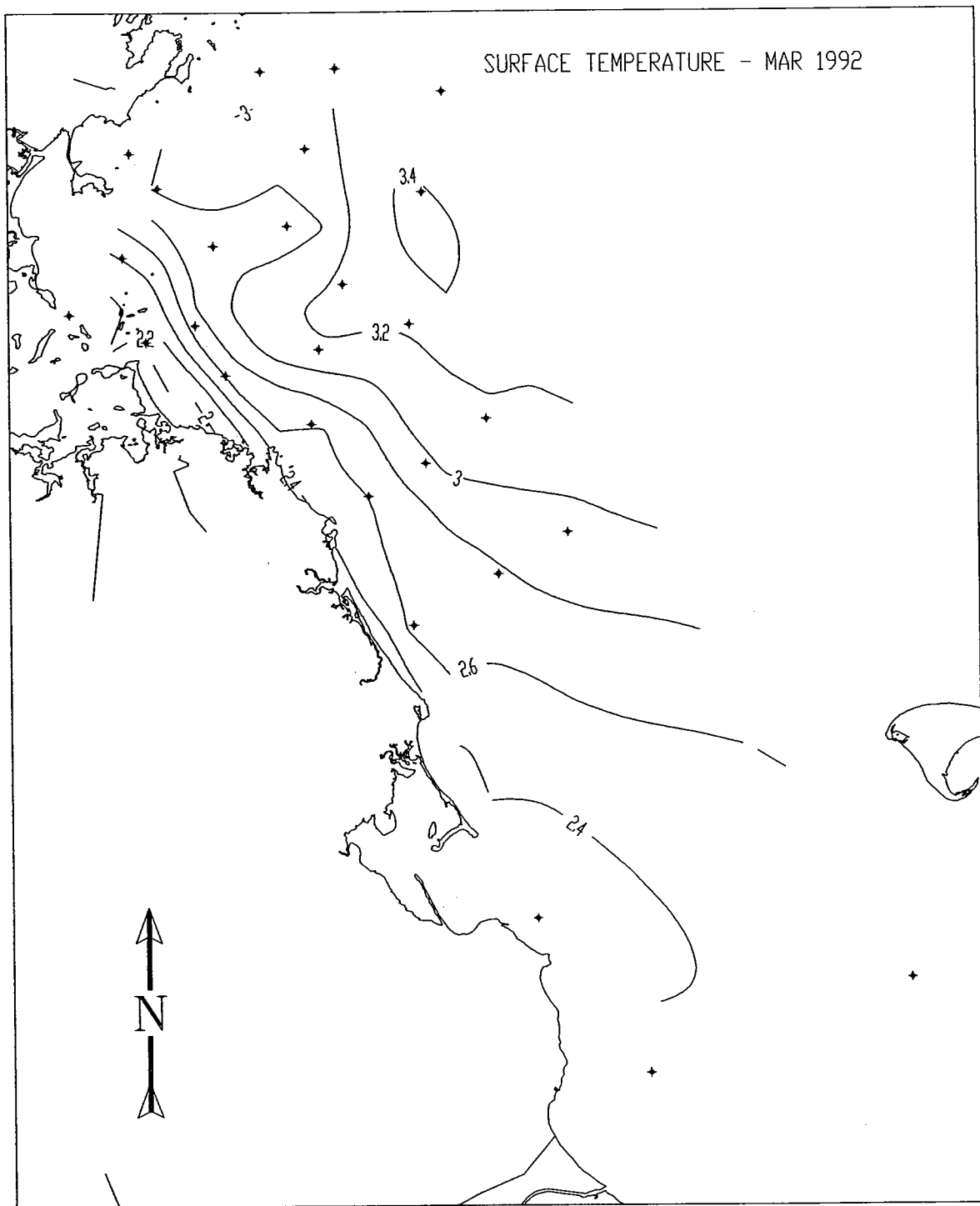
Water Type		Characteristics by Parameter				
Classification	Geographic Descriptor	T	S	Beam Attenuation	Chlorophyll Fluorescence	Nutrients
Coastal	Most of nearshore western Mass. Bay (~ less than 30m)	Cold	Freshest	High	Mixed, Intermediate	Intermediate
Northern Transect	Transect along northern entrance to Mass. Bay, (F20-F22) surface water	_____ not distinct _____ feature at this time				
Nearfield	Within nearfield Sampling Grid	Inter-mediate	Most Saline	Mixed	Mixed	Mixed, most with high SiO <sub>4</sub>
Offshore	Mainstem Mass. Bay (~ greater than 40m)	Warm	Most saline	Low	Low	Intermediate, but high SiO <sub>4</sub>
Cape Cod	All Cape Cod Bay Stations	_____ like Coastal _____				

TABLE 4-2. TOP 5 DOMINANT PHYTOPLANKTON TAXA, EXCLUDING MICROFLAGELLATES AND CRYPTOMONADS, IN NEAR SURFACE SAMPLES COLLECTED IN MARCH, 1992

Species	Station												
	F1P	F2P	F13P	F23P	N1P	N10P	N20P	N16P	N7P	N4P			
<i>Skeletonema costatum</i>													
<i>Leptocylindricus minimus</i>	(1) 0.329	(1) 0.911			(5) 0.017	(5) 0.015		(3) 0.031	(2) 0.058	(5) 0.022			
<i>Chaetoceros debilis</i>	(2) 0.109	(2) 0.314	(2) 0.110	(3) 0.122	(1) 0.112	(1) 0.214	(1) 0.170	(1) 0.190	(1) 0.151				
<i>Thalassiosira nordenskioeldii</i>			(3) 0.058	(1) 0.244			(4) 0.022	(4) 0.022					
<i>Thalassionema nitzschoides</i>	(3) 0.081	(4) 0.105			(4) 0.029	(4) 0.035	(5) 0.019						
<i>Detonula confervacea</i>			(1) 0.132	(2) 0.167									
<i>Chaetoceros</i> spp. (<10 mm)	(5) 0.019	(5) 0.070	(4) 0.030	(4) 0.051	(2) 0.071	(2) 0.091	(2) 0.039	(4) 0.022	(4) 0.048	(2) 0.154			
<i>Thalassiosira gravida</i>													
<i>Chaetoceros socialis</i>		(3) 0.199	(5) 0.027		(3) 0.031	(3) 0.053	(3) 0.025	(2) 0.041	(3) 0.055	(4) 0.028			
<i>Rhizosolenia delicatula</i>	(4) 0.036												
<i>Chaetoceros</i> spp. (>10mm)									(5) 0.021				
Unid. centrales				(5) 0.042									
Cyanophyceae													(1) 0.590
<i>Chaetoceros decipiens</i>													(3) 0.084

() = rank

Number = millions of cells L



**Figure 4-1** Surface temperature ( $^{\circ}\text{C}$ ) in the region in March 1992. Data are from Appendix B, the surfacemost sample at all farfield survey stations, including the BioProductivity stations within the nearfield grid. The contour interval is  $0.2^{\circ}\text{C}$ .

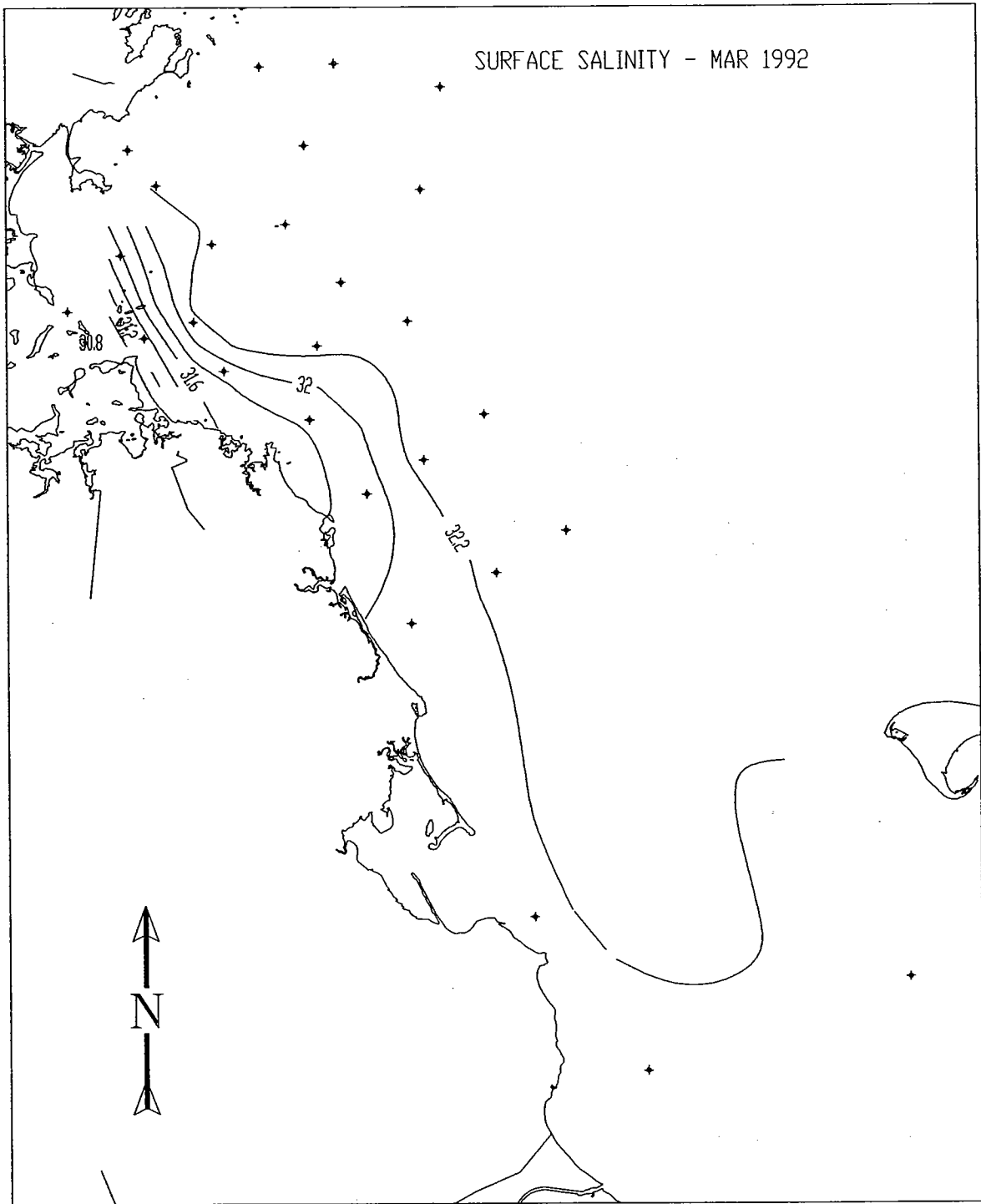


**Figure 4-2** Surface salinity (PSU) in the region in March 1992. Data are from Appendix B, the surfacemost sample at all farfield survey stations, including the BioProductivity stations within the nearfield grid. The contour interval is 0.2 PSU.

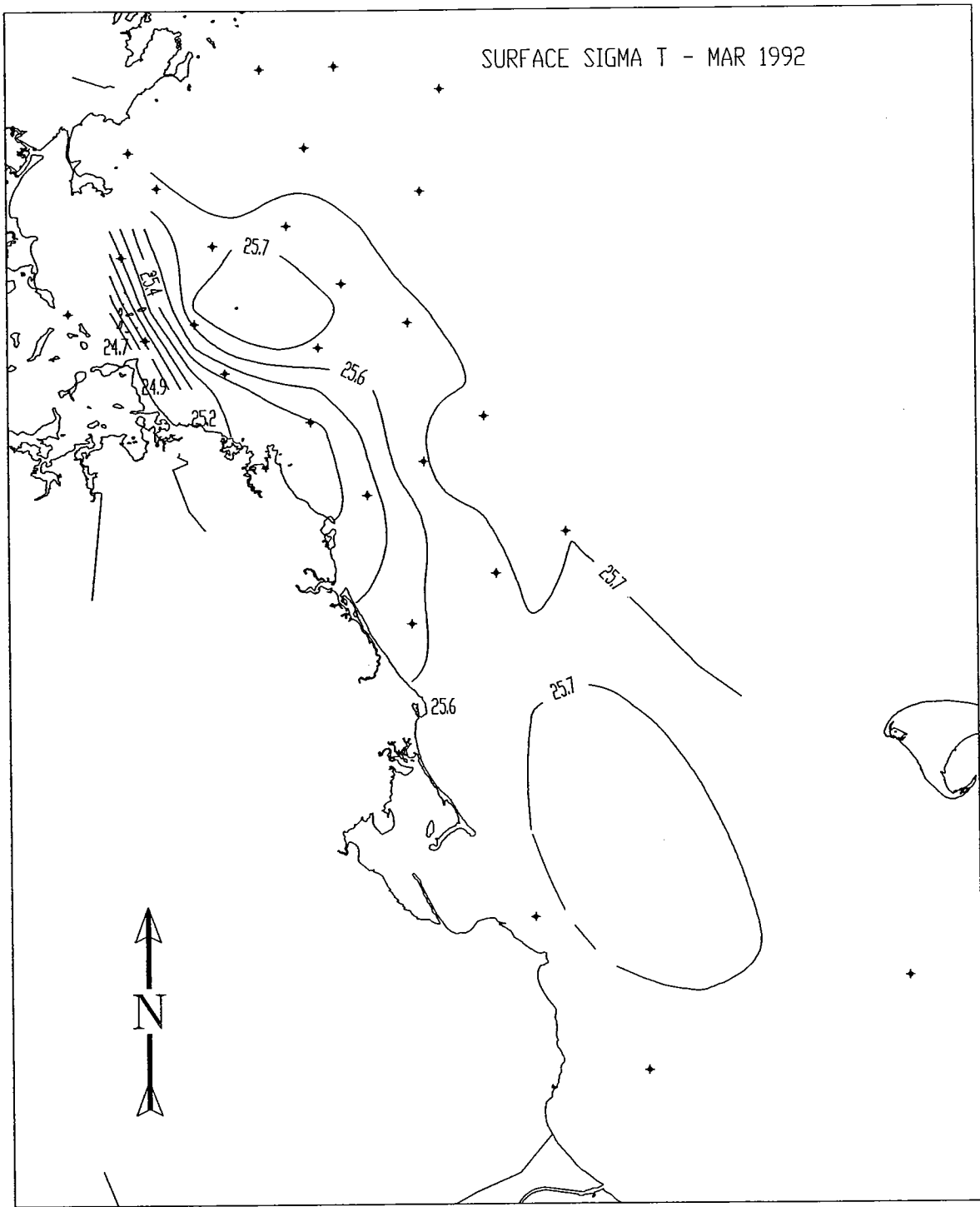


**Figure 4-3** Surface  $\sigma_T$  in the region in March 1992. Data are from Appendix B, the surfacemost sample at all farfield stations, including the BioProductivity stations within the nearfield grid. The contour interval is 0.1 units.

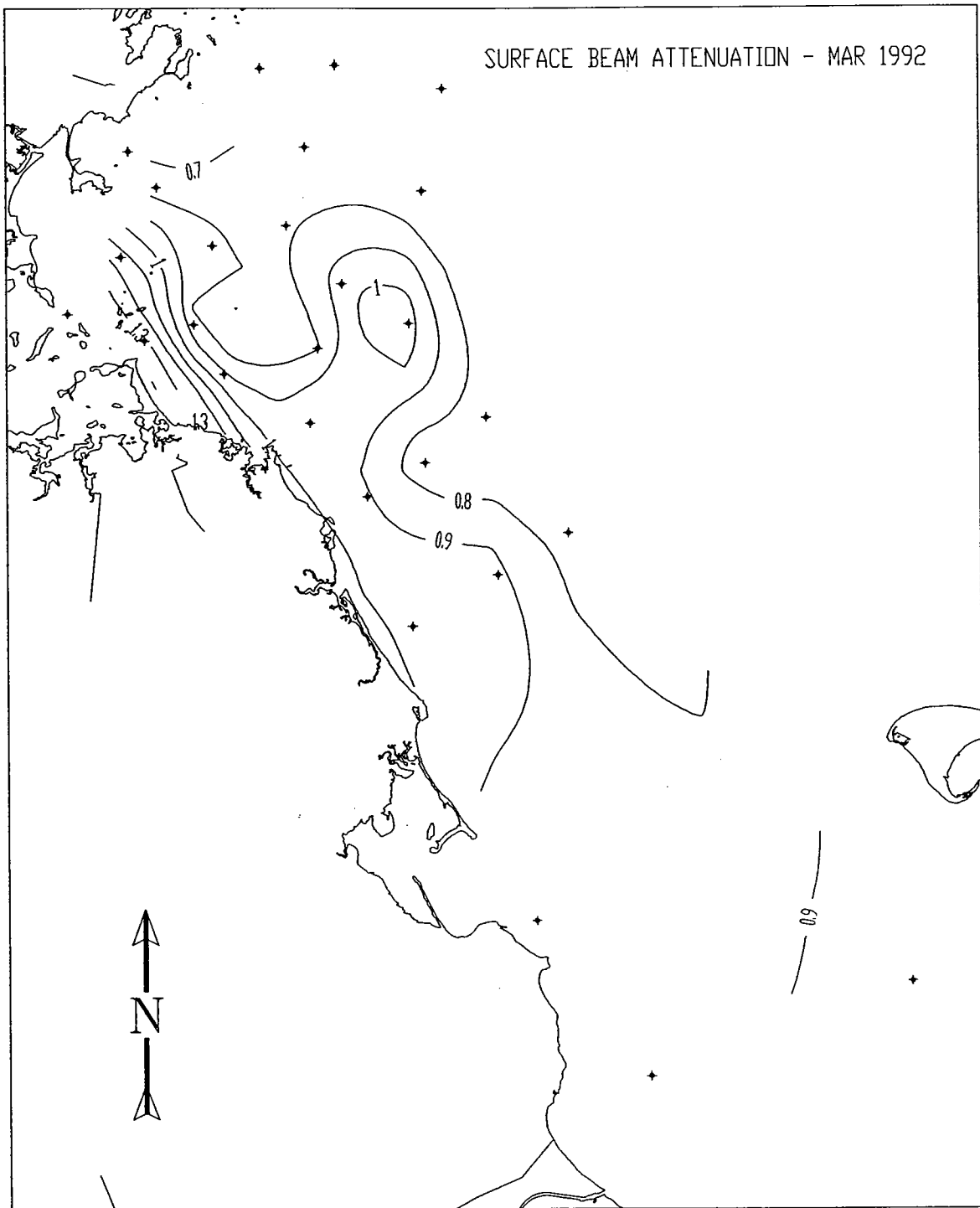


**Figure 4-4** Surface beam attenuation ( $m^{-1}$ ) in the region in March 1992. Data are from Appendix B, the surfacemost sample at all farfield survey stations, including the BioProductivity stations within the nearfield grid. The contour interval is  $0.1 m^{-1}$ .

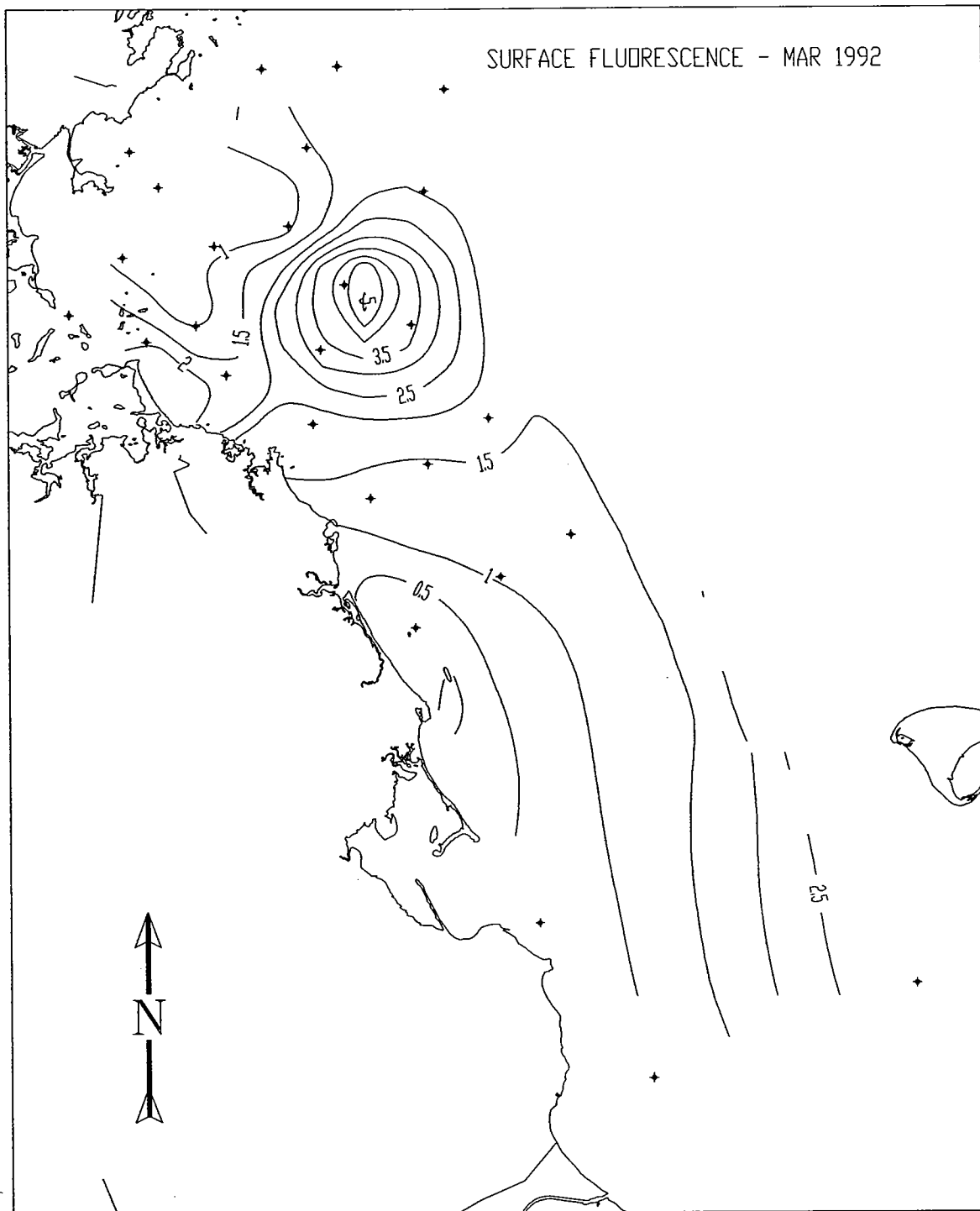


**Figure 4-5** Surface *in situ* fluorescence (as  $\mu\text{g Chl L}^{-1}$ ) in the region in March 1992. Data are from Appendix B, the surfacemost sample at all farfield survey stations, including the BioProductivity stations within the nearfield grid. The contour interval is  $0.5 \mu\text{g L}^{-1}$ .

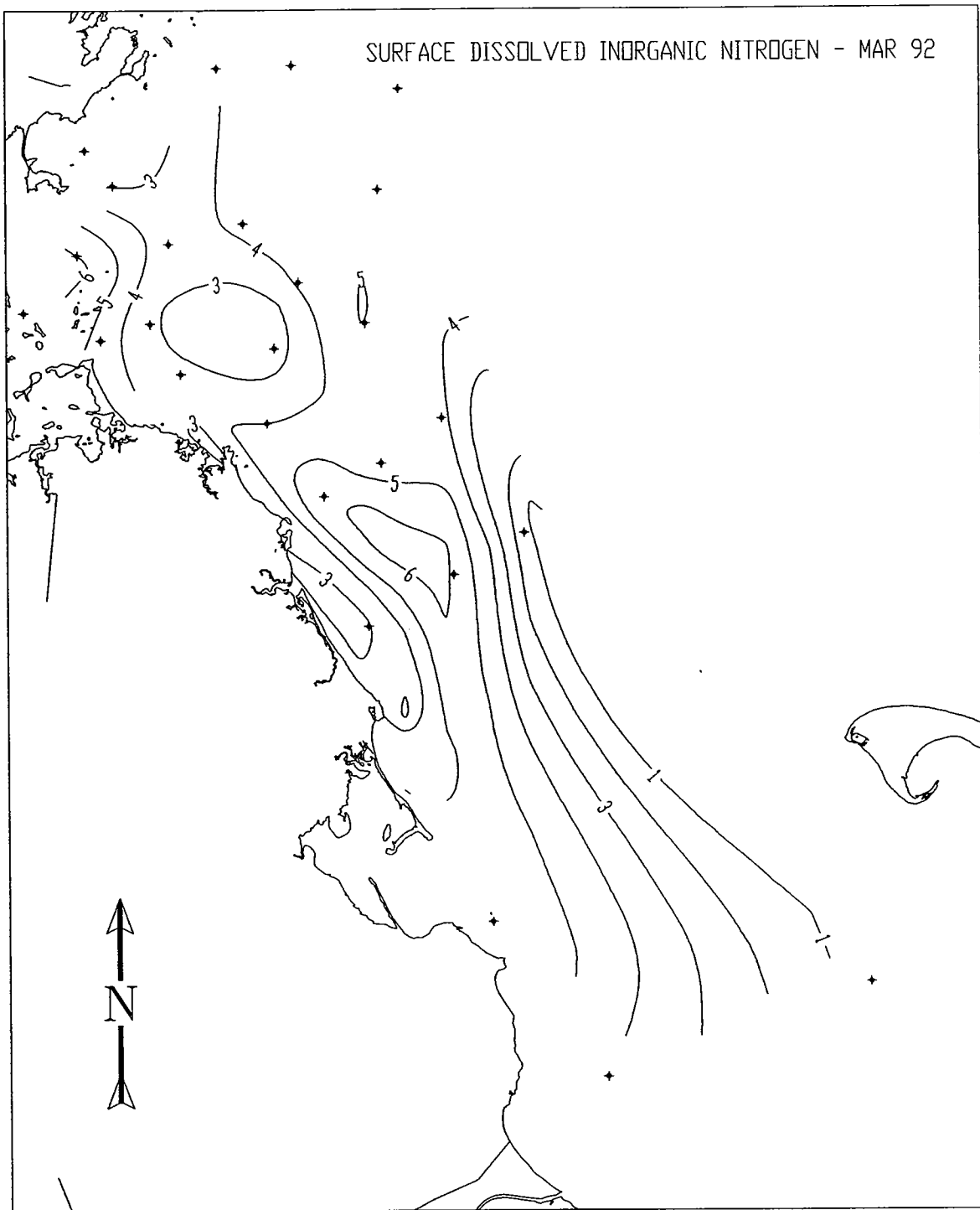


**Figure 4-6** Surface dissolved inorganic nitrogen (DIN  $\mu\text{M}$ ) in the region in March 1992. Data are from Appendix B, the surfacemost sample at all farfield survey stations, including the BioProductivity stations within the nearfield grid. The contour interval is 1.0  $\mu\text{M}$ .



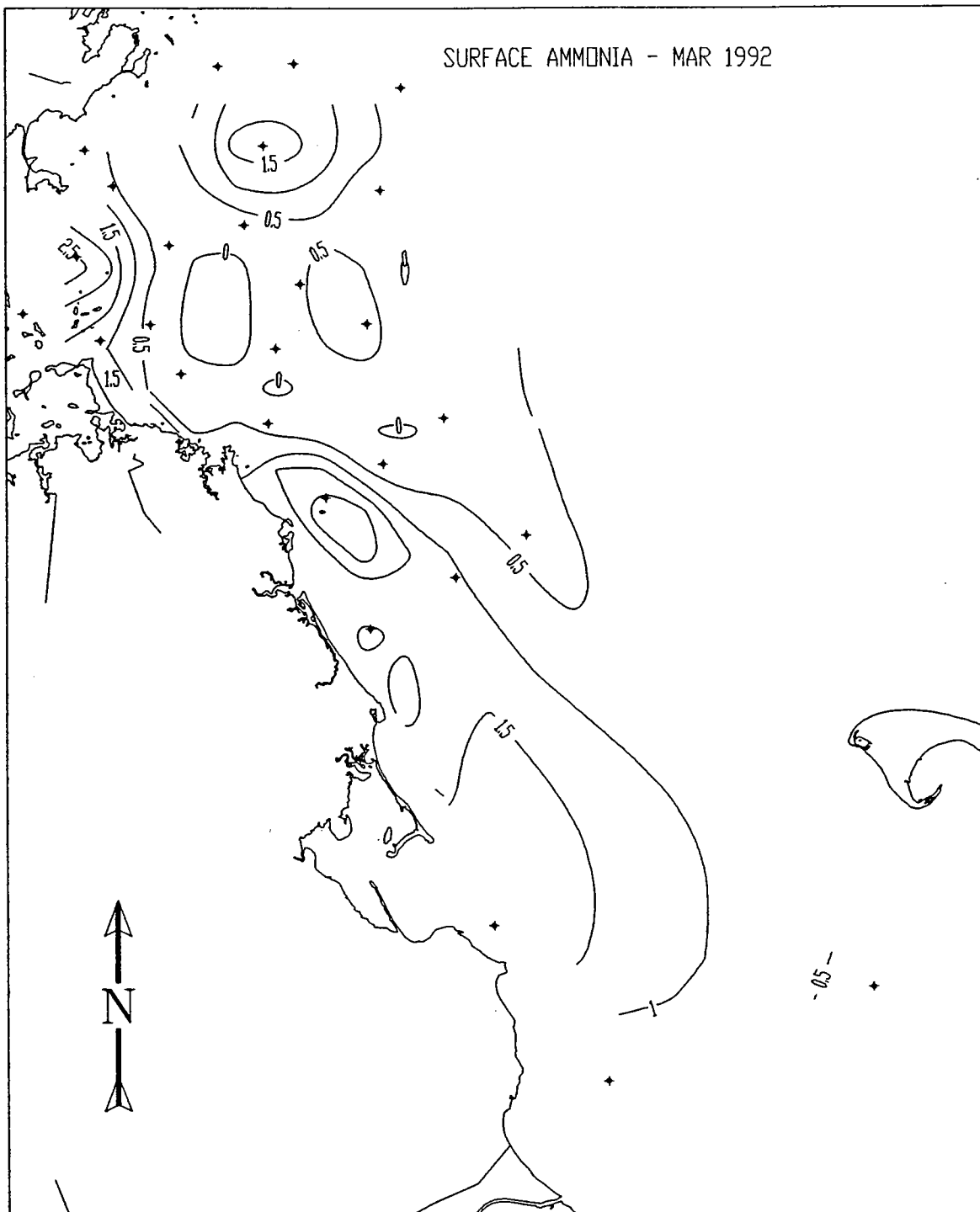


**Figure 4-7** Surface ammonia ( $\mu\text{M}$ ) in the region in March 1992. Data are from Appendix B, the surfacemost sample at all farfield survey stations, including the BioProductivity stations within the nearfield grid. The contour interval is 0.5  $\mu\text{M}$ .

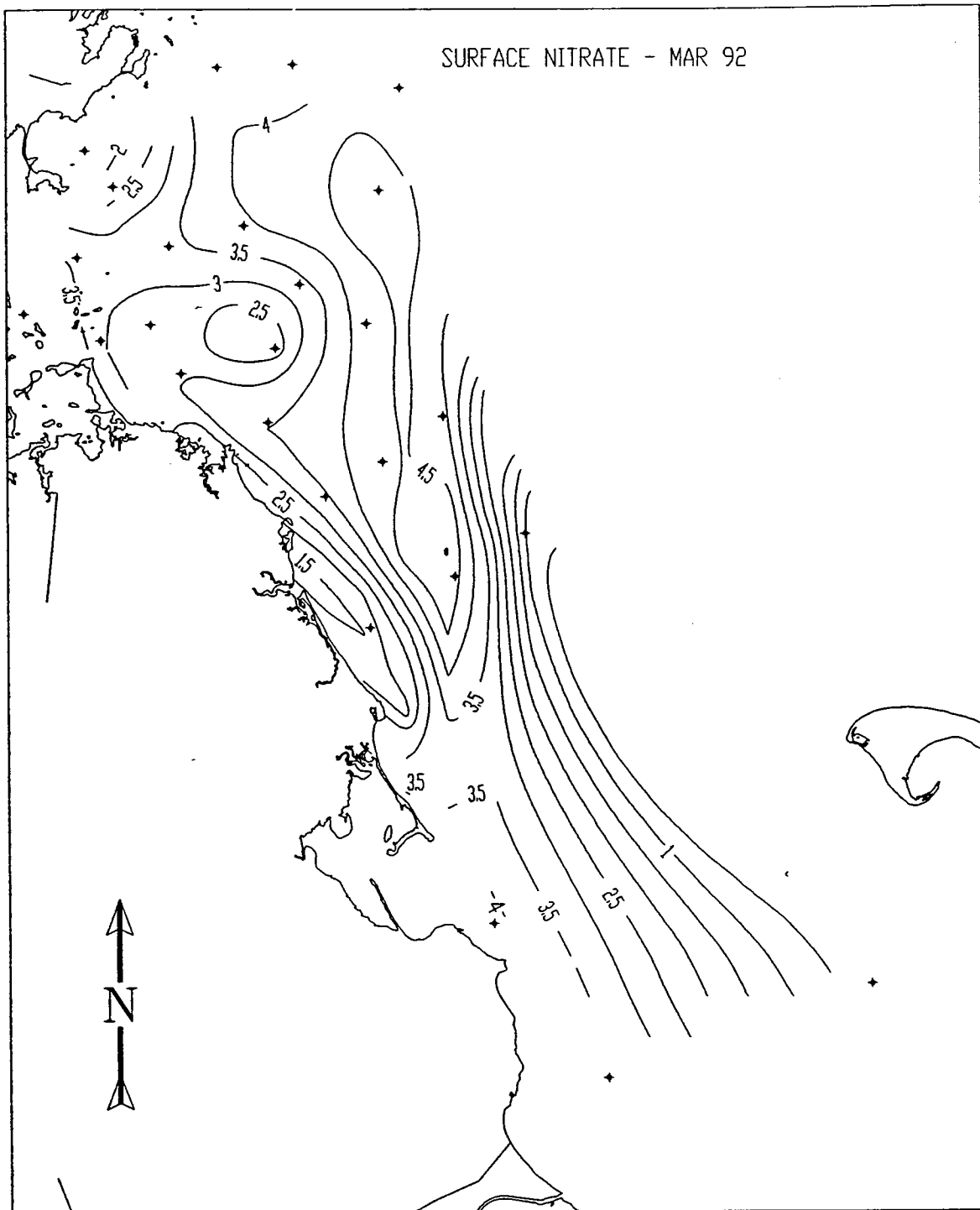


**Figure 4-8** Surface nitrate ( $\mu\text{M}$ ) in the region in March 1992. Data are from Appendix B, the surfacemost sample at all farfield stations, including the BioProductivity stations within the nearfield grid. The contour interval is 0.5  $\mu\text{M}$ .

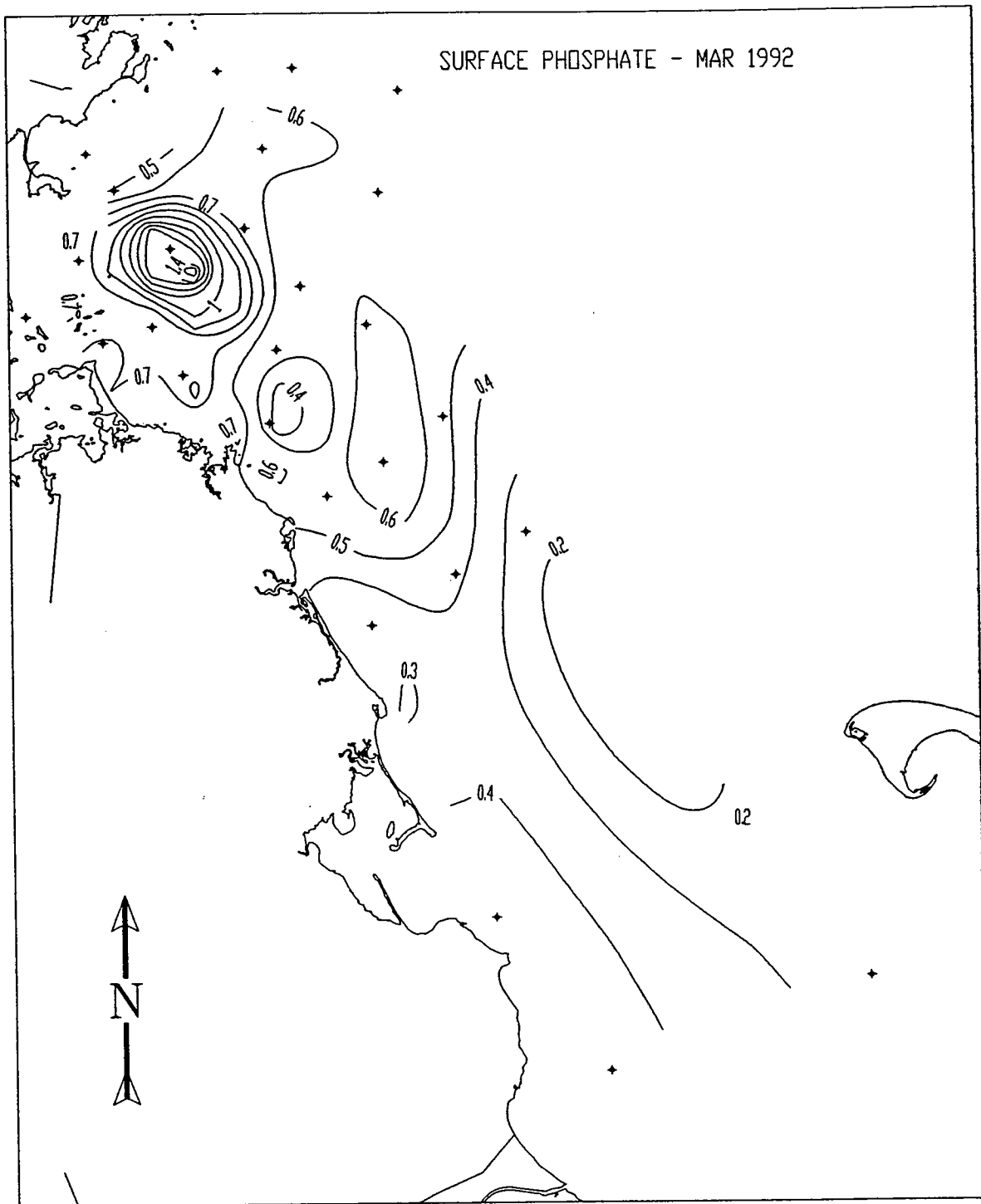


**Figure 4-9** Surface phosphate ( $\mu\text{M}$ ) in the region in March 1992. Data are from Appendix B, the surfacemost sample at all farfield survey stations, including the BioProductivity stations within the nearfield grid. The contour interval is 0.1  $\mu\text{M}$ .

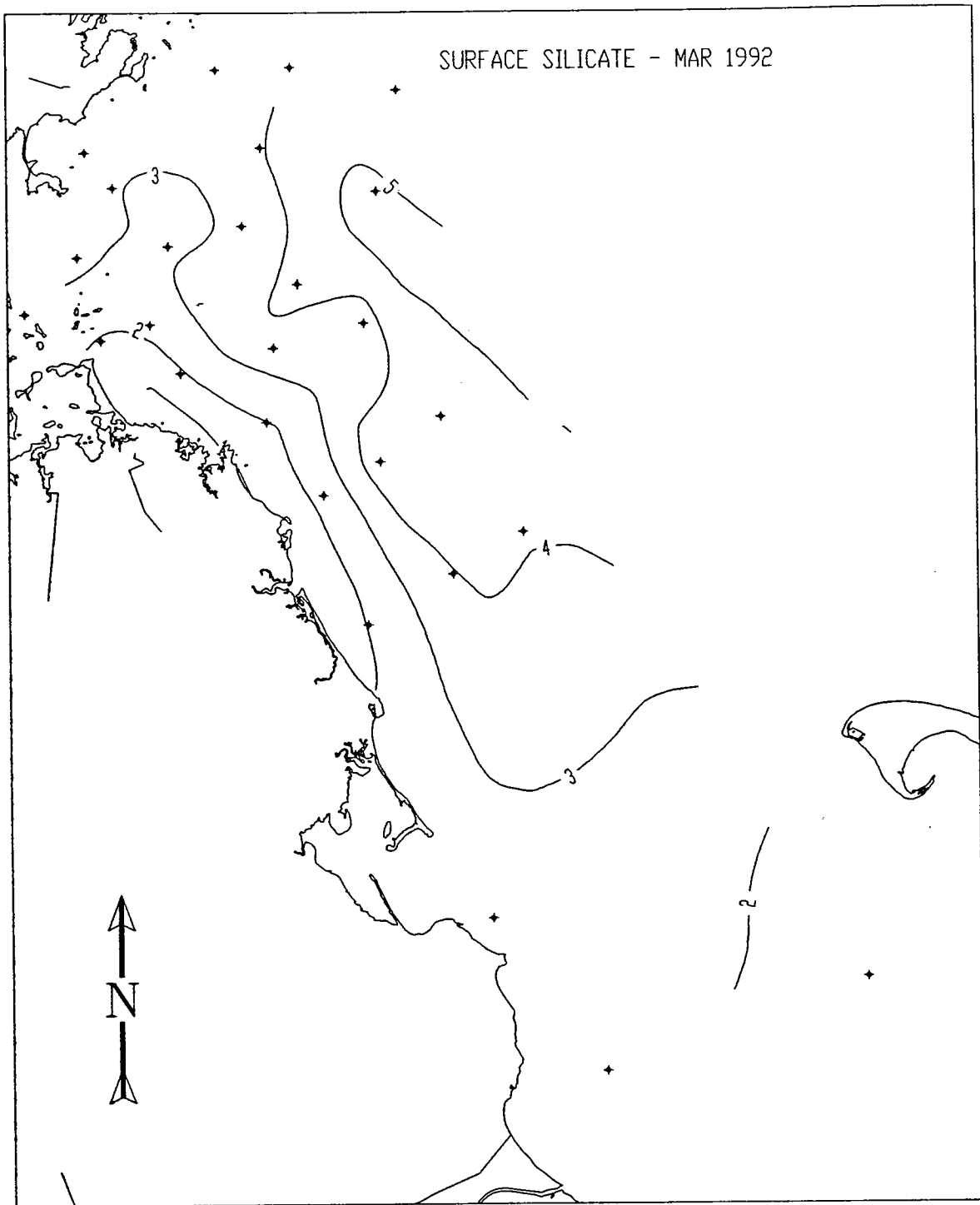


**Figure 4-10** Surface silicate ( $\mu\text{M}$ ) in the region in March 1992. Data are from Appendix B, the surfacemost sample at all farfield survey stations, including the BioProductivity stations within the nearfield grid. The contour interval is 1.0  $\mu\text{M}$ .

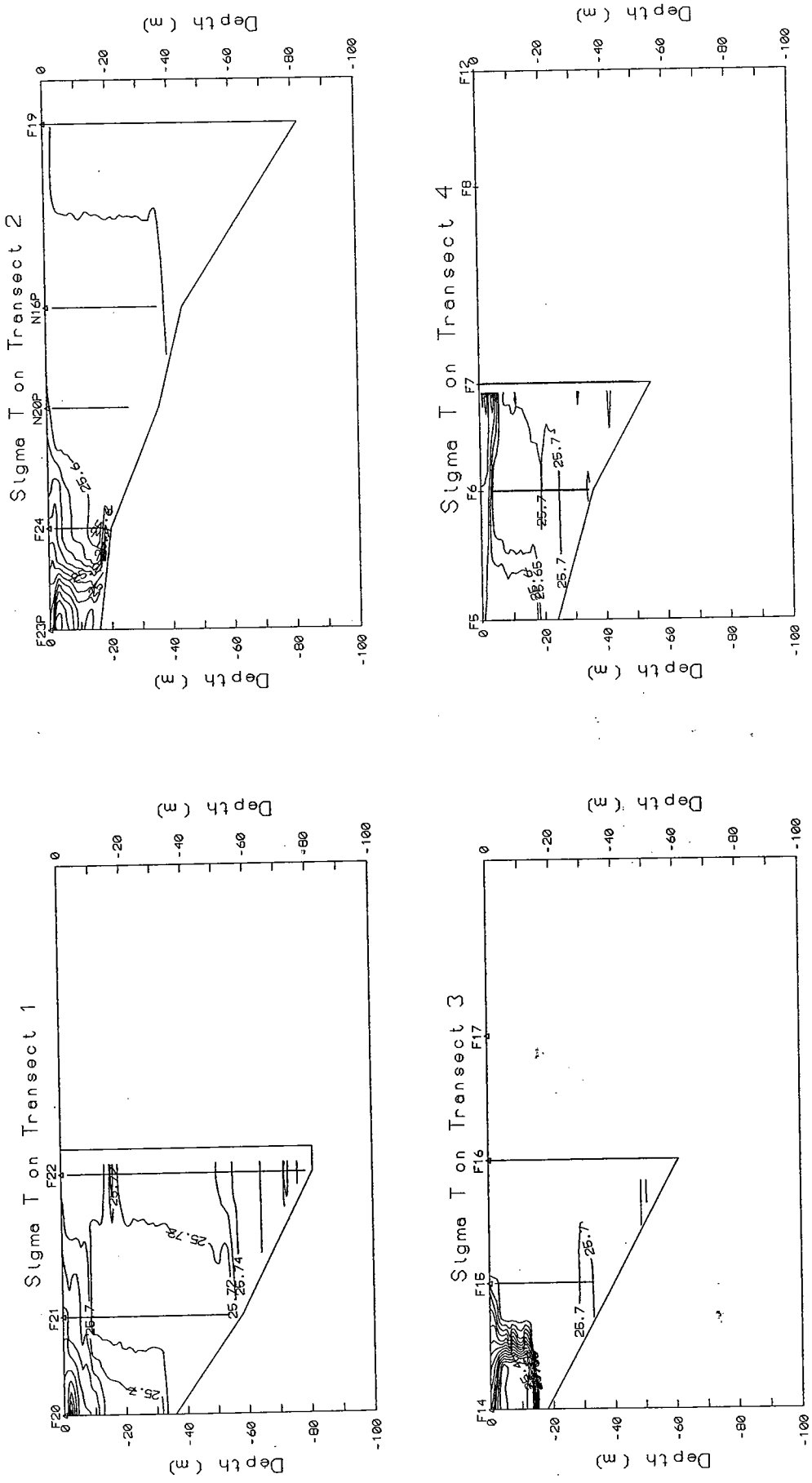


**Figure 4-11** Vertical section contours of  $\sigma_T$  in March for standard transects (see Figure 3-11). The data used to produce contours are from high-resolution continuous vertical profiles taken from the downcast at each station. The contour interval is from 0.02 to 0.05 units.

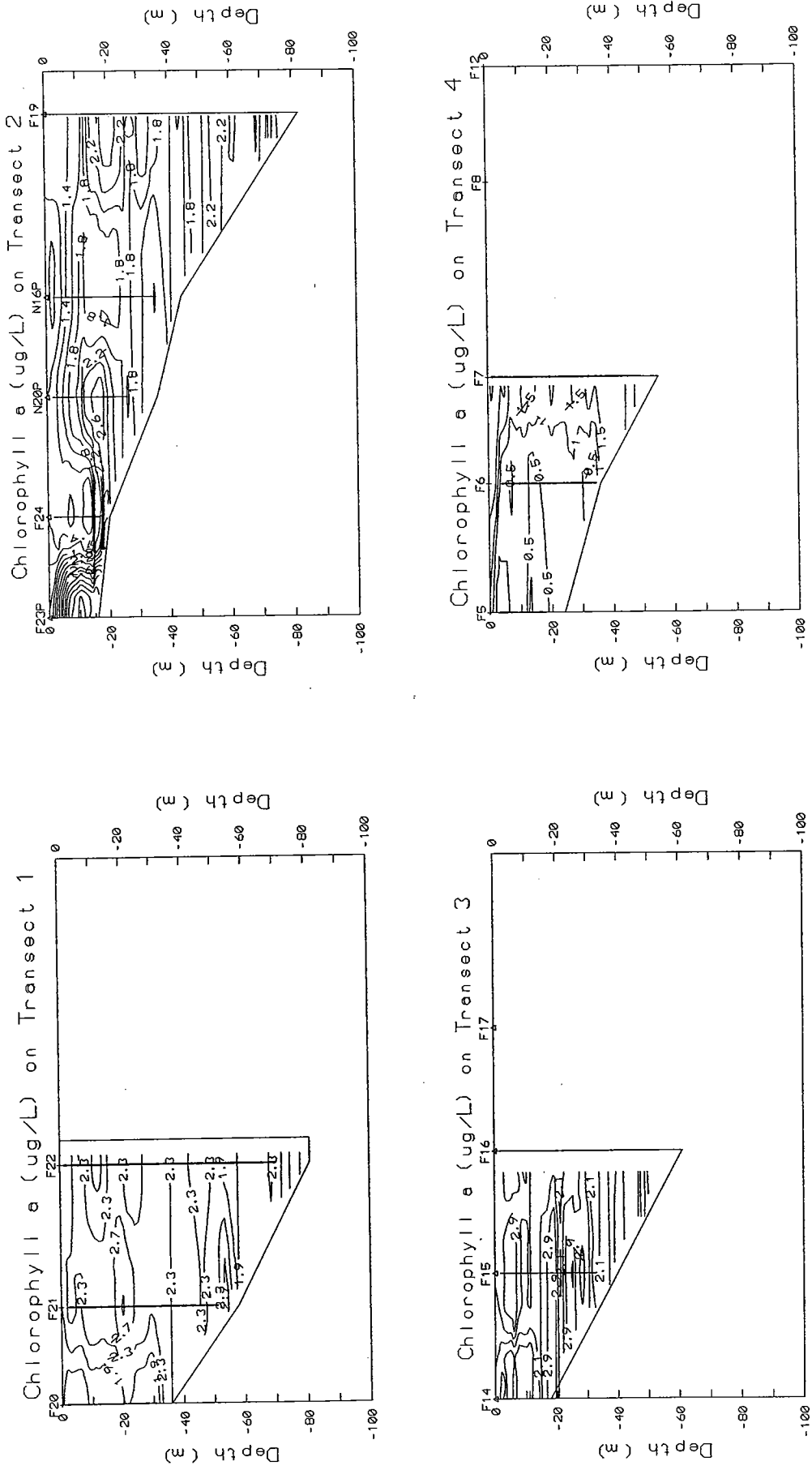


**Figure 4-12** Vertical section contours of fluorescence (as  $\mu\text{g Chl L}^{-1}$ ) in March for standard transects. The data used to produce contours are from high-resolution continuous vertical profiles taken from the downcast at each station. The contour interval is from 0.4 to 0.8  $\mu\text{g L}^{-1}$  units.

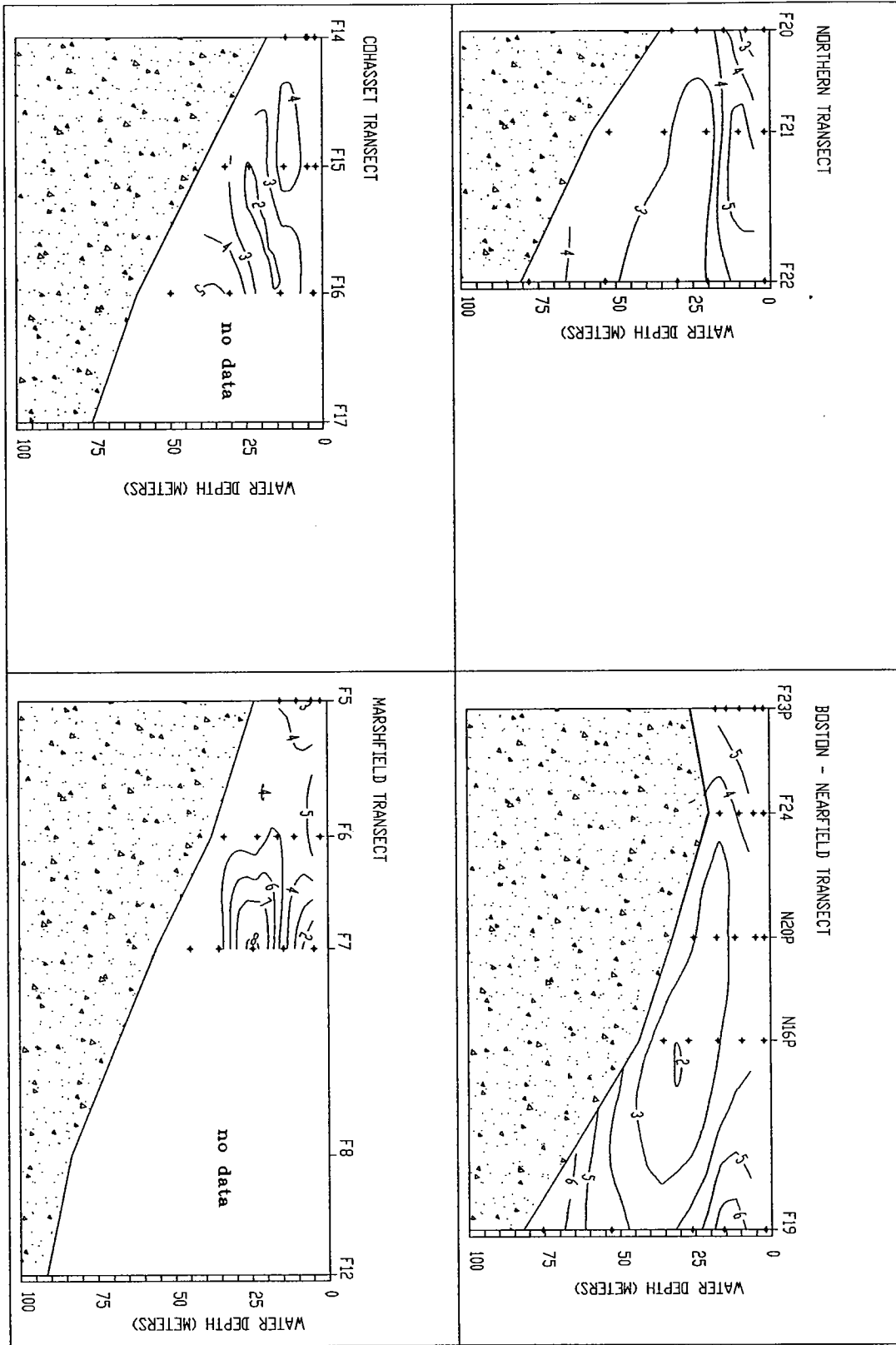


**Figure 4-13** Vertical section contours of dissolved inorganic nitrogen in March for standard transects. The data used to produce contours are from discrete bottle samples as given in Appendix B. The contour interval is 1  $\mu$ M.

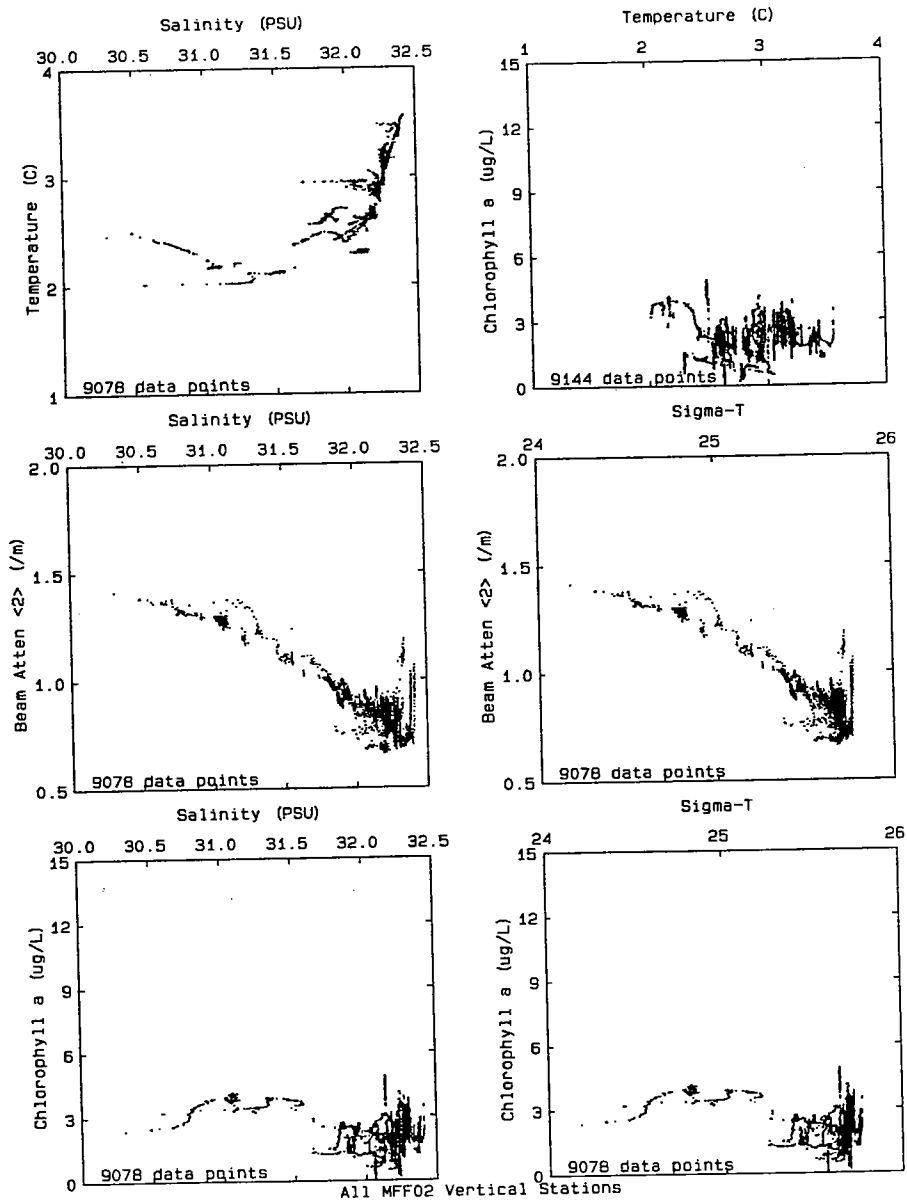


**Figure 4-14** Scatter plots of data acquired by *in situ* sensor package during vertical casts at all farfield and nearfield stations occupied in March 1992. Shallow coastal margin (approximately less than 30 m) stations had lower temperatures accompanied by high beam attenuation and higher than average chlorophyll. Individual station casts plots that were used to produce this composite are in Appendix E.



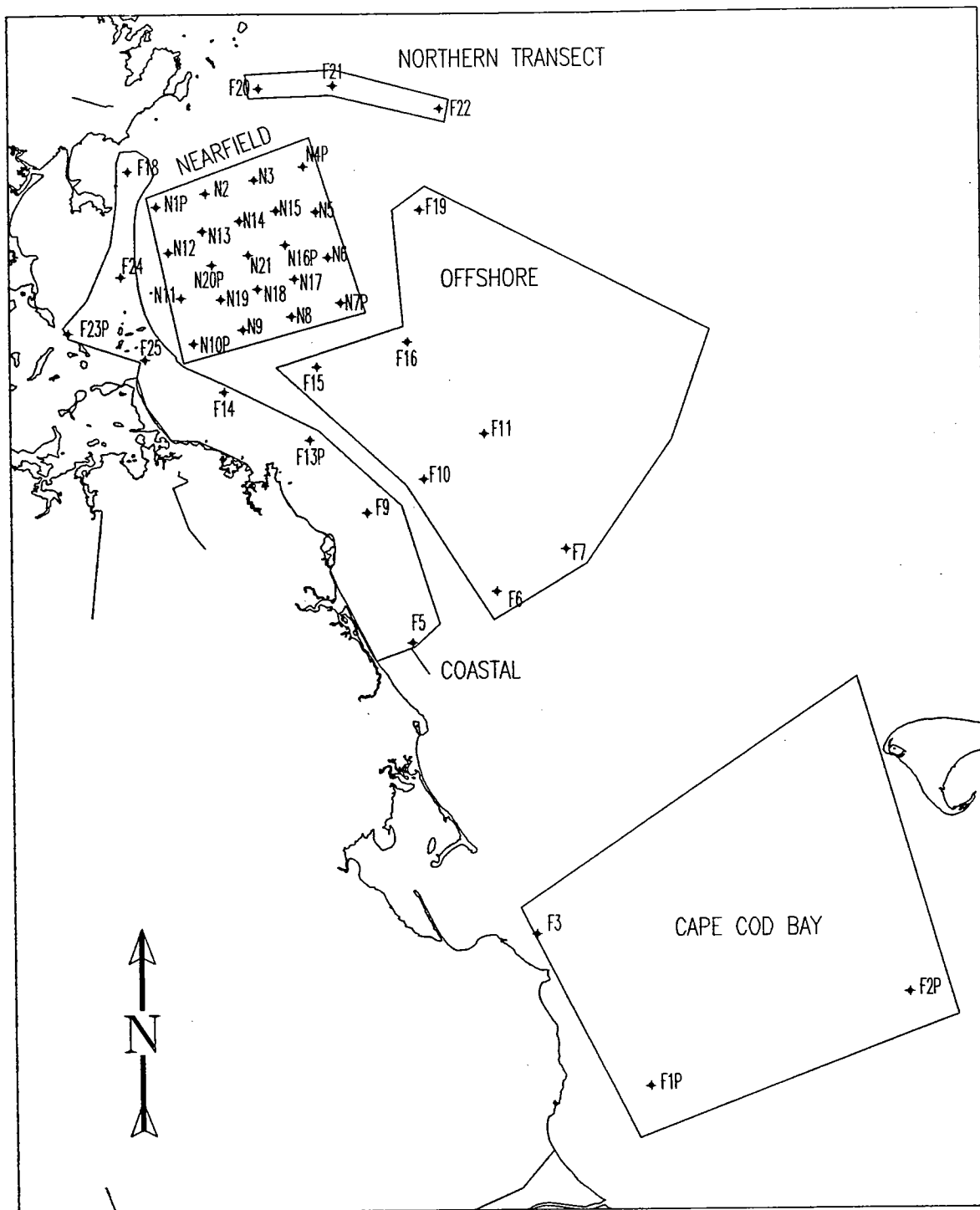


**Figure 4-15** Map to show station groups, the same as for February, designated in Figures 4-16 through 4-21. Stations F4, F8, F12, and F17 were not sampled in March due to poor weather.

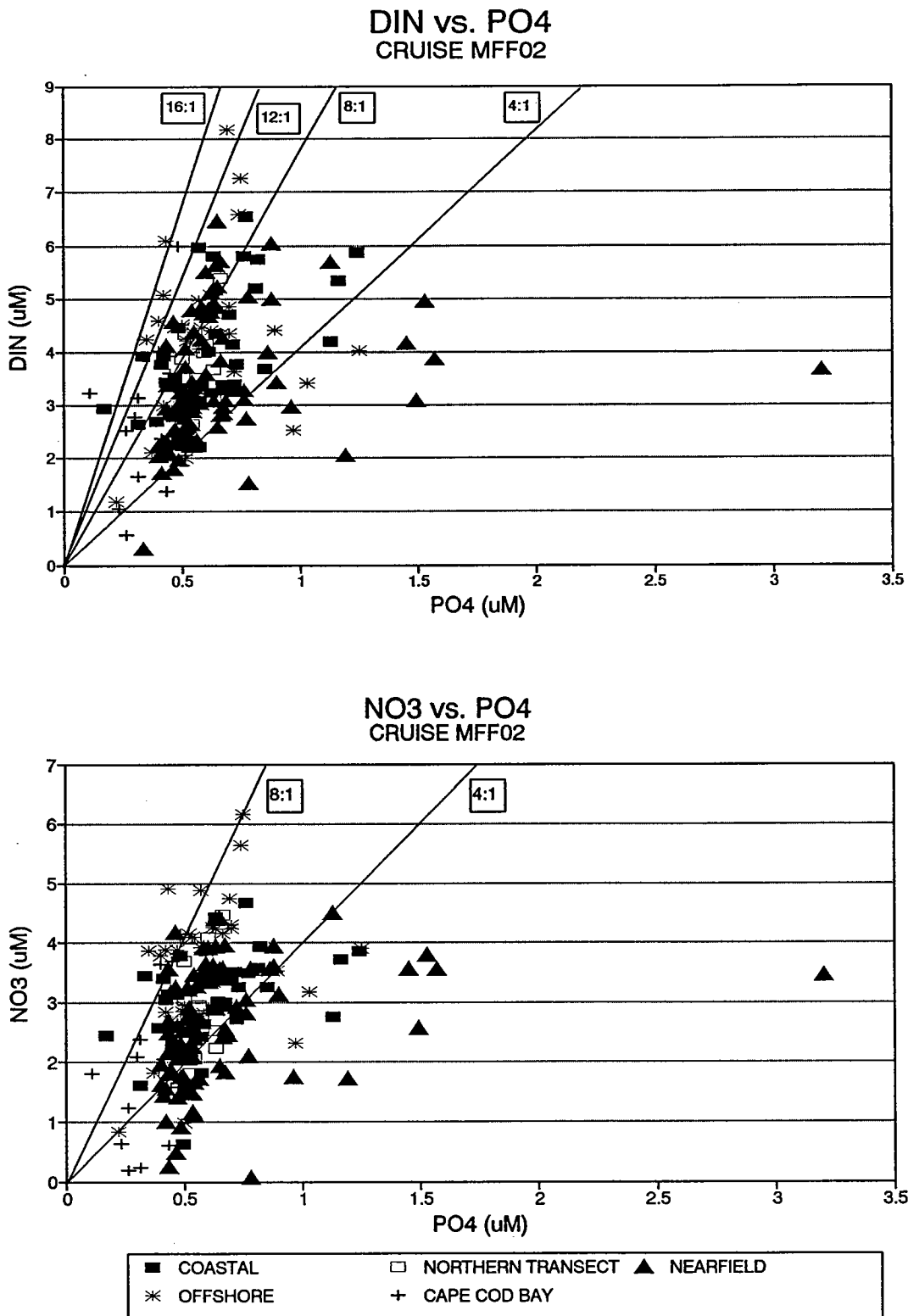


**Figure 4-16** Scatter plots of nitrogen forms vs. phosphate during March 1992. All stations and depths are included, and data are given in Appendix B. Lines show constant proportions of nitrogen relative to phosphorous across a range of N:P ratios.

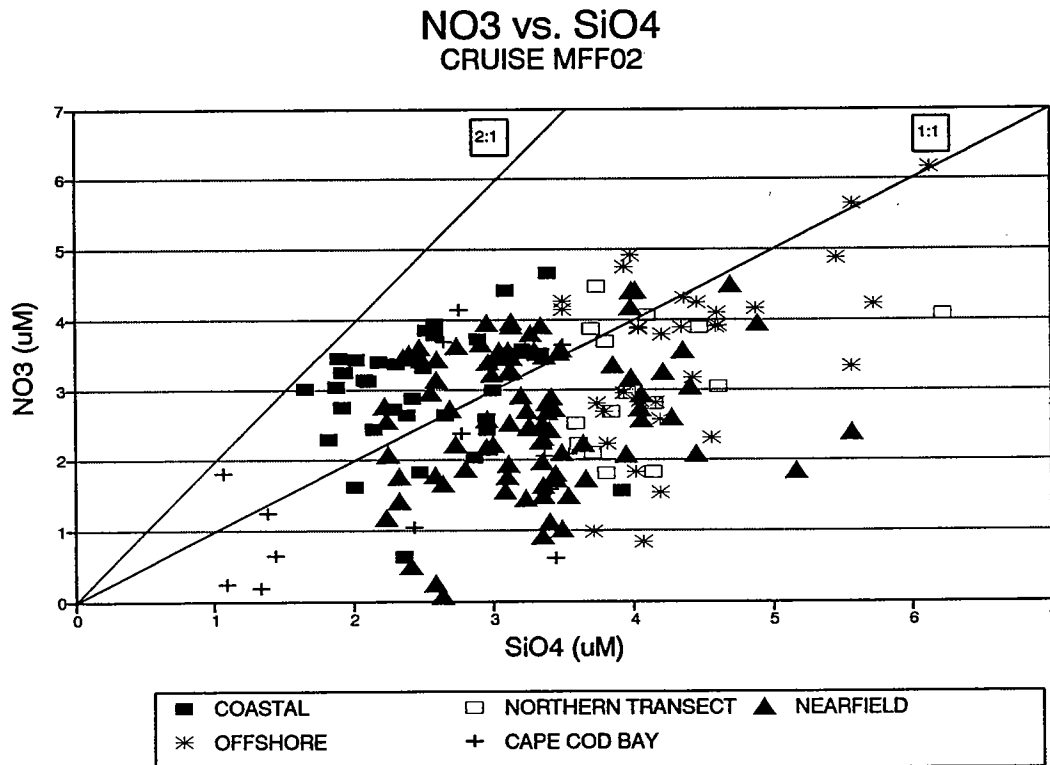
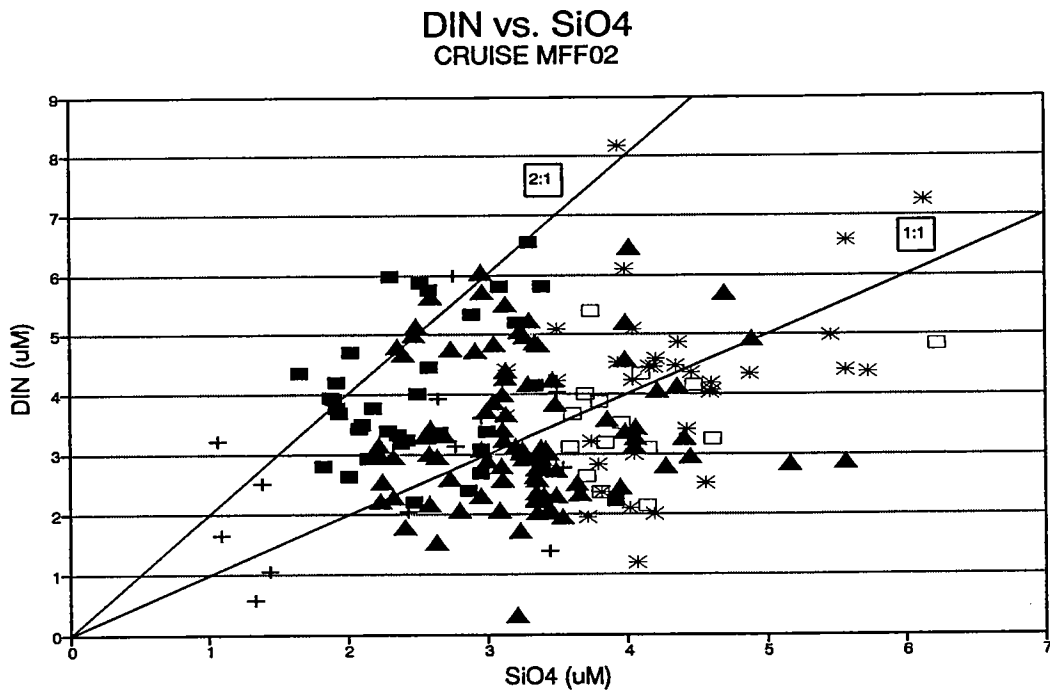
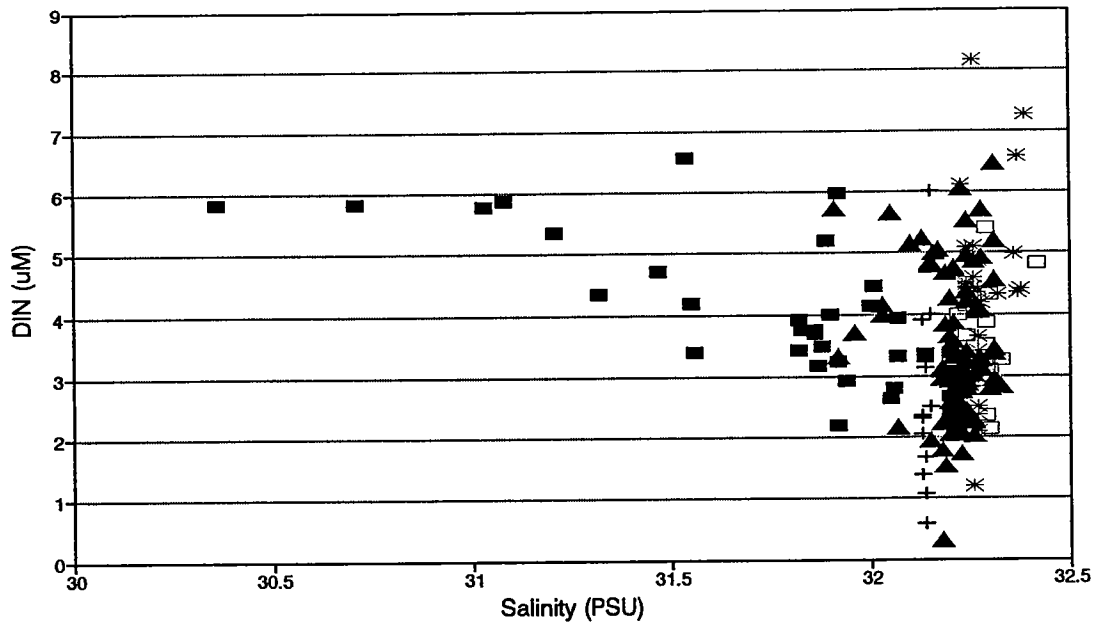


**Figure 4-17** Scatter plots of nitrogen vs. silicate during March 1992. All stations and depths are included, and data are given in Appendix B. Lines show constant proportions of nitrogen relative to silicate across a range of N:Si ratios.

DIN vs. Salinity  
CRUISE MFF02



DIN vs. SIGMA T  
CRUISE MFF02

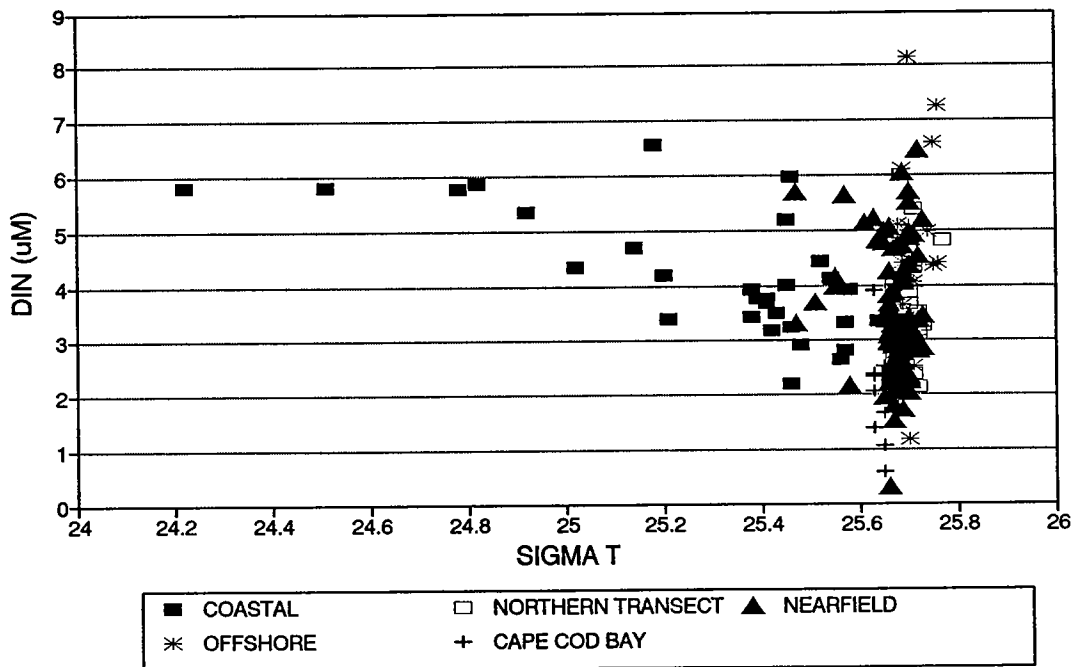
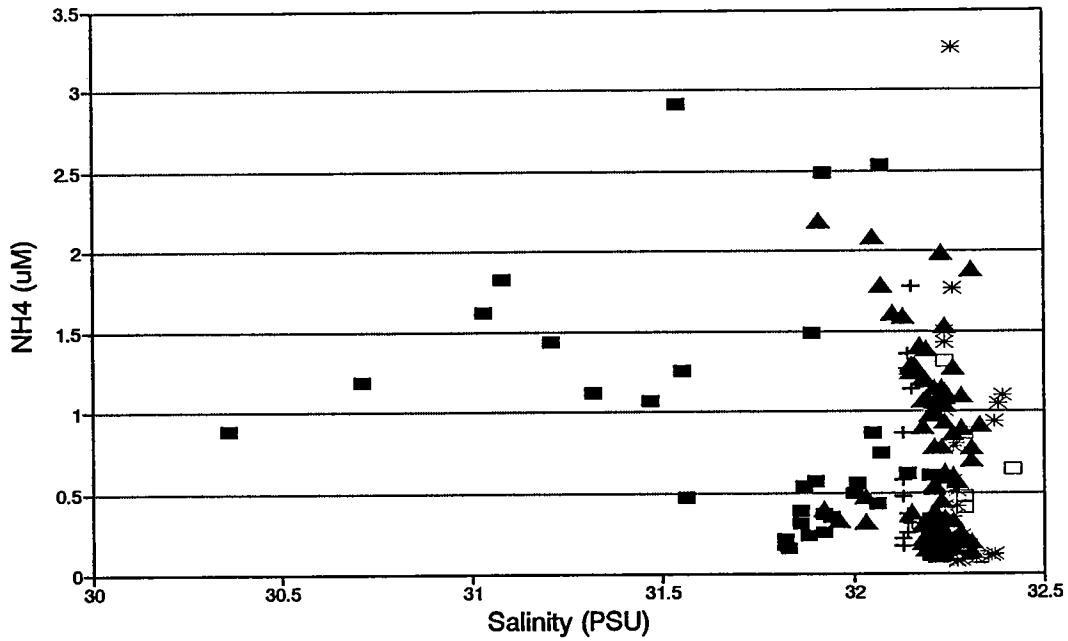


Figure 4-18 Dissolved inorganic nitrogen vs. salinity and  $\sigma_T$  in March 1992. All stations and depths are included, and data are given in Appendix B.

NH4 vs. Salinity  
CRUISE MFF02



NH4 vs. SIGMA T  
CRUISE MFF02

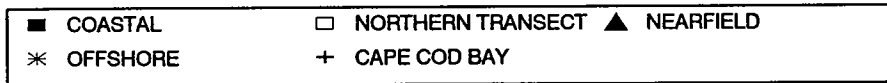
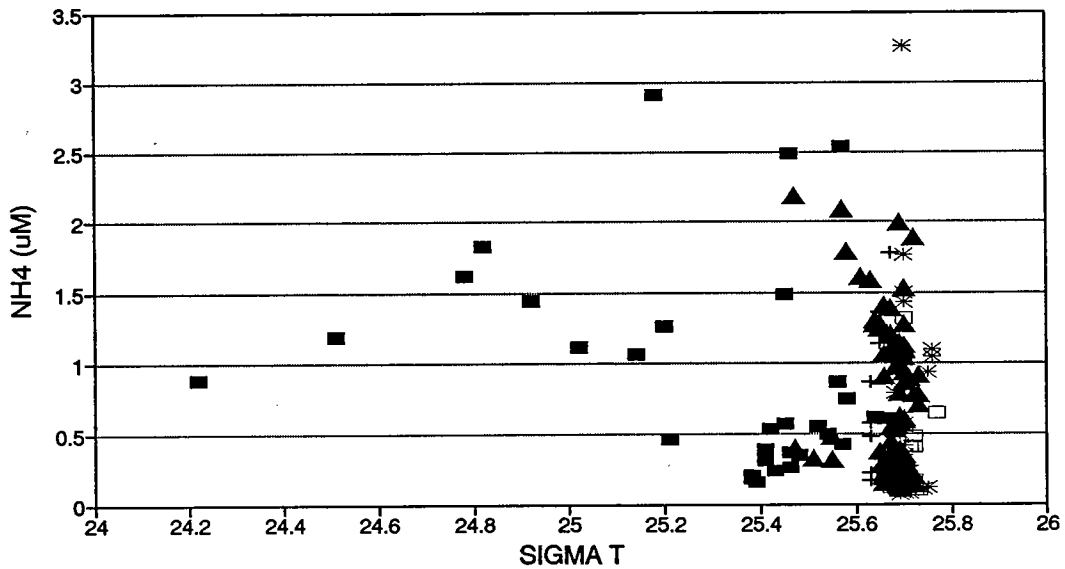
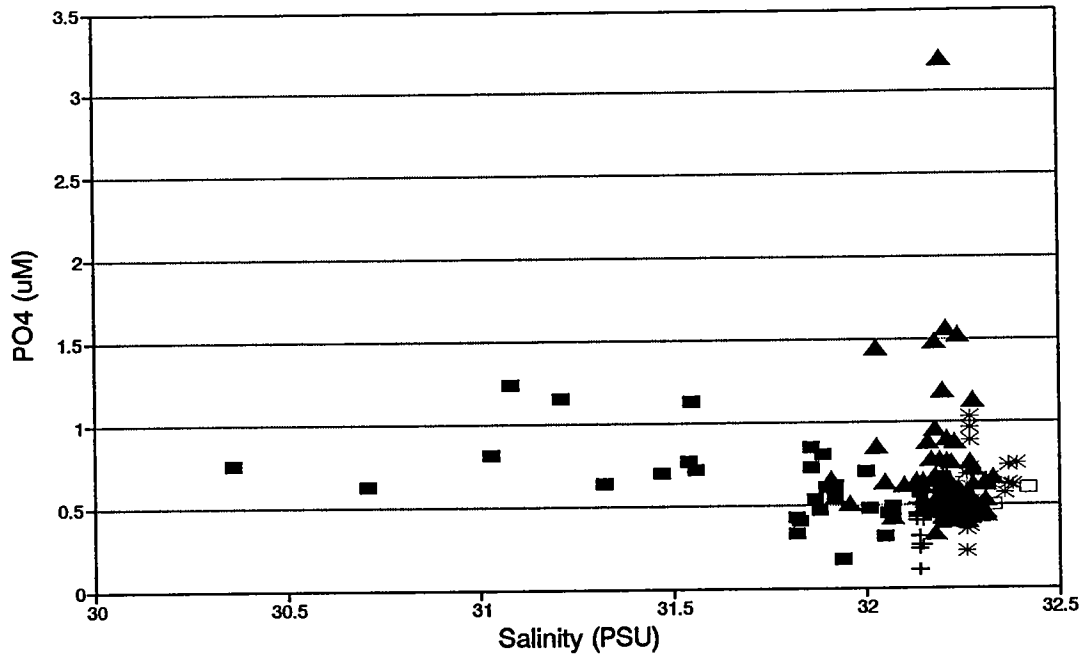


Figure 4-19 Ammonia vs. salinity and  $\sigma_T$  in March 1992. All stations and depths are included, and data are given in Appendix B.

PO4 vs. Salinity  
CRUISE MFF02



PO4 vs. SIGMA T  
CRUISE MFF02

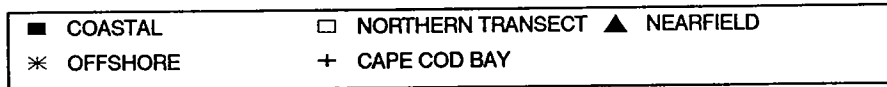
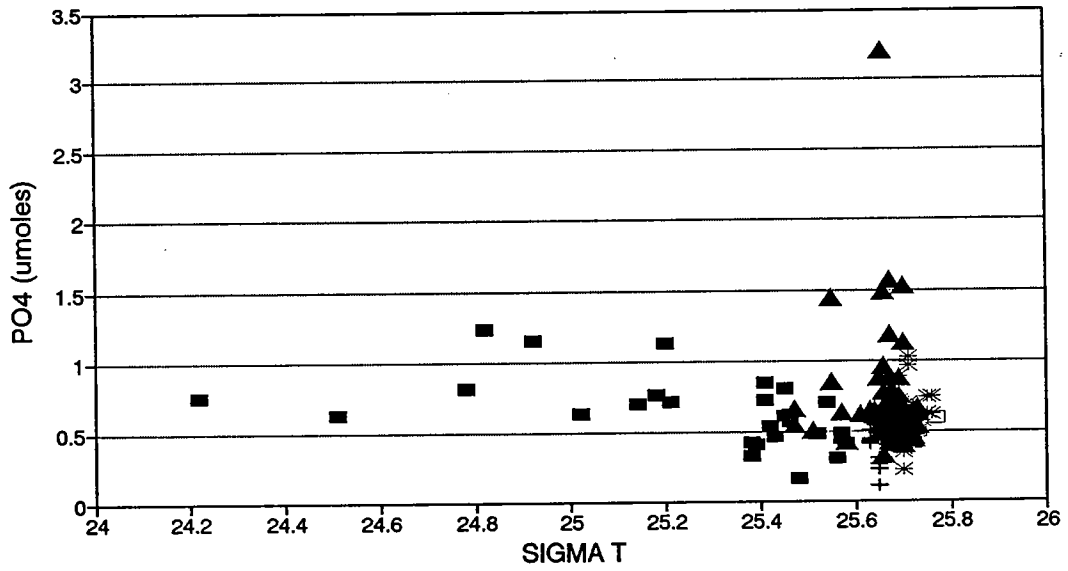
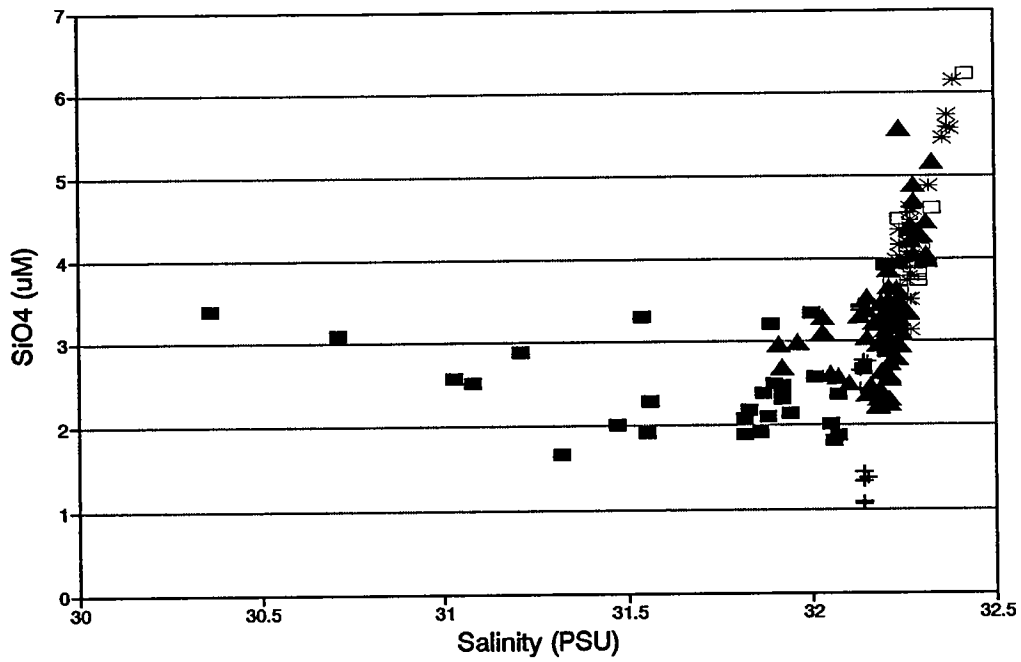


Figure 4-20 Phosphate vs. salinity and  $\sigma_T$  in March 1992. All stations and depths are included, and data are given in Appendix B.

SiO<sub>4</sub> vs. Salinity  
CRUISE MFF02



SiO<sub>4</sub> vs. SIGMA T  
CRUISE MFF02

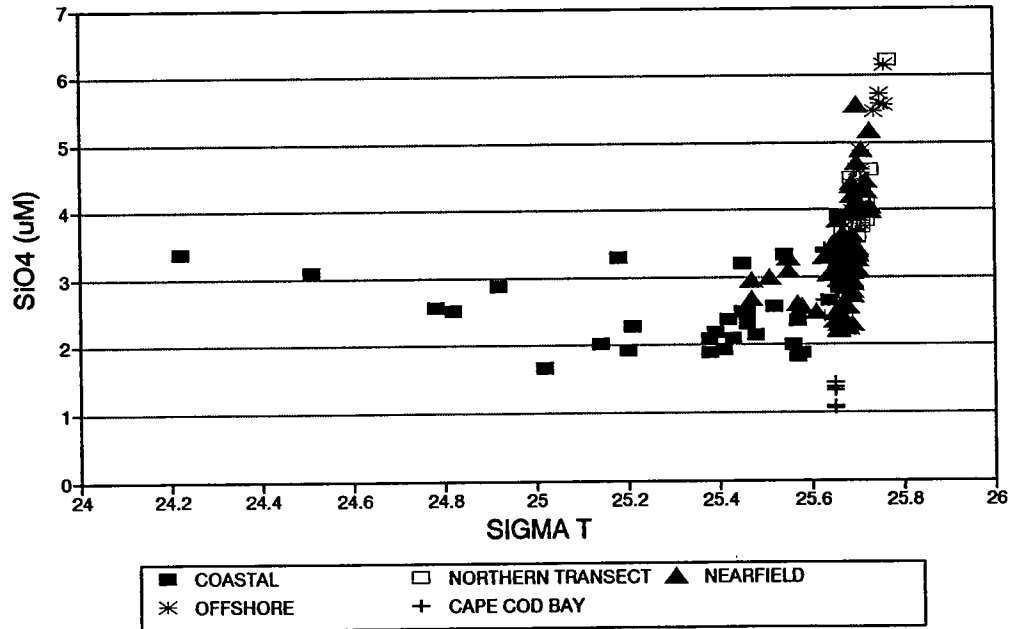
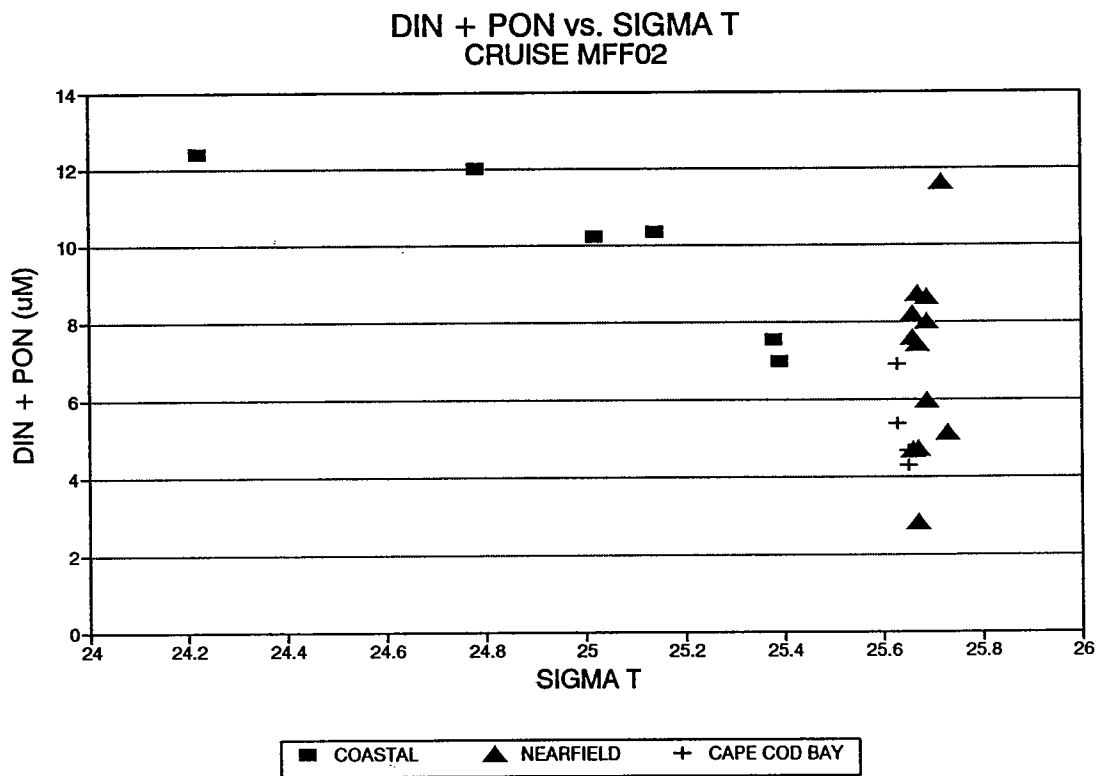
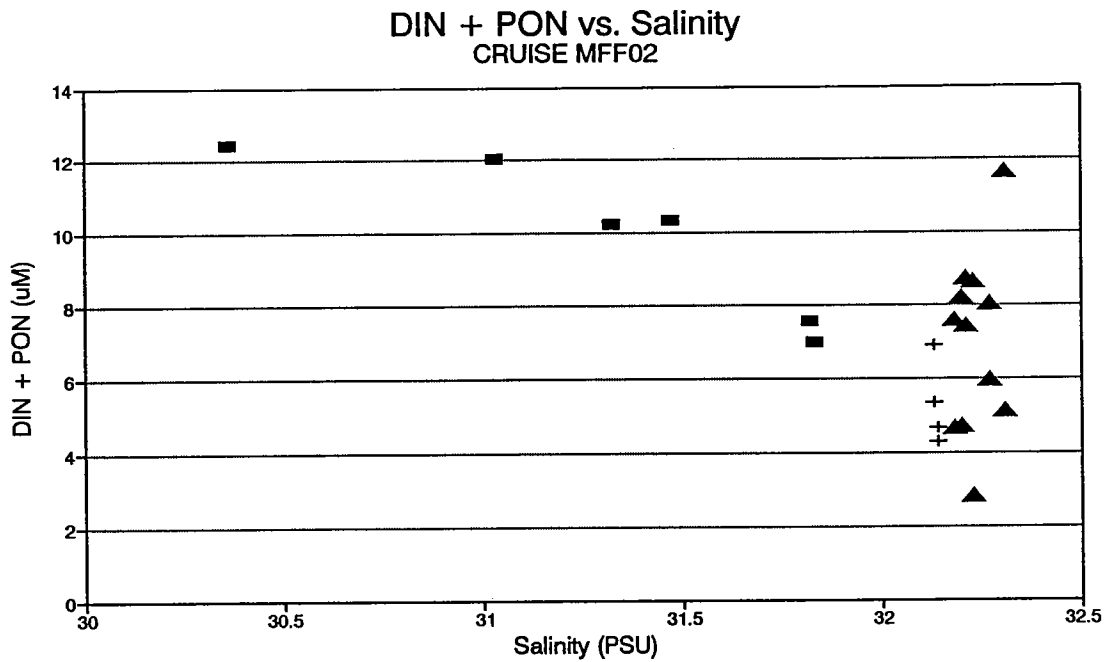
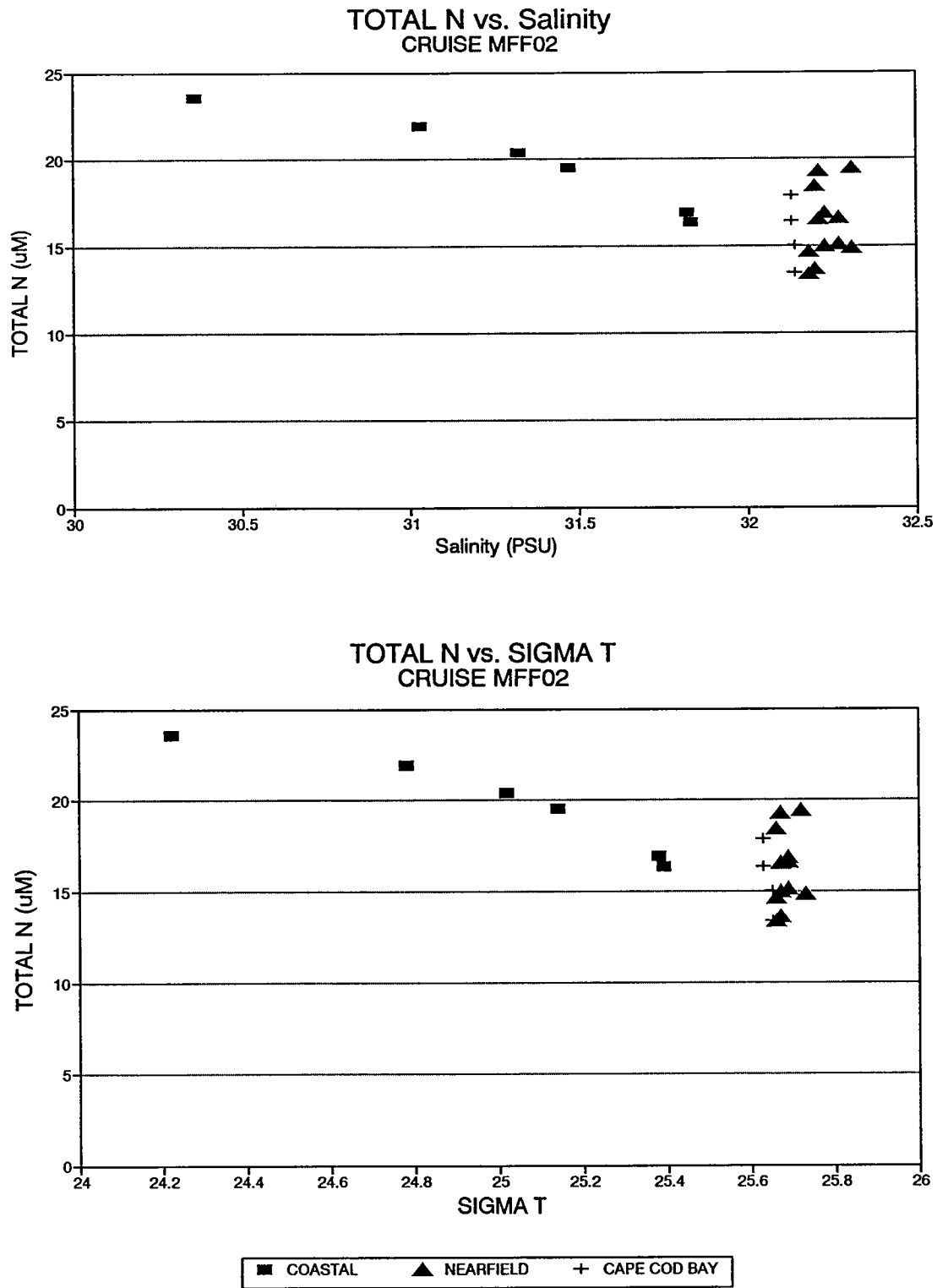


Figure 4-21 Silicate vs. salinity and  $\sigma_T$  in March 1992. All stations and depths are included, and data are given in Appendix B.



**Figure 4-22** The sum of dissolved inorganic nitrogen and particulate organic nitrogen vs salinity and  $\sigma_T$  in March 1992. Data are from BioProductivity stations and special station F25 and are given in Appendix B. The station groups are coded as given in Figure 4-15; there are no BioProductivity stations in the Offshore or Northern Transect groups.





**Figure 4-23** The sum of total dissolved nitrogen and particulate organic nitrogen (=total nitrogen) vs. salinity and  $\sigma_T$  in March 1992. Data are from BioProductivity stations and special station F25 and are given in Appendix B. Groups are the same Figure 4-22.

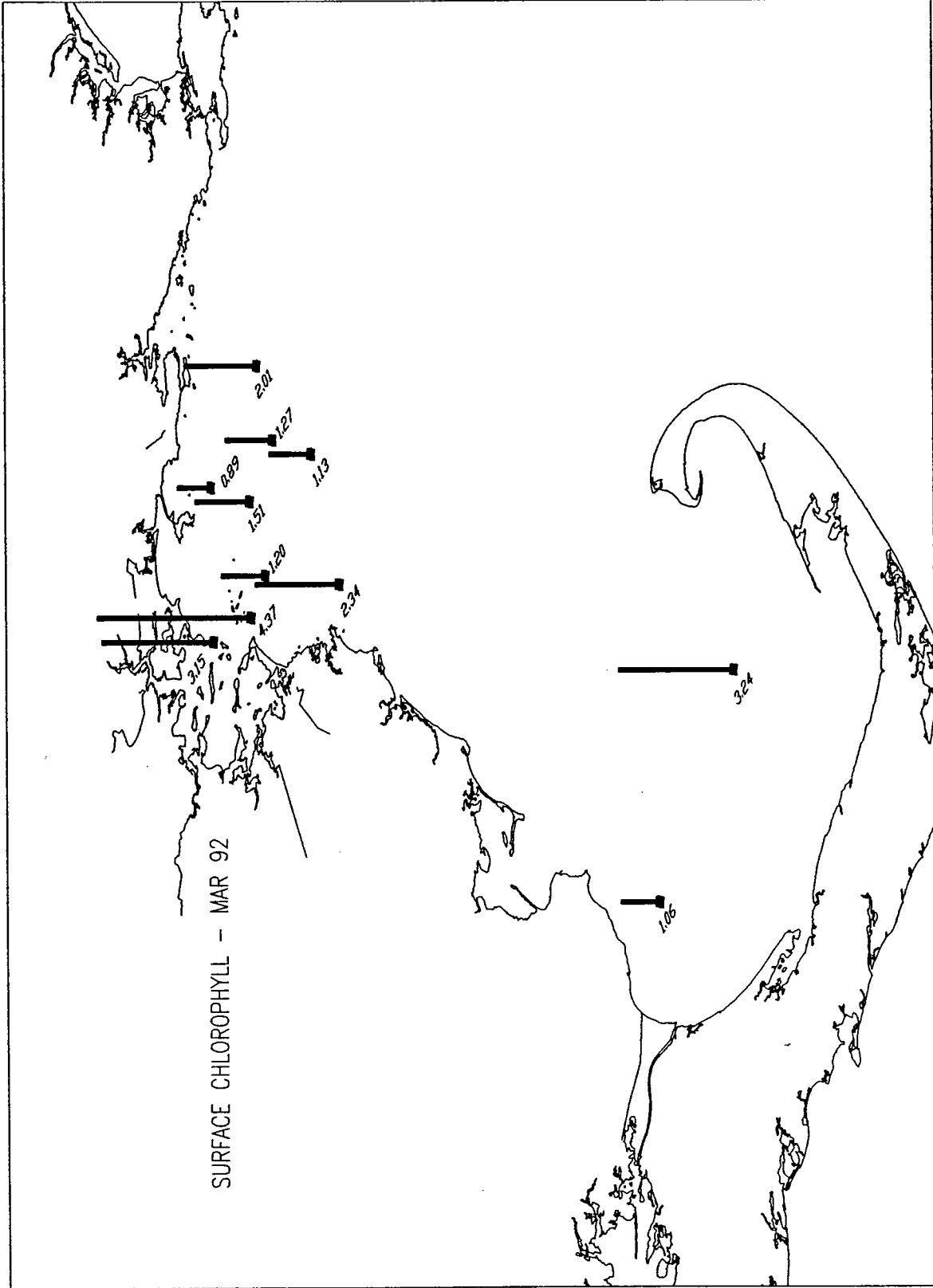


**Figure 4-24** Surface chlorophyll at BioProductivity stations and special station F25 in March 1992. Data are the average of duplicate determinations by standard chlorophyll extraction (Appendix B).

### Chl-A vs. Depth CRUISE MFF02

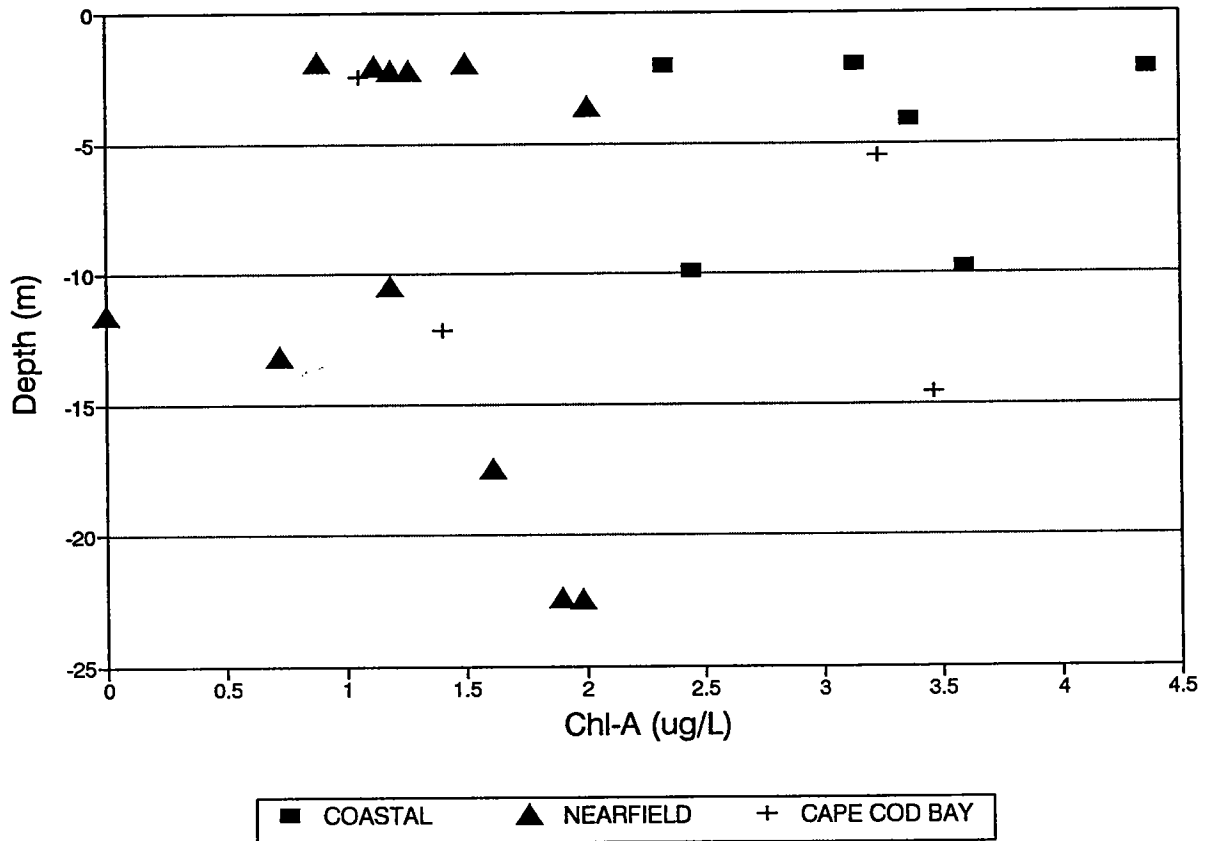


**Figure 4-25** Surface and deeper chlorophyll at BioProductivity stations and special station F25 in March 1992. Data are the average of duplicate determinations by standard chlorophyll extraction (Appendix B). Groups are the same as in Figure 4-22.

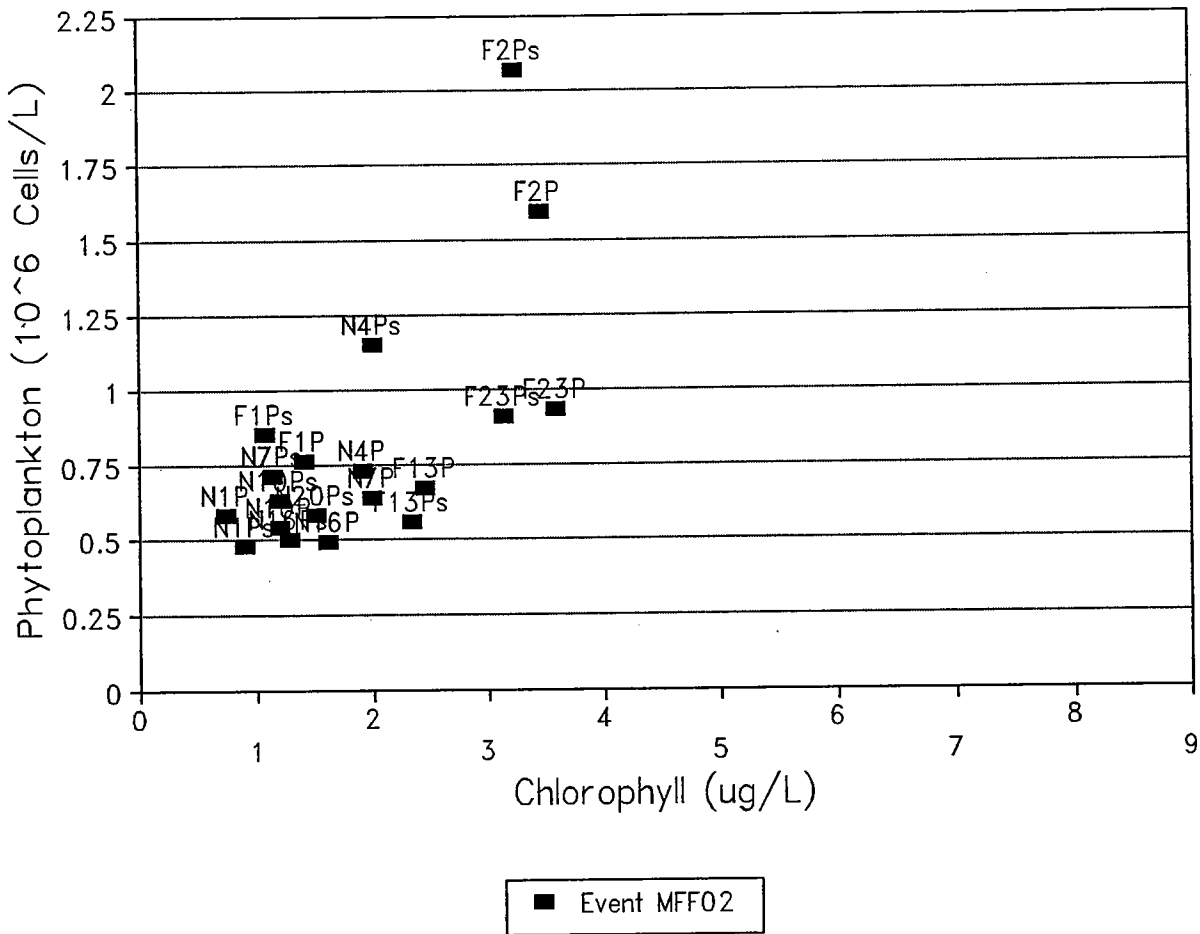


**Figure 4-26** Total phytoplankton abundance vs. extracted chlorophyll at BioProductivity stations in March 1992. Data are in Appendices B and J. An "s" for station label marks the surface sample at each station, without "s" marks the deeper sample.

# Phytoplankton - Mar 92

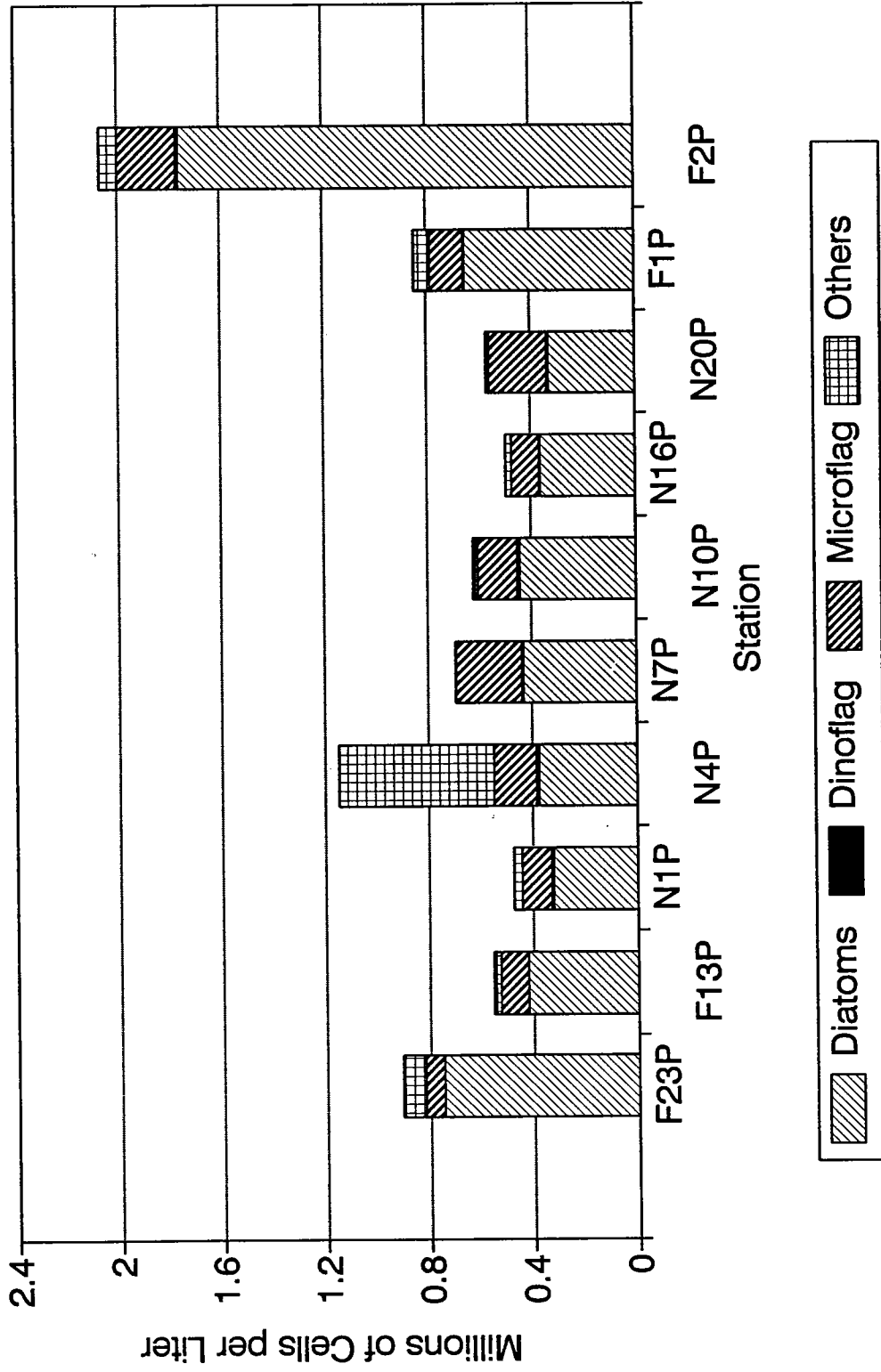
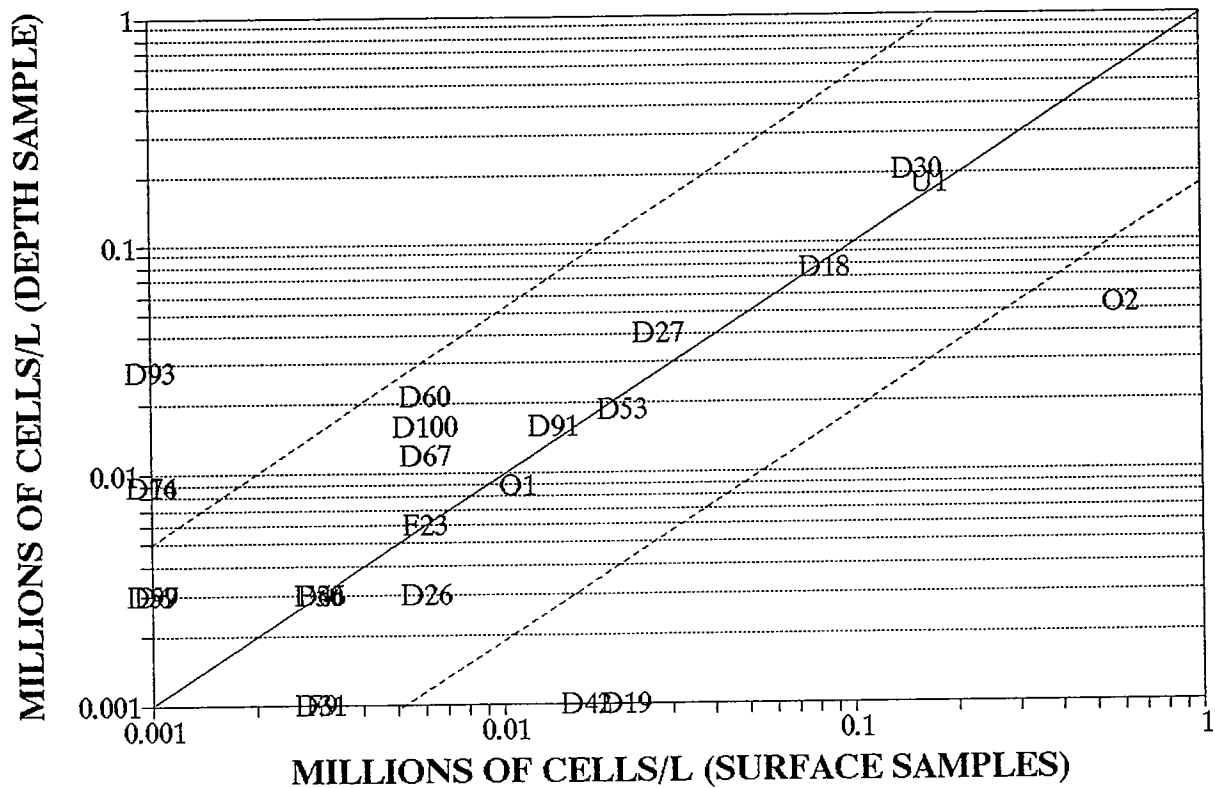


Figure 4-27 Total phytoplankton abundance in surface samples, by taxonomic groups, at BioProductivity stations in March 1992. Data are given in Appendix J.

## PHYTOPLANKTON SPECIES ABUNDANCE STATION N4P - CRUISE MFF02



**Figure 4-28** Comparison of phytoplankton taxonomic composition of surface and deeper samples at station N4P in March 1992. Full species codes are given in Appendix J, but the alphabetic code is as follows: D=diatoms, F=dinoflagellates, U= microflagellates, O= other. The solid lines shows a 1:1 relationship, the dotted lines show 1:5 and 5:1 isopleths.

# PHYTOPLANKTON SPECIES ABUNDANCE STATION F2P - CRUISE MFF02

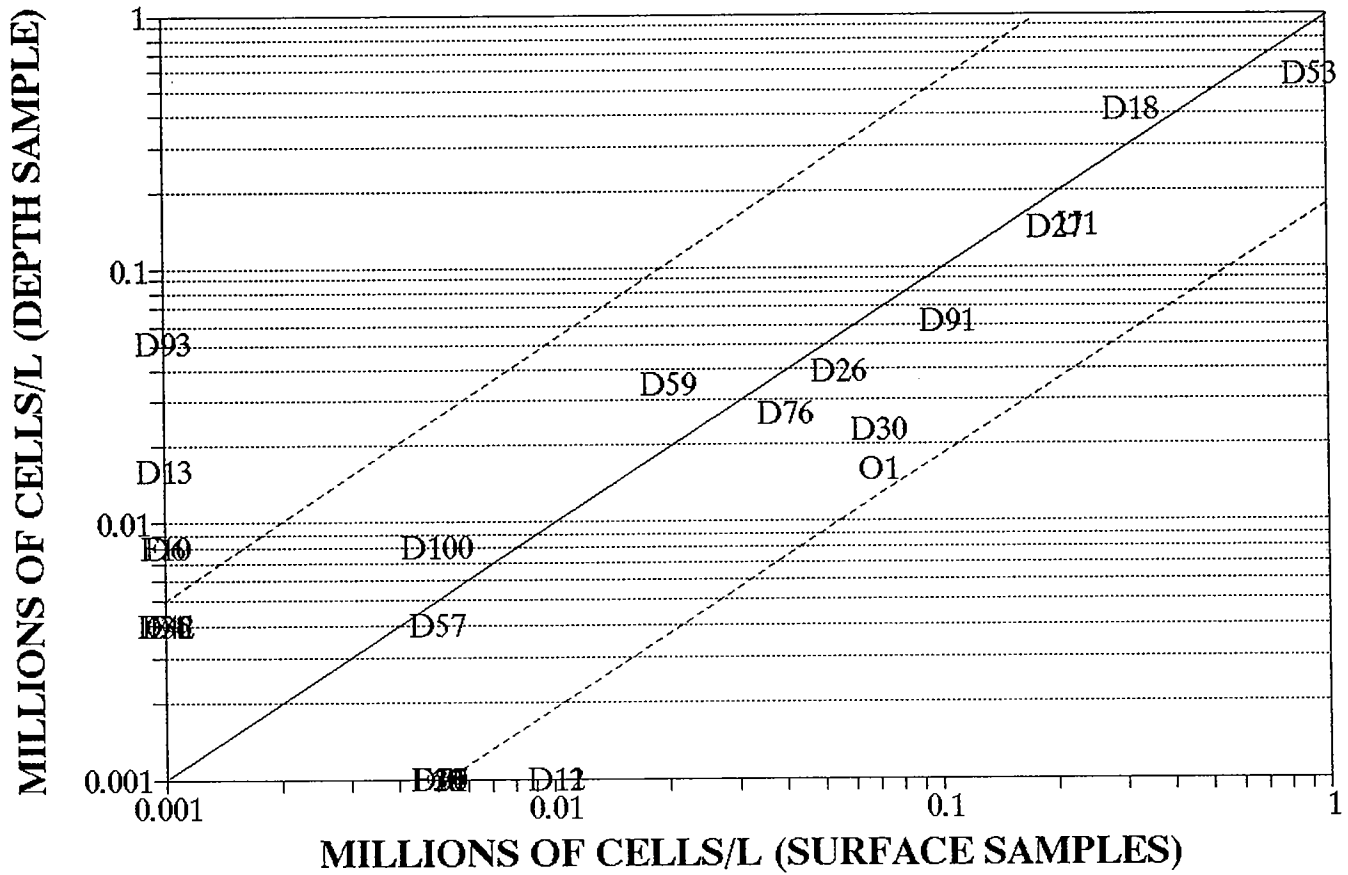


**Figure 4-29** Comparison of phytoplankton taxonomic composition of surface and deeper samples at station F2P in March 1992. Species codes are given in Appendix J.

# PHYTOPLANKTON SPECIES ABUNDANCE STATION F23P - CRUISE MFF02

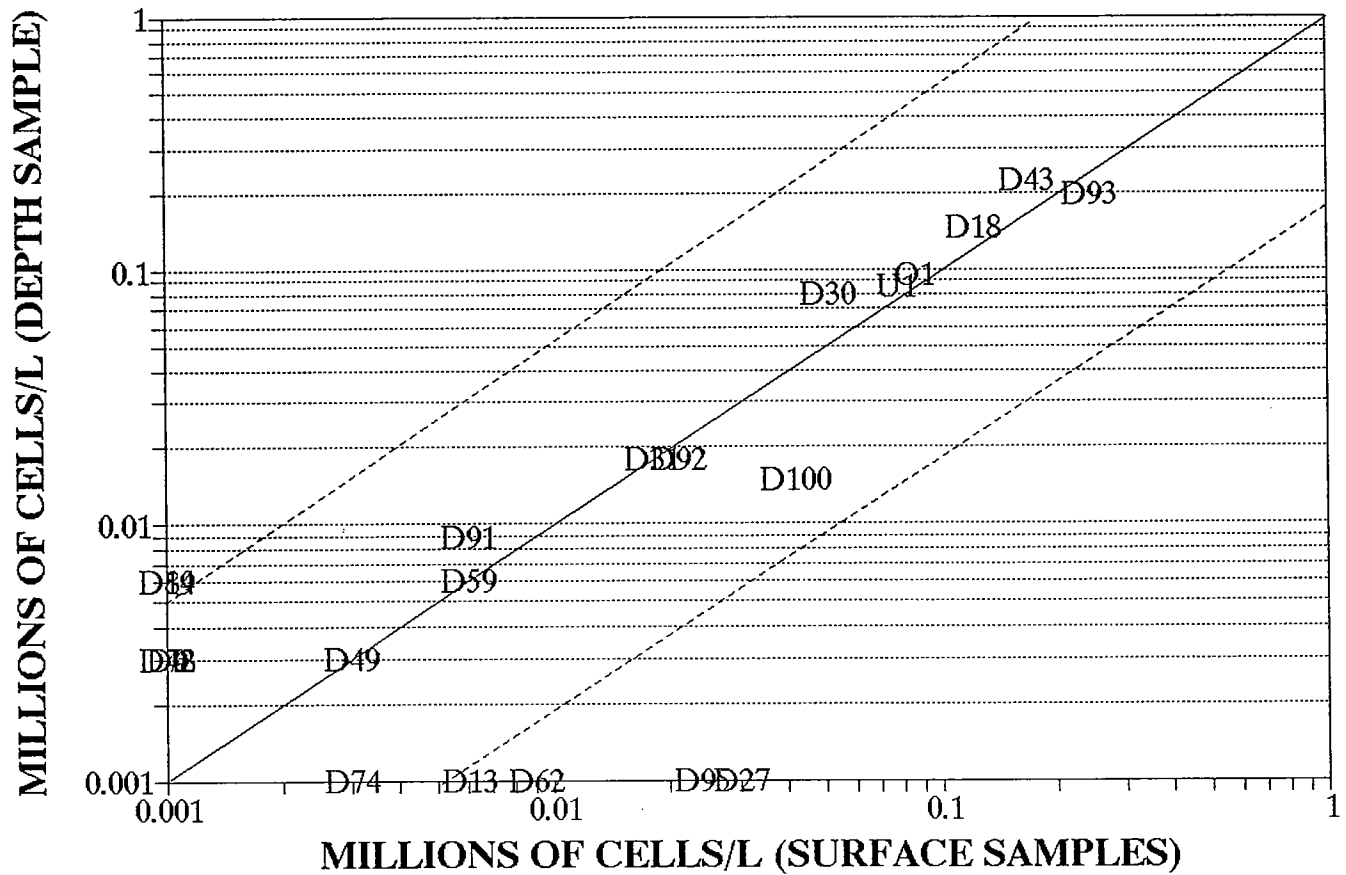


**Figure 4-30** Comparison of phytoplankton taxonomic composition of surface and deeper samples at station F23P in March 1992. Species codes are given in Appendix J.



## PHYTOPLANKTON SPECIES ABUNDANCE STATION F13P - CRUISE MFF02

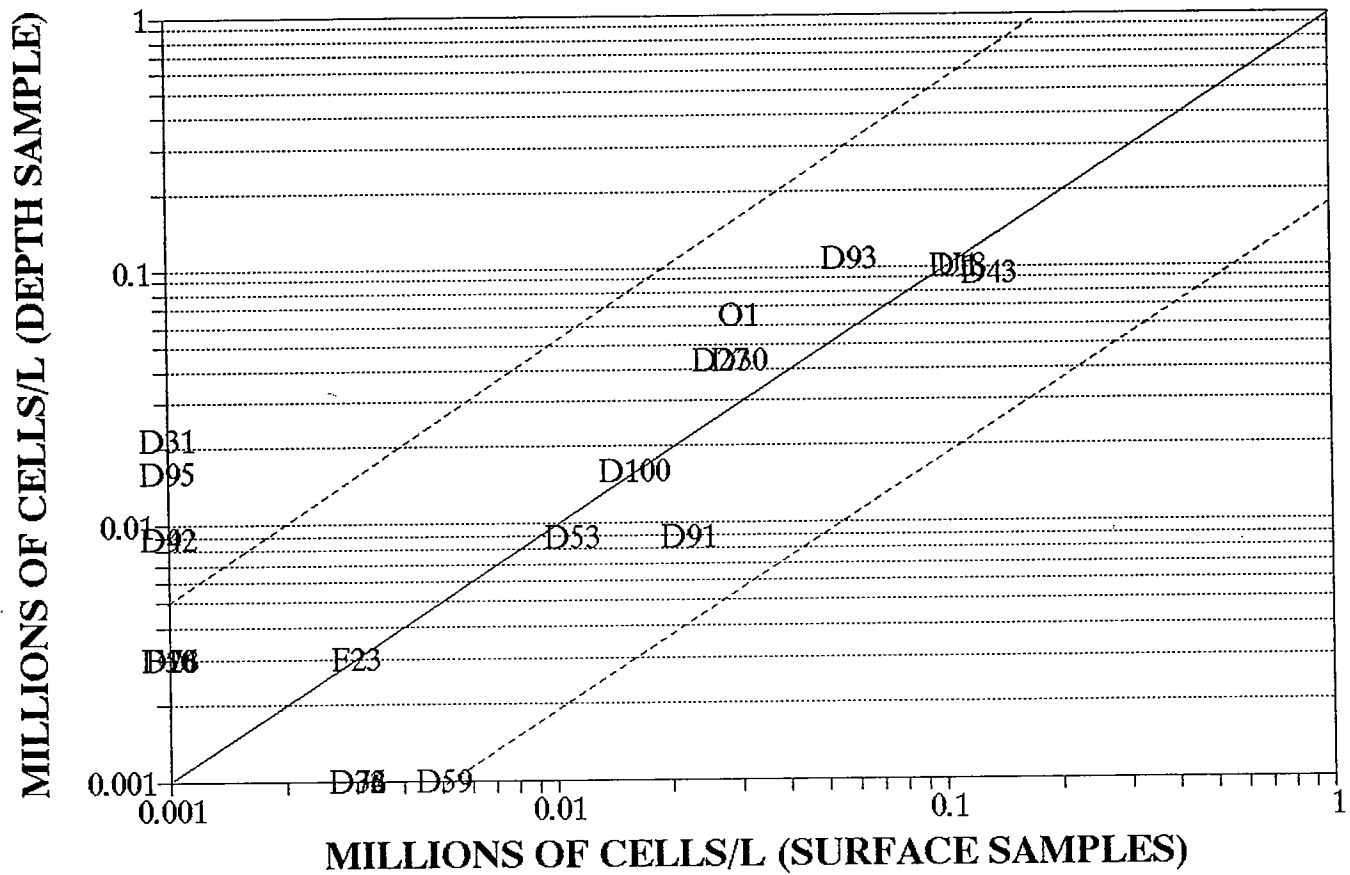


**Figure 4-31** Comparison of phytoplankton taxonomic composition of surface and deeper samples at station F13P in March 1992. Species codes are given in Appendix J.

# Zooplankton - Mar 92

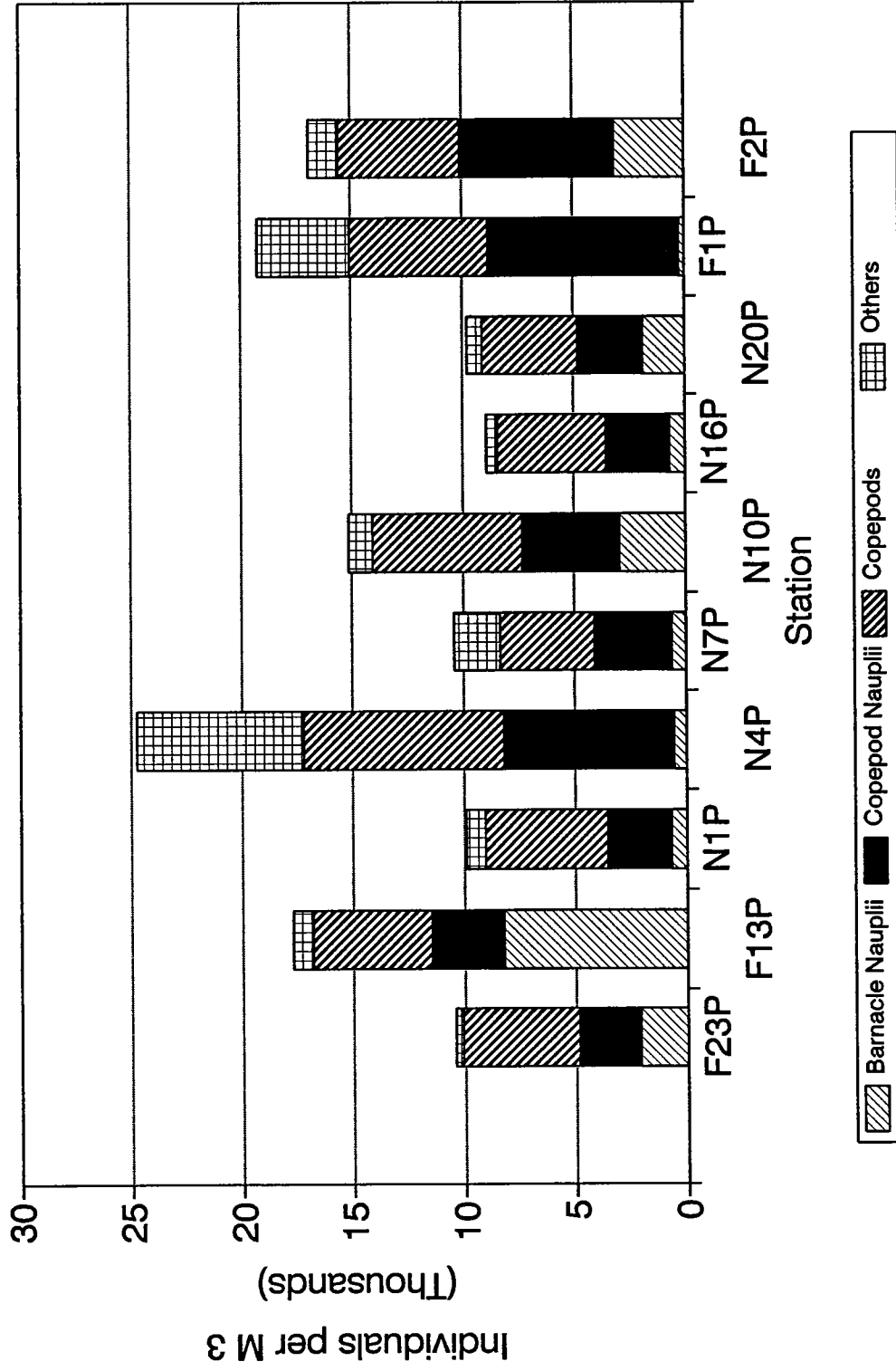


Figure 4-32 Zooplankton abundance, by groups, at BioProductivity stations in March 1992. Data are given in Appendix L.

# STATION N4P CRUISE 2

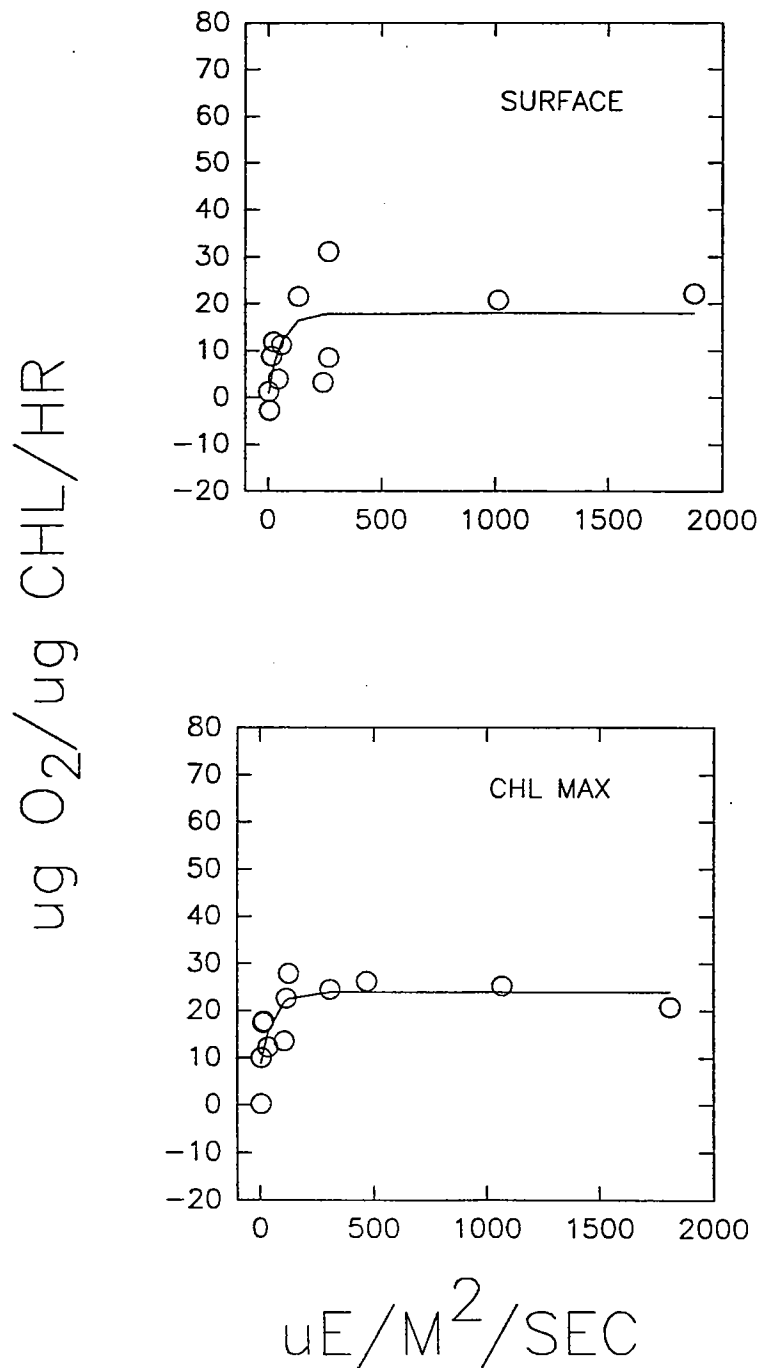


Figure 4-33 Net Production (P) vs. Irradiance (I) curves for station N4P in March 1992. Data are chlorophyll normalized rates see Appendix H.

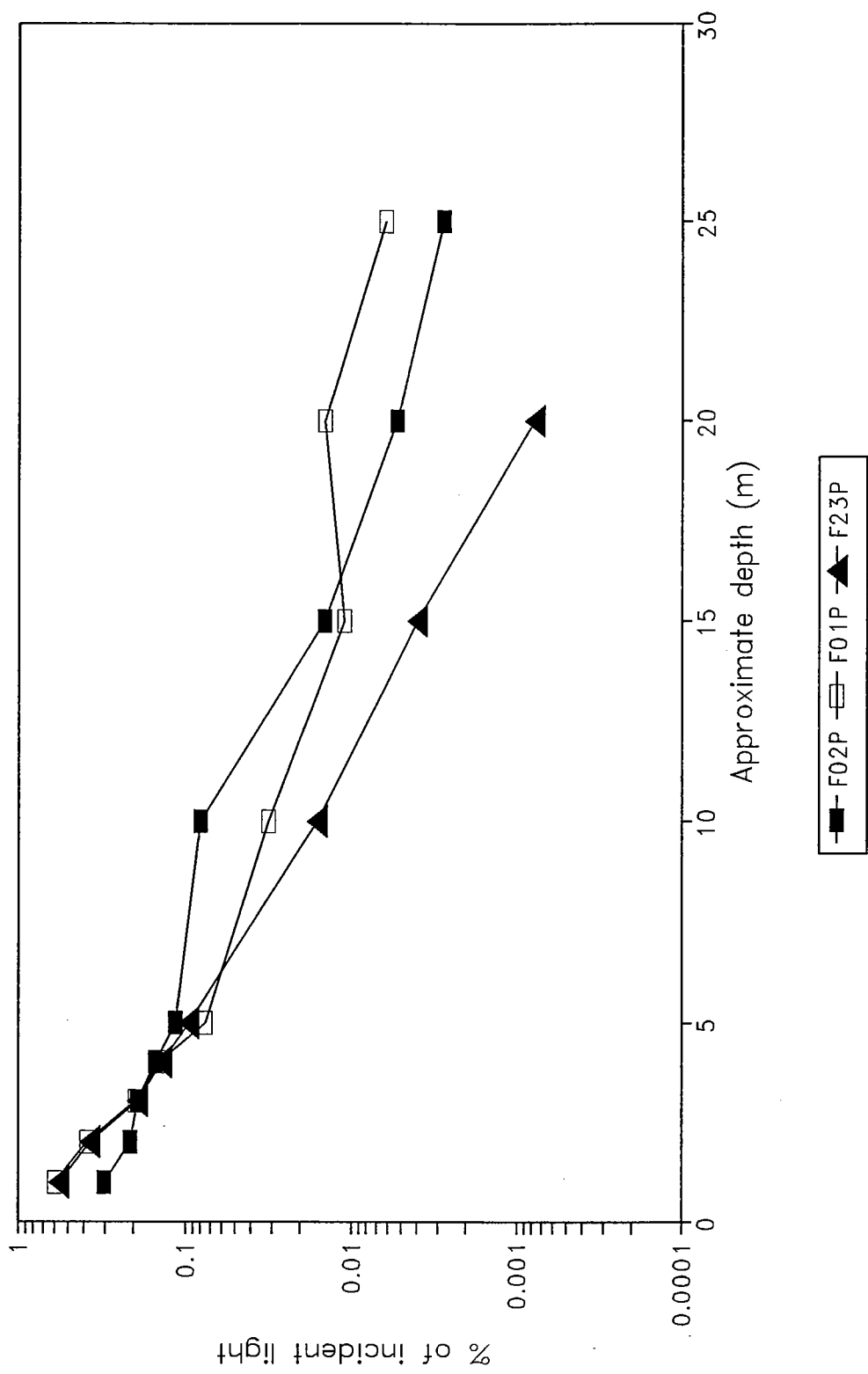


Figure 4-34. Light extinction at a selection of stations in March 1992. Data are given in Appendix H.

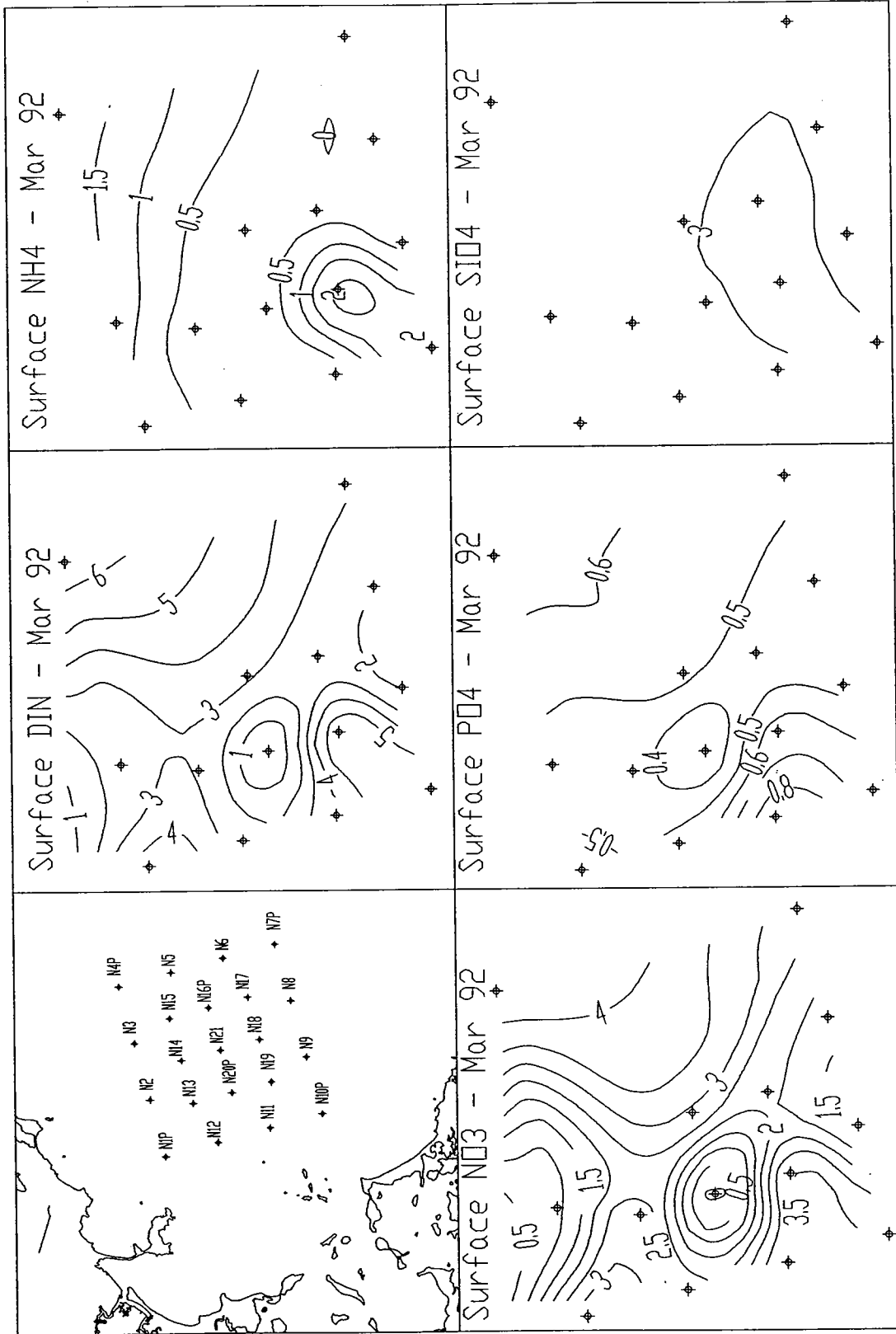
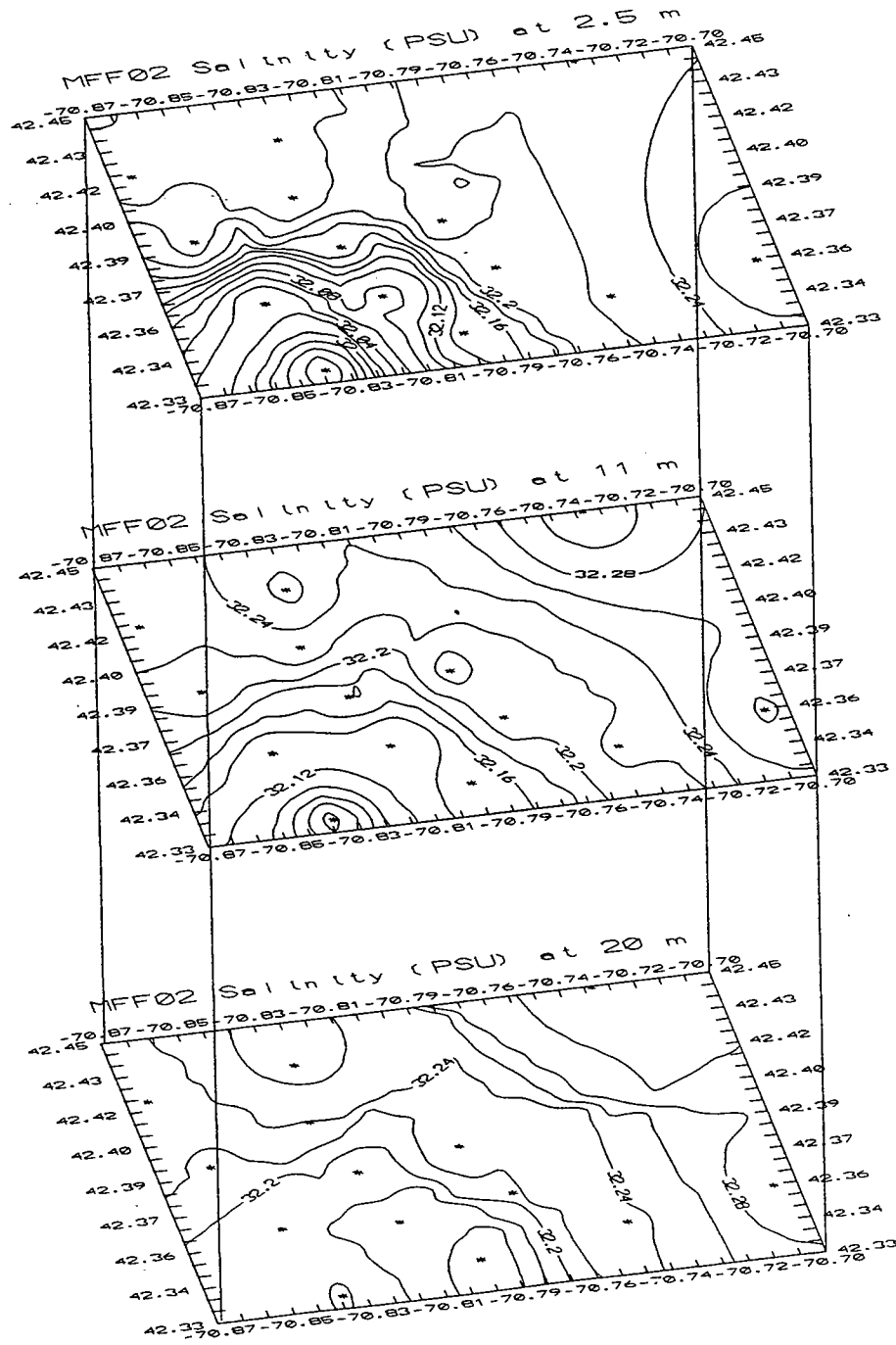
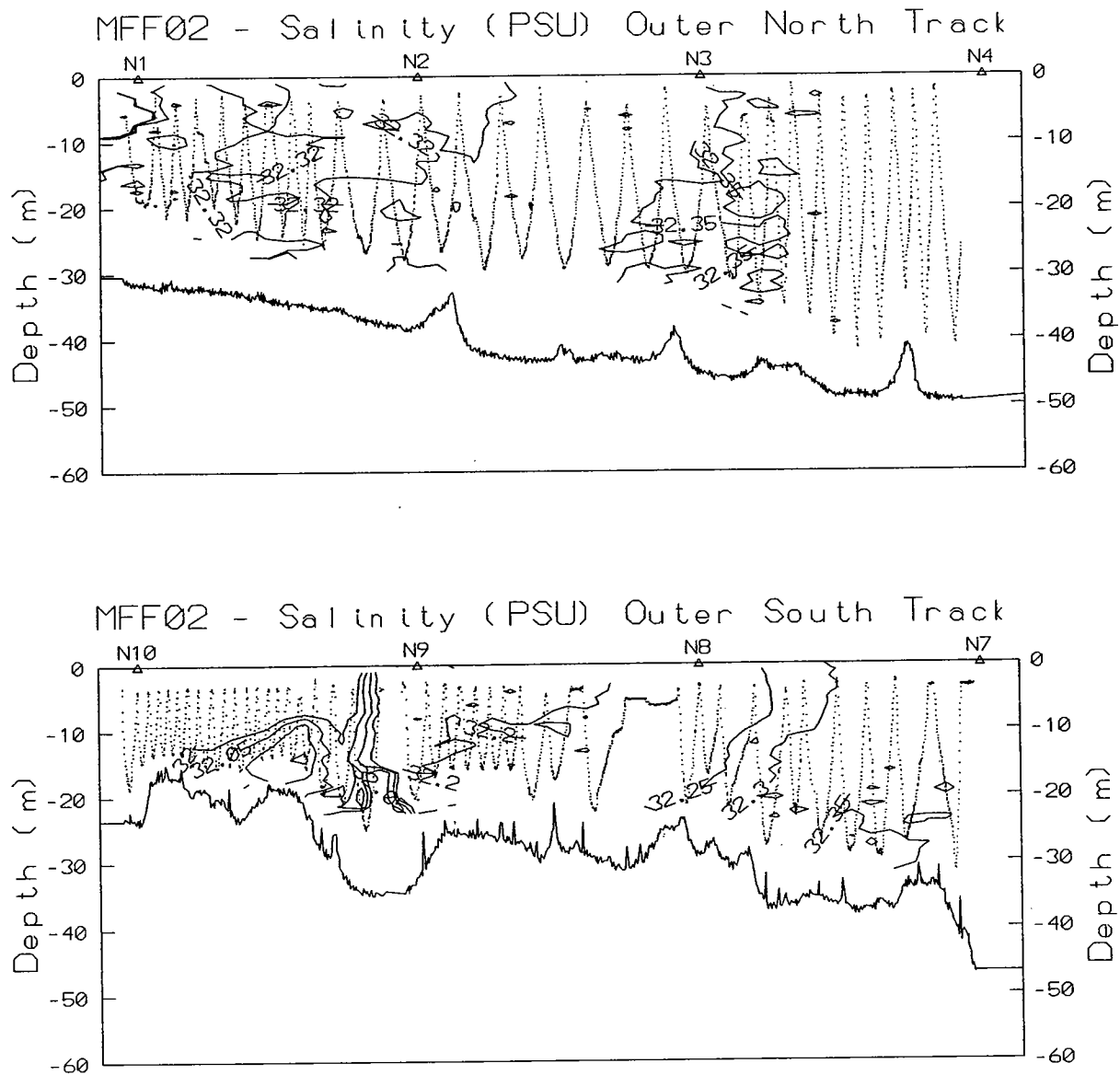


Figure 4-35 Surface nutrient concentrations ( $\mu\text{M}$ ) during day 1 of nearfield sampling in March 1992. Data are given in Appendix B. Contour intervals are  $1 \mu\text{M}$  for DIN and SiO<sub>4</sub>,  $0.5 \mu\text{M}$  for NH<sub>4</sub> and NO<sub>3</sub>, and  $0.1 \mu\text{M}$  for PO<sub>4</sub>.



**Figure 4-36**

The salinity field in the nearfield viewed as horizontal slices at 2.5, 11, and 20 m water depths. The water depth along the western edge (left) is as shallow as 25 m whereas, the water depth on the eastern edge (right) is on the order 45-50 m. Data are from vertical casts on nearfield day 1 at stations whose positions indicated. The contour interval is 0.02 PSU.



**Figure 4-37** Vertical section contours of salinity generated from tow-yos in March 1992. The view is towards the North, with a corner of the Nearfield grid at either end of a track. Bottom bathymetry is shown, with increasing water depth to the offshore (right). The V-pattern shows the position of the towfish along the track, where data were collected as the basis for the contouring.

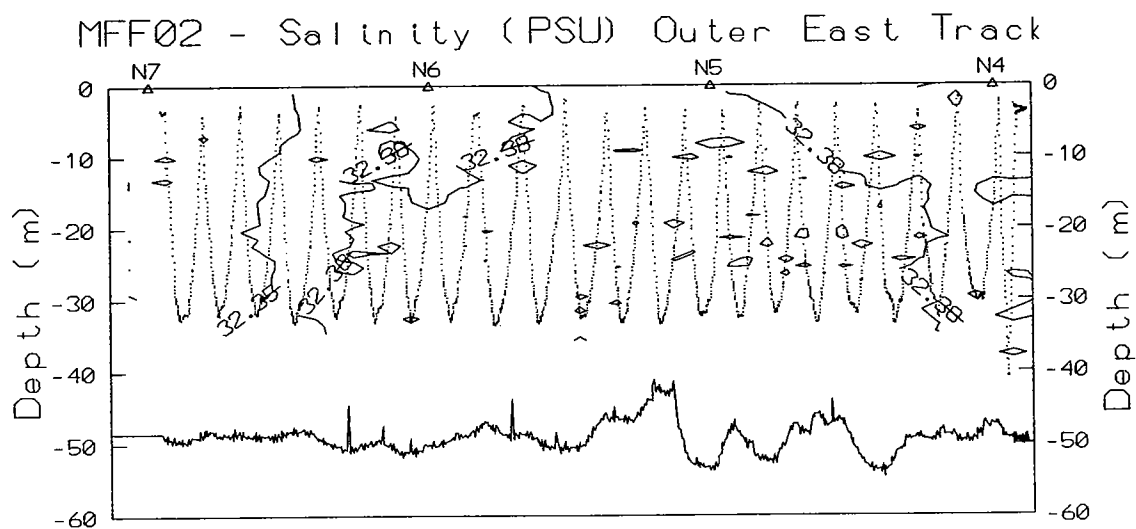
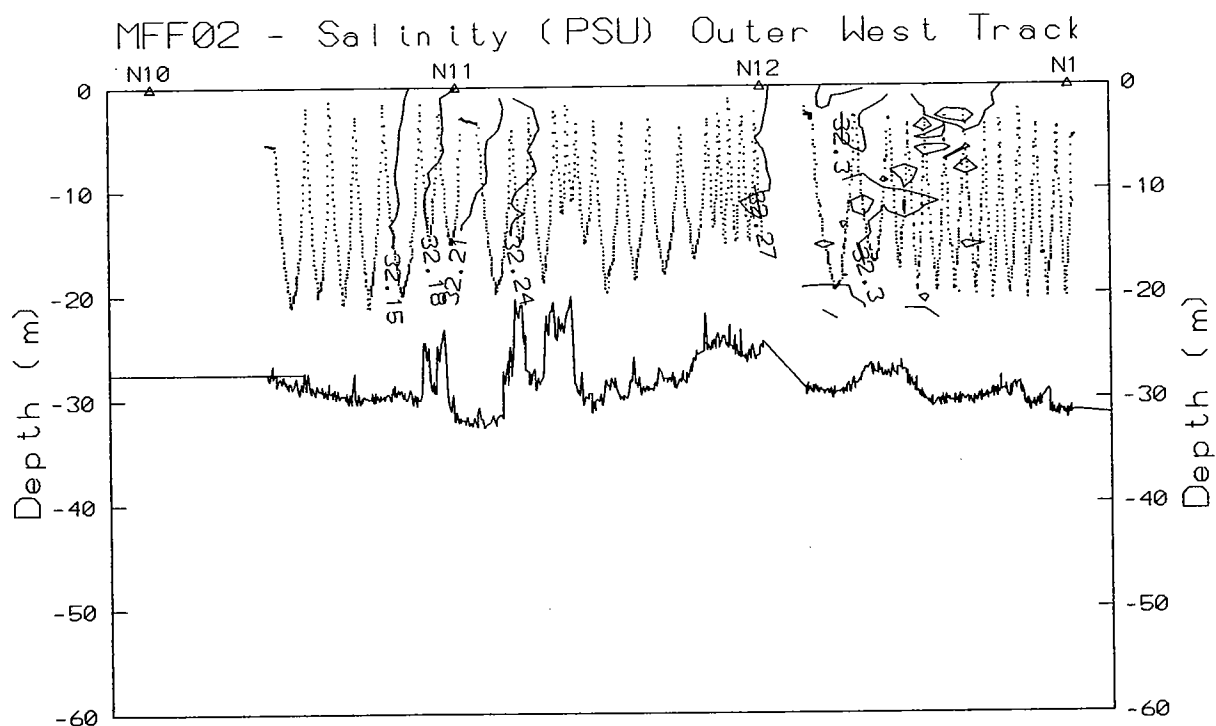


**Figure 4-38** Vertical section contours of salinity generated from tow-yos in March 1992. The view is towards Boston Harbor, with a corner of the Nearfield grid at either end of a track. Bottom bathymetry is shown, with increasing water depth to the offshore (bottom). The V-pattern shows the position of the towfish along the track, where data were collected as the basis for the contouring.





## **5.0 DISCUSSION**

### **5.1 Water Properties (Physical and Chemical)**

#### **5.1.1 Variability at the Regional Scale**

Broad regions were rather easily “typed,” even with the small range of physical parameters and with little vertical structure of the water column. At the regional level, a series of geographic/depth groupings of stations, at least partially distinguishable by physical measures, were easily discerned by nutrient content in February. For example, a plot of all stations and depths, grouped by stations as in Sections 3 and 4, readily showed the coastal group in western Massachusetts Bay was influenced strongly by the present outflow of dissolved inorganic nitrogen (DIN) from Boston Harbor (Figure 5-1). In contrast the Cape Cod Bay group, with an earlier winter-spring bloom initiation, stood out as low in DIN. In the middle stood the offshore (deeper) waters of Massachusetts Bay with a slight trend of increased DIN with depth. The regional picture became more muddled by March, when the North-South gradients were less strong and phytoplankton had begun to draw down the high dissolved nutrients in western Massachusetts Bay (Figure 5.2).

#### **5.1.2 Small-Scale Time and Space Variability in the Nearfield**

The nearfield was a dynamic region, as seen by several types of evidence. First, the boundary between coastal and offshore waters cut across it, but appeared to flex in and out with seasonal cooling and/or other events that changed conditions at stations both within and across days. Second, this region was clearly part of the present mixing zone of coastal nutrient export from Boston Harbor to offshore waters. Small-scale patches at the surface, as well as at depth, were routinely seen by high-resolution sampling/instrumentation. Some features were transient, and small, such as a lens of higher salinity water at the surface between two sampling stations, detected by tow-yo sampling. Others were persistent for at least several days, or recurrent, like the finger of surface water often extending out through the southwest corner. Finally there were meso-scale, advective events, like the high-chlorophyll water mass that appeared to cross the North track in February.

### 5.1.3 Coherence of Nearfield and Farfield Station Properties

As the season progressed from February to March, a disjunction in the timing of the winter-spring bloom and its associated ecological progression appeared to separate the nearfield from Cape Cod Bay. Clearly, stations within the nearfield were highly connected at times with surrounding offshore surface waters — North, East, and West waters impinged upon the nearfield. Figure 5-3 suggests how eastern offshore waters may have been shoaling into the nearfield to feed silica and other nutrients to nearfield surface waters. This shoaling would be a mechanism to continue depletion of deep-water nutrients as the season progresses, at least while the water column is well mixed. It was not obvious that surface or deep waters of the nearfield strongly communicated at this time with shallow inshore water to the south. There was a density structure suggesting coastal current flow from Hull down the coast past Cohasset that may not have interacted with the shallow nearfield. On the other hand, density structure along the outer edge of the nearfield grid strongly suggested that water from the North coursed down the Bay through the deeper section of the nearfield.

### 5.1.4 Comparison to Previous Studies

Overall, broad features for physical and chemical variables measured in the same areas in recent years were not remarkable in this year. It was a cold year, colder than measured by Geyer *et al.* (1992), but similar to February/March conditions described by Townsend *et al.* (1990). Coastal-offshore distinctions, shoreline cells of low salinity, and overall well-mixed vertical conditions have been the norm described in comparable studies.

## 5.2 Water-Column/Nutrient Dynamics

### 5.2.1 Vertical Structure

Only subtle layering of water was observed. For the most part, the water did not deviate strongly in  $\sigma_T$ , indicating how easily mixing could take place. Sometimes small, transient local features were observed, but there was no initiation of a seasonal stratification due to warming of the upper water column. Conditions overall cooled slightly from February to March.

Nutrient chemistry, for either total or dissolved forms, did not vary much at a station or a station grouping as a function of depth (e.g. Figure 5-4).

Silicate, however, was interesting because of an obvious increase in the deepest waters of Stellwagen Basin (Offshore group, Figure 5-5), partially a result of diatoms actively removing silicate near the surface. The well-mixed conditions apparently allowed removal of silicate from solution over the entire depth of most stations, as witnessed by the difference between concentrations from February to March. Even the deep offshore waters appeared to lose 2-3  $\mu\text{M}$  of  $\text{SiO}_4$  over this time. These conditions appeared to be progressively leading to diatom growth curtailment even if stratification were not initiated soon.

### **5.2.2 Inshore-Offshore Gradients, Including Boston Harbor Mouth**

Of all gradients, the high nutrient (N and P) concentrations decreasing from Boston Harbor outward and along the South shore, were most striking in February. Prior to significant biological activity, (i.e., February) the dissolved nutrients showed a strong decrease offshore. But the combined forms of nitrogen, either as TDN, PON + DIN, or Total N (TDN + PON) all demonstrated the gradient pattern to some degree. Overall, a relation between TDN and DIN was maintained over the region, especially showing the range from near the Harbor (highest of the coastal group) to the nearfield (Figure 5-6). The pattern for February suggested that DON (DON = TDN-DIN) also had a slight gradient out of the Harbor in that the coastal stations nearest the Harbor had DON in the range of about 10-12  $\mu\text{M}$ . Also a couple Cape Cod Bay Stations, where blooms were present, had slightly enriched DON concentrations, otherwise in February and March DON was fairly constant at roughly 8-9  $\mu\text{M}$  (as suggested by the y-intercept in Figure 5-6).

### **5.2.3 Influence of Water from Northern Rivers/Special Features**

In February, but not March, a distinct surface water mass from the North impinged on the nearfield. With it came high chlorophyll levels. This water was not found at the most shallow station of the northern transect, but was detected slightly offshore. Whether or not such water, which was warmer, originated from the Merrimack or other rivers, is not known. Being somewhat warm may suggest a complicated history, rather than a simple outflow of cold fresh water from the land.

### **5.2.4 Comparison to Previous Studies**

Nutrient levels, ratios, distribution, fluctuation, and patterns were broadly similar to those observed in recent studies of Townsend *et al.* (1990) and Geyer *et al.* (1992). Both of those studies extended into deeper waters, even outside the Bay, and some of their results showed higher nutrient concentrations. However, our February cruise may not have estimated the highest seasonal maximum for dissolved

nutrients in the Bays; it certainly didn't do so for Cape Cod Bay.

### **5.3 Biology in Relation to Water Properties and Nutrient Dynamics**

#### **5.3.1 Phytoplankton—Zooplankton Relationships**

Species composition of the phytoplankton and zooplankton communities were independent of stations, sampling depths, and cruises. There were minor variations in the top dominants across time and space, but mostly the typical winter-spring, diatom-dominated, coastal pelagic community was present.

From a trophic perspective, although we have no data on zooplankton grazing of phytoplankton, there was not a strong relationship between phytoplankton (numbers or chlorophyll biomass) and zooplankton numbers. During February, if anything, zooplankton were less abundant at high phytoplankton levels (Figure 5-7). That zooplankton were less numerous at stations with higher chlorophyll may simply reflect their slower, or lagged, development relative to rapid phytoplankton bloom events at very low temperatures. Such a lag in the peak of zooplankton would be typical for winter-spring pelagic dynamics. Even so, Station F23P at the mouth of Boston Harbor was especially low in zooplankton and remained so in March. The reason for this station's slightly different behavior, which was somewhat mimicked by Station F2P in Cape Cod, was not apparent.

Other than these two stations, the data started to suggest a tendency to have higher zooplankton at higher phytoplankton levels by March (Figure 5-8). Lest one conclude that a lagged zooplankton response was indeed catching up with phytoplankton to produce this tendency, it should be noted that zooplankton numbers on the whole were not different between February and March and weak patterns may be more a result of "noise" than a clear trophic response.

#### **5.3.2 Plankton Species and Water Properties**

As noted above, there were distinct distributional patterns evident on the basis of the physical and chemical environment, but the pelagic community was rather homogeneous throughout the Bays. There were anomalies at some stations, and these are described in Section 5.3.5.

The timing of biological events had some patchiness in expression, but there was a general latitudinal tendency, with the South preceding the North in development of high chlorophyll biomass on the broad scale. Such a gradient was most noticeable considering only the shallower stations of western

Massachusetts Bay and Cape Cod Bay. If these events were driven principally by light, as suggested below, one would expect energetic/trophic similarities across stations, but it is still surprising that the similarities were so strongly expressed in species composition. The similarities must be testament to the generally well-mixed conditions over the region and may imply that scales of horizontal and vertical physical processes are generally faster than biological growth rates at this time of the year.

Regardless, the similarity may imply that the Bay waters at this time were not highly isolated patches, biologically. The results also point out that, under the observed range of conditions, species composition was not very sensitive to DIN variations in the range of ~1 to 13  $\mu\text{M}$ . Otherwise, the area and stations just outside of Boston Harbor would have appeared much more distinct from other areas.

### 5.3.3 Chlorophyll Biomass and Nutrient Distribution

In contrast to *species* being somewhat insensitive to dissolved inorganic nutrients, the nutrients themselves were strongly affected by plankton *biomass* as suggested by chlorophyll. Thus, during February a strong inverse relation was apparent between phytoplankton (numbers or biomass) and DIN (Figures 5-9 and 5-10). At stations with high chlorophyll, the phytoplankton had drawn down nutrients to low levels, whereas around Boston Harbor nutrients were high and chlorophyll was low. By March, the plankton around Boston Harbor had helped to draw down DIN to intermediate levels (4.5-6  $\mu\text{M}$ ) (Figure 5-9) and the general relationship was less strong.

In Cape Cod Bay, there were some temporal differences among stations. Chlorophyll at Station F2P was somewhat sustained or at least similar, from February to March, and thus seemed to lag the dynamics of station F1P, where a peak had passed.

In general, there was a strong relation between chlorophyll and phaeopigments (Figure 5-11) on both cruises. In February, the phaeopigments, an indicator of degraded chlorophyll, were about 25% of the total in most cases. This percentage generally increased to about 30-50% in March.

In each case, stations that were relatively high in chlorophyll had the lowest percentage of phaeopigments (Figure 5-11), perhaps indicating more recent growth. Overall, the direction of change (during February-March) for the whole region was towards an aging phytoplankton community. This would be expected and may be the preface to the cessation of the winter-spring flowering, sinking of cells, and removal of nutrients from surface waters in subsequent months.

### 5.3.4 Metabolism and Environment

In theory, and as shown in previous bottle enrichment experiments (e.g., Smayda, in MWRA, 1988), both the initial rise in net production that takes place in response to irradiance (the model parameter,  $\alpha$ ) and the net production rate at light saturation (the model parameter,  $P_{\max}$ , normalized for chlorophyll biomass) should increase as nutrient concentrations (or supplies) increase. Using graphic estimates of  $P_{\max}$  (see Appendices G and H), which are admittedly rough, the data for P-I incubations for February suggest a trend of increasing  $P_{\max}$  with increasing DIN over the observed environmental range in concentration (Figure 5-12). Data for March, where some curves did not allow even a rough graphic estimation of  $P_{\max}$ , extended over about one-half the February DIN range and a  $P_{\max}$ -DIN relation is less striking.  $P_{\max}$  shows some promise as an additional indication of nutrient status.

No relation was obvious between normalized production and other environmental factors examined, such as temperature. For example, F23P, F2P, and F1P surface samples (see Figure 5-12) were within about 0.5°C of each other. Comparison of P-I curves, surface and deep, from station to station, did not suggest markedly different physiological status as a function of depth and phytoplankton species counts did not vary consistently with depth. These and other measures simply suggest a well-mixed ecological condition. P-I curves, together with *in situ* irradiance, suggested that daily and diurnal light fluctuations could govern net production rates at this time.

Thus, this group of observations support the notion of light as a limiting factor especially during the February cruise, but additionally suggest that where nutrients were highest, doubling and growth of phytoplankton could be most rapid if light were available. This hypothesis would predict that higher chlorophyll levels may appear to emerge from outside Boston Harbor as the season progresses and the light supply at that location becomes sufficient to initiate a bloom.

If light is indeed limiting the initiation of a winter-spring peak in chlorophyll, the appearance of generally higher chlorophyll earlier in Cape Cod Bay than in most of Massachusetts Bay may be due to several factors. Coastal winter-spring bloom events appear to require a critical daily threshold of light for initiation (Hitchcock and Smayda, 1977) and timing from year to year or place to place over a geographical range may be keyed to such a threshold. The daily source intensity of light is a function of daylength and sun angle (season-latitude), as well as atmospheric transparency (cloudiness) and surface water reflectance. The light supply actually experienced by phytoplankton is modified in part by the water clarity; attenuation is a function of suspended particles (inorganic or organic) and dissolved matter as well as seawater's own attenuation. The rate and depth of vertical mixing can help regulate the position of plankton cells, their light field over a day, and in this way, the average daily intensity of the population (e.g. Sverdrup, 1953; Smetacek and Passow, 1990). It is not clear from the data at hand how much each of these factors may have contributed to the observations and the earlier bloom in Cape Cod

Bay could have been in partial consequence of several. Finally, the sky condition, if generally clearer over Cape Cod Bay than Massachusetts Bay, could be a contributing factor.

A final note on metabolism and system dynamics. Respiration was not detectable, and the system as a whole was likely showing net system production (excess of production over respiration). Oxygen during the February cruise was generally 110-120% of saturation, giving strong evidence of net system production. The degree to which sinking of this net production occurred from February to March would be best indicated by changes in total nitrogen in the water column over time (expressed as a function of  $\sigma_T$  or salinity). The bulk of the data on combined nitrogen forms showed only slight diminishment from February to March. This suggests that while dissolved nutrients were being taken up and bundled into particles, these particles, to a large degree, may not have yet fallen from the upper water column within the Bay outside of the Boston Harbor region.

### 5.3.5 Special Features/Anomalous Stations

Biologically, there were a few situations that stood out from the norm. Station N4P was distinctive for the dominance, in March, by high numbers of blue-greens (Cyanophyceae) as well as phytoplankton and zooplankton species indicative of a more oceanic water mass. The biology seemed in this case a reflection of physical conditions that brought higher salinity waters with distinctive surface geochemistry to this location.

A previously noted special feature was the presence of barnacle larvae in coastal surroundings of Boston Harbor. There were subtle differences also in diatoms, such as the presence of the small diatom *Detonula confervacea* around Boston Harbor in March while the small diatom *Leptocylindricus minimus* was dominant in Cape Cod Bay (Table 4-2), but these were neither persistent across cruises, nor of any likely large ecological consequence.

### 5.3.6 Comparison to Previous Studies

The range of chlorophyll concentrations were similar to recent studies of Massachusetts Bay by Townsend *et al.* (1991), Cura (1990), and Smayda (in MWRA, 1988). Light extinction, and the depth of the 1% light level were similar to results in February/March of Townsend *et al.* (1991) in northern and western Massachusetts Bay.

Zooplankton species and counts for other recent studies were unavailable, but data here were typical of other coastal waters (Turner, personal observation). The phytoplankton species composition observed



in this program had the primary complement of species routinely observed in recent Massachusetts Bay Studies (Townsend *et al.*, 1991; Cura, 1990; Smayda, in MWRA 1988). Abundances were in expected ranges (Cura, 1990), although results vary as a function of methodology.

Metabolism results were similar to some previous studies. The P-I data showed fundamentally the same high  $\alpha$ , sharply saturated response that was evident in the short-term  $^{14}\text{C}$  incubations of Townsend *et al.* (1991), and the longer-term incubations of Smayda (MWRA, 1988).

Enrichment studies of Smayda (MWRA, 1988) showed an increase of normalized  $P_{\text{max}}$  with increased nutrient concentrations. Smayda also showed no significant species changes as a result of short-term (several days) experimental enrichment with DIN concentrations that were higher than observed in this study. Longer-term studies (years) at the Marine Ecosystem Research Laboratory (MERL) have demonstrated that shifts and oscillations among resident phytoplankton species regularly occur with nutrient enrichment, but persistent shifts of the community to dominance by initially rare forms has not been found to occur. Interestingly, the data from the February and March survey support such findings:  $P_{\text{max}}$  had a tendency to increase with nutrients in spite of only small variations in the dominant phytoplankton species (Tables 3-2 and 4-2).

The P-I data gathered on the monitoring surveys are most suitably used as an indicator of station and depth differences related to nutrient status, light limitation, or comparison of  $P_{\text{max}}$ . However, the data on chlorophyll-normalized net production (P) as a function of irradiance (I) may be coupled with light extinction and the fluorescence-estimated vertical distribution of chlorophyll at a station to model net production rates over the photic zone.

Such modeling requires a number of assumptions, and results are sensitive to these. A full sensitivity analysis is beyond the scope of this report, but a simple example calculation was made with data from one station in order to provide a rough idea of integrated water column rates.

For Station N4P in February, a good model fit was obtained for the P-I data. We assumed  $P_{\text{max}} = 17$  and  $\alpha/P_{\text{max}} = 0.016$  for the whole water column. The incident light during daylight hours ( $\sim 800$ - $1600\text{h}$ ) was measured at various stations and times (over the survey period) and averaged about  $260 \mu\text{E m}^{-2} \text{sec}^{-1}$ , quite low, as it was cloudy. Using the light extinction profile from 0-25 m, we calculated average daily light levels at depth increments. These were entered into the model,  $P_B = P_{\text{max}} (1 - e^{-(\alpha I/P_{\text{max}})})$ , to calculate  $P_B$  at that depth increment. Rates were multiplied by average chlorophyll (fluorescence) appropriate for that depth (Appendix C). Conversion was then made to express rates as per  $\text{m}^3$ , rather than per L, and increments summed 0-25 m, to arrive at a rate per  $\text{m}^2$  of water surface. This rate was multiplied by an assumed 8-h daylength to arrive at a daily rate of  $5272 \text{ mg O}_2 \text{ m}^{-2} \text{ d}^{-1}$ . The lower 10 m of the column had calculated  $P_B$  rates that were well within the error of respiration estimates; if the

net production of this layer were subtracted, the integrated water column rate was  $4632 \text{ mg O}_2 \text{ m}^{-2} \text{ d}^{-1}$ . Assuming a PQ (PQ = Photosynthetic Quotient, the ratio of  $\text{O}_2$  produced per  $\text{CO}_2$  utilized) of 1.25, the resultant rates, converted to carbon units, ranged from  $1386\text{-}1578 \text{ mg C m}^{-2} \text{ d}^{-1}$ , or roughly  $1.5 \text{ g C m}^{-2} \text{ d}^{-1}$ . Note that this was at a station that had relatively high chlorophyll levels, and that the entire field had relatively low light levels because of clouds.

There is only a small historical base of measurements that have been made and these have been performed and calculated using quite different methods. Summarized by Cura (1991), there have been about 10 separate primary production estimates in the nearfield vicinity reported during the February to March period and these range from 0.2 to almost  $7 \text{ g C m}^{-2} \text{ d}^{-1}$ , the higher being in March and at higher observed chlorophyll levels. It is difficult to make much of limited comparison, given the many inherent differences in methods and assumptions necessary to make these calculations, but the example shows that the monitoring data can be further exploited to make such estimates.

## **5.4 Recommendations**

### **5.4.1 Station Locations**

The placement and spacing of stations was sufficient to capture numerous details of the physical, chemical, and biological character within the nearfield region. Even with a well-mixed field and a small range of most parameters, the relationship between the nearfield and its surrounding waters was described very powerfully. Thus, the array of farfield stations for conditions at this time of year allowed a strong description of sources and influences on the nearfield, such as from existing Boston Harbor water outflows and offshore waters surrounding the eastern edge of the nearfield. Additionally, the farfield stations allowed reasonable characterization of Cape Cod Bay, and elucidated some difference in timing in seasonal ecological dynamics in that region compared to Massachusetts Bay. The choice of stations for more comprehensive measurements (BioProductivity stations) provided a good data set to confirm and refine features evident from the hydrology/nutrient stations. Their positioning allowed strong description of regional-scale latitudinal patterns, as well as the relationship between shallow near-coastal and nearfield stations; the outer corners of the nearfield provided refinement on the nature of offshore-nearfield relationships.

Finally, the sampling strategy that characterizes the farfield area surrounding the nearfield just prior to repeated visits to the nearfield, has the advantage of detecting some of the short-term, fine-scale variability that seemed associated with physical dynamics.

#### 5.4.2 Field and Laboratory Procedures

The combination of the physical, geochemical, and biological measurements presented above enabled high-level resolution of ecological variability through the Bays; a virtue of having different types of measures is that they may be used as complementary/corroborating indicators of oceanographic features. In general, the field and laboratory procedures went well. Due to poor performance of the oxygen sensors under extreme cold/freezing conditions on deck, it is necessary either to add more bottle sampling and DO titrations to provide *consistent* coverage in the event of such extreme conditions or to consider dropping this measure during cold winter-spring months. The DO titrations that were performed showed relative homogeneity and little pattern that cannot be better determined by other (non-gaseous) measures. Since this measure as an endpoint also has greatest relevance at warm temperatures, it seems reasonable to conduct this analysis starting sometime later in the year. Likewise, considering the low rates of respiration at these very low temperatures, and the difficulty of measuring significant rates and the expenditure to perform incubations, it would be reasonable to limit this measure also to warmer/stratified conditions when oxygen levels are of immediate concern.

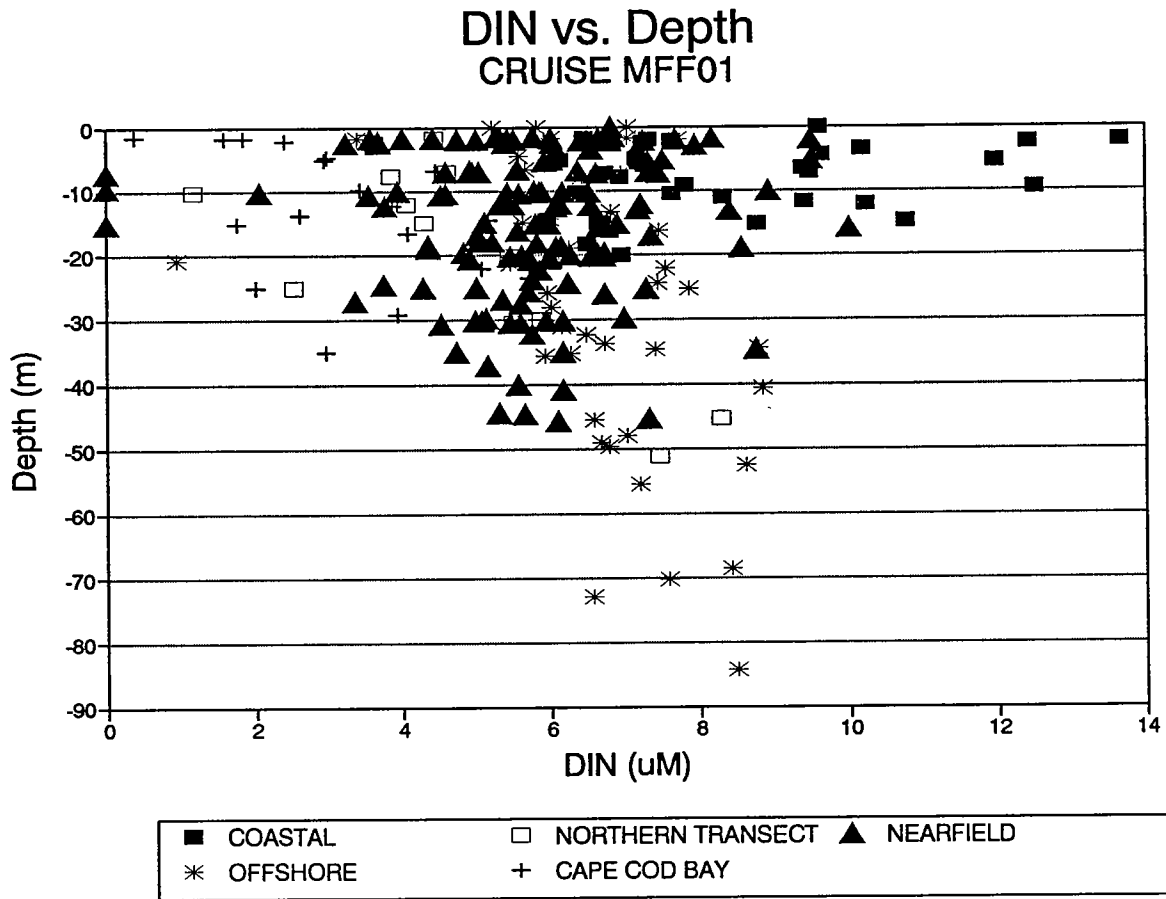


**Figure 5-1** Dissolved inorganic nitrogen vs. depth for all stations in February 1992. Station groups are as given in Figure 3-16. Data are given in Appendix A.

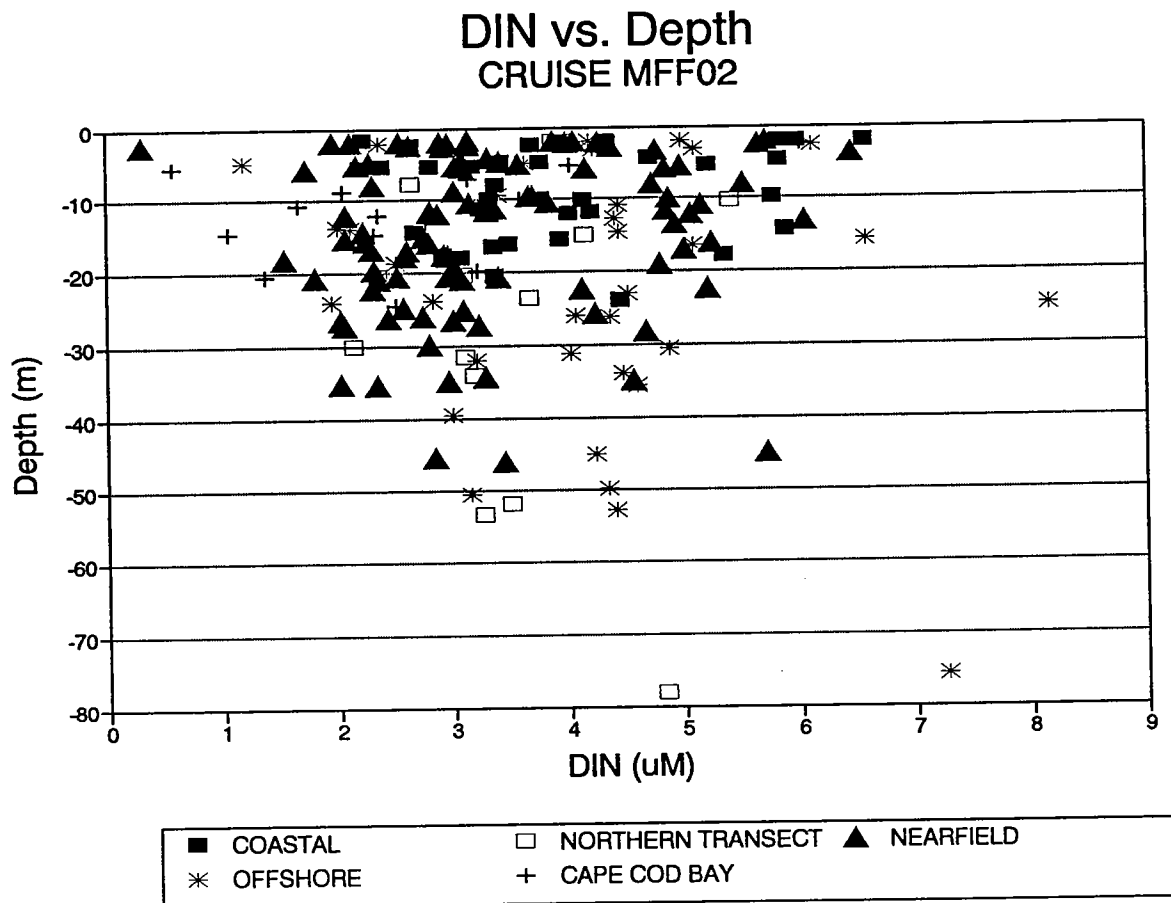


**Figure 5-2** Dissolved inorganic nitrogen vs. depth for all stations in March 1992. Station groups are as given in Figure 4-15. Data are given in Appendix B.

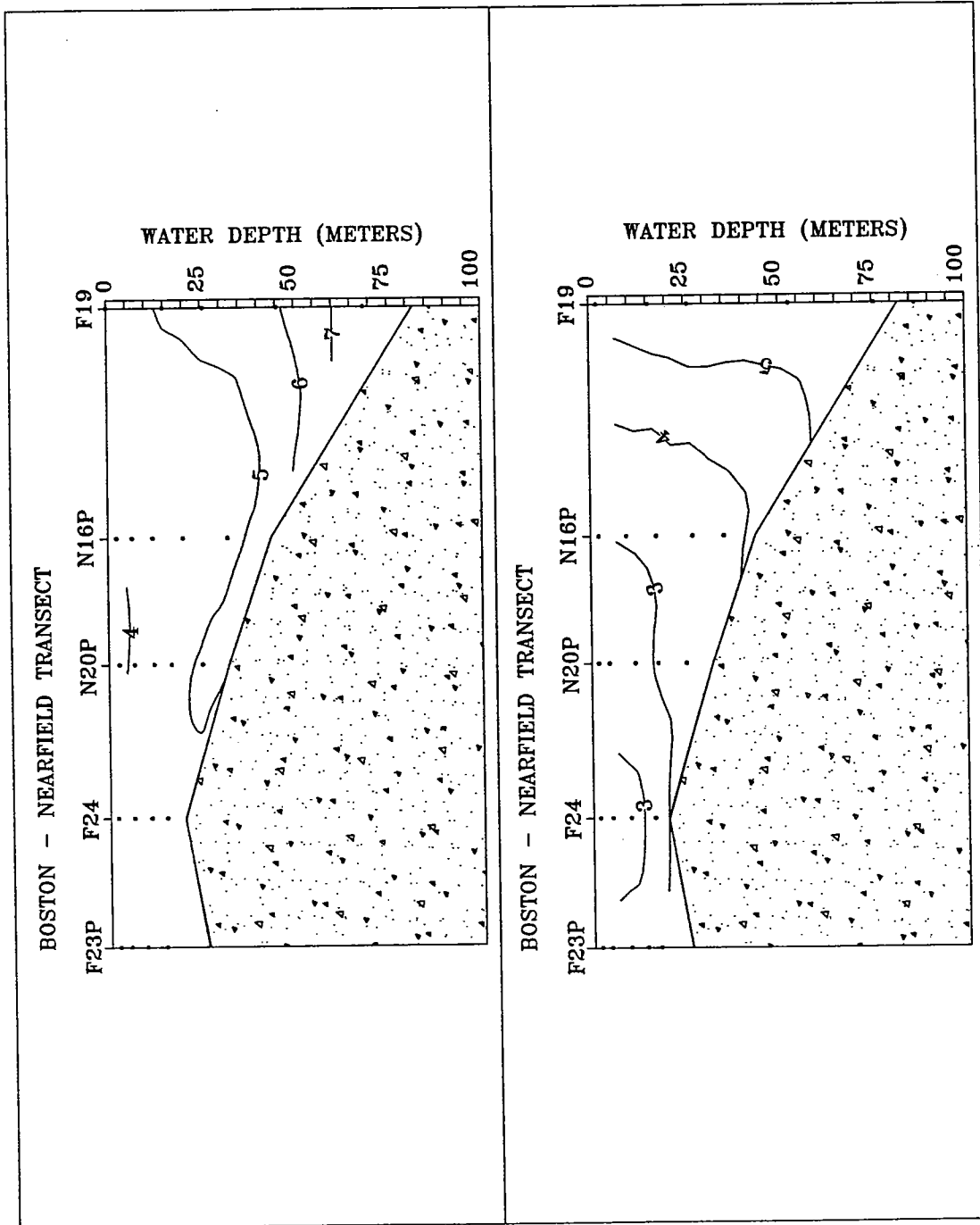
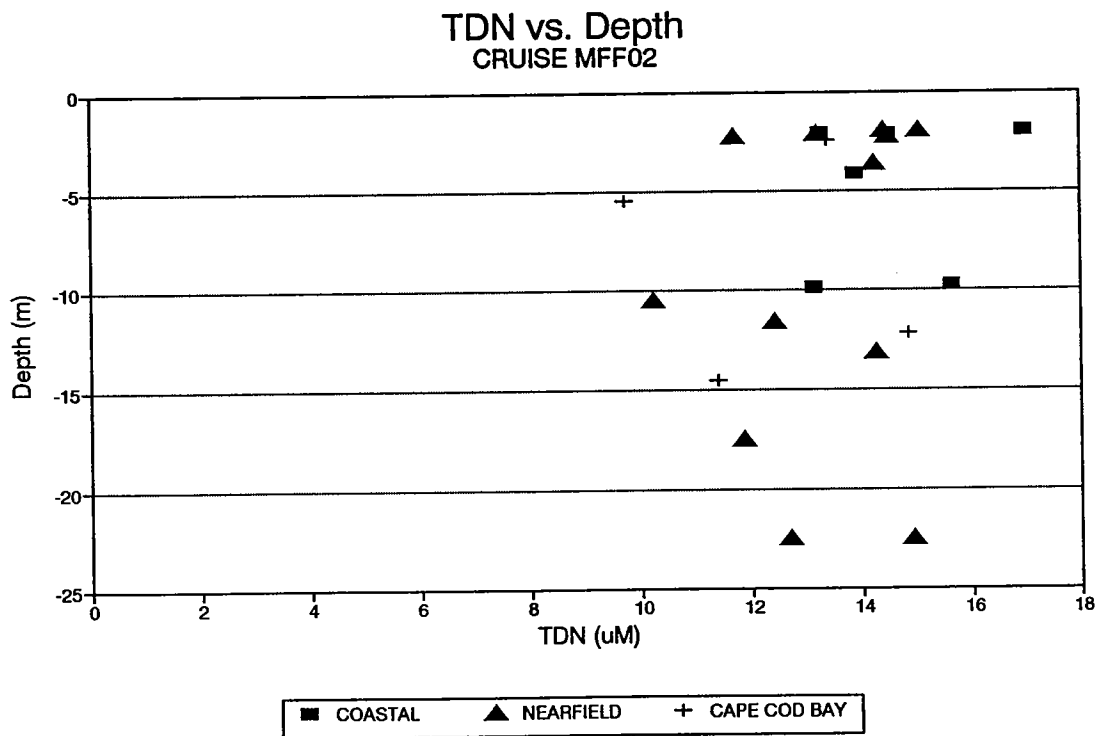
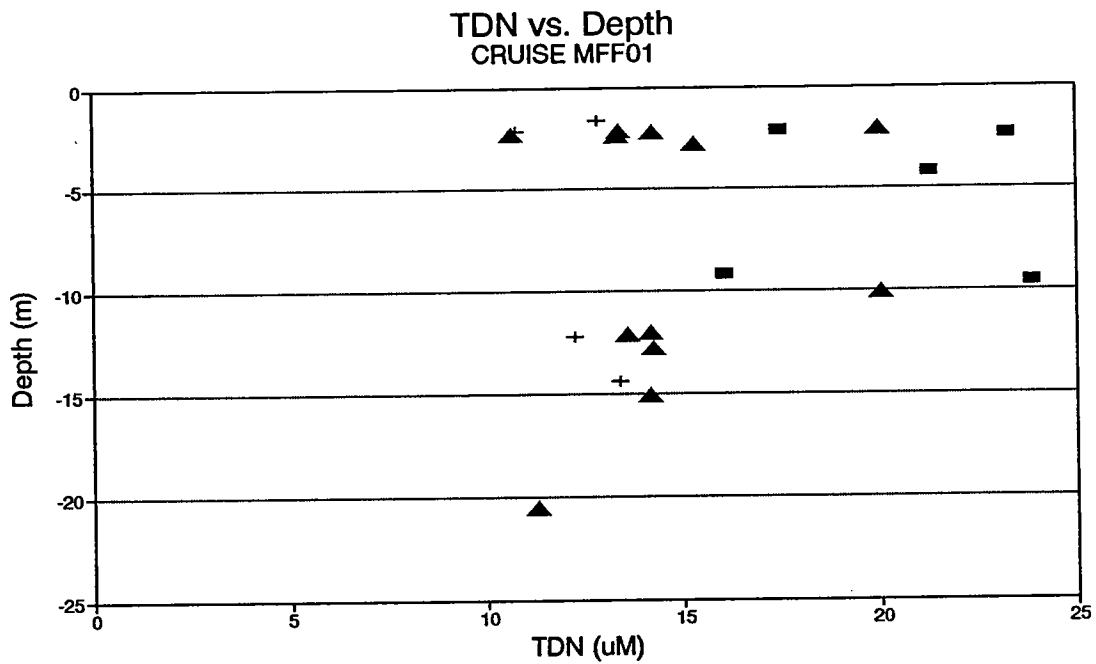
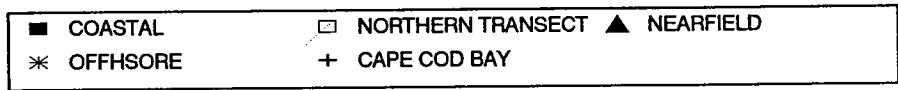
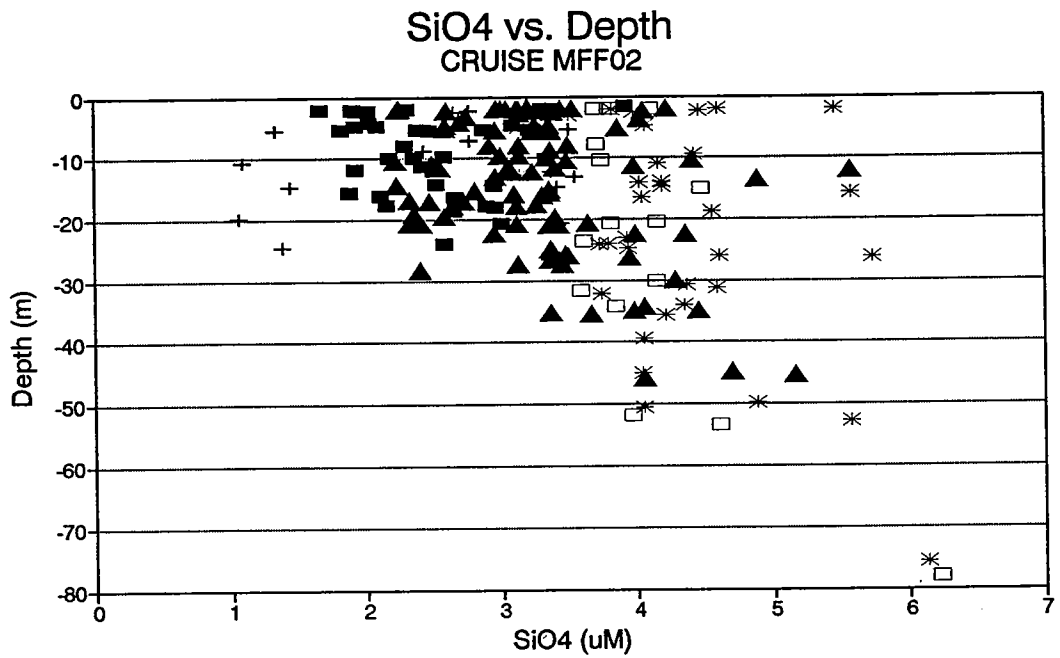
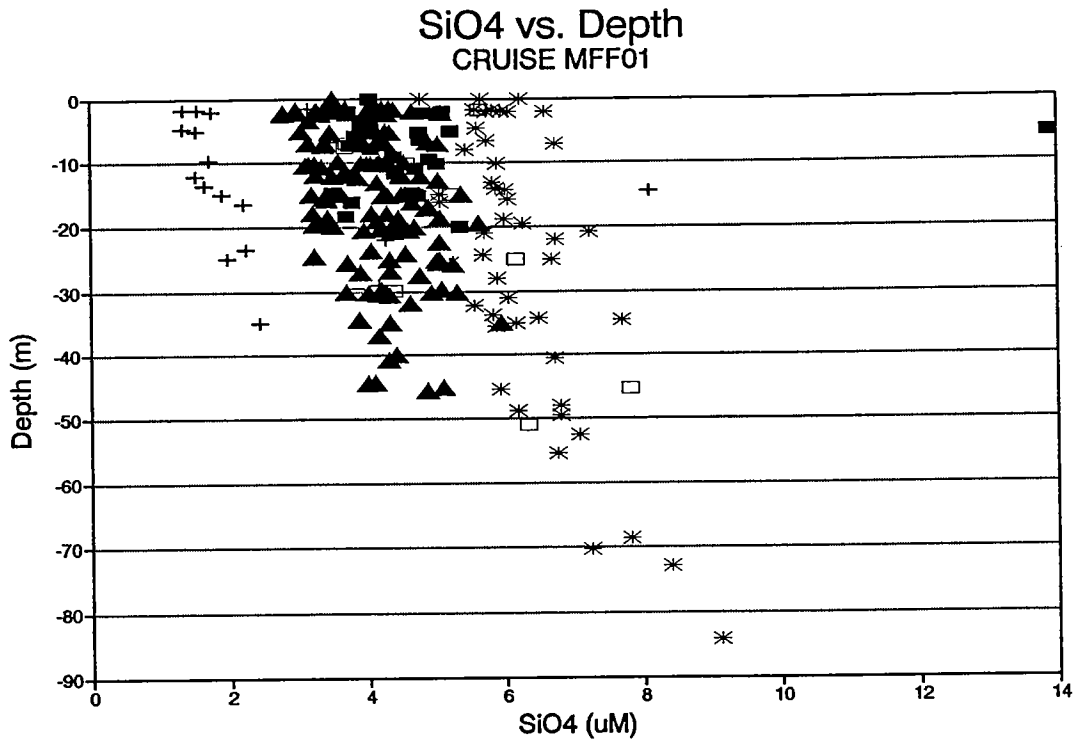


Figure 5-3 Vertical section plots for silicate ( $\mu\text{M}$ ) across the Boston - Nearfield Transect 2 in February (top) and in March (bottom) 1992. Data are from discrete bottle samples as given in Appendices A and B, contour interval is  $1.0 \mu\text{M}$ .



**Figure 5-4** Total dissolved nitrogen vs. depth from BioProductivity stations and special station F25 in February (top) and March (bottom) 1992. Data are given in Appendices A and B. Station groups are as given in Figure 5-1.



**Figure 5-5** Silicate vs. depth for all stations in February (top) and March (bottom) 1992. Station groups are as given in Figure 5-1. Data are given in Appendices A and B.



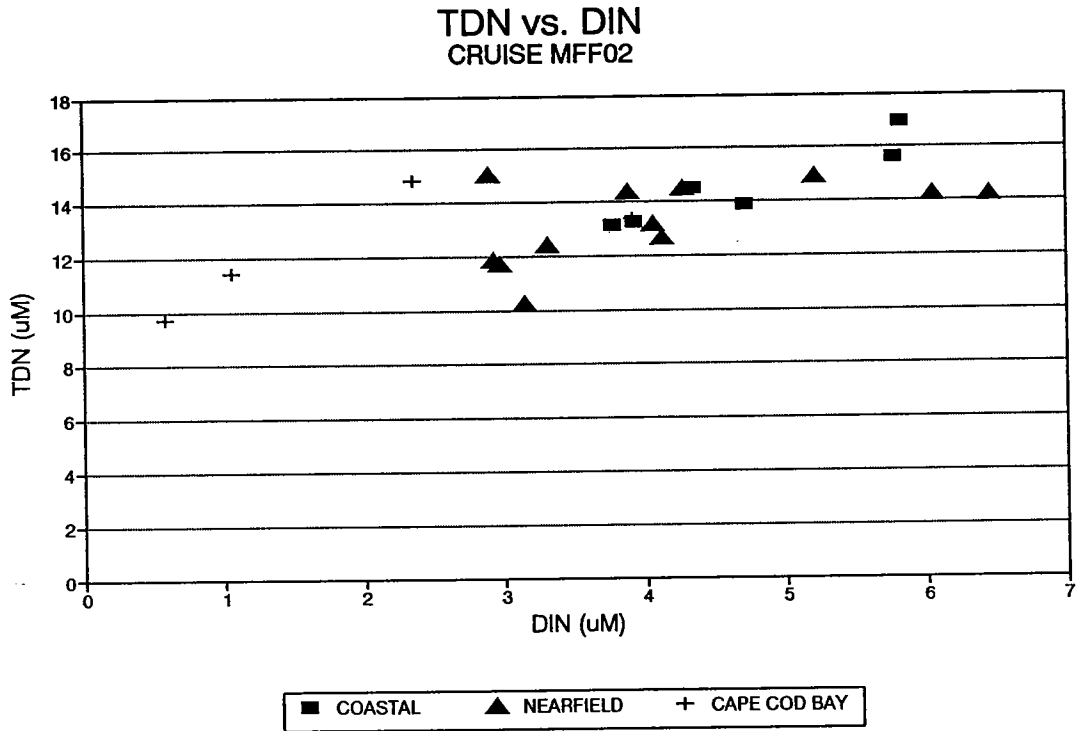
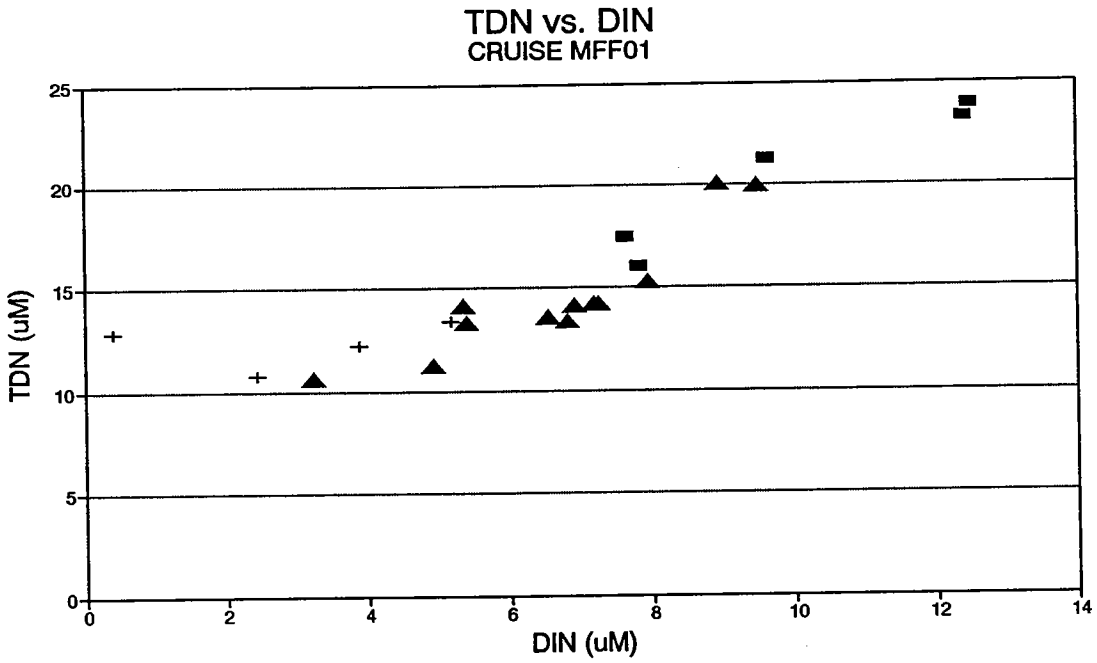


**Figure 5-6** Total dissolved nitrogen vs. dissolved inorganic nitrogen in February (top) and March (bottom) 1992. Data from all BioProductivity Stations are in Appendices A and B.

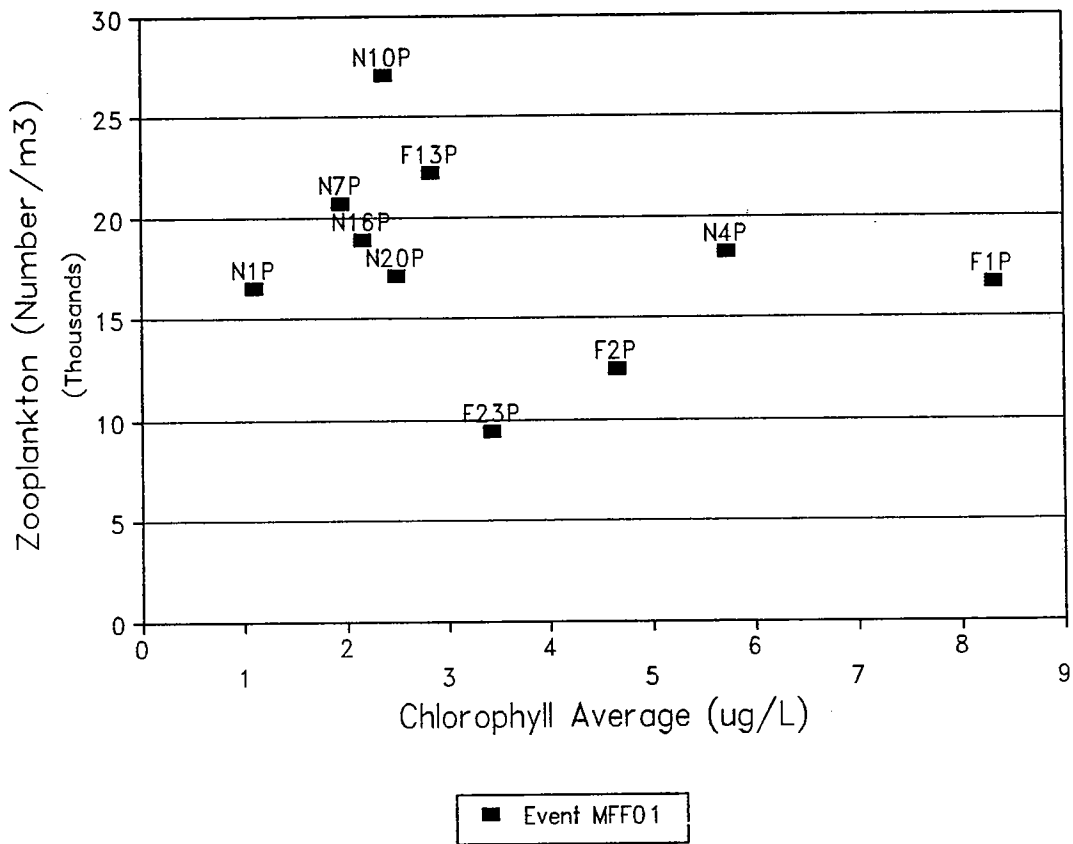
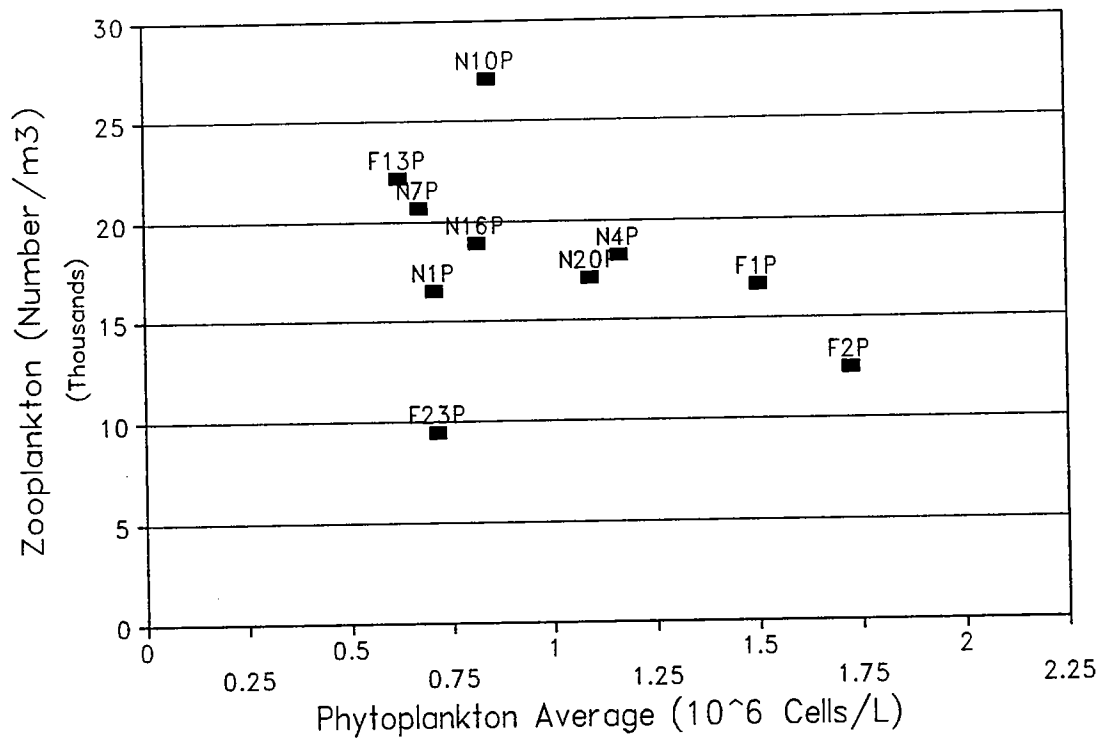


**Figure 5-7 Zooplankton abundance vs. phytoplankton abundance (top) and chlorophyll (bottom) from all BioProductivity stations in February 1992. Phytoplankton samples from surface and depth were averaged; data are from Appendices A, I, and K.**

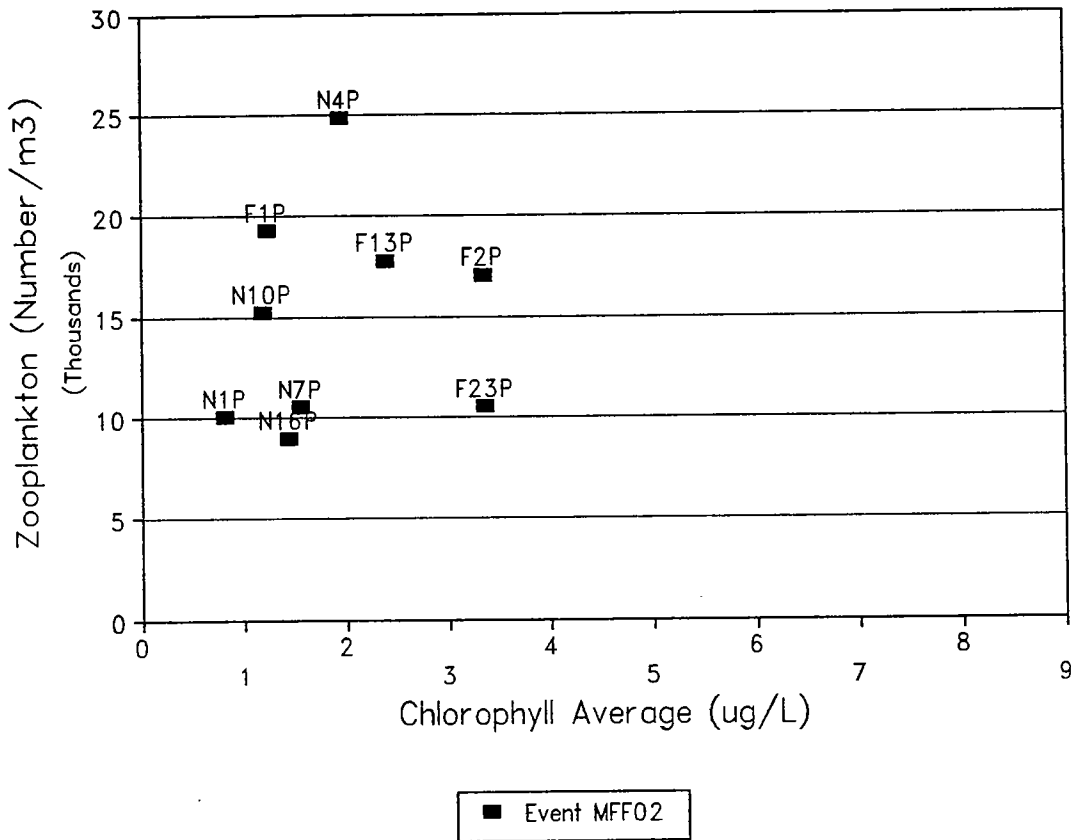
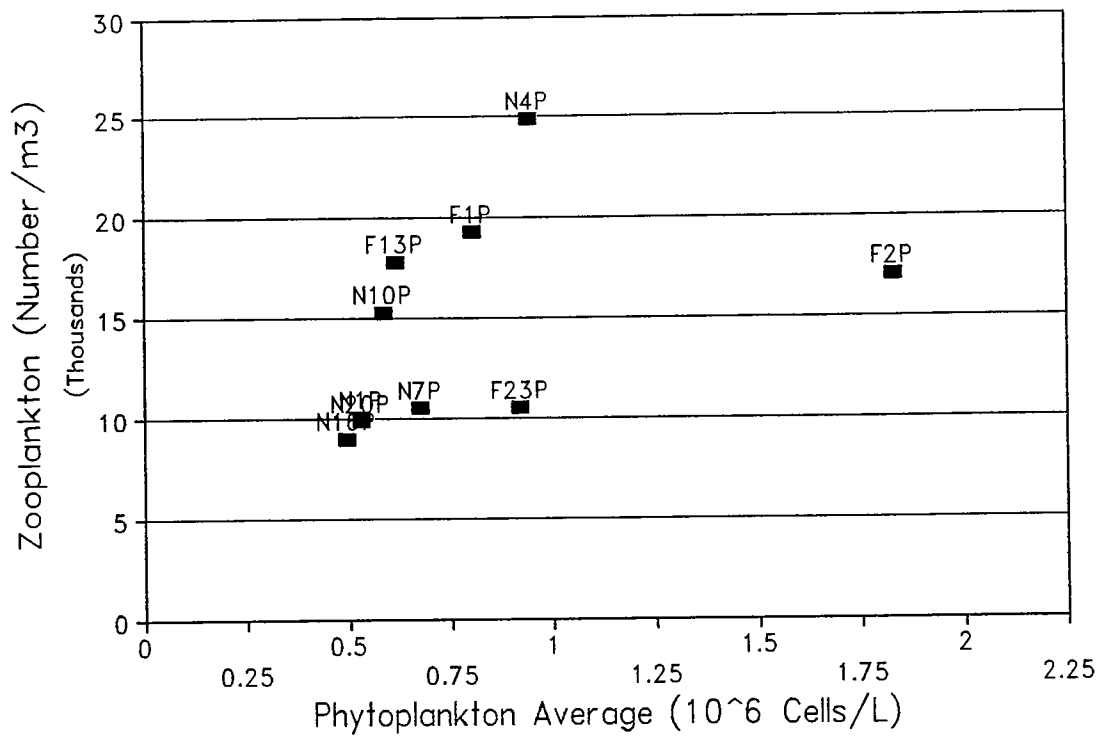


**Figure 5-8** Zooplankton abundance vs. phytoplankton abundance (top) and chlorophyll (bottom) from all BioProductivity stations in March 1992. Samples from surface and depth were averaged; data are from Appendices B, J, and L.

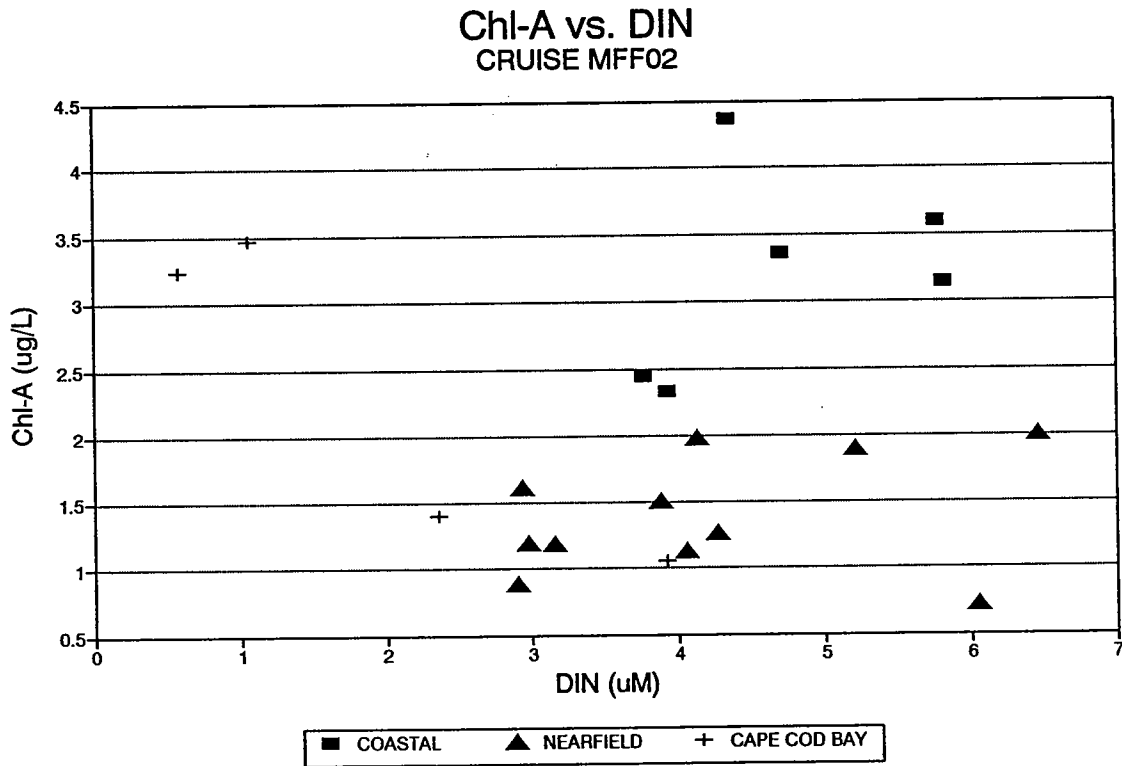
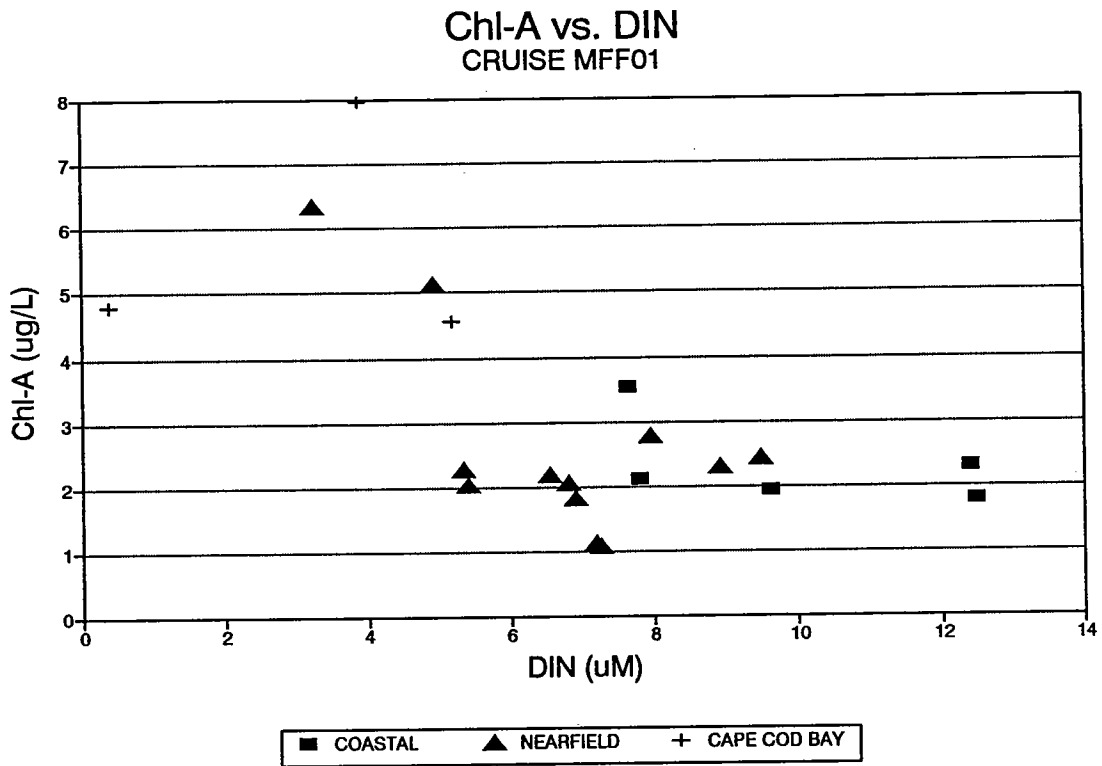


**Figure 5-9** Chlorophyll vs dissolved inorganic nitrogen from all BioProductivity stations in February (top) and March (bottom) 1992 at two depths. Data are given in Appendices A and B.

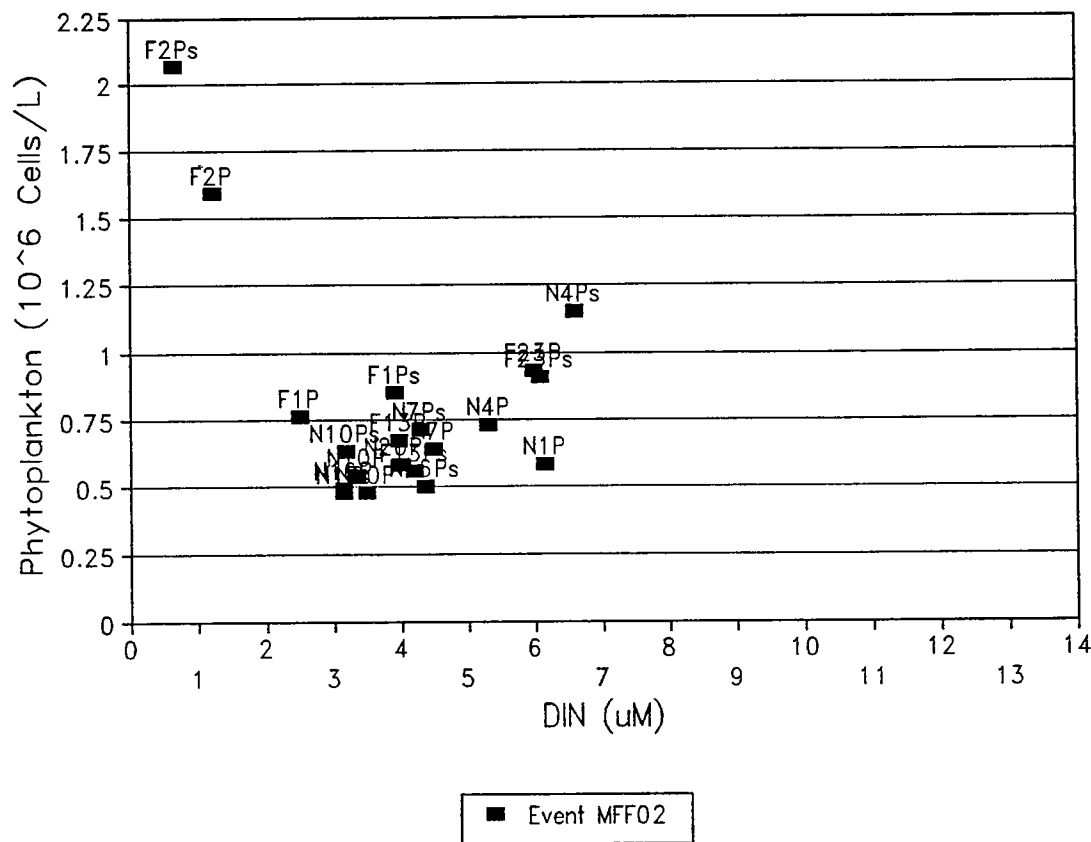
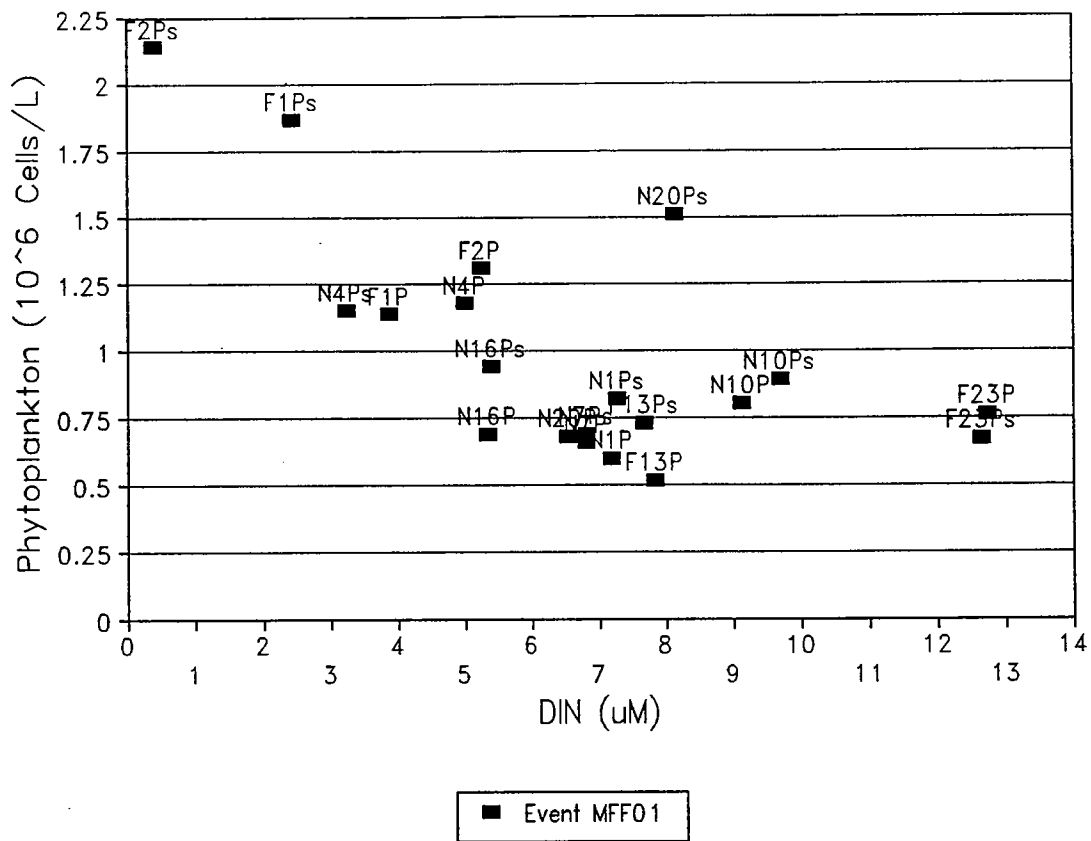
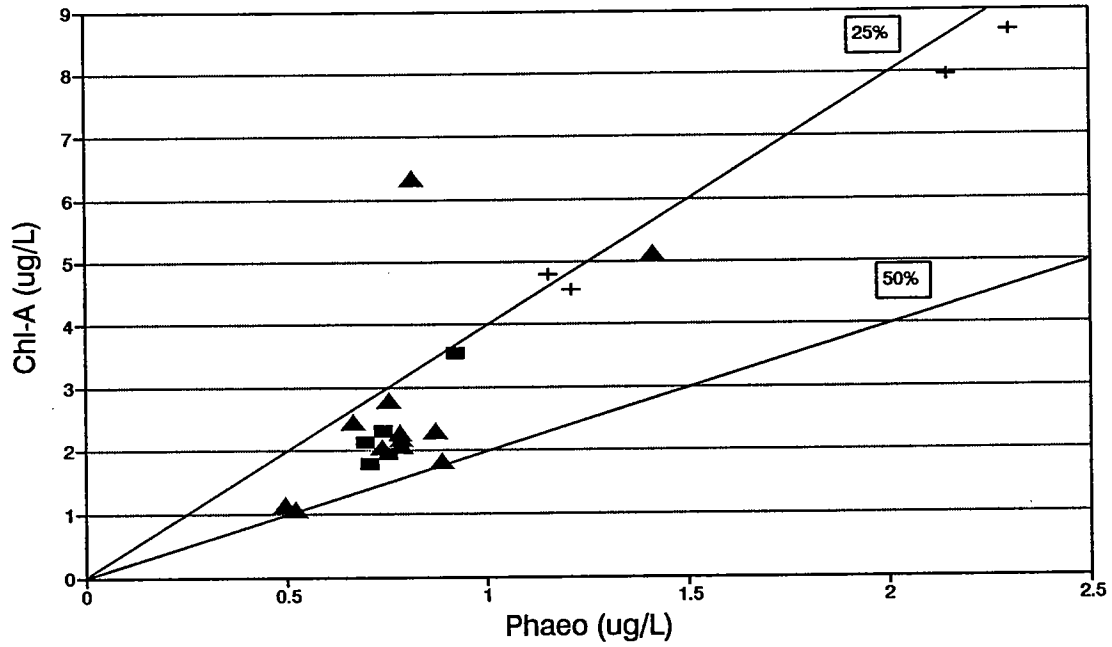


**Figure 5-10** Phytoplankton abundance vs dissolved inorganic nitrogen from all BioProductivity stations in February (top) and March (bottom) 1992 at two depths. Data are given in Appendices A, B, I, and J. The "s" marks surface samples, as distinct from deeper sample.

Chl-A vs. Phaeopigments  
CRUISE MFF01



Chl-A vs. Phaeopigments  
CRUISE MFF02

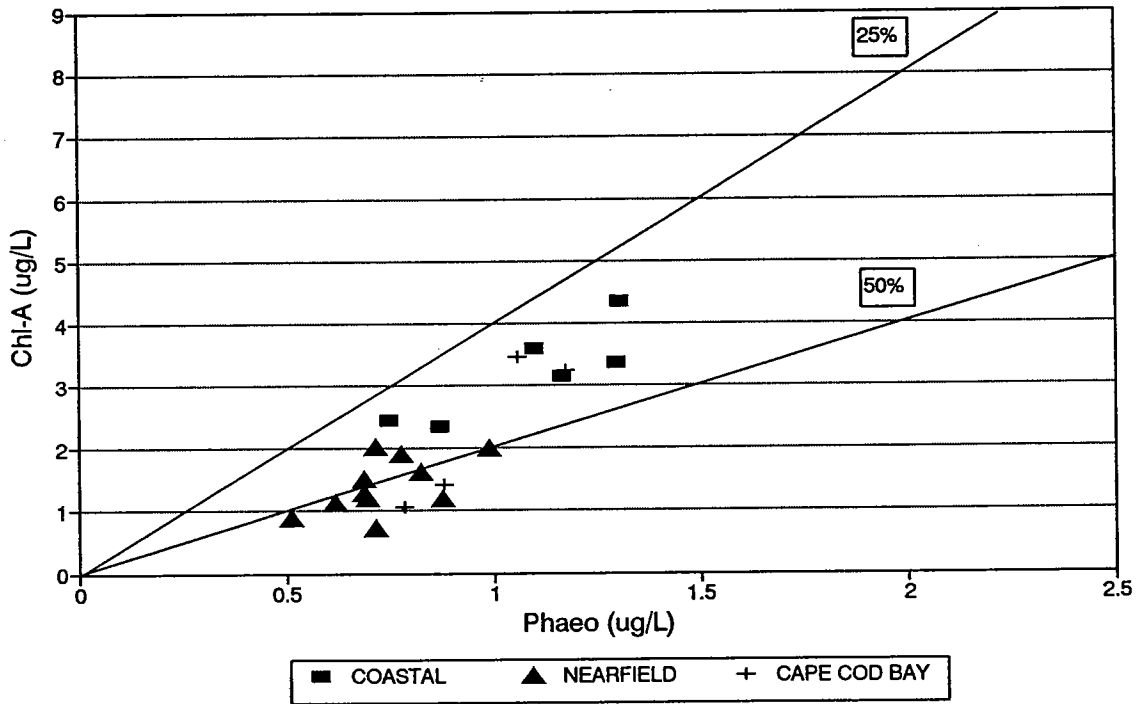


Figure 5-11 Chlorophyll vs. phaeopigments from all BioProductivity stations in February (top) and March (bottom) at two depths. Data are given in Appendices A and B.

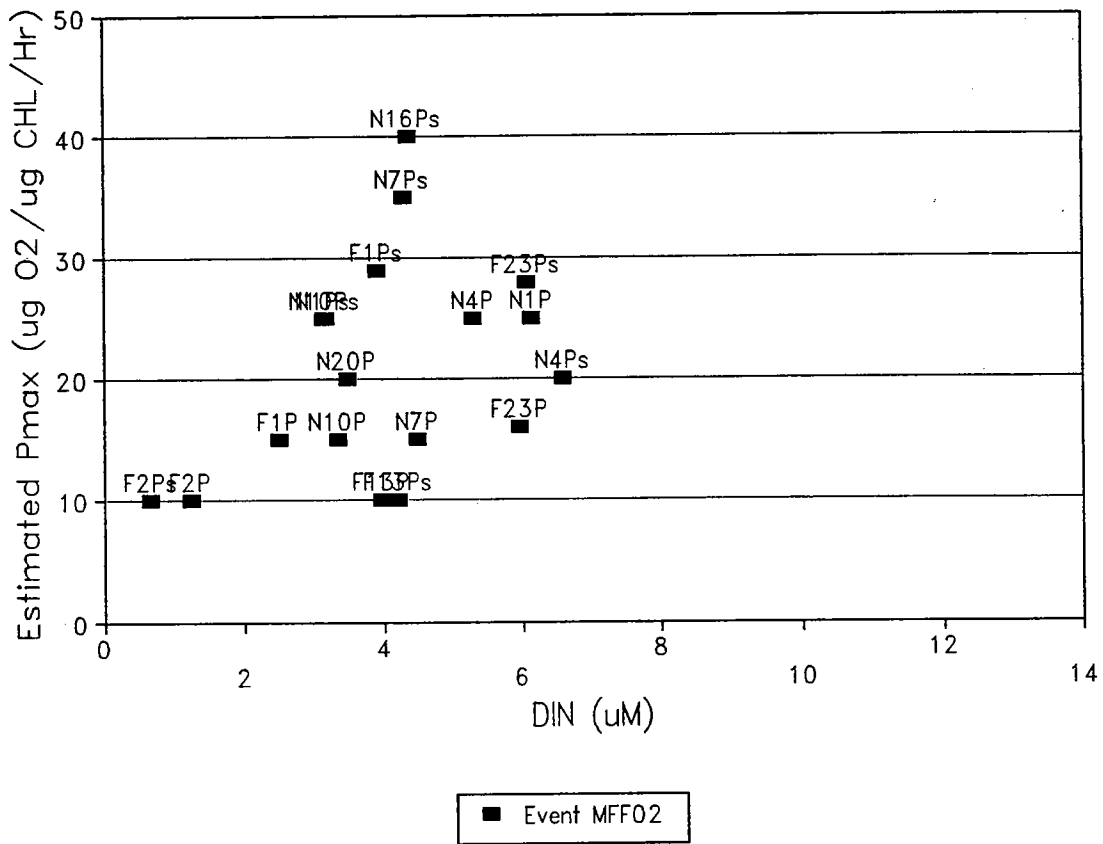
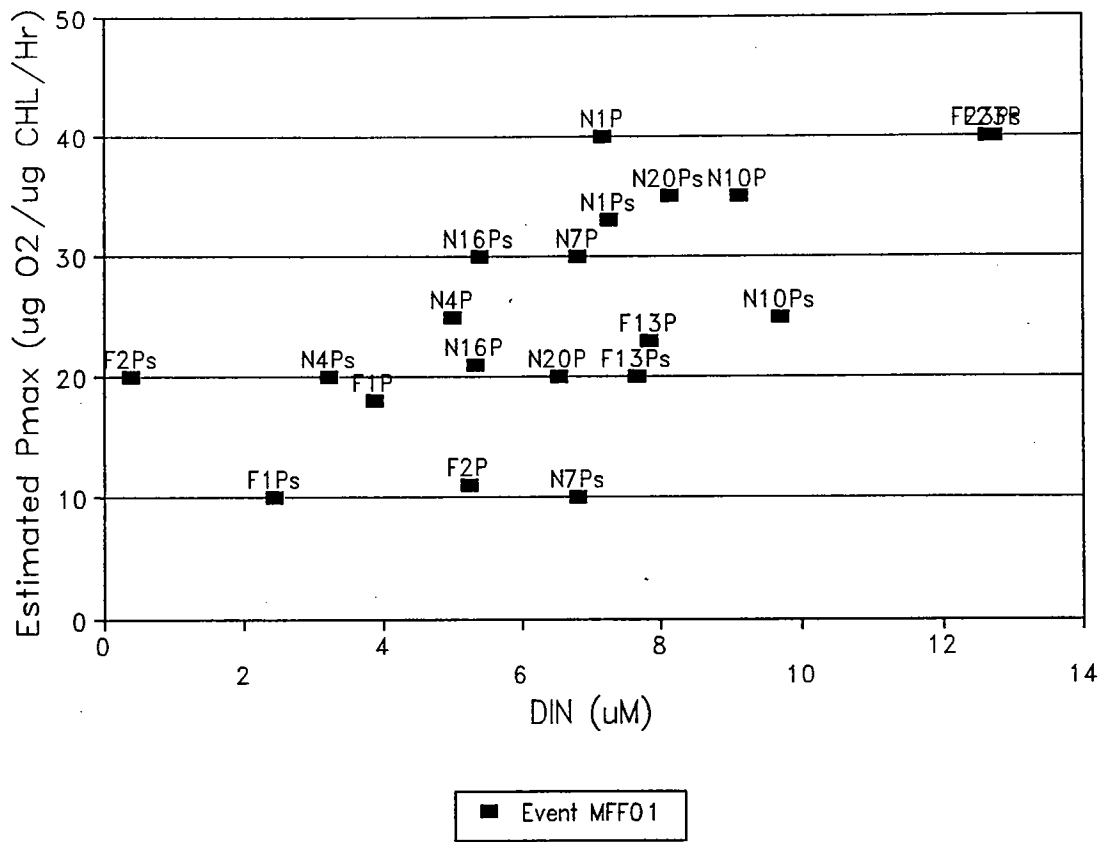


Figure 5-12 Estimated P<sub>max</sub> from P-I curves vs. dissolved inorganic nitrogen in February (top) and March (bottom) 1992. P<sub>max</sub> was estimated from plots given in Appendices G and H, DIN is from Appendices A and B. The "s" marks surface samples, as distinct from deeper sample.





## 6.0 SUMMARY INTERPRETATION OF WINTER-SPRING SEASON DYNAMICS

### 6.1 Farfield Scale

#### 6.1.1 Water Properties in Space and Time

The principal physical heterogeneities in the water column of Massachusetts and Cape Cod Bays were 1) rather subtle layers of lighter surface waters in the northern area of the survey, 2) outward flow from Boston Harbor, and 3) shoreward intrusion of water from the northeast into the nearfield region of western Massachusetts Bay. The observations suggested a coastal-offshore horizontal boundary running southward and weakening well before reaching Cape Cod Bay, which was vertically well mixed and horizontally homogenous at the surface of stations surveyed. Vertical layering in all cases was extremely weak and the water column thus could be easily mixed with the cooling that occurred over the period. In March, the "frontal" or "mixing" zone between the coastal margin water and offshore water appeared to be compressed towards the shore relative to conditions in February. The concomitant nutrient distribution across these subtle horizontal and vertical inhomogeneities was more striking than the physical features. Differences in nutrients were amplified across latitude, as well as from shore-to-sea, by variability in the activity of the phytoplankton.

#### 6.1.2 Ecological Dynamics

The broad-scale features of the ecosystem, given this physical template, are well represented by the composite summary in Figure 6-1, which shows the distribution of total nitrogen (TDN + PON) at the surface of ten BioProductivity stations contoured over the pattern of *in situ* fluorescence. Total nitrogen concentrations depicted the sharp gradient away from the nutrient source in Boston Harbor. At this time, Cape Cod Bay was in the midst of a winter-spring bloom, so fluorescence readings were high (Figure 6-1). Although total nitrogen was similar to that observed as background in the nearfield, the dissolved nutrients were low. The insinuation is that differences in light supply, being the obvious limiting factor at this time of year, initiated phytoplankton growth earlier in the south. However, growth also appeared initiated in the clear waters of northern Massachusetts Bay, creating a second patch of high chlorophyll extending to the edge of the nearfield. In contrast, plankton in the inshore waters, which were more turbid although very rich in nutrients (especially nitrogen), appeared not to be receiving sufficient light to sustain bloom conditions. The hypothesis is that these set of conditions created the general north-south gradient in nutrients, inversely related to chlorophyll. With little action by biology, the chemical gradients out of the Harbor approximated conservative mixing to

the middle of the nearfield region and along the shoreward flow to the south. The suggestion must be that the rates of biological processes across this distance gradient from the Harbor (the strongest nutrient point-source in the region) were slower than the rates of physical processes mixing and dissipating the nutrient concentrations.

Over the February to March period, biological processes started to dominate; chlorophyll outside of the Harbor rose and the sharp distinction in nutrients across water masses began to blur. Against this suspected dynamic, there was little striking variation in the mix of species of the pelagic community. The relative consistency in plankton across stations and depth was likely attributable to the mixed conditions and the lack of strong influence of nutrient variability on species composition at this time, when diatoms characteristically dominate.

## **6.2 Nearfield Scale**

### **6.2.1 Water Properties in Space and Time**

A lesson learned in mathematical ecology during the 1980's was that perception is a function of the scale used to make the observation. Not surprisingly, looking at the nearfield as nested in the farfield scale, or at the different spatial and temporal scales described in this report, the image changed in sometimes subtle and sometimes rather marked ways, such as when a front apparently slipped past a fixed sampling point, changing major aspects of the water quality properties.

### **6.2.2 Ecological Dynamics**

Nevertheless, the physical and ecological variations in the nearfield could be seen as simply a subset of the larger set of variability expressed over latitude. The nearfield was clearly a region influenced from many directions and where active mixing and advection occurred. What was striking was that the measurements that were taken, from physical to chemical to biological, tracked each other well and allowed a strong understanding of rather subtle changes at ecologically relevant scales. This bodes well for the strength of the monitoring program to detect changes as a function of relocation of the discharge of the strong nutrient source in the area.

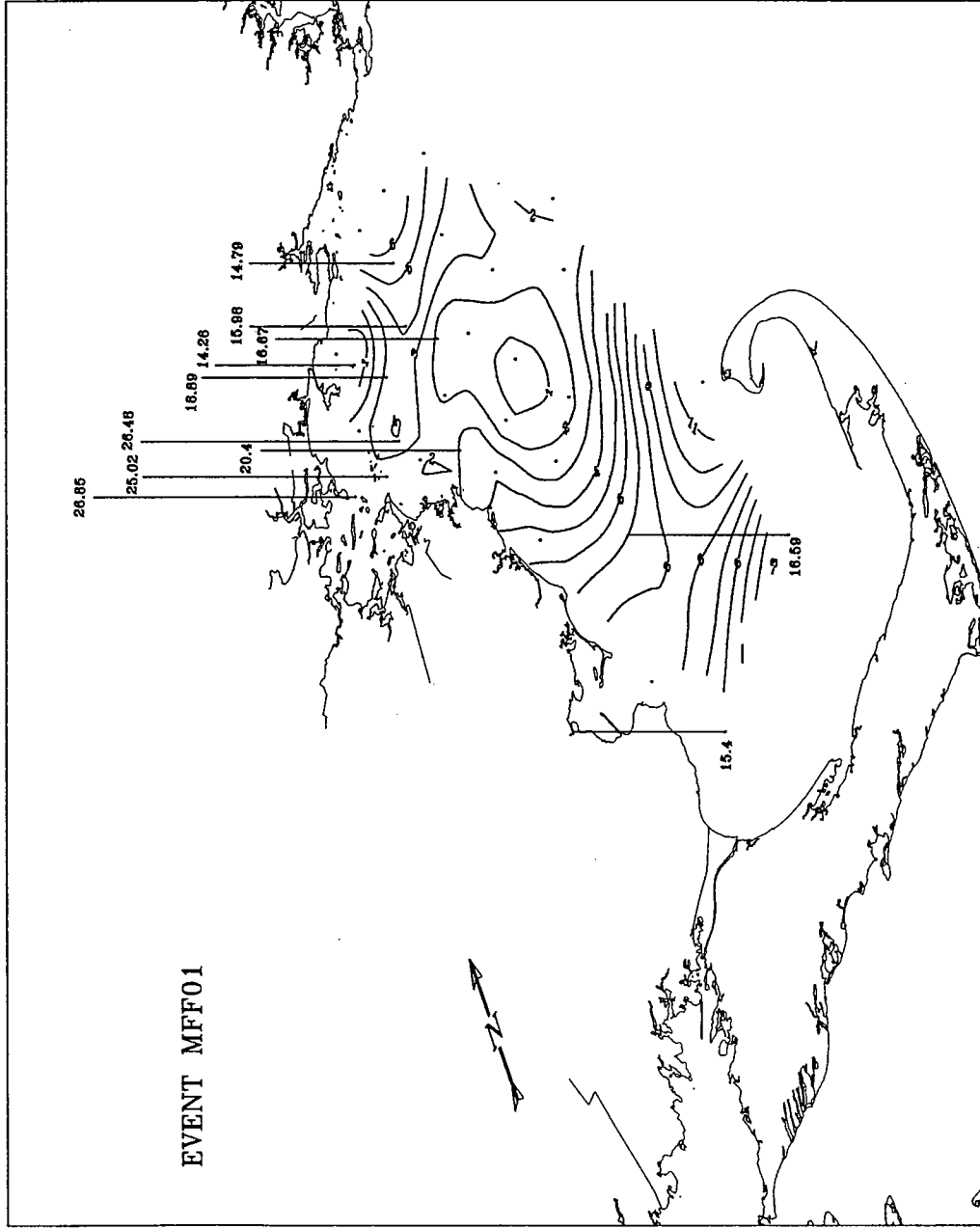


**Figure 6-1** Surface concentrations of total nitrogen ( $\Sigma$ TDN + PON,  $\mu$ M) at BioProductivity stations and special station F25 shown as relative height bars overlain upon horizontal contours of surface fluorescence (as  $\mu$ g Chl  $L^{-1}$ ) during February 1992. Data are given in Appendix A, contour interval is  $1.0 \mu$ g  $L^{-1}$ .

## 7.0 REFERENCES

- Anonymous. 1978. *Phytoplankton Manual*. Monographs on Oceanographic Methodology, 6th Edition. Sournia, (Editor). UNESCO, Paris. (Especially sections 2.1, 5.1, 5.2, 7.1.1, 7.1.2, 7.2.2)
- Bendschneider, K. and R.J. Robinson. 1952. A new spectrophotometric determination of nitrite in seawater. *J. Mar.Res.* 11:87-96.
- Brewer, P.G. and J.P. Riley. 1966. The automatic determination of silicate silicon in natural waters with special reference to seawater. *Anal. Chim. Acta.* 35:514-519.
- Cura, J.J. 1991. Review of phytoplankton data for Massachusetts Bay. Draft report to MWRA. February 1991. 26+ pp.
- Geyer, W.R., G.B. Gardner, W.S. Brown, J. Irish, B. Butman, T. Loder, and R.P. Signell. Draft Final Report: Physical Oceanographic Investigation of Massachusetts and Cape Cod Bays. To Massachusetts Bays Program. March 4, 1992.
- Guillard, R.R.L. 1973. Division Rates, pp. 289-311. In: J.R. Stein, (Editor), *Phycological Methods*. Cambridge University Press.
- Hitchcock, G.L. and T.J. Smayda. 1977. The importance of light in the initiation of the 1972-1973 winter-spring diatom bloom in Narragansett Bay. *Limnol. Oceanogr.* 22:126-134.
- Kelly, J.R. 1991. Nutrients and Massachusetts Bay: A Synthesis of Eutrophication Issues. Report to the MWRA. 58+ pp.
- Lambert, C.E. and C.A. Oviatt. 1986. Manual of biological and geochemical techniques in coastal areas. MERL Series, Report No. 1, Second Edition. Marine Ecosystems Research Laboratory, University of Rhode Island, Narragansett, RI 02882-1197.
- Lewis, M.R. and J.C. Smith. 1983. A small volume, short-incubation-time method for measurement of photosynthesis as a function of incident irradiance. *Marine Ecology Progress Series.* 13:99-102.
- Lorenzen, C.J. 1966. A method for the continuous measurement of *in vivo* chlorophyll concentration. *Deep Sea Res.* 13:223-227.
- Morris, A.W. and J.P. Riley. 1963. The determination of nitrate in seawater. *Analytica chim acta.* 29:272-279.
- Murphy, J. and J.P. Riley. 1962. A modified single solution method for the determination of phosphate in natural waters. *Anal. Chim. Acta.* 27:31.

- MWRA. 1988. Secondary Treatment Facilities Plan. Massachusetts Water Resources Authority, Boston, MA. March 1998.
- MWRA. 1991. Massachusetts Water Resources Authority effluent outfall monitoring plan phase I: baseline studies. MWRA Enviro. Quality Depart., November 1991. Massachusetts Water Resources Authority, Boston, MA. 95 pp.
- Oudot, C., R. Gerard and P. Morin. 1988. Precise shipboard determination of dissolved oxygen (Winkler procedure) for productivity studies with a commercial system. *Limnol. and Oceanogr.* 33:146-150.
- Ricker, W.E. 1973. Linear regressions in fishery research. *J. Fish. Res. Bd. Can.* 30:409-434.
- Ryther, J. 1992a. Survey report for the February 1992 Combined Nearfield-Farfield Water Quality Survey. Survey report to MWRA.
- Ryther, J. 1992b. Survey report for the March 1992 Combined Nearfield-Farfield Water Quality Survey. Survey report to MWRA.
- SAS. 1985. SAS Users Guide: Statistics. SAS Institute, Inc., Cary, NC. 956 pp.
- Shea, D., J. Ryther, and J. Kelly. 1992. Quality assurance project plan for MWRA effluent outfall monitoring program: Baseline Water Quality Monitoring of Massachusetts Bay. Battelle Ocean Sciences Report to Massachusetts Water Resources Authority, Boston, MA. 41 pp.
- Smetacek, V. and U. Passow. 1990. Spring bloom initiation and Sverdrup's critical-depth model. *Limnol. Oceanogr.* 35:228-234.
- Solorzano, L. 1969. Determination of ammonia in natural waters by the phenol hypochlorite method. *Limnol. and Oceanogr.* 14:799-801.
- Strickland, J.D.H. and T.R. Parsons. 1972. A practical handbook of seawater analysis. *Fish. Res. Bd. Can. Bull.* 167:310 pp.
- Sugimura, Y. and Y. Suzuki. 1988. A high temperature catalytic oxidation method for the determination of non-volatile dissolved organic carbon in sea water by direct injection of liquid samples. *Mar. Chem.* 24:105-131.
- Sverdrup, H. U. 1953. On conditions for the vernal blooming of phytoplankton. *J. Const. COns. Int. Explor. Mer.* 18:287-295.

- Townsend, D. and others. 1990. Seasonality of oceanographic conditions in Massachusetts Bay. Bigelow Laboratory for Ocean Sciences Technical Report No. 83, December 1990. Massachusetts Water Resources Authority, Boston, MA. 114 pp.
- Valderama, J.C. 1981. The simultaneous analysis of total nitrogen and total phosphorus in natural waters. *Mar. Chem.* 10:109-122.
- Yentsch, C.S. and D.W. Menzel. 1963. A method for the determination of phytoplankton chlorophyll and phaeophytin by fluorescence. *Deep Sea Res.* 10:221-231.

Note to reader: Appendices A-L are bound separately from this technical report. To request the Appendices contact the MWRA and ask for one of the MWRA Miscellaneous Publications entitled "APPENDICES TO WATER QUALITY MONITORING IN MASSACHUSETTS AND CAPE COD BAYS: FEBRUARY-MARCH 1992."



The Massachusetts Water Resources Authority  
Charlestown Navy Yard  
100 First Avenue  
Charlestown, MA 02129  
(617) 242-6000